FRAM POLLUTION OBSERVATORY

ANTHROPOGENIC DEBRIS POLLUTION IN THE ARCTIC

Dem Fachbereich Geowissenschaften

der

UNIVERSITÄT BREMEN

Dr. rer. nat.

vorgelegte

DISSERTATION

von

Mine Banu Tekman

Gutachter der Dissertation:
Prof. Dr. Morten Iversen
Dr. Holger Freund

Ph.D. Colloquium

20.01.2023

Marine debris and microplastic distribution in different ecosystem compartments in the Arctic

Versicherung an Eides Statt / *Affirmation in lieu of an oath*

gem. § 5 Abs. 5 der Promotionsordnung vom 28.04.2021 /
according to § 5 (5) of the Doctoral Degree Rules and Regulations of 28 April, 2021

Ich / I, Mine Banu Tekman, Kadiköy-Istanbul-Turkei
(Vorname / First *Name*, Name / *Name*, Anschrift / *Address*, ggf. Matr.-Nr. / *student ID no., if applicable)*

versichere an Eides Statt durch meine Unterschrift, dass ich die vorliegende Dissertation selbständig und ohne fremde Hilfe angefertigt und alle Stellen, die ich wörtlich dem Sinne nach aus Veröffentlichungen entnommen habe, als solche kenntlich gemacht habe, mich auch keiner anderen als der angegebenen Literatur oder sonstiger Hilfsmittel bedient habe und die zu Prüfungszwecken beigelegte elektronische Version (PDF) der Dissertation mit der abgegebenen gedruckten Version identisch ist. / *With my signature I affirm in lieu of an oath that I prepared the submitted dissertation independently and without illicit assistance from third parties, that I appropriately referenced any text or content from other sources, that I used only literature and resources listed in the dissertation, and that the electronic (PDF) and printed versions of the dissertation are identical.*

Ich versichere an Eides Statt, dass ich die vorgenannten Angaben nach bestem Wissen und Gewissen gemacht habe und dass die Angaben der Wahrheit entsprechen und ich nichts verschwiegen habe. / *I affirm in lieu of an oath that the information provided herein to the best of my knowledge is true and complete.*

Die Strafbarkeit einer falschen eidesstattlichen Versicherung ist mir bekannt, namentlich die Strafandrohung gemäß § 156 StGB bis zu drei Jahren Freiheitsstrafe oder Geldstrafe bei vorsätzlicher Begehung der Tat bzw. gemäß § 161 Abs. 1 StGB bis zu einem Jahr Freiheitsstrafe oder Geldstrafe bei fahrlässiger Begehung. / *I am aware that a false affidavit is a criminal offence which is punishable by law in accordance with § 156 of the German Criminal Code (StGB) with up to three years imprisonment or a fine in case of intention, or in accordance with § 161 (1) of the German Criminal Code with up to one year imprisonment or a fine in case of negligence.*

Istanbul, 05.08.2022

Ort / *Place*, Datum / *Date*

Unterschrift / *Signature*

The more I learn, the more I realize how much I don't know.

Albert Einstein

Table of Contents

Summary vii

Zusammenfassung ix

1 Introduction 1

1.1 Global Plastic Pollution 1

1.2 The Arctic Ocean 5

1.3 FRAM Pollution Observatory 6

1.4 The Aim and Structure of the Dissertation 7

1.5 References 8

1.6 Declaration of Author's Contribution 12

2 The spatiotemporal distribution of macro-debris pollution in the Arctic 15

2.1 Marine debris floating in Arctic and temperate Northeast Atlantic waters 15

2.1.1 Introduction 16

2.1.2 Material and Methods 18

2.1.3 Results 24

2.1.4 Discussion 33

2.1.5 Conflict of Interest 42

2.1.6 Author Contributions 43

2.1.7 Funding 43

2.1.8 Acknowledgements 43

2.1.9 References 43

2.2 Marine litter on deep Arctic seafloor continues to increase and spreads to the North at *the* HAUSGARTEN observatory 51

2.2.1 Introduction 52

2.2.2 Material and Methods 53

2.2.3 Result 58

2.2.4 Discussion 67

2.2.5 Conclusions 72

2.2.6 Acknowledgements 73

2.2.7 References 73

3 Tying up Loose Ends of Microplastic Pollution in the Arctic: Distribution from the Sea Surface through the Water Column to Deep-Sea Sediments at the HAUSGARTEN Observatory 79

3.1 Introduction 80

3.2 Material and Methods 82

3.3 Results 88

3.4 Discussion 94

3.5 Acknowledgements 100

3.6 References 101

4 General Discussion 108

4.1 Overview 108

4.2 Sea Surface, Sea Ice and Snow 113

4.3 Arctic Beaches (Svalbard) 121

4.4 The Water Column 128

4.5 The Deep Seafloor 130

4.6 Comparison of polymer compositions in snow, water column and sediment 138

4.7 Impacts on Arctic biota 141

4.8 Outlook 148

4.9 References 151

5 Supporting Information 162

5.1 Marine debris floating in Arctic and temperate Northeast Atlantic waters 162

5.2 Marine litter on deep Arctic seafloor continues to increase and spreads to the North at the HAUSGARTEN observatory 172

5.3 Tying up Loose Ends of Microplastic Pollution in the Arctic: Distribution from the Sea Surface through the Water Column to Deep-Sea Sediments at the HAUSGARTEN Observatory 174

6 Further scientific publications 202

7 Acknowledgements 204

Summary

The exponential increase in plastic production is reflected in the amount of waste produced, yet the waste management infrastructures and practices have been insufficient to regulate and govern the extensive plastic waste entering the environment, which was estimated as 19 – 23 million metric tons in 2016 for aquatic systems. Disturbing footage of pervasive pollution or an increasing number of sightings of encounters with charismatic species not only draw public attention but also boosted an interest within the scientific community. Soon enough, it was realized that anthropogenic debris pollution has even reached uninhabited remote islands and polar regions. Globally, there are thousands of studies on regional or large-scale anthropogenic debris pollution, yet a holistic approach to identify the distribution patterns is mostly lacking. In this regard, with the aim of measuring anthropogenic debris and microplastic pollution levels in all ecosystem compartments in the Arctic, the FRAM Pollution Observatory represents a rare case. The comparison of findings from different ecosystem compartments allowed us to explore and identify the sources, transportation pathways and sinks of anthropogenic debris in the Arctic.

In this dissertation, I summarise the findings obtained by the studies of the FRAM Pollution Observatory. The main chapters deal with the distribution of macro-debris floating in Arctic surface waters (Chapter 2.1) and on the deep seafloor (Chapter 2.2) and with the distribution of microplastic throughout the water column and in deep-sea sediments (Chapter 3). However, in the general discussion (Chapter 4), I focused on the findings from all ecosystem compartments including sea ice, snow, Svalbard beaches and biota. Overall, the majority of anthropogenic macro-debris in the Arctic is plastic. In all ecosystem compartments, high levels of pollution were detected, which are comparable to those reported from more densely populated regions of the world. Quantities of floating macro-debris in Arctic waters were not different to those in the North Sea. Higher concentrations of floating macro-debris measured in summer than in autumn and spring highlighted the indirect effect of decreasing sea ice extent, which has opened new passages for maritime activities. Between 2002 and 2014, a significant increase in macro-debris concentrations on the deep seafloor was identified. Deep-sea sediments are an ultimate sink for microplastic pollution. Throughout the water column, highest microplastic concentrations were observed in the ocean surface layer and decreased towards greater depths as did organic matter distribution, too. Microplastic particles between 10 and 100 µm accounted for 99.9% of the microplastics detected in the water column, raising concerns about their bioavailability. A different vertical profile at the Molloy Deep suggested

that local oceanographic conditions and bathymetry affect microplastic distribution. The simulation of drift trajectories indicated the North Atlantic Current as the main carrier of anthropogenic debris to the Fram Strait, yet with a contribution of the Transpolar Drift carrying debris from the Siberian Arctic. Sea ice drift trajectories identified the Kara and Laptev Seas as another source of pollution in the Fram Strait. As for the other studies of the FRAM Pollution Observatory, Arctic sea ice is a temporary sink of microplastic, scavenging particles from surrounding waters during ice formation and releasing them upon melting. Microplastic concentrations in Arctic snow, as an indicator of atmospheric microplastic pollution, showed considerable concentrations, which are comparable to those from urban areas. A preliminary analysis of microplastic distribution in the water column, sediment and snow showed significant differences in concentrations between sediment and other ecosystem compartments, but not between those obtained from the water column and snow. This finding points out a turnover at the sea-air interface. Last but not least, zooplankton organisms in the Fram Strait were found to have ingested microplastic, confirming the bioavailability of these anthropogenic pollutants.

Although, a substantial number of findings helped me to understand the pollution levels and trends of anthropogenic debris in the Arctic, they raised a lot more questions to be answered. We still do not know, how and when such a pervasive pollutant will affect the biodiversity, biogeochemical cycles in the Arctic and eventually global climate patterns. I hope, we will be able to regulate our plastic production, consumption and waste management before such destructive impacts occur.

Zusammenfassung

Der exponentielle Anstieg der Kunststoffproduktion spiegelt sich in der Menge des erzeugten Abfalls wider, doch die Infrastrukturen und Praktiken der Abfallbewirtschaftung reichen nicht aus, um die umfangreichen Kunststoffabfälle, die in die Umwelt gelangen, zu regulieren und zu kontrollieren. 2016 wurden diese für aquatische Systeme auf 19 bis 23 Millionen Tonnen geschätzt. Beunruhigende Aufnahmen der allgegenwärtigen Umweltverschmutzung oder eine zunehmende Zahl von Sichtungen von Begegnungen mit charismatischen Arten erregen nicht nur die öffentliche Aufmerksamkeit, sondern wecken auch das Interesse der wissenschaftlichen Gemeinschaft. Schon bald wurde klar, dass die vom Menschen verursachte Verschmutzung sogar unbewohnte, abgelegene Inseln und Polarregionen erreicht hat. Weltweit gibt es Tausende von Studien zur regionalen oder großräumigen anthropogenen Müllverschmutzung, doch fehlt es meist an einem ganzheitlichen Ansatz zur Ermittlung der Verteilungsmuster. In dieser Hinsicht stellt das FRAM Pollution Observatory mit dem Ziel, die anthropogene Verschmutzung durch Müll und Mikroplastik in allen Ökosystemkompartimenten der Arktis zu messen, einen seltenen Fall dar. Der Vergleich der Ergebnisse aus verschiedenen Ökosystemkompartimenten ermöglichte es uns, die Quellen, Transportwege und Senken von anthropogenem Müll in der Arktis zu untersuchen und zu identifizieren.

In dieser Dissertation fasse ich die Erkenntnisse zusammen, die durch die Studien des FRAM Pollution Observatory gewonnen wurden. Die Hauptkapitel befassen sich mit der Verteilung von Makromüll, der in arktischen Oberflächengewässern (Kapitel 2.1) und auf dem Meeresboden (Kapitel 2.2) schwimmt, sowie mit der Verteilung von Mikroplastik in der Wassersäule und in Tiefseesedimenten (Kapitel 3). In der allgemeinen Diskussion (Kapitel 4) konzentrierte ich mich jedoch auf die Ergebnisse aus allen Ökosystemkompartimenten, einschließlich Meereis, Schnee, Svalbard-Strände und Biota. Insgesamt besteht der Großteil des anthropogenen Makromülls in der Arktis aus Plastik. In allen Ökosystemkompartimenten wurden hohe Verschmutzungsgrade festgestellt, die mit denen vergleichbar sind, die aus dichter besiedelten Regionen der Welt gemeldet werden. Die Mengen an schwimmendem Makromüll in arktischen Gewässern unterschieden sich nicht von denen in der Nordsee. Höhere Konzentrationen von schwimmendem Makromüll, die im Sommer gemessen wurden, als im Herbst und Frühjahr, verdeutlichen die indirekte Auswirkung der abnehmenden Meereisausdehnung, die neue Passagen für maritime Aktivitäten eröffnet hat. Zwischen 2002 und 2014 wurde ein signifikanter Anstieg der Makromüllkonzentrationen auf dem tiefen

Meeresboden festgestellt. Die Tiefseesedimente sind eine ultimative Senke für die Verschmutzung durch Mikroplastik. In der gesamten Wassersäule wurden die höchsten Mikroplastikkonzentrationen in der Oberflächenschicht des Ozeans beobachtet, die mit zunehmender Tiefe abnahmen, ebenso wie die Verteilung organischer Stoffe. Mikroplastikpartikel zwischen 10 und 100 µm machten 99,9 % des in der Wassersäule nachgewiesenen Mikroplastiks aus, was Anlass zur Sorge über seine Bioverfügbarkeit gibt. Ein anderes vertikales Profil im Molloy Deep deutet darauf hin, dass die lokalen ozeanografischen Bedingungen und die Bathymetrie die Verteilung des Mikroplastiks beeinflussen. Die Simulation von Driftbahnen ergab, dass der Nordatlantikstrom der Hauptträger von anthropogenem Müll in der Framstraße ist, wobei jedoch auch die Transpolardrift mit Müll aus der sibirischen Arktis einen Beitrag leistet. Die Meereis-Drifttrajektorien wiesen die Kara- und die Laptewsee als weitere Quelle der Verschmutzung in der Framstraße aus. Wie in den anderen Studien der FRAM-Beobachtungsstelle für Verschmutzung ist das arktische Meereis eine vorübergehende Senke für Mikroplastik, da es während der Eisbildung Partikel aus den umliegenden Gewässern aufnimmt und sie beim Schmelzen wieder freisetzt. Die Mikroplastikkonzentrationen im arktischen Schnee als Indikator für die Verschmutzung der Atmosphäre durch Mikroplastik wiesen erhebliche Konzentrationen auf, die mit denen in städtischen Gebieten vergleichbar sind. Eine vorläufige Analyse der Verteilung von Mikroplastik in der Wassersäule, im Sediment und im Schnee ergab signifikante Unterschiede in den Konzentrationen zwischen Sediment und anderen Ökosystemkompartimenten, jedoch nicht zwischen den Konzentrationen in der Wassersäule und im Schnee. Diese Feststellung deutet auf einen Umsatz an der Schnittstelle zwischen Meer und Luft hin. Nicht zuletzt wurde festgestellt, dass Zooplanktonorganismen in der Framstraße Mikroplastik aufgenommen haben, was die Bioverfügbarkeit dieser anthropogenen Schadstoffe bestätigt.

Obwohl mir eine ganze Reihe von Erkenntnissen geholfen hat, die Verschmutzungsgrade und -trends des anthropogenen Mülls in der Arktis zu verstehen, haben sie viele weitere Fragen aufgeworfen, die es zu beantworten gilt. Wir wissen immer noch nicht, wie und wann sich ein solch allgegenwärtiger Schadstoff auf die biologische Vielfalt, die biogeochemischen Zyklen in der Arktis und schließlich auf die globalen Klimamuster auswirken wird. Ich hoffe, dass wir in der Lage sein werden, unsere Kunststoffproduktion, unseren Verbrauch und unsere Abfallwirtschaft zu regulieren, bevor es zu solch zerstörerischen Auswirkungen kommt.

1 Introduction

1.1 Global Plastic Pollution

The first synthetic material based on nitrocellulose was produced in 1862 by Parkes and in 1866 by Hyatt. Hyatt used camphor as an additive producing the first thermoplastic, which then was used to produce a movie film (Feldman, 2008). In 1907, the first synthetic thermoset polymer Bakelite was produced and the commercial production of Bakelite after a few years is considered as the beginning of the plastic industry (Feldman, 2008). The most commonly produced plastics are polypropylene (PP), polyethylene (PE), polyvinyl chloride (PVC), polystyrene (PS) and polyethylene terephthalate (PET), which are considered commodity plastics due to their high volume and low cost (Andrady and Neal, 2009). PVC was developed in 1872, PS in 1930, PE in 1933, PET in 1941 and PP in 1954 and their commercial production started between the late 1920's and 1950's (Andrady and Neal, 2009), yet plastic was started to be widely used after the World War II (Geyer et al., 2017). Since then, the value of the global plastic market has increased to 580 billion U.S. dollars in 2020 (Source: statista.com).

In the two decades following World War II, studies on plastic pollution started to emerge. Kenyon and Kridler (1969) reported container caps and toys ingested by Laysan Albatrosses, plastics floating in the Sargasso Sea were observed (Carpenter and Smith, 1972) and polystyrene granules were found in the coastal waters off southern New England (Carpenter et al., 1972). However, it is worth mentioning here that Eugene Willis Gudger (Gudger, 1928) already reported a mackerel grown with a roved rubber band in 1928, a very early sign of a nowadays very common interaction between fish and man-made material (Colmenero et al., 2017). In 1973, Venrick et al. (1973) reported floating anthropogenic items from the Central North Pacific Ocean by visual surveys. Soon after, marine debris including plastic was reported from the Antarctic seafloor (Dayton and Robilliard, 1971), bottom trawl samples taken in the deep Skagerrak, Sweden (Holmström, 1975), Bering Sea seafloor (Feder et al., 1978) and northeast Gulf of Alaska (Jewett, 1976). The plastic films from the Skagerrak were found at depths between 180 and 400 m. The author of the study, Arne Holmström, suggested that floating plastics gets weathered due to the UV exposure, simultaneously bryozoa begin to grow on them so that they begin to sink towards the pycnocline, where brown algae *Lithoderma* take over and eventually the items sink to the seafloor. Meanwhile, plant-eating molluscs consume plastic together with *Lithoderma*, causing "eating traces" on the films. Personally, I find it astonishing that during the last 50 years, hundreds even thousands of studies (Source:

litterbase.org) have identified these mechanisms and although the scientists warned the world back then, we still cannot take environmental plastic pollution under control.

The aim here is not to provide a full history of research on plastic pollution, but to emphasize that as early as in the 1970's, plastic waste was identified as an environmental problem. In five decades, its annual production reached to 450 million metric tons (Geyer, 2020; PlasticsEurope, 2021) and more than 2,981 studies were published on plastic pollution (litterbase.org), reporting sightings from all marine compartments, freshwater systems, soils and even from mountaintops, air, snow and sea ice (MacLeod et al., 2021) or fragile ecosystems such as mangrove forests and coral reefs (Tekman et al., 2022). A total of 2,144 marine species have been documented to encounter plastics in the oceans and another 400 have been reported to interact with plastic in experimental conditions (Tekman et al., 2022).

Geyer et al. (2017) estimated that 8.3 billion metric tons of virgin plastic had been produced between 1950 and 2015, of which 6.3 billion metric tons had become waste. They estimated that a mere 9% of the waste was recycled, 12% was incinerated, whereas the remainder went into landfills or to the environment. Between 2016 and 2020, another 1.8 billion metric tons of virgin plastic was added to this 'picture' (PlasticsEurope, 2021), which corresponds to 21% of the mass of plastic produced between 1950 and 2015. Accordingly, if we apply the percentages of recycled and incinerated amounts to the updated dataset, as of 2021, the mass of plastic waste in landfills or in the environment accounts for 7.96 billion metric tons. Borrelle et al. (2020) estimated the amount of plastic waste that entered aquatic environments in 2016 from land-based sources at 19 to 23 million metric tons, which is expected to reach to a value between 36 and 90 million metric tons in 2030 if plastic production and waste generation continue to grow at the same rate as in 2016. This estimate does yet not include the recent 'plastic surge' of the COVID-19 pandemic. Globally, 129 billion face masks and 65 billion gloves were estimated to be consumed monthly during the COVID-19 pandemic. Moreover, the increase of take-away food and mail delivery during the quarantine periods boosted up the amount of plastic waste produced (Prata et al., 2020).

In general, sources of plastic debris are categorised as land-based and sea-based and it is often stated that 80% of marine plastic debris items by number originates from land-based sources. However, firstly, the terms "land-based" and "sea-based" sources need to be considered here. Probably, the best definitions have been put forward by the Joint Group of Experts on the Scientific Aspects of Marine Environmental Protection (GESAMP). They categorised the consumer sectors as sources and on top of these sources, they identified the

entry points (GESAMP, 2016). Land-based sectoral consumers are agriculture, construction, transportation on land and tourism industry, whereas sea-based sectoral consumers comprised fisheries, aquaculture, shipping and offshore industry. They suggested individual consumers as an additional group for food and drinking packaging as well as for textile and clothing waste. Waste management was also identified as a source sector, since solid waste and particles from wastewater are known to leak into the oceans. Plastics enter the oceans from rivers, coastlines, oceans and the atmosphere, which can all be considered as entry points. As an addition, long-distance transport of debris and local inputs should be mentioned here for a complete picture of how anthropogenic debris moves along marine environments. Once a plastic item enters the ocean, the fate of it depends on material type and shape as well as environmental conditions and biological interactions (van Sebille et al., 2020). In general, non-buoyant items are expected to sink directly (Engler, 2012), whereas positively buoyant debris floats until its density increases by organisms that have settled on it (Fazey and Ryan, 2016). Floating items can strand on the coastlines (Ryan et al., 2019), until they are picked up during clean-ups or return to the sea along with the waves and winds (Ryan et al., 2020) possibly after becoming fragmented (Kaandorp et al., 2021). Fragmentation occurs due to environmental conditions such as UV light, wave actions or by organisms (Fazey and Ryan, 2016). These debris items can also be deposited at the coastlines. The fate of sinking pieces and particles are similar to those moving towards the coasts: Sinking pieces and particles eventually reach the seafloor, where they can either move to upper layers due to wind and wave actions (Kooi et al., 2017) or deposited on the deep ocean floor (Chapter 2.2 and Chapter 3). One interesting suggestion is that after plastic debris starts to sink due to the biofilm load, which attracts organisms to graze on them, removing the additional organic load so that it resurfaces (Ye and Andrady, 1991). While settling, particles can be consumed in the pelagic realm (Choy and Drazen, 2013), so that they can be transported within the organisms, until they are egested and return to the "plastic movement loop" again (Wieczorek et al., 2019). Clearly, such a complicated and highly parametrised cycle is very hard to investigate and model.

Plastic pollution in the environment is poorly reversible because its accumulation occurs at a rate, which outpaces the capacity of natural removal processes and cleaning actions (MacLeod et al., 2021). The durability of the plastic material leads to a persistence in the environment for long but yet unknown periods of time (Ward and Reddy, 2020) and continuous fragmentation processes lead to smaller particles namely micro- and nanoplastics (MacLeod et al., 2021). Therefore, plastic pollution was recently identified as a planetary boundary threat

together with other novel chemicals (Persson et al., 2022). Effects on species depend on the size of plastic debris. Impacts of marine macro plastics interactions have been well-acknowledged by the research and public (Bucci et al., 2020; Tekman et al., 2022). Entanglements in plastic debris can lead to suffocation and restrained mobility (Kühn et al., 2015). Ingestion of plastic debris can cause internal injury, blockage, a false sense of satiety, decreased food uptake and as a consequence possibly to reduced fertility, growth and mortality (Kühn et al., 2015). Colonisation of plastic items by rafting organisms can boost the dispersal of organisms to habitats where they can become invasive (Kiessling et al., 2015; Tekman et al., 2022). When covered with plastic debris, habitats or species below can suffer from oxygen-deficiency (Green et al., 2015) and decreased food supply (Mouchi et al., 2019). As the other less-known impacts, macro plastic debris on the beaches can become an obstacle for the sea turtle hatchlings preventing them to reach the ocean (Aguilera et al., 2018) or fishing net fragments in the nests of seabirds can lead to suffocation of the juveniles (Tekman et al., 2022). Hundreds of studies have confirmed ingestion of micro- (< 5mm) and nanoplastics (< 1µm), yet the ecotoxicological impacts of ingestion are still under debate due to the 'unrealistic' concentrations used in many laboratory studies and differences in the responses of different organisms (Mehinto et al., 2022).

The spatial distribution of microplastic is highly variable and the concentrations reported depend strongly on the mesh and pore size of sampling gears and analysis filters used. Apart from the hotspots, even in a certain area (such as the Fram Strait, Chapter 3) local environmental conditions might lead to different patterns of distribution, not to mention the large differences in concentrations between different marine compartments. For example, beaches and the seafloor are characterised by the highest concentrations of microplastics (Tekman et al., 2022). Moreover, globally, only a few laboratories have the technology to detect particles between 10 and 100 µm, which in fact account for the majority of the microplastics in the water column, sea ice, snow and sediments of the Arctic [Chapter 3 and (Bergmann et al., 2017b; Peeken et al., 2018; Bergmann et al., 2019)], in snow from urban centres of Europe and the Alps (Bergmann et al., 2019), in surface waters and sediments of the North Sea (Lorenz et al., 2019), an urban fjord in Norway (Haave et al., 2019), in sediments of the Rhine River (Mani et al., 2019) and in hadal sediments (Abel et al., 2021). A recent study on microplastic ingestion by zooplankton organisms from the Fram Strait also revealed that the smallest size class accounts for most of the ingested particles (Botterell et al., 2022). Therefore, laboratory studies on the effects of microplastic exposure on organisms should consider

different particle sizes and concentrations. Nevertheless, ingestion of microplastic by organisms can lead to injury of the digestive track and changes in physiology, feeding, growth, reproduction, and oxygen consumption rates (Prinz and Korez, 2020).

Additives such as Bisphenol A (BPA), phthalates, flame retardants, pigments and metals are added to achieve certain material properties and can leach from plastic debris to the surrounding waters and when ingested, to the tissues of the organisms where they can elicit toxic effects. It was estimated that 190 million metric tons of chemical additives entered the oceans in 2015 (De Frond et al., 2019). These substances can be carcinogenic, alter hormonal functions, movement, feeding behaviour of organisms and cause inflammatory and autoimmune diseases. Hazardous substances can also adsorb to plastic from the surrounding waters and sediments, yielding concentrations higher than those in the environment that they came from (Ogata et al., 2009). Sorption and desorption of these pollutants make plastic both a source and sink of toxicity (Koelmans, 2015).

1.2 The Arctic Ocean

The Arctic is under spotlight because its physical and ecological processes are transforming fast as a reaction to climate forcing (Thomas et al., 2022). Until recently, public perception was that plastic pollution is not an issue in polar regions, as these areas are not densely populated. This view highlights how the complexity of the problem can be underrated. A decade of research has established that polar regions are not immune to plastic pollution and this highlights that direct land-based inputs are only one part of the problem. The presence of macro-plastic in the Arctic highlighted the high contribution of sea-based inputs (Bergmann et al., 2017a; Węsławski and Kotwicki, 2018), long-distance transport (Cózar et al., 2017) and accumulation on the seafloor (Parga Martínez et al., 2020). The Arctic Ocean is connected to the global circulation of water masses via the Bering Strait, Canadian Arctic Archipelago, Davis Strait, Fram Strait, and the entrance to the Barents Sea (Beszczynska-Möller et al., 2011). As for the European Arctic, Atlantic waters enter through the Fram Strait as West Spitzbergen Current and this warm inflow facilitates melting of sea ice and subsequent release of particles entrained. The East Greenland Current carries polar freshwater and sea ice through the Fram Strait out of the Arctic Ocean towards the North Atlantic (Wekerle et al., 2018). The eastern branch of the North Atlantic current feeds the Barents Sea and coincides with the polar waters originating from the Siberian Seas (Beszczynska-Möller et al., 2011).

Even though, the Arctic Ocean accounts for about +1% of the global ocean volume, it receives 11% of the global river discharge (Aagaard and Carmack, 1989). The Mackenzie, Yukon, Kolyma, Lena, Yenisei, Ob, Pechora, and Severnaya Dvina rivers together account for 60% of the river inflow into the Arctic Ocean with an increasing trend of Siberian river discharges (Holmes et al., 2021). Harms et al. (2000) modelled the Siberian river runoff with a focus on contaminants suggesting that river tracers from Ob and Yenisei rivers spread to the central Kara Sea in spring, whereas in autumn, they are directed eastward towards the Laptev Sea. In spring, a discharge rate of more than 100,000 m^3 s^{-1}, the wind and the extensive turbulence caused by the break-up of river ice flushed the tracers to the Kara Sea, which then left and joined the Siberian branch of the Transpolar Drift within one year (Harms et al., 2000). Particulate matter is not only transported by surface waters but also spreads to waters deeper than 150 m for more than 250 km off the coast of the Kara Sea, circulating there for several years (Harms et al., 2000). However, how plastic debris trajectories align with these currents is currently unknown mostly, because sampling campaigns can only be performed during short time spans. Golubeva et al. (2019) simulated different scenarios based on the Arctic Ocean Oscillation index, which represents the intensity and sense (clockwise / anticyclonic or counter clockwise / cyclonic) of the upper Arctic Ocean circulation based on a wind-driven sea surface height field. A simulation of a cyclonic circulation as observed between 1989 and 1996 directed the tracers into the central Arctic with a part of them reaching the north Canadian Basin, whereas an anticyclonic circulation moved the tracers into the Eurasian basin and Fram Strait.

Such a complex circulation pattern complicates the efforts to understand sources and pathways of plastic pollution. Moreover, climate induced changes are expected to cause disruptions in Arctic circulations. The warming of the Arctic region was suggested to interrupt the Transpolar Drift with less sea ice reaching to the Fram Strait due to less ice forming in shallow areas, whereas more ice-rafted material is released in the northern Laptev Sea and central Arctic Ocean (Krumpen et al., 2019). Proxy calculations found a weakening of the Atlantic Meridional Overturning Circulation over recent decades (Caesar et al., 2021).

1.3 FRAM Pollution Observatory

In 1999, the Alfred Wegener Institute Helmholtz Centre for Polar and Marine Research (AWI) established the HAUSGARTEN long-term ecological observatory in the eastern Fram Strait in order to assess temporal variability in faunal, bacterial, biogeochemical and geological properties as well as on hydrography and sedimentation patterns that could be affected by global change. Currently, it comprises 21 stations along a bathymetric gradient and a latitudinal

gradient (Soltwedel et al., 2016). During every expedition to HAUSGARTEN, the deep seafloor was photographed to assess changes in the epibenthic megafauna (Bergmann et al., 2011). In 2012, Bergmann and Klages published the first report on marine debris pollution detected in these seafloor images. In 2016, sightings of floating marine debris in the Fram Strait and Barents Sea were reported based on opportunistically conducted ship-based and aerial visual surveys (Bergmann et al., 2016). The presence of marine debris in these remote Arctic marine environments led to the establishment of the FRAM Pollution Observatory with the aim to investigate the distribution of marine debris including microplastic in all ecosystem compartments. Since 2015, marine debris data have been collected by citizen scientists on beaches of Svalbard. Visual ship-based surveys and photographical surveys of the seafloor were conducted to analyse the spatiotemporal distribution of marine debris in the Arctic Ocean. Since increasing numbers of small debris items were observed on the deep seafloor, microplastic analyses in the water column, sediments, sea ice and snow became part of the investigations, too.

1.4 The Aim and Structure of the Dissertation

This dissertation is divided into four main chapters, containing introductory and background information (Chapter 1), the scientific manuscripts (Chapter 2 and 3), and a summary of the results obtained from the FRAM Pollution Observatory (Chapter 4). Chapters 2 and 3 contain three manuscripts that were published in peer-reviewed scientific journals. Chapter 2 focuses on temporal and spatial distribution of marine macro-debris in surface waters (Chapter 2.1) and on the deep seafloor (Chapter 2.2). Chapter 3 focuses on microplastic pollution and reports the spatial distribution of microplastic particles throughout the whole water column, from the sea surface to deep-sea sediments. However, the research of the FRAM Pollution observatory is not limited to these studies. The presence of plastic debris at the beaches of Svalbard (Bergmann et al., 2017a; Meyer, 2022), in snow samples (Bergmann et al., 2019), sea ice (Peeken et al., 2018), and biota (Kühn et al., 2018; Botterell et al., 2022) have also been reported. Microplastic pollution in Arctic sediments was not only assessed in Chapter 3 but also in Bergmann et al. (2017b). In the general discussion (Chapter 4), I aim to synthesise all results of the FRAM Pollution Observatory and will outline the distribution, transportation pathways, accumulation of marine debris including microplastic in different Arctic ecosystem compartments (sea surface, Svalbard beaches, sea ice, snow, water column and seafloor) and its impacts on biota in a holistic approach. Moreover, I will present the results

of a new comparison of polymer compositions in different ecosystem compartments (water column, sediment and snow).

1.5 References

Aagaard, K., and Carmack, E.C. (1989). The role of sea ice and other fresh water in the Arctic circulation. *Journal of Geophysical Research: Oceans* 94(C10)**,** 14485-14498. doi: 10.1029/JC094iC10p14485.

Abel, S.M., Primpke, S., Int-Veen, I., Brandt, A., and Gerdts, G. (2021). Systematic identification of microplastics in abyssal and hadal sediments of the Kuril Kamchatka trench. *Environ. Pollut.* 269**,** 116095. doi: 10.1016/j.envpol.2020.116095.

Aguilera, M., Medina-Suárez, M., Pinós, J., Liria-Loza, A., and Benejam, L. (2018). Marine debris as a barrier: Assessing the impacts on sea turtle hatchlings on their way to the ocean. *Mar. Pollut. Bull.* 137**,** 481-487. doi: 10.1016/j.marpolbul.2018.10.054.

Andrady, A.L., and Neal, M.A. (2009). Applications and societal benefits of plastics. *Philos Trans R Soc Lond B Biol Sci* 364(1526)**,** 1977-1984. doi: 10.1098/rstb.2008.0304.

Bergmann, M., Lutz, B., Tekman, M.B., and Gutow, L. (2017a). Citizen scientists reveal: Marine litter pollutes Arctic beaches and affects wild life. *Mar. Pollut. Bull.* 125(1-2)**,** 535-540. doi: 10.1016/j.marpolbul.2017.09.055.

Bergmann, M., Mutzel, S., Primpke, S., Tekman, M.B., Trachsel, J., and Gerdts, G. (2019). White and wonderful? Microplastics prevail in snow from the Alps to the Arctic. *Sci. Adv.* 5(8)**,** eaax1157. doi: 10.1126/sciadv.aax1157.

Bergmann, M., Sandhop, N., Schewe, I., and D'Hert, D. (2016). Observations of floating anthropogenic litter in the Barents Sea and Fram Strait, Arctic. *Polar Biol.* 39**,** 553-560. doi: 10.1007/s00300-015-1795-8.

Bergmann, M., Soltwedel, T., and Klages, M. (2011). The interannual variability of megafaunal assemblages in the Arctic deep sea: Preliminary results from the HAUSGARTEN observatory (79°N). *Deep Sea Res. Part I Oceanogr. Res. Pap.* 58(6)**,** 711-723. doi: 10.1016/j.dsr.2011.03.007.

Bergmann, M., Wirzberger, V., Krumpen, T., Lorenz, C., Primpke, S., Tekman, M.B., et al. (2017b). High Quantities of Microplastic in Arctic Deep-Sea Sediments from the HAUSGARTEN Observatory. *Environ. Sci. Technol.* 51(19)**,** 11000-11010. doi: 10.1021/acs.est.7b03331.

Beszczynska-Möller, A., Woodgate, R.A., Lee, C., Melling, H., and Karcher, M. (2011). A synthesis of exchanges through the main oceanic gateways to the Arctic Ocean. *Oceanography* 24(3)**,** 82-99. doi: 10.5670/oceanog.2011.59.

Borrelle, S.B., Ringma, J., Law, K.L., Monnahan, C.C., Lebreton, L., McGivern, A., et al. (2020). Predicted growth in plastic waste exceeds efforts to mitigate plastic pollution. *Science* 369(6510)**,** 1515-1518. doi: 10.1126/science.aba3656.

Botterell, Z.L.R., Bergmann, M., Hildebrandt, N., Krumpen, T., Steinke, M., Thompson, R.C., et al. (2022). Microplastic ingestion in zooplankton from the Fram Strait in the Arctic. *Sci. Total Environ.* 831**,** 154886. doi: 10.1016/j.scitotenv.2022.154886.

Bucci, K., Tulio, M., and Rochman, C.M. (2020). What is known and unknown about the effects of plastic pollution: A meta-analysis and systematic review. *Ecol. Appl.* 30(2)**,** e02044. doi: 10.1002/eap.2044.

Caesar, L., McCarthy, G.D., Thornalley, D.J.R., Cahill, N., and Rahmstorf, S. (2021). Current Atlantic Meridional Overturning Circulation weakest in last millennium. *Nat. Geosci.* 14(3)**,** 118-120. doi: 10.1038/s41561-021-00699-z.

Carpenter, E.J., Anderson, S.J., Harvey, G.R., Miklas, H.P., and Peck, B.B. (1972). Polystyrene spherules in coastal waters. *Science* 178(4062)**,** 749-750.

Carpenter, E.J., and Smith, K.L., Jr. (1972). Plastics on the Sargasso sea surface. *Science* 175(4027)**,** 1240-1241. doi: 10.1126/science.175.4027.1240.

Choy, C.A., and Drazen, J.C. (2013). Plastic for dinner? Observations of frequent debris ingestion by pelagic predatory fishes from the central North Pacific. *Mar. Ecol. Prog. Ser.* 485(Marine Ecology Progress Series 2013 485 155-163)**,** 155-163. doi: 10.3354/meps10342.

Colmenero, A.I., Barria, C., Broglio, E., and Garcia-Barcelona, S. (2017). Plastic debris straps on threatened blue shark *Prionace glauca*. *Mar. Pollut. Bull.* 115(1-2)**,** 436-438. doi: 10.1016/j.marpolbul.2017.01.011.

Cózar, A., Marti, E., Duarte, C.M., Garcia-de-Lomas, J., van Sebille, E., Ballatore, T.J., et al. (2017). The Arctic Ocean as a dead end for floating plastics in the North Atlantic branch of the Thermohaline Circulation. *Sci. Adv.* 3(4)**,** e1600582. doi: 10.1126/sciadv.1600582.

Dayton, P.K., and Robilliard, G.A. (1971). Implications of pollution to the McMurdo Sound benthos. *Antarctic Journal***,** 53-56.

De Frond, H.L., van Sebille, E., Parnis, J.M., Diamond, M.L., Mallos, N., Kingsbury, T., et al. (2019). Estimating the Mass of Chemicals Associated with Ocean Plastic Pollution to Inform Mitigation Efforts. *Integr. Environ. Assess. Manag.* 15(4)**,** 596-606. doi: 10.1002/ieam.4147.

Engler, R.E. (2012). The complex interaction between marine debris and toxic chemicals in the ocean. *Environ. Sci. Technol.* 46(22)**,** 12302-12315. doi: 10.1021/es3027105.

Fazey, F.M., and Ryan, P.G. (2016). Biofouling on buoyant marine plastics: An experimental study into the effect of size on surface longevity. *Environ. Pollut.* 210**,** 354-360. doi: 10.1016/j.envpol.2016.01.026.

Feder, H.M., Jewett, S.C., and Hilsinger, J.R. (1978). Man-made debris on the Bering Sea floor. *Mar. Pollut. Bull.* 9(2)**,** 52-53. doi: 10.1016/0025-326X(78)90534-9.

Feldman, D. (2008). Polymer History. *Des. Monomers Polym.* 11(1)**,** 1-15. doi: 10.1163/156855508X292383.

GESAMP (2016). "Sources, fate and effects of microplastics in the marine environment: part 2 of a global assessment", (ed.) P.J. Kershaw, and Rochman, C.M.: IMO/FAO/UNESCO-IOC/UNIDO/WMO/IAEA/UN/UNEP/UNDP Joint Group of Experts on the Scientific Aspects of Marine Environmental Protection).

Geyer, R. (2020). "A Brief History of Plastics," in *Mare Plasticum - The Plastic Sea: Combatting Plastic Pollution Through Science and Art,* eds. M. Streit-Bianchi, M. Cimadevila & W. Trettnak. (Cham: Springer International Publishing), 31-47.

Geyer, R., Jambeck, J.R., and Law, K.L. (2017). Production, use, and fate of all plastics ever made. *Sci. Adv.* 3(7)**,** e1700782. doi: 10.1126/sciadv.1700782.

Golubeva, E., Platov, G., Iakshina, D., and Kraineva, M. (2019). A simulated distribution of Siberian river runoff in the Arctic Ocean. *IOP Conf. Ser.: Earth Environ. Sci.* 386(1)**,** 012022. doi: 10.1088/1755-1315/386/1/012022.

Green, D.S., Boots, B., Blockley, D.J., Rocha, C., and Thompson, R. (2015). Impacts of discarded plastic bags on marine assemblages and ecosystem functioning. *Environ. Sci. Technol.* 49(9)**,** 5380-5389. doi: 10.1021/acs.est.5b00277.

Gudger, E.W. (1928). A mackerel (Scomber scombrus) with a rubber band rove through its body. American Museum novitates; no. 310.

Haave, M., Lorenz, C., Primpke, S., and Gerdts, G. (2019). Different stories told by small and large microplastics in sediment - first report of microplastic concentrations in an urban recipient in Norway. *Mar. Pollut. Bull.* 141**,** 501-513. doi: 10.1016/j.marpolbul.2019.02.015.

Harms, I.H., Karcher, M.J., and Dethleff, D. (2000). Modelling Siberian river runoff — implications for contaminant transport in the Arctic Ocean. *J. Mar. Syst.* 27(1)**,** 95-115. doi: 10.1016/S0924-7963(00)00062-2.

Holmes, R.M., Shiklomanov, A.I., Suslova, A., Tretiakov, M., McClelland, J.W., Scott, L., et al. (2021). "River Discharge". National Oceanic Atmospheric Administration.).

Holmström, A. (1975). Plastic films on the bottom of the Skagerack. *Nature* 255(5510)**,** 622-623. doi: 10.1038/255622a0.

Jewett, S.C. (1976). Pollutants of the northeast gulf of Alaska. *Mar. Pollut. Bullet.* 7(9)**,** 169. doi: 10.1016/0025-326X(76)90213-7.

Kaandorp, M.L.A., Dijkstra, H.A., and van Sebille, E. (2021). Modelling size distributions of marine plastics under the influence of continuous cascading fragmentation. *Environ. Res. Lett.* 16(5)**,** 054075. doi: 10.1088/1748-9326/abe9ea.

Kenyon, K.W., and Kridler, E. (1969). Laysan albatrosses swallow indigestible matter. *The Auk* 86(2)**,** 339-343.

Kiessling, T., Gutow, L., and Thiel, M. (2015). "Marine litter as habitat and dispersal vector," in *Marine anthropogenic litter,* eds. M. Bergmann, L. Gutow & M. Klages. Springer, Cham), 141-181.

Koelmans, A.A. (2015). "Modeling the role of microplastics in bioaccumulation of organic chemicals to marine aquatic organisms. A critical review," in *Marine anthropogenic litter,* eds. M. Bergmann, L. Gutow & M. Klages. Springer Open), 309-324.

Kooi, M., Nes, E.H.v., Scheffer, M., and Koelmans, A.A. (2017). Ups and Downs in the Ocean: Effects of Biofouling on Vertical Transport of Microplastics. *Environ. Sci. Technol.* 51(14)**,** 7963-7971. doi: 10.1021/acs.est.6b04702.

Krumpen, T., Belter, H.J., Boetius, A., Damm, E., Haas, C., Hendricks, S., et al. (2019). Arctic warming interrupts the Transpolar Drift and affects long-range transport of sea ice and ice-rafted matter. *Sci. Rep.* 9(1)**,** 5459. doi: 10.1038/s41598-019-41456-y.

Kühn, S., Bravo Rebolledo, E.L., and van Franeker, J.A. (2015). "Deleterious effects of litter on marine life," in *Marine anthropogenic litter,* eds. M. Bergmann, L. Gutow & M. Klages. Springer Open), 75-116.

Kühn, S., Schaafsma, F.L., van Werven, B., Flores, H., Bergmann, M., Egelkraut-Holtus, M., et al. (2018). Plastic ingestion by juvenile polar cod (Boreogadus saida) in the Arctic Ocean. *Polar Biol.* 41(6)**,** 1269-1278. doi: 10.1007/s00300-018-2283-8.

Lorenz, C., Roscher, L., Meyer, M.S., Hildebrandt, L., Prume, J., Löder, M.G.J., et al. (2019). Spatial distribution of microplastics in sediments and surface waters of the southern North Sea. *Environ. Pollut.* 252(Pt B)**,** 1719-1729. doi: 10.1016/j.envpol.2019.06.093.

MacLeod, M., Arp, H.P.H., Tekman, M.B., and Jahnke, A. (2021). The global threat from plastic pollution. *Science* 373(6550)**,** 61-65. doi: 10.1126/science.abg5433.

Mani, T., Primpke, S., Lorenz, C., Gerdts, G., and Burkhardt-Holm, P. (2019). Microplastic Pollution in Benthic Midstream Sediments of the Rhine River. *Environ Sci Technol* 53(10)**,** 6053-6062. doi: 10.1021/acs.est.9b01363.

Mehinto, A.C., Coffin, S., Koelmans, A.A., Brander, S.M., Wagner, M., Thornton Hampton, L.M., et al. (2022). Risk-based management framework for microplastics in aquatic ecosystems. *Microplastics and Nanoplastics* 2(1)**,** 17. doi: 10.1186/s43591-022-00033-3.

Meyer, A.N. (2022). *Deep Dives into Arctic Beach Debris. Analysing its Composition and Origin.* Bachelor, Christian-Albrecht University of Kiel.

Mouchi, V., Chapron, L., Peru, E., Pruski, A.M., Meistertzheim, A.L., Vetion, G., et al. (2019). Long-term aquaria study suggests species-specific responses of two cold-water corals to macro-and microplastics exposure. *Environ. Pollut.* 253**,** 322-329. doi: 10.1016/j.envpol.2019.07.024.

Ogata, Y., Takada, H., Mizukawa, K., Hirai, H., Iwasa, S., Endo, S., et al. (2009). International Pellet Watch: global monitoring of persistent organic pollutants (POPs) in coastal waters. 1. Initial phase data on PCBs, DDTs, and HCHs. *Mar. Pollut. Bull.* 58(10)**,** 1437-1446. doi: 10.1016/j.marpolbul.2009.06.014.

Parga Martínez, K.B., Tekman, M.B., and Bergmann, M. (2020). Temporal trends in marine litter at three stations of the HAUSGARTEN observatory in the Arctic deep sea. *Front. Mar. Sci.* 7**,** 321.

Peeken, I., Primpke, S., Beyer, B., Gutermann, J., Katlein, C., Krumpen, T., et al. (2018). Arctic sea ice is an important temporal sink and means of transport for microplastic. *Nat. Commun.* 9(1)**,** 1505. doi: 10.1038/s41467-018-03825-5.

Persson, L., Carney Almroth, B.M., Collins, C.D., Cornell, S., de Wit, C.A., Diamond, M.L., et al. (2022). Outside the Safe Operating Space of the Planetary Boundary for Novel Entities. *Environ. Sci. Technol.* 56(3)**,** 1510-1521. doi: 10.1021/acs.est.1c04158.

PlasticsEurope (2021). "Plastics - the Facts 2021". (Brussels).

Prata, J.C., Silva, A.L.P., Walker, T.R., Duarte, A.C., and Rocha-Santos, T. (2020). COVID-19 Pandemic Repercussions on the Use and Management of Plastics. *Environ. Sci. Technol.* 54(13)**,** 7760-7765. doi: 10.1021/acs.est.0c02178.

Prinz, N., and Korez, Š. (2020). "Understanding how microplastics affect marine biota on the cellular level is important for assessing ecosystem function: A review," in *YOUMARES 9 - The oceans: Our research, our future,* eds. S. Jungblut, V. Liebich & M. Bode-Dalby. Springer Open), 101-120.

Ryan, P.G., Dilley, B.J., Ronconi, R.A., and Connan, M. (2019). Rapid increase in Asian bottles in the South Atlantic Ocean indicates major debris inputs from ships. *Proc. Natl. Acad. Sci. U.S.A.* 116(42)**,** 20892-20897. doi: 10.1073/pnas.1909816116.

Ryan, P.G., Pichegru, L., Perolod, V., and Moloney, C.L. (2020). Monitoring marine plastics - will we know if we are making a difference? *S. Afr. J. Sci.* 116**,** 1-9. doi: 10.17159/sajs.2020/7678.

Soltwedel, T., Bauerfeind, E., Bergmann, M., Bracher, A., Budaeva, N., Busch, K., et al. (2016). Natural variability or anthropogenically-induced variation? Insights from 15 years of multidisciplinary observations at the arctic marine LTER site HAUSGARTEN. *Ecol. Indic.* 65**,** 89-102. doi: 10.1016/j.ecolind.2015.10.001.

Tekman, M. B., Walther, B. A., Peter, C., Gutow, L. and Bergmann, M. (2022): Impacts of plastic pollution in the oceans on marine species, biodiversity and ecosystems, 1–221, WWF Germany, Berlin. Doi: 10.5281/zenodo.5898684

Thomas, D.N., Arévalo-Martínez, D.L., Crocket, K.C., Große, F., Grosse, J., Schulz, K., et al. (2022). A changing Arctic Ocean. *Ambio* 51(2)**,** 293-297. doi: 10.1007/s13280-021-01677-w.

van Sebille, E., Aliani, S., Law, K.L., Maximenko, N., Alsina, J.M., Bagaev, A., et al. (2020). The physical oceanography of the transport of floating marine debris. *Environ. Res. Lett.* 15(2)**,** 32. doi: 10.1088/1748-9326/ab6d7d.

Venrick, E.L., Backman, T.W., Bartram, W.C., Platt, C.J., Thornhill, M.S., and Yates, R.E. (1973). Man-made Objects on the Surface of the Central North Pacific Ocean. *Nature* 241(5387)**,** 271-271. doi: 10.1038/241271a0.

Ward, C.P., and Reddy, C.M. (2020). We need better data about the environmental persistence of plastic goods. *Proc. Natl. Acad. Sci. U.S.A.* 117(26)**,** 14618-14621. doi: 10.1073/pnas.2008009117.

Wekerle, C., Krumpen, T., Dinter, T., von Appen, W.J., Iversen, M.H., and Salter, I. (2018). Properties of Sediment Trap Catchment Areas in Fram Strait: Results From Lagrangian Modeling and Remote Sensing. *Front. Mar. Sci.* 5**,** 407. doi: 10.3389/fmars.2018.00407.

Węsławski, J., and Kotwicki, L. (2018). Macro-plastic litter, a new vector for boreal species dispersal on Svalbard. *Pol. Polar Res.* 39**,** 165-174. doi: 10.24425/118743.

Wieczorek, A.M., Croot, P.L., Lombard, F., Sheahan, J.N., and Doyle, T.K. (2019). Microplastic ingestion by gelatinous zooplankton may lower efficiency of the biological pump. *Environ. Sci. Technol.* 53(9)**,** 5387-5395. doi: 10.1021/acs.est.8b07174.

Ye, S., and Andrady, A.L. (1991). Fouling of floating plastic debris under Biscayne Bay exposure conditions. *Mar. Pollut. Bull.* 22(12)**,** 608-613.

1.6 Declaration of Author's Contribution

This cumulative PhD thesis compromises a collection of three joint-authorship manuscripts, which were published in recognized scientific journals. The author contribution and the contributions of the co-authors to the manuscripts are as follows:

Chapter 2.1. Marine debris floating in Arctic and temperate Northeast Atlantic waters

Authors: Mine Banu Tekman, Lars Gutow, Melanie Bergmann.

Published in Frontiers in Marine Science (2022), doi: 10.3389/fmars.2022.933768

All authors conceived of the presented idea, contributed to the design and implementation of the research. M.B.T. processed the data, performed the analysis, drafted the manuscript. All authors discussed the results, commented on the manuscript, read and approved the submitted version.

Chapter 2.2. Marine litter on deep Arctic seafloor continues to increase and spreads to the North at the HAUSGARTEN observatory

Authors: Mine Banu Tekman, Thomas Krumpen, Melanie Bergmann.

Published in Deep Sea Research Part I: Oceanographic Research Papers (2017), doi: 10.1016/j.dsr.2016.12.011

M.B. conceived of the presented idea, M.B.T. and M.B. contributed to the design and implementation of the research. M.B.T. processed the data, performed the analysis, drafted the manuscript. T.K. implemented sea ice trajectories. All authors discussed the results, commented on the manuscript, read and approved the submitted version.

Chapter 3. Tying up Loose Ends of Microplastic Pollution in the Arctic: Distribution from the Sea Surface through the Water Column to Deep-Sea Sediments at the HAUSGARTEN Observatory

Authors: Mine Banu Tekman, Claudia Wekerle, Claudia Lorenz, Sebastian Primpke, Christiane Hasemann, Gunnar Gerdts, Melanie Bergmann

Published in Environmental Science & Technology (2020), doi: 10.1021/acs.est.9b06981

M.B.T and M.B. conceived of the presented idea, contributed to the design and implementation of the research. M.B.T. processed the data, performed the microplastic analyses with support from G.G., C.L. and S.P. and statistical analyses with support from C.H.

C.W. implemented drift trajectories. M.B.T. drafted the manuscript. All authors discussed the results, commented on the manuscript, read and approved the submitted version.

2 The spatiotemporal distribution of macro-debris pollution in the Arctic

2.1 Marine debris floating in Arctic and temperate Northeast Atlantic waters

Mine B. Tekman*, Lars Gutow*, Melanie Bergmann*

* Alfred-Wegener-Institut, Helmholtz-Zentrum für Polar- und Meeresforschung, Am Handelshafen 12, 27570 Bremerhaven, Germany

Frontiers in Marine Science, July 2022, doi: 10.3389/fmars.2022.933768

Abstract

Floating marine debris is ubiquitous in marine environments but knowledge about quantities in remote regions is still limited. Here, we present the results of an extensive survey of floating marine debris by experts, trained scientists from fields other than pollution or non-professional citizen scientists. A total of 276 visual ship-based surveys were conducted between 2015 and 2020 in the Northeast (NE) Atlantic from waters off the Iberian Peninsula to the Central Arctic, however, with a focus on Arctic waters. Spatiotemporal variations among regional seas (Central Arctic, Barents Sea, Greenland Sea, Norwegian Sea, North Sea) and oceanic regions (Arctic waters and the temperate NE Atlantic) were explored. The overall median debris concentration was 11 items km^{-2}, with considerable variability. The median concentration was highest in the North Sea with 19 items km^{-2}. The Nordic seas, except the Central Arctic showed median concentrations ranging from 9 to 13 items km^{-2}. Plastic accounted for 91% of all floating items. Miscellaneous fragments, films, ropes and nets, packaging materials, expanded polystyrene and straps were the most frequently observed plastic types. Although the median debris concentration in the Central Arctic was zero, this region was not entirely free of floating debris. The variations between regional seas and oceanic regions were statistically not significant indicating a continuous supply by a northward transportation of floating debris. The data show a slight annual decrease and clear seasonal differences in debris concentrations with higher levels observed during summer. A correlation between debris concentrations and environmental and spatial variables was found, explaining partly the variability in the observations. Pollution levels were 500 times lower than those recorded on the seafloor indicating the seafloor as a sink for marine debris. The Arctic was characterised by similar pollution levels as regions in temperate latitudes highlighting that Arctic ecosystems face threats from plastic pollution, which add to the effects of rapid climate change.

2.1.1 Introduction

Marine debris refers to "any solid, manufactured or processed material disposed of or abandoned in marine environments" (UNEP, 2005). By definition, this comprises materials such as glass, metal or processed wood. However, plastics account for the great majority of marine debris in most regions of the oceans (Bergmann et al., 2017b). Global plastic emissions from land into aquatic environments were estimated at 19 – 23 million metric tons (MMT) in 2016, which constitute 11% of the annual global plastic production and are projected to reach up to 90 MMT by 2030 under current growth trajectories (Borrelle et al., 2020). Its accumulation in the environment is poorly reversible, especially in the aquatic realm, where it affects biogeochemical processes, habitats and species and has societal impacts (MacLeod et al., 2021). Since plastic production has outpaced the global capacity for monitoring and governance, plastic pollution, along with other man-made contaminants, is assumed to exceed safe planetary boundaries (Persson et al., 2022).

More than 2,000 marine species have been reported to encounter plastics in their natural habitats (Tekman et al., 2022). The severity and type of impact is mostly evaluated in relation to the size of the plastic debris. For example, there is still debate about the effects of microplastic (< 5mm) on marine organisms because of unrealistically high particle concentrations applied in many laboratory experiments (Koelmans et al., 2022). On the contrary, the effects of interactions with macroplastics are well-established. Entanglement with and ingestion of macroplastics can cause suffocation, restrained mobility, obstruction, false sense of satiety and, ultimately, also the death of marine organisms (Kühn and van Franeker, 2020; Tekman et al., 2022). Because of continuous campaigns by NGOs driven by the intensive scientific research efforts in recent years, plastic pollution has become widely acknowledged as a global threat. Accordingly, the fifth United Nations Environment Assembly adopted a resolution to negotiate a legally binding global treaty by 2024 to combat plastic pollution (Bundela et al., 2022).

An estimated amount of more than 5 trillion plastic pieces are floating at the surface of the oceans (Eriksen et al., 2014). Floating marine debris is known to accumulate in subtropical gyres (Lebreton et al., 2018), enclosed basins (Everaert et al., 2020), or coastal margins (Olivelli et al., 2020). However, relatively little is known about concentrations of floating marine debris over vast stretches of the open ocean, especially in remote geographic regions such as the polar oceans (Bergmann et al., 2022). Recent surveys revealed substantial amounts of marine debris on Arctic beaches (Bergmann et al., 2017a; Falk-Andersson et al., 2019; Haarr

et al., 2020) and on the deep Arctic seafloor (Parga Martínez et al., 2020). Meanwhile, it has been well established that polar regions have become significantly polluted by plastics and that direct land-based input is only one part of the problem (Bergmann et al., 2017a; Suaria et al., 2020). The Arctic Ocean is connected to the global oceanic circulation system via the Bering Strait, the Canadian Arctic Archipelago, Davis Strait, Fram Strait, and the entrance to the Barents Sea (Beszczynska-Möller et al., 2011). This complex circulation pattern complicates the identification of sources and pathways of Arctic plastic pollution. Nevertheless, a decade of intense research highlighted the high contribution of sea-based input (Bergmann et al., 2017a; Węsławski and Kotwicki, 2018), long-distance transport (Cózar et al., 2017), and deposition and accumulation on the seafloor (Parga Martínez et al., 2020).

A wide variety of sampling and analysis methods are used to investigate the distribution of floating debris. Neuston nets have been widely used, yet this method allows to sample only a limited surface area for macroplastic and requires dedicated ship time (Ryan et al., 2020). Floating marine debris has also been reported from aerial surveys or satellite imagery (Pichel et al., 2007; Bergmann et al., 2016; Lebreton et al., 2018; Biermann et al., 2020; Unger et al., 2021). However, small items are easily missed by these methods. On visual ship-based surveys, trained observers (Chiu et al., 2020) can quantify and characterise floating debris even without specific scientific expertise. These surveys can be conducted opportunistically from virtually any kind of ship, including ferries (Campana et al., 2018) or pole-and-line tuna fishing boats (Chambault et al., 2018). However, survey locations are bound to the ship's route and dependent on the availability of observers and conditions (Chambault et al., 2018; Gutow et al., 2018; Connan et al., 2021), which can induce bias in surveyed regions. Moreover, different qualification and characterisation criteria can impede the comparability of debris concentrations among studies.

Standardised sampling campaigns by citizen scientists have been widely used to assess marine debris pollution (e.g. Hidalgo-Ruz and Thiel, 2015; Nelms et al., 2017; Falk-Andersson et al., 2019; Haarr et al., 2020; Gacutan et al., 2022). Even in the remote Arctic, the distribution of marine debris was reported based on the data and samples collected by trained non-professionals or local people (Bergmann et al., 2017a; Bergmann et al., 2019; Bourdages et al., 2020; Ershova et al., 2021). Unlike public campaigns for beach debris, visual surveys of floating debris by citizen scientists (Chiu et al., 2020) are not common. Currently, the OSPAR marine debris monitoring program for the Northeast (NE) Atlantic involves beach surveys as well as quantification of ingested plastics by northern fulmars (*Fulmarus glacialis*) in the North

Sea only. Extending the program by standardized quantifications of floating marine debris by ship-based visual surveys could fill some blind spots, and promote environmental awareness, especially if citizen scientists were involved in data collection. Accordingly, a recent experimental evaluation of visual surveys in the Mediterranean Sea suggested a standardisation, which considers the potentially confounding effects of ship type, speed, survey effort, size detection limits, observer experiences and weather conditions on the results (Arcangeli et al., 2020).

In the present study, we investigate the spatial and temporal distribution of floating marine debris in the NE Atlantic and Arctic Ocean by ship-based visual surveys partly conducted by citizen scientists during ten expeditions between 2015 and 2020. The effect of spatial, annual and seasonal variations on debris concentrations as well as on size and material compositions of floating anthropogenic items in Arctic waters, in the temperate NE Atlantic and in the regional seas (Central Arctic, Barents Sea, Norwegian Sea, Greenland Sea, North Sea) were explored. Specific environmental variables were tested for their potential to control the distribution of floating marine debris. Moreover, debris captured opportunistically in pelagic and bottom trawls around Svalbard and hand-picked floating plastics from the Fram Strait provided additional information regarding the origin and distribution of marine debris in Arctic waters. Finally, the floating debris data gathered in the Greenland Sea were compared with quantities reported from the seafloor in the same study region to identify potential sinks of plastic debris in this area and help answering the question 'Where is all the plastic?' (Thompson et al., 2004; van Sebille et al., 2015).

2.1.2 Material and Methods

Visual surveys

A vessel-based surface observer programme (visual surveys) was conducted in the Northeast (NE) Atlantic between 2015 and 2020 during ten expeditions of the German research vessels Heincke, Maria S. Merian and Polarstern, and the sailing vessel Antigua (Fig. 2.1.1). The amount of floating debris was assessed from the moving ship (average speed ± SD: 9.4 ± 2.2 kn) during times of daylight whenever the weather and sea conditions were suitable for the observers to perform a visual survey and the waves were deemed not too high to submerge debris items. In addition to marine debris experts, trained scientists from fields other than marine pollution and non-professional citizen scientists composed of cruise tourists and crew of SV Antigua were carefully instructed and conducted surveys to increase the spatial coverage. The surveys were conducted by one observer, unless a practical training was required for

others. A total of 276 visual surveys was conducted [Chapter 5. Supporting Information (SI), Table 5.1.1]. Overall, the duration of each survey was approximately 1 hour (average ± SD duration: 59 ± 16 minutes). Sometimes it had to be shortened when the ship stopped for station work, or due to deteriorating weather and sea conditions.

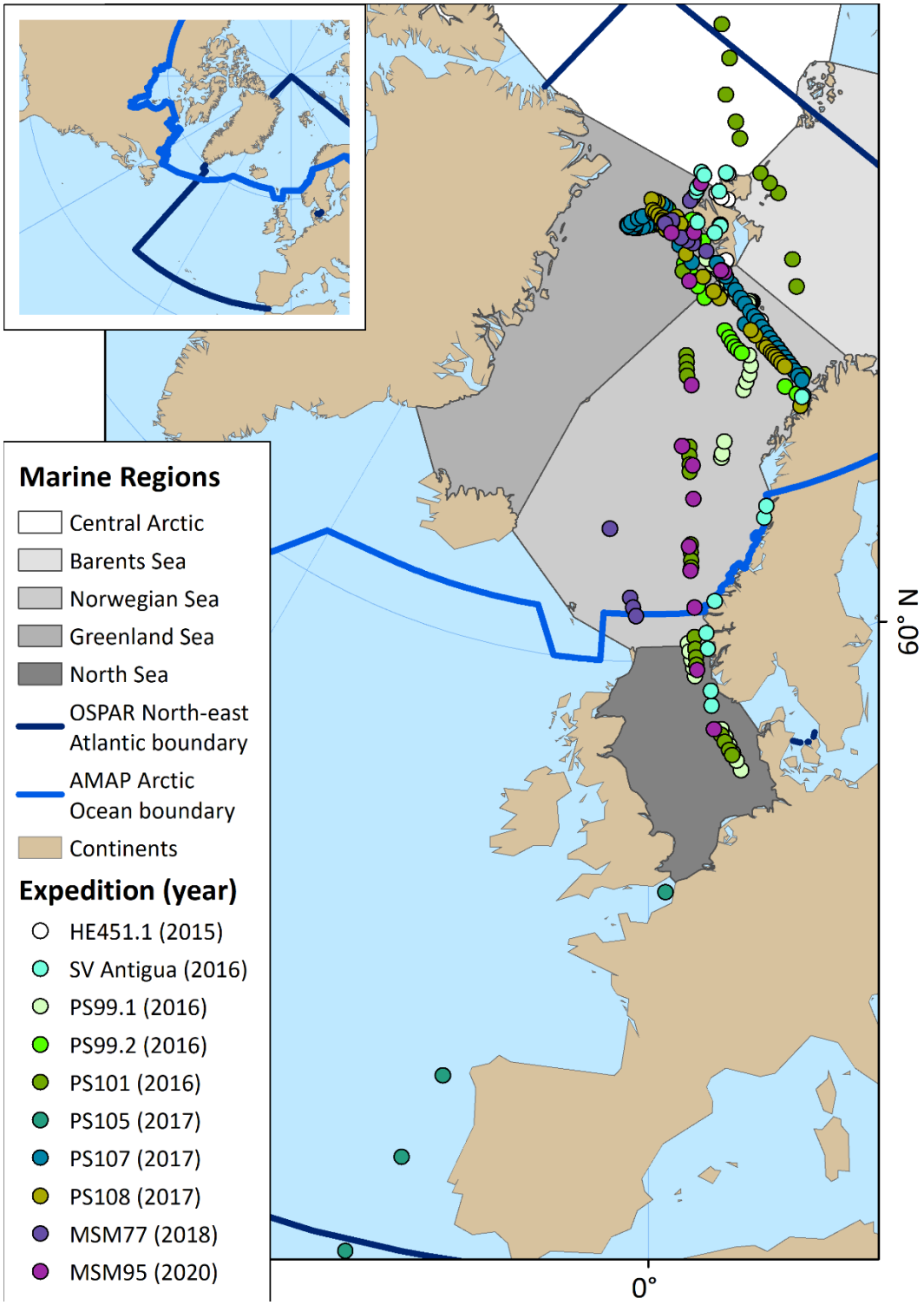

Figure 2.1.1 Location of visual surveys conducted in the study area between 2015 and 2020. Each circle corresponds to a visual survey. Marine regions are discerned by different

colours. The Arctic Ocean boundary of the Arctic Monitoring & Assessment Programme (AMAP) divides the Arctic waters from the temperate Northeast Atlantic. The close-up map shows the AMAP Arctic Ocean boundary and the OSPAR Northeast Atlantic boundary within the study region.

During surveys, a strip width of 10 m next to the ship starting behind the bow wave of the research vessel was inspected for floating items. Since SV Antigua is a relatively small vessel, the bow wave was negligible and the strip width was recorded for each transect depending on weather, wind conditions and visibility. The position of the observers above the sea level varied between 3 m (SV Antigua), 5.5 m (RV Heincke), 7.2 m (RV Maria S Merian) and 7.5 m (RV Polarstern). Each floating item was noted in protocol forms (SI, 5.1). Objects seen in the distance outside the observation corridor were recorded but omitted from the analysis. A handheld Global Positioning System (GPS) device was used to record the position of the observer and the time of each observation. Aggregations of debris were observed occasionally. For some of these aggregations the abundance of floating debris was estimated. For two aggregations, "several dozen" were recorded in the protocols and to be conservative, the number of anthropogenic items was considered as 12 for the analysis. For three aggregations, no quantitative information was given. They were thus treated as single items.

The survey tracks (transects) of research cruises were extracted from the ships' position acquisition system (D-SHIP) at one-minute intervals. The coordinates were imported into ArcMap 10.6.1, converted into line features and the geodesic length of each transect was computed using the "Add Geometry" function. For the SV Antigua cruise, all available waypoints and observations were utilised to estimate the lengths of the transects. The area covered by each survey was calculated by multiplying the length of the transect with the strip width, and debris concentrations were expressed as (number of) items per km2. On cruises of SV Antigua, HE451.1 and PS99.2, the observers managed occasionally to take images of floating items.

Categorization of the floating items

Whenever possible, floating debris items were characterised in terms of material, plastic type or usage, size and colour. In case of uncertainty, or if the detail of the object was not recorded, the information was categorised as "not available" (N/A). The material was categorised as plastic, rope and nets, glass, metal, timber, organic or paper (including cardboard). Ropes and nets were considered in a separate material category although FTIR

measurements of beached nets and ropes from Svalbard showed that all items were made of plastic (Meyer, 2022). Additionally, plastic items were recorded according to type or usage (e.g., fragment, film, box, bottle, packaging). Films, foils, sheets and bags were assigned to the same category. Identification of floating items from a moving ship is challenging, especially for non-experts, because the observers have only a few seconds to observe and record the items. Therefore, pre-defined categories of plastic items were not used and the observers were instructed to record as many details of the floating objects (material, type, usage, shape, size) as possible, which were then evaluated and grouped during the data analysis.

Items were categorised according to their estimated sizes as small (<10cm), medium (10≤ x ≤ 50cm) or large (>50 cm) to allow for a comparison of the size distribution of debris items from the sea surface (this study) and the deep seafloor (Bergmann and Klages, 2012; Tekman et al., 2017; Parga Martínez et al., 2020). The minimum size of floating debris recorded by the observers was 1 cm. Objects partly or completely submerged were marked in the protocols except for expedition PS99.1. Occasionally, the observers noted the fouling status of plastics, especially for strongly bio-fouled items. Along with anthropogenic items, natural flotsam was recorded during 173 surveys.

Environmental parameters

Together with the ship positions, environmental parameters were obtained from the D-SHIP data acquisition system at one-minute intervals. The average values of salinity, chlorophyll *a*, air and water temperature and wind speed were obtained for each transect in order to explore the relationships between the debris distribution and environmental variables. These parameters were not available for RV *Maria S. Merian* (MSM77 and MSM95 expeditions) and SV *Antigua* cruises. In total, the relationships with environmental variables were explored for 211 transects. Longitude, latitude, ship speed and distance to the nearest point at the European coastline (EEA, 2015) were also tested. The distances were calculated with the "Near" tool of ArcMap 10.6.1 by selecting the geodesic length.

Marine regions

To evaluate regional variations in debris concentrations, the transects were assigned to regional seas as suggested for the world marine regions (NE, 2019) using ArcMap 10.6.1 (Fig 2.1.1). The analyses were performed for the Central Arctic, Barents Sea, Greenland Sea, Norwegian Sea, North Sea and North Atlantic sector. The four transects in waters off the Iberian Peninsula and English Channel were grouped within the North Atlantic sector for

statistical analyses (Fig. 2.1.1). Additionally, the transects were grouped according to their position relative to the Arctic Ocean boundary of AMAP (AMAP, 2013) and median concentrations were calculated for Arctic waters (OSPAR Region I) and for the temperate NE Atlantic (OSPAR Region II – IV) (OSPAR, 2016). All maps were produced using ArcMap 10.6.1.

Statistical analysis

Univariate statistical analyses were performed using Sigmaplot 14.0. Normality tests revealed that concentrations of debris and natural objects were not normally distributed (Shapiro-Wilk: $P < 0.050$). Accordingly, these parameters were displayed as median values for the regional seas and for the oceanic regions (i.e., Arctic waters and the temperate NE Atlantic Ocean). Minimum and maximum values as well the first and third quartile were given as measures of variability. A Kruskal-Wallis One Way Analysis of Variance on Ranks was performed to explore overall differences in debris concentrations between regional seas, oceanic regions, years, seasons and different ships. A significant difference in the debris quantities recorded from different ships could indicate that its size and thus the distance between an observer and a floating item affects the results. In case of significant differences, Dunn's post-hoc test was used to perform pairwise comparisons. The correlations between the concentrations of debris and natural objects as well as between debris concentrations and environmental variables were tested by a Spearman's rank order correlation test. The proportions of the materials (combined with types/usages of plastic items), size groups and colours within the regional seas were calculated to check for possible patterns.

Multivariate statistical analyses were performed using PRIMER-e version 6.1.16 and PERMANOVA 1.0.6. Spatial and temporal differences in material, size and type compositions were investigated with permutational multivariate analysis of variance (PERMANOVA) using a two-way crossed design of fixed factors ('regional sea' × year and 'oceanic region' × year). PERMANOVA is robust against zero inflation and deviations from a normal distribution of the data (Anderson and Walsh, 2013). Bray-Curtis resemblance matrices were created from 4^{th}-root transformed debris concentrations per km^{-2}. Subsequently, a PERMANOVA routine with 999 permutations with sums of squares type of Type III was carried out to test for differences in the material and size compositions. For PERMANOVA analyses, plastic and ropes (including nets) were considered as separate categories. The PERMANOVA for comparison of the plastic type/usage compositions revealed inconsistent results when the N/A category was

either included or excluded. Therefore, the plastic type/usage composition was not analysed statistically. Differences were explored between the regional seas (Central Arctic, Barents Sea, Greenland Sea, Norwegian Sea, North Sea, North Atlantic sector) and oceanic regions (Arctic waters and the temperate NE Atlantic) combined with sampling years (2015 – 2020) and seasons (spring, summer and autumn). Moreover, a PERMANOVA was performed to assess the effects of different ships on the material and size compositions by using the vessel as a fixed factor. In case of significant differences, pairwise comparisons were conducted to identify differences between individual factor levels. Additionally, similarity percentage (SIMPER) analyses were performed to quantify the contribution of each material or size group to the dissimilarity between factor levels.

Principal coordinates analysis (PCO) was applied using PRIMER-e to visualise the environmental variables of *a priori* defined regional seas. Multivariate multiple regressions between environmental variables and the material and size compositions and environmental parameters were explored using the distance-based linear model (DistLM) routine of PRIMER-e after checking autocorrelations between environmental parameters with a Draftsman plot to avoid multi-collinearity. The average values of environmental parameters were normalised and marginal tests were run with 999 permutations to identify correlations between resemblance matrices of environmental variables and materials and size classes. The "Best" selection procedure based on the "Akaike information criterion (AIC)" was selected to find the best fitting regression models. Relations were visualised with distance-based redundancy analysis (dbRDA).

Opportunistically collected physical samples

During research cruise HE451.1 around Svalbard (Mark, 2015), debris items were retrieved from a fish lift that was connected to a juvenile fish trawl (Holst and McDonald, 2000) (SI, Fig. 5.1.1). A fish lift is an aquarium at the trawl cod end, aiming to capture the fish unharmed by minimising the turbulence inside. The fish lift was deployed for 15 minutes at depths, where fish schools had been detected by a Simrad EK60 hydro-acoustic system. Debris items were retrieved from the fish-lift samples taken in the south of Hinlopen Strait at 56 m depth, in Kongsfjorden at 30 m depth and in Billefjorden during four deployments at 150 – 160 m depth and from bottom trawls conducted in Billefjorden to assess fish stocks around Svalbard. The bottom trawl samples were not systematically screened for marine debris. Debris sorted from fish-lift and bottom trawl samples was photographed. In addition, during cruise

PS99.2, floating plastic items were collected in Fram Strait (~79.07N, 4.34E, 12/07/2016) from an inflatable boat.

2.1.3 Results

Spatiotemporal distribution of floating objects

A total of 276 visual surveys were conducted over 272.5 hours covering a total length of 4,793 km and an area of 47.35 km^2 (Table 2.1.1, Fig. 2.1.2). A total of 1,149 anthropogenic items were observed on 191 transects while no debris was detected on 85 transects. This total amount includes aggregations of anthropogenic items observed on three transects, for which the number of items was estimated as 30, 30 and 50, while three aggregations observed during the SV *Antigua* cruise were counted as single items. Debris concentrations did not vary significantly between regional seas (Kruskal-Wallis: H = 2.9, P = 0.712), oceanic regions (H = 0.160, P = 0.689) and different ships (H = 2.8 P = 0.428) when the data were consolidated for years and seasons. The overall median concentration of all transects conducted in this study was 11 items km^{-2} and ranged from 0 to 356 items km^{-2}, with the highest concentration recorded on a transect in the Greenland Sea off Longyearbyen, Svalbard (Table 2.1.1, Fig. 2.1.2). The highest annual median debris concentration of 38 items km^{-2} was recorded in the Barents Sea in 2016. For all sampling years combined, the North Sea showed the highest median debris concentration (19 items km^{-2}) of any region, while a median value of zero was obtained for the Central Arctic transects. In Arctic waters and in the temperate NE Atlantic Ocean, the median concentrations across all years were 11 items km^{-2} each.

Table 2.1.1 Concentrations of floating marine debris in different regions, years and seasons. Concentrations are presented as median, minimum, 1st quartile, 3rd quartile and maximum values. All concentrations are given as number of items (N) km^{-2}.

		Year	Total transect count (N)	Total observation Time (h)	Surveyed distance (km)	Surveyed area (km^2)	Total debris count (items)	Plastic (%) *	Median concentration (items km^{-2})	Minimum (items km^{-2})	Maximum (items km^{-2})	1st quartile (items km^{-2})	3rd quartile (items km^{-2})
Ocean	Arctic waters	2015-2020	247	244	4264	42.14	989	91	11	0	356	0	29
	Temperate NE Atlantic	2015-2020	29	29	529	5.20	160	93	11	0	117	0	32
Region	Central Arctic	2015	2	2	25	0.25	8	63	32	30	35	31	34
		2016	8	7	87	0.78	22	100	0	0	178	0	30
		Total**	10	9	113	1.03	30	90	0	0	178	0	34
	Barents Sea	2015	3	3	48	0.48	2	0	0	0	11	0	6
		2016	6	5	102	1	105	98	38	11	275	15	112
		Total**	9	8	150	1.48	107	96	13	0	275	11	56
	Greenland Sea	2015	7	7	94	0.94	19	89	19	0	49	0	31
		2016	52	57	986	9.69	313	88	18	0	356	3	48
		2017	51	51	836	8.36	130	98	8	0	80	0	16
		2018	13	11	226	2.26	26	96	8	0	107	0	11
		2020	7	7	94	0.94	13	100	5	0	60	0	14
		Total**	130	133	2,236	22.18	501	91	9	0	356	0	29
	Norwegian Sea	2015	1	2	28	0.28	2	50	7	7	7	7	7
		2016	51	46	862	8.35	184	86	16	0	115	6	28
		2017	38	38	724	7.24	154	92	13	0	162	4	28
		2018	4	4	67	0.67	14	93	20	7	36	15	25
		2020	7	6	136	1.36	4	100	0	0	9	0	5
		Total**	101	96	1,817	17.9	358	89	13	0	162	4	27
	North Sea	2016	20	20	377	3.75	127	93	18	0	116	0	36
		2020	2	2	37	0.37	5	100	13	0	25	6	19
		Total**	22	22	414	4.12	132	93	19	0	116	0	34
	North Atlantic sector	2017	4	4	63	0.63	21	90	10	0	117	7	38
Year		2015	13	14	195	1.95	31	74	11	0	49	0	31
		2016	137	135	2,414	23.57	751	90	16	0	356	0	42
		2017	93	93	1,623	16.23	305	94	9	0	162	0	20
		2018	17	15	293	2.93	40	95	8	0	107	5	17
		2020	16	15	267	2.67	22	100	2	0	60	0	10
Season	Spring	2015-2020	12	13	196	2	72	1	10	–	117	0	39
	Summer	2015-2020	107	106	1,888	19	640	1	26	–	356	9	50
	Autumn	2015-2020	157	153	2,709	27	437	1	6	–	275	0	16
Grand Total***			276	273	4,793	47.35	1,149	91	11	0	356	0	30

* The proportion of plastic items including ropes and nets are shown in the "Plastic" column as the percentage of the total debris count within the given category.

** "Total" shows the overall value of the corresponding column for all sampling years in a region.

*** "Grand Total" represents the overall value of the corresponding column for all sampling years and regions.

The overall debris concentration decreased slightly over the study period (SI, Fig. 5.1.2, linear regression: $r^2 = 0.024$; Analysis of Variance of the regression model: $F = 6.81$, $P = 0.010$). Accordingly, the debris concentrations varied significantly between years ($H = 13.2$, $P = 0.010$) with higher concentrations in 2016 than in 2020 (Table 2.1.1, Dunn's post-hoc: $Q = 2.825$, $P = 0.047$). Moreover, the overall debris concentration varied seasonally ($H = 42.8$, $P < 0.001$) with higher concentrations in summer than in autumn ($Q = 6.3$, $P < 0.001$). Generally, debris

concentrations in summer were about three to four times higher than in the other seasons (Table 2.1.1).

2,645 natural floating objects from 173 transects comprised items such as bird feathers, seaweed, patches of the ice alga *Melosira* sp., natural wood, a bird carcass and leaves. The overall median concentration of natural flotsam was 31 items km^{-2} with a range of 0 – 817 items km^{-2}. Seaweed was the most abundant natural flotsam with a median of 18 items km^{-2} (range: 0 – 462 items km^{-2}). All other natural objects were rare (median of 0 items km^{-2}). A weak positive but significant correlation was found between the concentrations of debris and natural items (Spearman: $\rho = 0.29$, $P < 0.001$) and between plastics and seaweed ($\rho = 0.39$, $P < 0.001$).

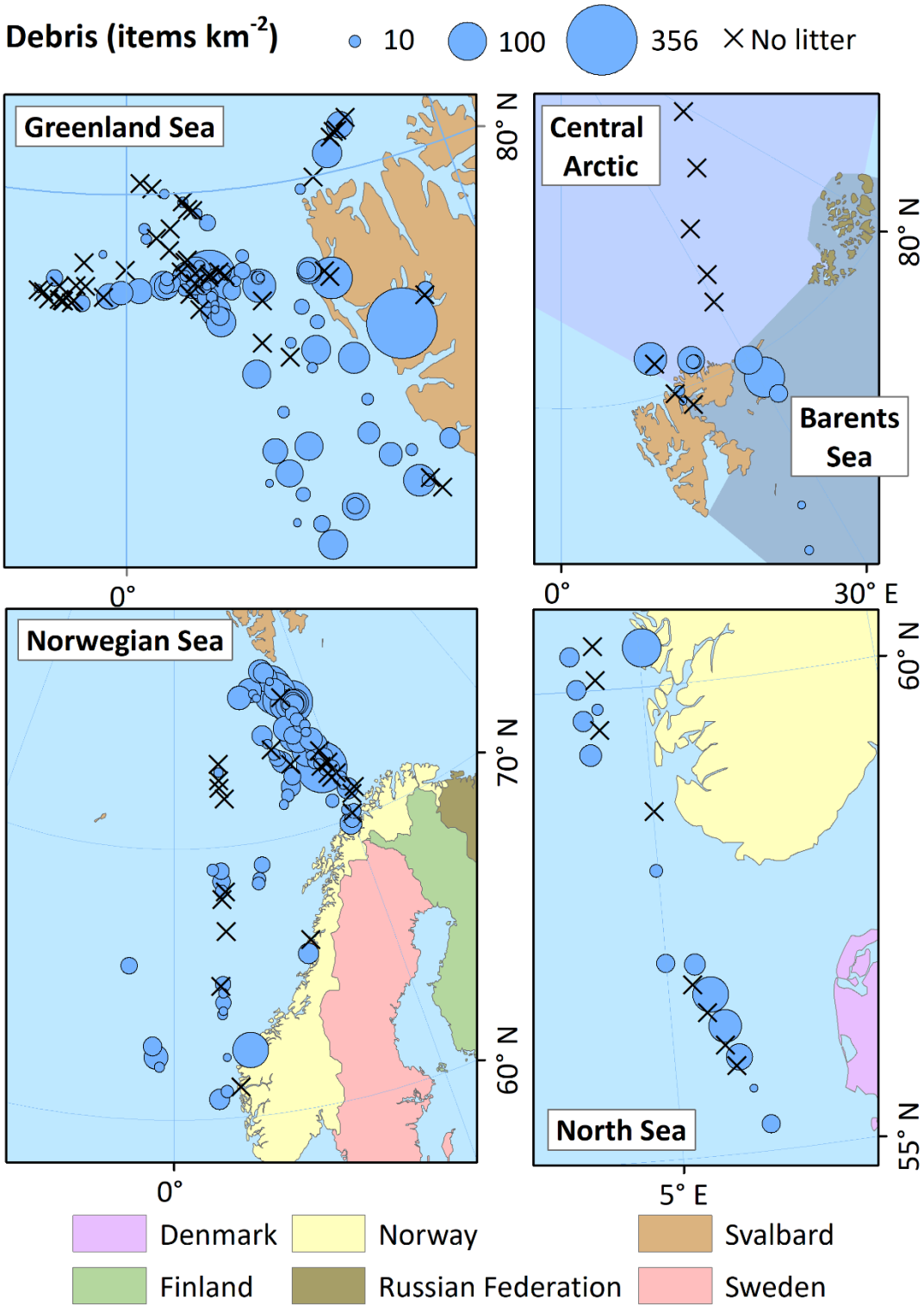

Figure 2.1.2 Concentrations of anthropogenic debris (number of items km^{-2}) recorded in visual surveys in the Central Arctic, Barents Sea, Greenland Sea, Norwegian Sea and North Sea. The four southern transects in the North Atlantic region are not shown to improve the scaling of the maps. The sizes of the bubbles are proportional to the debris concentrations of the transects. Crosses denote transects with zero records.

Composition of floating debris

A total of 1,046 plastic items, including ropes and nets accounted for 91% of all debris items recorded (Fig. 2.1.3). Other types of anthropogenic items included glass, timber, metal, paper, organic waste (28 items, 3%). Six percent (73 items) of the debris could not be assigned to any material category (N/A). However, 33 of these unidentified items (i.e., 3% of all debris items) were noted as "potential plastic items". Types or usages could be identified for 62% or 651 of the plastic items. The contribution of plastic to the total floating debris concentration was highest in the Barents Sea (96%) and lowest in the Norwegian Sea (89%). The most frequently observed plastic items were fragments, films, ropes and nets, packaging materials, expanded polystyrene and straps (Fig. 2.1.4).

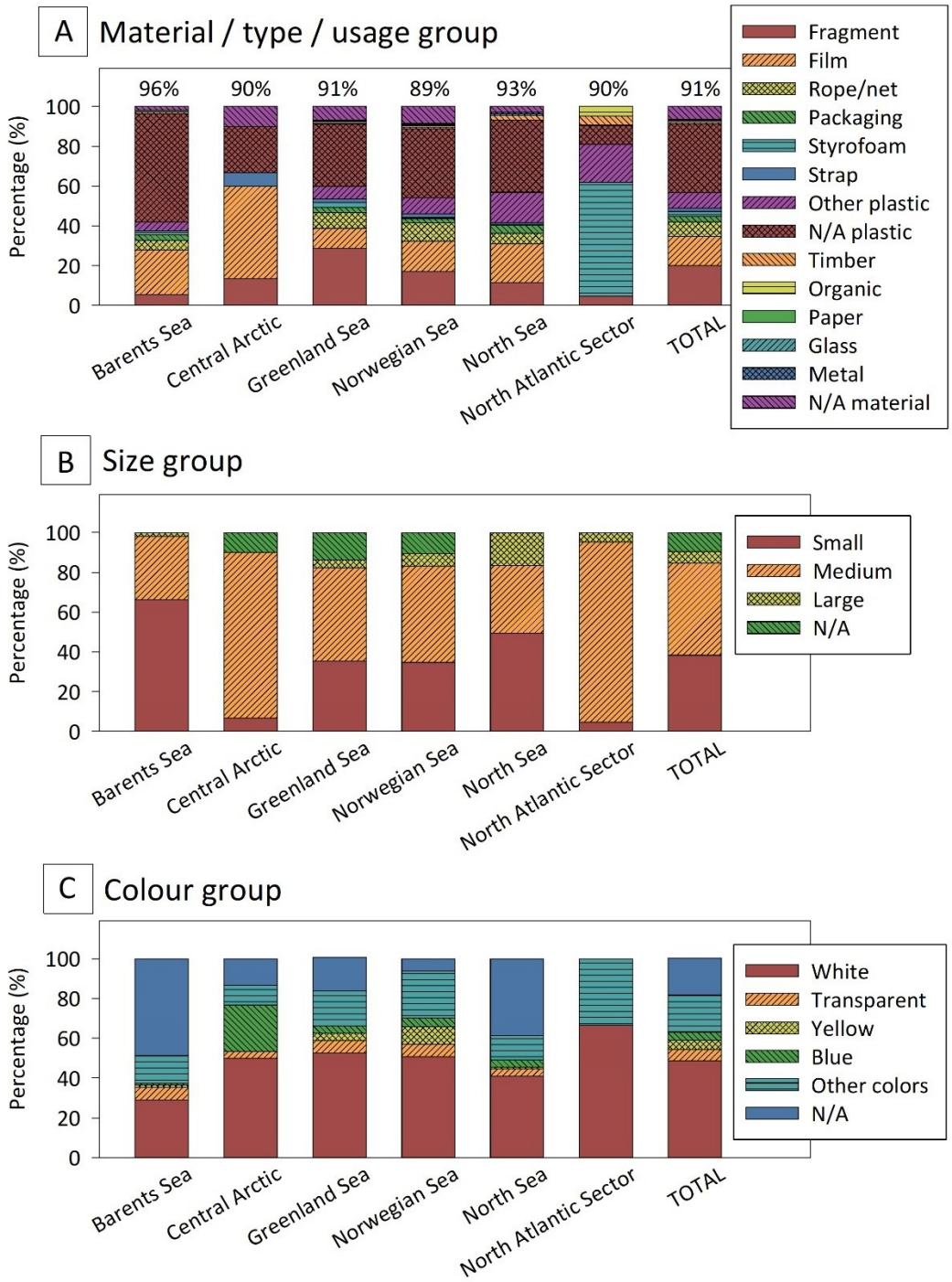

Figure 2.1.3 Proportions of debris items according to material, type or usage (A), size (B) and colour (C) groups. The values refer to proportions (%) within a region and the whole study area (TOTAL). The percentages in (A) above the bars represent the proportion of total plastic items. "N/A" refers to the proportion of the total observed debris within a region and/or category, for which the corresponding detail was not identified. Other plastic items included: bottle, cup, box, buoy/ball, cartridge, chip, cigarette bud, container, sanitary towel, disc, glove, grid, handle, helmet, hose, lid, paint container, photo, printed label, ribbon, ring, rubber, ship paint, sponge, stick, straw, syringe, tube, cotton bud.

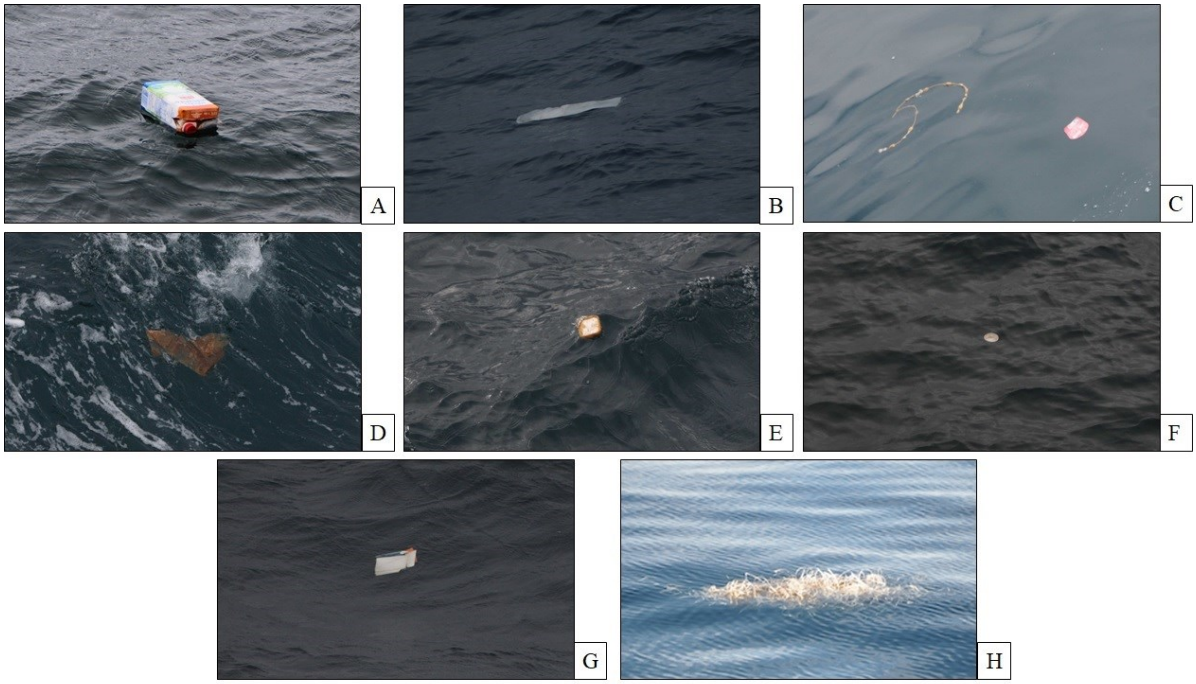

Figure 2.1.4 Photographs of floating plastic items observed during RV *Polarstern* cruise PS99.1 (A), PS99.2 (B-G) and *SV Antigua* (H). **A.** Tetra Pak (credit: Christoph Le Gall). **B.** White plastic sheet. **C.** Red-coloured hard plastic item and fouled rope. **D.** Heavily colonised plastic sheet. **E.** Plastic lid. **F.** Single-use container **G.** Piece of cardboard packaging. **H.** A bundle of tangled plastic straps (credit: Birgit Lutz). The original images can be found in the Supporting Information (Chapter 5.1).

Size was classified for 90% or 1,039 of the 1,149 debris items (Fig. 2.1.3). Medium-sized items dominated in the study area (532 items, 46%), followed by small-sized (440 items, 38%) and large-sized (67 items, 6%) items. Small items constituted the largest fraction in the Barents Sea with 66% (71 out of 107 items) and in the North Sea with 49% (65 out of 132 items, 49%) whereas medium-sized items dominated in the Central Arctic, Greenland Sea, Norwegian Sea and on transects in the temperate Northeast (NE) Atlantic. Among these, the Central Arctic had the highest fraction of medium-sized items (25 out of 30 items, 83%).

The multivariate PERMANOVA identified a statistically significant interactive effect of regional seas and sampling year suggesting significant differences in the annual dynamics of the material and size composition among the regions (SI, Table 5.1.2). In 2016, the Central Arctic differed from the Norwegian, Greenland and Barents Seas in the material and size composition of the floating debris (SI, Table 5.1.2). The SIMPER analyses revealed that the

higher abundances of plastics, ropes and nets in the Norwegian, Greenland and Barents Seas accounted for more than 60% in the dissimilarity to the material composition in the Central Arctic. Differences in the concentrations of small- and medium-sized items accounted for more than 80% of the dissimilarity between the Central Arctic and other regions and was primarily due to the low quantities in the Central Arctic. In 2017, the Norwegian and Greenland Seas differed in the material types of debris (SI, Table 5.1.2). No annual or spatial variations could be found by the corresponding analysis for Arctic waters and the temperate NE Atlantic. The PERMANOVA for different ships did not show any significant effect on the material and size compositions (SI, Table 5.1.2).

At both spatial scales of the regional seas and the oceanic regions, seasonal variations were evident (SI, Table 5.1.2). The material and size composition in summer differed from the composition in autumn and spring (SI, Table 5.1.2) due to higher abundances of plastics. However, a significant interaction with seasonality was only observed for the oceanic regions in material composition (SI, Table 5.1.2) suggesting differences in the temporal dynamics in debris composition among the two oceanic basins but not among regional seas.

Colour information was recorded for 81% or 935 of all items. Almost half of the items were white (49% or 560 items), 46% (530 items) of which being plastics (Fig. 2.1.3). Another 14% (164 items) were transparent, yellow or blue. Other colours accounted for 14% (161 items). Except for the submerged items within the aggregations, 105 single items (9%) floated partially or completely below the surface. In the aggregations, submerged items were noticed but not quantified. Forty-four items (4%) were recorded with obvious signs of bio-fouling.

Correlation with environmental and spatial variables

The principal coordinates of the environmental parameters confirmed variations in several variables between the regional seas (SI, Fig. 5.1.3). The debris concentration had a weak significant positive correlation with salinity (SI, Fig. 5.1.4; $\rho = 0.29$, $P < 0.001$), and a weak significant negative correlation with wind speed (SI, Fig. 5.1.5; $\rho = -0.26$, $P < 0.001$) and distance to the nearest European coast (SI, Fig. 5.1.6; $\rho = -0.25$, $P < 0.001$).

According to distance-based linear model, material and size compositions of the floating debris correlated significantly with all tested environmental parameters and ship speed, latitude, and distance to the nearest European coast (SI, Table 5.1.3 and S4, respectively). Air temperature was excluded because of a strong autocorrelation with water temperature

(correlation coefficient > 0.9). For the material and size compositions, the multivariate regression models of salinity, water temperature, wind and ship speed and nearest distance to the European coastline were selected as distance-based linear models (SI, Fig. 5.1.7, $r^2 = 0.21$, AIC = 1,420, and SI, Fig. 5.1.8, $r^2 = 0.23$, AIC = 1,439, respectively), which explained 21% and 23% of the variation, respectively.

Characterization of collected debris items

Nine plastic items were obtained from six fish-lift samples around Svalbard. One transparent plastic fragment was found inside a jellyfish captured in the south of Hinlopen Strait at a depth of 56 m (Fig. 2.1.5A). A yellow fragment was collected in Kongsfjorden at 30 m depth. The remaining items were recovered from four fish-lift deployments made at ~160 m depth, 0 – 11 m above the Billefjorden seafloor (Fig 2.1.5 B – H). The items from Billefjorden were strongly weathered except for the fisheries ropes (Fig. 2.1.5 G – H) and a transparent plastic fragment (Fig. 2.1.5B). Moreover, a strongly fouled leather shoe was retrieved from a bottom trawl at Billefjorden (Fig. 2.1.5I).

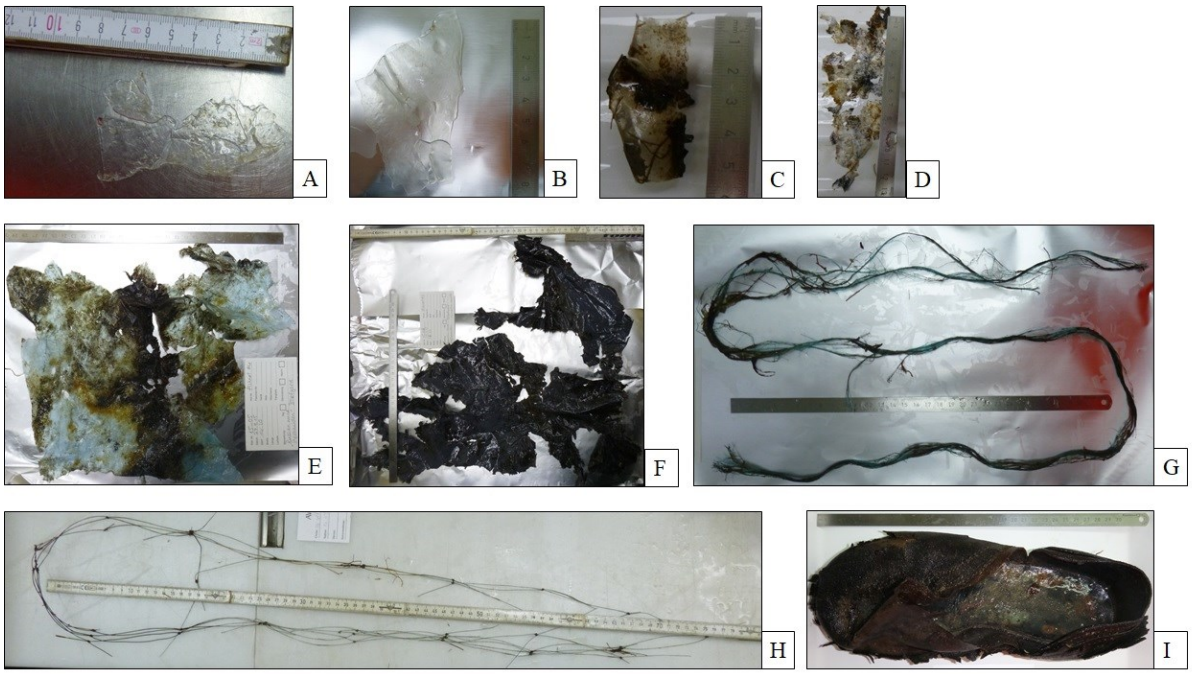

Figure 2.1.5 Photographs of debris items found in pelagic and bottom trawls during RV *Heincke* expedition around Svalbard in 2015. (A) Transparent plastic fragment secured from a jellyfish caught at 56 m depth in the Hinlopen Strait; (B – H) plastic debris collected from fish lift samples taken above the seafloor of Billefjorden; (I) weathered leather shoe collected by a bottom trawl in Billefjorden.

A fisheries glove, a kefir Tetra Pak manufactured in Latvia, two pieces of buckets and a bundle of ropes entangled with a transparent soft fragment (Fig. 2.1.6 A – F) were collected by hand in the Fram Strait. One box fragment was densely colonised by filamentous seaweeds and hydrozoans and hosted a rafting isopod of the genus *Idotea* and a cf. *Dendronotus* sp. nudibranch (Fig. 2.1.6 G – H).

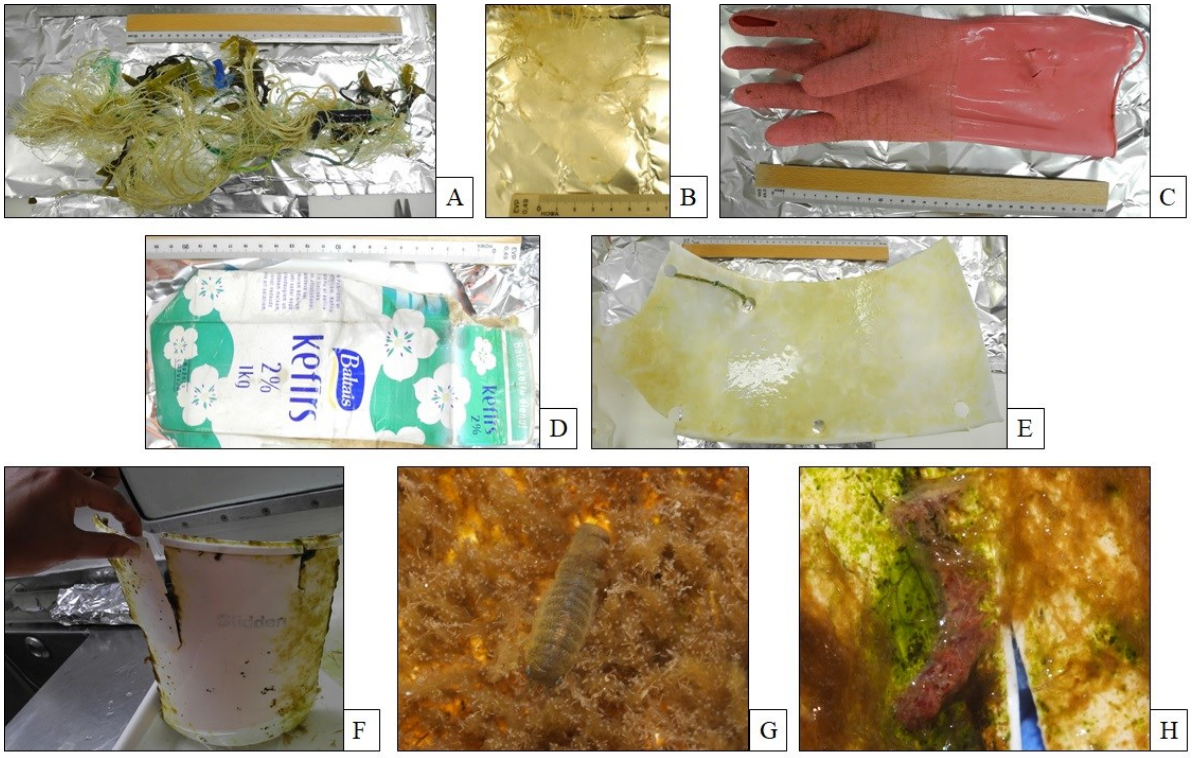

Figure 2.1.6 Photographs of plastic debris hand-picked from the sea surface in Fram Strait in 2016: **(A)** a bundle of tangled ropes, **(B)** a transparent soft fragment that had been entangled with the ropes, **(C)** fisheries glove, **(D)** a Kefir Tetra Pak manufactured in Latvia, **(E)** bucket fragment, **(F)** fragment of a more than 20-year-old bucket of the paint manufacturer Glidden, a piece of a plastic box that was densely colonised by hydrozoans and algae with **(G)** a rafting isopod *Idotea* sp. and **(H)** a nudibranch cf. *Dendronotus* sp. (credit: G, H by Andrey Vedenin).

2.1.4 Discussion

Spatial distribution

The aim of this study was to quantify the pollution of floating macro-debris in Arctic and Northeast (NE) Atlantic waters. Our results highlight that floating marine debris, mainly plastics, is widespread in the North as it was observed on 69% of the transects. While the whole

study area of 47.35 km^{-2} was covered to a considerable spatial extent by visual ship-based surveys, the availability of ship transit time and the fixed cruise program resulted in an unbalanced distribution of surveys among the regional seas. For example, most surveys in 2016 and 2017 were located in the Greenland and Norwegian Seas and overall, only 11% of the total surveyed area was located south of the Arctic Ocean boundary. The median debris concentration in the whole study area ranged from zero to 356 items km^{-2}. The highest concentration in Arctic waters was 356 items km^{-2} and 117 items km^{-2} in the temperate NE Atlantic.

Most polar seas showed similar median concentrations of floating marine debris ranging from 9 to 13 items km^{-2}, except for the Central Arctic. In 2016, when half of all visual surveys were conducted, no floating debris was observed on 75% of the transects in the Central Arctic, leading to a median concentration of zero for this region. While a total survey area of 0.8 km^2 is hardly representative for the whole of the Central Arctic, it could still be argued that a low probability of encountering floating marine debris in this region can be assumed since no debris was observed during six out of eight transects beyond 80° N. The observers occasionally reported sea ice at a coverage of 50 – 100% of the sea surface during the surveys without any debris sighting. Similarly, Bergmann *et al.* (2016) did not record any flotsam on transects with sea ice. While the presence of sea ice clearly affects debris counts, we do not yet know the fate of floating macro-debris during ice formation or when encountering ice floes. Debris items could become either submerged, or pushed aside, crushed/fragmented or entrained in sea ice. As with driftwood (Murphy et al., 2021), plastic items could then be carried with the sea ice, which is known to transport microplastic entrapped from the water (Peeken et al., 2018; Hoffmann et al., 2020). Clearly, the interaction and fate of macroplastics encountering sea ice merits further investigation. Still, occasional records of floating marine debris (Aliani et al., 2020) and even a large aggregation beyond 80° N (this study) demonstrate that the Central Arctic is not free of plastic debris.

Previous visual surveys on the quantity of floating marine debris in the Arctic Ocean yielded densities of 0.006 items km^{-1} in the Greenland Sea and 0.004 items km^{-1} in the Barents Sea (Bergmann et al., 2016). Those concentrations are substantially lower than the 0.09 to 0.13 items km^{-1} (Table 2.1.2) counted in the same regional seas in our study, potentially because Bergmann et al. (2016) reported only floating items larger than 20 cm, which were recorded as a by-product of seabird and mammal surveys conducted at a greater distance from the forward-

looking ship's bridge or a helicopter, while we specifically targeted any item visible from the rail of the moving vessel. Pogojeva et al. (2021) detected no debris in Siberian waters but reported 0.92 items km^{-2} in the Barents Sea. Again, we measured a 14 times higher median concentration of 13 items km^{-2} (Table 2.1.1) in the Barents Sea, suggesting substantial temporal and/or spatial variations in floating marine debris amounts.

Table 2.1.2 Floating marine debris concentrations reported in items km^{-2} by visual surveys after 2010.

Region	Location	Concentration (items km^{-2})	Concentration measure	Minimum size detection limit	Plastic (%)	Reference
Arctic Ocean	Barents, Greenland, Norwegian Seas	11	Median	> 1cm	91	This study
Arctic Ocean	Kara, Laptev and East Siberian Seas	0.002	Mean	> 2.5 cm		(Pogojeva et al., 2021)
Arctic Ocean	Barents Sea	0.92	Mean	> 2.5 cm		(Pogojeva et al., 2021)
Baltic Sea	Northern Baltic Sea	0.2 ± 0.1	Mean	> 5 cm	96	(Rothausler et al., 2019)
North Sea	German Bight	20	Median		64	(Thiel et al., 2011; Gutow et al., 2018)
North Sea	North Sea	19	Median	> 1 cm		This study
North Atlantic	North Sea, Norwegian Sea	11	Median	> 1 cm	91	This study
North Atlantic	Azores archipelago, Madeira	0.78g ± 0.07	Mean	> 2.5 cm	69	(Chambault et al., 2018)
North Atlantic	Portuguese waters	2.98	Mean	Items smaller than 2.5 cm were reported		(Sa et al., 2016)
South Atlantic	Coastal waters	67	Mean	> 1 cm	97	(Ryan, 2014)
South Atlantic	Oceanic waters	2.9	Mean	> 1 cm	97	(Ryan, 2014)
North Pacific Ocean	Station 1 (20–40°N, 120–155°W)	1400	Median	> 2cm	~100	(Goldstein et al., 2013)
North Pacific Ocean	Station 2 (20–40°N, 120–155°W)	3200	Median	> 2cm	~100	(Goldstein et al., 2013)
North Pacific Ocean	Station 3 (20–40°N, 120–155°W)	1500	Median	> 2cm	~100	(Goldstein et al., 2013)
North Pacific Ocean	Station 4 (20–40°N, 120–155°W)	1600	Median	> 2cm	~100	(Goldstein et al., 2013)
Central Pacific Ocean	Mexican Central Pacific	40 to 2440	Range		80	(Diaz-Torres et al., 2017)
Indian Ocean	Bay of Bengal	8.8 ± 1.4	Mean	>1 cm	96	(Ryan, 2013)
Indian Ocean	Straits of Malacca	578 ± 219	Mean	>1 cm	99	(Ryan, 2013)
Indian Ocean	Sub-Tropical, Sub-Antarctic and Antarctic Polar fronts	5.94	Mean	> 1cm	99	(Connan et al., 2021)
Southern Ocean	North of the Subtropical front	0.28–0.51	Range	>1 cm	(93 - 94)	(Suaria et al., 2020)
Southern Ocean	South of the Subtropical front	0.021–0.030	Range	>1 cm	(86 - 83)	(Suaria et al., 2020)
Southern Ocean	North of the Subtropical front	0.58	Mean	>1 cm	96	(Ryan et al., 2014)
Southern Ocean	South of the Subtropical front	0.032	Mean	>1 cm	96	(Ryan et al., 2014)
Southern Ocean	Central–southern Chile and Patagonian fjords	0 – 300	Range			(Hinojosa et al., 2011)
Mediterranean Sea	Balearic, Sardinian and Tyrrhenian Seas	2.3	Mean	> 20 cm	> 69	(Campana et al., 2018)
Mediterranean Sea	Adriatic Sea	251 ± 601	Mean	> 2.5	91	(Zeri et al., 2018)
Mediterranean Sea	Liguro-Provençal Sea	14.98 ± 22.84	Mean	> 1 cm	87	(Di-Meglio and Campana, 2017)
Mediterranean Sea	Central & western Mediterranean Sea	24.9	Mean	> 2 cm	96	(Suaria and Aliani, 2014)
Mediterranean Sea	Adriatic Sea	175	Mean	> 2.5 cm		(Palatinus et al., 2019)
Mediterranean Sea	Ligurian Sea, Sardinian-Balearic basin, Bonifacio Strait, Central Tyrrhenian Sea, Sicilian-Sardinian Channels, Adriatic Sea, Ionian Sea	2–5	Mean	> 20 cm	> 80	(Arcangeli et al., 2018)
Black Sea	NW Black Sea	30.9 ± 7.4	Mean	> 2 cm	89	(Suaria et al., 2015)

Floating marine debris has been quantified visually in various regions of the world's ocean (Table 2.1.2). Low concentrations of floating debris were recorded in the Southern Ocean (0.021 – 0.58 items km^{-2}) (Ryan et al., 2014; Suaria et al., 2020). Ryan et al. (2014) reported an average concentration of floating marine debris of 6.2 items km^{-2} in the South Atlantic between Cape Town and Tristan da Cunha, suggesting that this area represented the southern edge of a large accumulation zone. Concentrations of 3 – 14 items km^{-2} were reported from the Southern Indian Ocean (Connan et al., 2021) and 9 items km^{-2} from the Bay of Bengal in the Northern Indian Ocean (Ryan, 2013). Floating marine debris concentrations in the Mediterranean Sea ranged from 15 to 251 items km^{-2} in different sectors (Suaria and Aliani, 2014; Di-Meglio and Campana, 2017; Campana et al., 2018; Zeri et al., 2018). The North Pacific subtropical gyre is a well-established accumulation area of floating marine debris (Law et al., 2014). Between 1,400 and 3,200 items km^{-2} were reported from the region located between 20-40°N and 120–155°W (Goldstein et al., 2013) while 40 – 2,440 items km^{-2} were reported in the sub-tropical East Pacific off Mexico (Diaz-Torres et al., 2017). Only few visual surveys on floating debris have been conducted in the North Atlantic Ocean (Thiel et al., 2011; Sa et al., 2016; Chambault et al., 2018; Gutow et al., 2018). Chambault et al. (2018) reported debris concentrations of 0.78 items km^{-2} in Portuguese waters off the Azores and Madeira, which were much lower than the median concentration of 11 items km^{-2} observed on our three transects off the Iberian Peninsula. An earlier study in the North Sea reported median floating marine debris concentration of 20 items km^{-2} for the period of 2006 to 2016 (Gutow et al., 2018). Consistently, a median of 19 items km^{-2} was recorded during our study between 2016 and 2020. In summary, floating debris concentrations in the Arctic Ocean are lower than in the heavily polluted regions of the Central and North Pacific and the Mediterranean Sea but in a similar range as in the North Sea and higher than in the Indian, Southern and South Atlantic Ocean.

Almost half of the sea surface observations in our study were from the Fram Strait in the Arctic Ocean. In that region, the seafloor happened to be photographically surveyed regularly for the HAUSGARTEN time series and analysed for marine debris since 2002 (Tekman et al., 2017; Parga Martínez et al., 2020; Bergmann et al., 2022). The mean concentration on the deep Arctic seafloor across years and stations (4,571 ± 1,628 items km^{-2}) is about 500 times higher than the median concentration of floating marine debris in the Greenland Sea (9 items km^{-2}). By contrast, in the North Sea, the mean concentration on the seafloor was only some 40 times higher than at the sea surface (Gutow et al., 2018). The much higher ratio of seafloor to surface

concentrations in the Greenland Sea could be due to frequent resuspension of benthic debris in the much shallower and more dynamic North Sea whereas the deep sea seems to constitute a sink continuously accumulating marine debris (Pham et al., 2014). The composition of the debris material differs between the seafloor and sea surface. Plastic, rubber, Styrofoam, and fisheries-related plastic clearly dominated the composition at the surface by 91%, whereas these types accounted only for 56% on the seafloor (Parga Martínez et al., 2020). Glass pieces sink directly to the seafloor. Accordingly, only 0.2% of the floating items were glass, while it was the second most abundant debris type on the seafloor (21%). The overall composition of marine debris on the seafloor and at the sea surface depends strongly on material density. Several processes initiate the sinking process of positively buoyant plastics, which then become also subject to lateral advection processes during their passage to the seafloor (Li et al., 2020; Tekman et al., 2020). Bio-fouling can enhance the specific gravity of an item and cause it to sink. The relative surface area increases as the size of the item becomes smaller and therefore, small items lose their buoyancy faster than larger ones (Fazey and Ryan, 2016). Accordingly, small debris items dominated on the deep seafloor of the Fram Strait, whereas floating items in the Greenland Sea were mostly medium-sized. The large box fragment collected in the Fram Strait was still afloat although it was densely colonised by organisms (Fig 2.1.6 F – H). Empirical observations off South Africa showed that large and thick fragments float for longer than thin items, such as plastic bags (Ryan, 2015). Marine organisms can also facilitate the transport of anthropogenic debris to the seafloor (Choy and Drazen, 2013; Choy et al., 2019). The plastic film fragment inside the jellyfish collected by the fish lift in the Hinlopen Strait demonstrates that ingested plastics can be transported by pelagic organisms through the water column. Grøsvik et al. (2018) also reported marine debris in pelagic trawls taken close to the Norwegian and Svalbard coasts.

Temporal variability

Overall, there was a weak declining trend in floating debris concentrations from 2016 to 2020. However, longer-term investigations with sufficient annual counts are needed to confirm a continuous long-term decrease in marine debris pollution. A long-term study in the North Sea did not find persistent temporal changes between 2006 and 2016 (Gutow et al., 2018) but reported an order of magnitude increase between first assessments in 1983 (Dixon and Dixon, 1983) and later surveys in 2006 – 2008 (Thiel et al., 2011). Other studies from different marine compartments have suggested both decreasing and increasing trends. Citizen-science data from

over 200 beach locations at the Lofoten archipelago, Norway, collected from 2011 to 2018 revealed a decrease in marine debris, potentially in response to regular beach clean-ups and a change in consumer behaviour (Haarr et al., 2020). However, a continuous 7-fold increase from 2004 to 2017 was documented for the deep Arctic seafloor (Bergmann and Klages, 2012; Tekman et al., 2017; Parga Martínez et al., 2020).

Seasonal differences in marine debris concentrations are unlikely where human activities constantly emit debris (Hinojosa et al., 2011). Still, we observed a much higher debris concentration in summer than in autumn, which could be due to increased touristic and maritime activities in the absence of sea ice in summer (Stocker et al., 2020). Seafloor debris concentrations in that region correlated positively with fishing and tourism in the Fram Strait (Parga Martínez et al., 2020). A similar pattern was reported for beach debris from the Mediterranean (Campana et al., 2018) and Baltic Seas (Rothäusler et al., 2019) and attributed to seasonally increased recreational activities and tourism.

Floating objects

Plastics, including ropes and nets accounted for 91% of all floating debris. Small- and medium-sized fragments were the most common type of floating items. Similarly, plastic fragments were particularly abundant in offshore waters of the Indian Ocean whereas nearshore waters in that region had a higher proportion of consumer-related items (Ryan, 2013). A high fraction of undefined plastic fragments can be characteristic of remote regions off the centres of human activities, such as the Arctic Ocean due to extensive weathering processes during the long passage at sea.

The majority of plastic fragments were white or transparent concurring with studies from other regions (Ryan, 2014; Campana et al., 2018; Marti et al., 2020; Connan et al., 2021). Photooxidation causes discoloration or whitening, which shifts to yellow and then to brown upon extended exposure to solar radiation (Andrady, 2017; Marti et al., 2020), indicating progressive weathering. For densely colonised items, such as the box fragment collected in Fram Strait (Fig. 2.1.6 G – H), the determination of the colour can be challenging. The colour of an item can be important for interactions of species with floating debris (Ory et al., 2017; Marti et al., 2020).

Seaweeds were the dominant natural floating objects and were encountered in all regional seas, except for the Barents Sea. However, seaweeds were counted only on half of the transects

in the Barents Sea, where no floating debris was detected either. Our analysis suggests a weak but significant correlation between the distribution of debris and natural items, which can be explained by common transport mechanisms for all types of flotsam (Campana et al., 2018; Pogojeva et al., 2021). However, natural and anthropogenic items likely have different source regions, which could explain the weakness of the correlation.

The effect of environmental conditions and spatial variables

The debris concentration in our study area correlated positively with salinity but negatively with wind speed and nearest distance to the European coastline. Additionally, multivariate regression analysis revealed correlations with salinity, latitude, water temperature, wind speed and distance to the nearest European coast. As expected, both analyses confirm that environmental conditions as well as the latitude and distance to the coast (i.e. potential source regions) partly explain the variability in the distribution of floating marine debris, since there are other factors, which are not considered in this study (van Sebille et al., 2020).

The salinity gradient in the Nordic Seas is governed by the Norwegian Atlantic Current, which is a northward extension of the North Atlantic Current (the West Spitsbergen Current) with salinities exceeding 35 psu and the East Greenland Current with polar waters of lower salinities (< 34 psu). Waters of even lower salinities (32–34 psu) from the Skagerrak and the North Sea flowing along the Norwegian coast influence the eastern and north eastern sector of the Nordic Seas (Furevik et al., 2002; Strand et al., 2021). Backward drift simulations based on currents, wave action and wind forcing showed that floating debris from the North Sea and the temperate NE Atlantic is transported northwards towards Arctic waters within a year (Strand et al., 2021). However, a horizontal random spread of debris was also suggested (Strand et al., 2021). Our transects in the Barents Sea were mostly located around Svalbard, which is influenced by both, Atlantic and polar waters. Pogojeva et al. (2021) did not find floating debris in the eastern part of the Kara Sea, which is a source of polar waters (Wilson et al., 2021), suggesting that the high amounts of debris in the north and north east of Svalbard in our study originated primarily from local sources and maritime activities in that region or from transport from Atlantic sources. The contribution of maritime activities as a source of marine debris pollution has been reported by an assessment of plastic drinking bottles on an inhabited island in the Tristan da Cunha archipelago, central South Atlantic (Ryan et al., 2019). European debris is known to be transported to the north (Cózar et al., 2017; Tekman et al., 2020; Pogojeva et al., 2021). Indeed, 43% of the debris beached on Svalbard with embossed writing consisted of

objects manufactured in Europe (Björn et al., 2019). Debris on the beaches of western Svalbard, in the Greenland Sea, originate primarily from around Svalbard and the Barents Sea with additional minor contributions from Iceland and the Norwegian Sea (Strand et al., 2021). In our study, the proportion of small plastics was highest in the Barents Sea, followed by the North Sea. This distribution corroborates the drift trajectories projected for microplastic (Strand et al., 2021), and suggests the North Sea as a source region for microplastics in the Norwegian and Barents Seas. Moreover, the relatively high proportion of small plastic items in the Barents Sea can be explained by a continuous fragmentation of floating plastic items during extended residence times in the Barents Sea, supporting the projection of an accumulation area in the Barents Sea (van Sebille et al., 2012).

A decrease of marine debris concentrations with distance to land was also observed on the seafloor of the Norwegian and Barents Seas (Buhl-Mortensen and Buhl-Mortensen, 2017). High amounts of marine debris, especially plastic, have been reported at the coasts of Labrador, West Greenland (Mallory et al., 2021), Norway (Falk-Andersson et al., 2019; Haarr et al., 2020) and Svalbard beaches (Bergmann et al., 2017a). Higher concentrations in coastal waters than in offshore waters do not necessarily indicate land-based sources, especially in Arctic waters. Several studies highlighted fisheries, i.e. sea-based inputs, as a prime source of marine debris in the Arctic and the North Sea (Bergmann et al., 2017a; Buhl-Mortensen and Buhl-Mortensen, 2017; Gutow et al., 2018; Vesman et al., 2020; Benzik et al., 2021; Strand et al., 2021). Wind and currents can promote the transport and deposition of floating debris towards coasts (Ryan, 2013; van Sebille et al., 2020), resulting in a negative correlation of the debris concentration with nearest distance to the European coastline.

Wind-induced vertical mixing supports the vertical transport of floating marine debris through the water column down to hundreds of metres depth (Kukulka et al., 2012; Reisser et al., 2013; Suaria et al., 2016), which could explain the negative correlation between the debris concentrations and wind speed. Accordingly, 19% of the floating items in the South Atlantic were completely submerged by an estimated depth of 0.2 – 5 m (Ryan, 2014). In our study, we did not consistently record the position of floating items relative to the sea surface but at least 9% of the items were noted as being partly or completely submerged.

Conclusion

Floating marine debris was encountered on the great majority of transects suggesting a substantial pollution of Northeast Atlantic waters. The same median value of debris concentration was obtained for both sides of the Arctic Ocean boundary. Overall, the regional seas showed similar debris concentrations, except for the central Arctic, where despite occasional sightings, the majority of transects were free of floating debris. Clear seasonal trends were found, with higher pollution levels in summer than in other seasons, which could be attributed to seasonally elevated tourism and shipping activities in the region. Although the examination of environmental and spatial variables confirmed a distinction between the regional seas, their relation to the debris concentration partly explained the variability, possibly due to the complex hydrography in the area, the existence of other factors, and a random horizontal spread of floating items. A high proportion of unidentified fragments and films is characteristic for plastic pollution in remote open waters.

Visual surveys do not require the use of specific sampling gear and are, therefore, relatively easy to perform even for people without scientific training or specific expertise. The extensive dataset compiled in this study would not have been possible without non-experts and citizen scientists, highlighting that collaboration with citizen scientists can help us to fill important knowledge gaps. Moreover, observations of floating plastics can be used to validate and improve the modelled simulations and predictions regarding the distribution of flotsam, which are essential for ecological risk assessments (Compa et al., 2019) and assessments of the efficiency of new regulations such as a UN Plastic Treaty. Interactions comprising entanglement, ingestion and colonisation of debris have already been reported for species from the bottom of the food chain to top predators in Arctic waters (Parga Martínez et al., 2020; Collard and Ask, 2021; Bergmann et al., 2022; Botterell et al., 2022). While the effects of these interactions are largely unknown, Arctic ecosystems are already under threat from climate change (Thomas et al., 2022) and plastic pollution can only exacerbate its effects (Tekman et al., 2022). Action is thus urgently required to efficiently reduce plastic pollution from both local and distant sources.

2.1.5 Conflict of Interest

The authors declare that the research was conducted in the absence of any commercial or financial relationships that could be construed as a potential conflict of interest.

2.1.6 Author Contributions

All authors conceived of the presented idea, contributed to the design and implementation of the research. M.B.T. processed the data, performed the analysis, drafted the manuscript with support from L.G. and M.B. All authors discussed the results, commented on the manuscript, read and approved the submitted version.

2.1.7 Funding

This work contributes to the Pollution Observatory of the Helmholtz-funded infrastructure program FRAM (Frontiers in Arctic Marine Research), which funded MBT. M.B. and L.G. were funded by the Helmholtz-Gemeinschaft Deutscher Forschungszentren. The grant number of HE451.1 is AWI_HE451_01.

2.1.8 Acknowledgements

The data for this study has been collected by dozens of helpers. We cannot provide all names but would like to sincerely thank the crew, (principal) scientists, and students of the cruises HE451.1, PS99.1, PS99.2, PS101, PS105, PS107, PS108, MSM77, MSM95 and crew and tourists of the SV *Antigua* cruise. The authors organized the data collection on HE451.1, PS99.1, PS99.2, PS108, MSM77. Jennifer Dannheim organized the data collection on PS101, Simon Dreutter on PS105, Melissa Käß on PS107 and Lilian Boehringer conducted the visual surveys during MSM95. We gratefully acknowledge the efforts of Birgit Lutz, who organized the data collection by citizen scientists during sailing cruises. Sandra Tippenhauer collected floating items in the Fram Strait. Andrey Vedenin provided photos of collected debris items. Corina Peter and Erik Dauer digitalized visual survey protocols. We also thank Simon Dreutter and Tilo Birnbaum for their help with ArcGIS analyses. This publication is Eprint ID 55885 of the Alfred-Wegener-Institut Helmholtz-Zentrum für Polar- und Meeresforschung.

2.1.9 References

Aliani, S., Casagrande, G., Catapano, P., and Catapano, V. (2020). "Polarquest 2018 Expedition: Plastic Debris at 82°07' North," in *Mare Plasticum - The Plastic Sea,* eds. M. Streit-Bianchi, M. Cimadevila & W. Trettnak. (Cham: Springer International Publishing), 89-116.

[Dataset] AMAP (2013). *AMAP area / boundary, line and polygon shapefiles.* Available: https://www.amap.no/work-area/document/868.

Anderson, M.J., and Walsh, D.C.I. (2013). PERMANOVA, ANOSIM, and the Mantel test in the face of heterogeneous dispersions: What null hypothesis are you testing? *Ecol. Monogr.* 83(4)**,** 557-574. doi: 10.1890/12-2010.1.

Andrady, A.L. (2017). The plastic in microplastics: A review. *Mar. Pollut. Bull.* 119(1)**,** 12-22. doi: 10.1016/j.marpolbul.2017.01.082.

Arcangeli, A., Campana, I., Angeletti, D., Atzori, F., Azzolin, M., Carosso, L., et al. (2018). Amount, composition, and spatial distribution of floating macro litter along fixed trans-

border transects in the Mediterranean basin. *Mar. Pollut. Bull.* 129(2)**,** 545-554. doi: 10.1016/j.marpolbul.2017.10.028.

Arcangeli, A., David, L., Aguilar, A., Atzori, F., Borrell, A., Campana, I., et al. (2020). Floating marine macro litter: Density reference values and monitoring protocol settings from coast to offshore. Results from the MEDSEALITTER project. *Mar. Pollut. Bull.* 160**,** 111647. doi: https://doi.org/10.1016/j.marpolbul.2020.111647.

Benzik, A.N., Orlov, A.M., and Novikov, M.A. (2021). Marine seabed litter in Siberian Arctic: A first attempt to assess. *Mar. Pollut. Bull.* 172**,** 112836. doi: 10.1016/j.marpolbul.2021.112836.

Bergmann, M., Collard, F., Fabres, J., Gabrielsen, G.W., Provencher, J.F., Rochman, C.M., et al. (2022). Plastic pollution in the Arctic. *Nat. Rev. Earth Environ.* 3(5)**,** 323-337. doi: 10.1038/s43017-022-00279-8.

Bergmann, M., and Klages, M. (2012). Increase of litter at the Arctic deep-sea observatory HAUSGARTEN. *Mar. Pollut. Bull.* 64(12)**,** 2734-2741. doi: 10.1016/j.marpolbul.2012.09.018.

Bergmann, M., Lutz, B., Tekman, M.B., and Gutow, L. (2017a). Citizen scientists reveal: Marine litter pollutes Arctic beaches and affects wild life. *Mar. Pollut. Bull.* 125(1-2)**,** 535-540. doi: 10.1016/j.marpolbul.2017.09.055.

Bergmann, M., Mutzel, S., Primpke, S., Tekman, M.B., Trachsel, J., and Gerdts, G. (2019). White and wonderful? Microplastics prevail in snow from the Alps to the Arctic. *Sci. Adv.* 5(8)**,** eaax1157. doi: 10.1126/sciadv.aax1157.

Bergmann, M., Sandhop, N., Schewe, I., and D'Hert, D. (2016). Observations of floating anthropogenic litter in the Barents Sea and Fram Strait, Arctic. *Polar Biol.* 39**,** 553-560. doi: 10.1007/s00300-015-1795-8

Bergmann, M., Tekman, M.B., and Gutow, L. (2017b). Marine litter: Sea change for plastic pollution. *Nature* 544(7650)**,** 297. doi: 10.1038/544297a.

Beszczynska-Möller, A., Woodgate, R.A., Lee, C., Melling, H., and Karcher, M. (2011). A synthesis of exchanges through the main oceanic gateways to the Arctic Ocean. *Oceanogr.* 24(3)**,** 82-99.

Biermann, L., Clewley, D., Martinez-Vicente, V., and Topouzelis, K. (2020). Finding plastic patches in coastal waters using optical satellite data. *Sci. Rep.* 10(1)**,** 1-10. doi: 10.1038/s41598-020-62298-z

Björn, A., Peter, H., Tiina, K., Tina, S., Pame, 2019. Desktop Study on Marine Litter Including Microplastics in the Arctic, Grid-Arendal. Retrieved from https://policycommons.net/artifacts/2390702/desktop-study-on-marine-litter-including-microplastics-in-the-arctic/3412124/ on 22 Jun 2022. CID: 20.500.12592/grg7dg.

Borrelle, S.B., Ringma, J., Law, K.L., Monnahan, C.C., Lebreton, L., McGivern, A., et al. (2020). Predicted growth in plastic waste exceeds efforts to mitigate plastic pollution. *Science* 369(6510)**,** 1515-1518. doi: 10.1126/science.aba3656.

Botterell, Z.L.R., Bergmann, M., Hildebrandt, N., Krumpen, T., Steinke, M., Thompson, R.C., et al. (2022). Microplastic ingestion in zooplankton from the Fram Strait in the Arctic. *Sci. Total Environ.* 831**,** 154886. doi: 10.1016/j.scitotenv.2022.154886.

Bourdages, M.P.T., Provencher, J.F., Sudlovenick, E., Ferguson, S.H., Young, B.G., Pelletier, N., et al. (2020). No plastics detected in seal (Phocidae) stomachs harvested in the eastern Canadian Arctic. *Mar. Pollut. Bull.* 150**,** 110772. doi: 10.1016/j.marpolbul.2019.110772.

Buhl-Mortensen, L., and Buhl-Mortensen, P. (2017). Marine litter in the Nordic Seas: Distribution composition and abundance. *Mar. Pollut. Bull.* 125(1-2)**,** 260-270. doi: 10.1016/j.marpolbul.2017.08.048.

Bundela, A.K., Pandey, K.K. The United Nations General Assembly Passes Historic Resolution to Beat Plastic Pollution. Anthr. Sci. (2022). https://doi.org/10.1007/s44177-022-00021-5

Campana, I., Angeletti, D., Crosti, R., Di Miccoli, V., and Arcangeli, A. (2018). Seasonal patterns of floating macro-litter across the Western Mediterranean Sea: a potential threat for cetacean species. *Rend. Lincei Sci. Fis. Nat.* 29(2)**,** 453-467. doi: 10.1007/s12210-018-0680-0.

Chambault, P., Vandeperre, F., Machete, M., Lagoa, J.C., and Pham, C.K. (2018). Distribution and composition of floating macro litter off the Azores archipelago and Madeira (NE Atlantic) using opportunistic surveys. *Mar. Environ. Res.* 141**,** 225-232. doi: 10.1016/j.marenvres.2018.09.015.

Chiu, C.-C., Liao, C.-P., Kuo, T.-C., and Huang, H.-W. (2020). Using citizen science to investigate the spatial-temporal distribution of floating marine litter in the waters around Taiwan. *Mar. Pollut. Bull.* 157**,** 111301.

Choy, C.A., and Drazen, J.C. (2013). Plastic for dinner? Observations of frequent debris ingestion by pelagic predatory fishes from the central North Pacific. *Mar. Ecol. Prog. Ser.* 485(Marine Ecology Progress Series 2013 485 155-163)**,** 155-163. doi: 10.3354/meps10342.

Choy, C.A., Robison, B.H., Gagne, T.O., Erwin, B., Firl, E., Halden, R.U., et al. (2019). The vertical distribution and biological transport of marine microplastics across the epipelagic and mesopelagic water column. *Sci. Rep.* 9(1)**,** 7843. doi: 10.1038/s41598-019-44117-2.

Collard, F., and Ask, A. (2021). Plastic ingestion by Arctic fauna: A review. *Sci. Total Environ.* 786**,** 147462. doi: 10.1016/j.scitotenv.2021.147462.

Compa, M., Alomar, C., Wilcox, C., van Sebille, E., Lebreton, L., Hardesty, B.D., et al. (2019). Risk assessment of plastic pollution on marine diversity in the Mediterranean Sea. *Sci. Total Environ.* 678**,** 188-196. doi: 10.1016/j.scitotenv.2019.04.355.

Connan, M., Perold, V., Dilley, B.J., Barbraud, C., Cherel, Y., and Ryan, P.G. (2021). The Indian Ocean 'garbage patch': Empirical evidence from floating macro-litter. *Mar. Pollut. Bull.* 169**,** 112559. doi: 10.1016/j.marpolbul.2021.112559.

Cózar, A., Marti, E., Duarte, C.M., Garcia-de-Lomas, J., van Sebille, E., Ballatore, T.J., et al. (2017). The Arctic Ocean as a dead end for floating plastics in the North Atlantic branch of the Thermohaline Circulation. *Sci. Adv.* 3(4)**,** e1600582. doi: 10.1126/sciadv.1600582.

Di-Meglio, N., and Campana, I. (2017). Floating macro-litter along the Mediterranean French coast: Composition, density, distribution and overlap with cetacean range. *Mar. Pollut. Bull.* 118(1-2)**,** 155-166. doi: 10.1016/j.marpolbul.2017.02.026.

Diaz-Torres, E.R., Ortega-Ortiz, C.D., Silva-Iniguez, L., Nene-Preciado, A., and Orozco, E.T. (2017). Floating Marine Debris in waters of the Mexican Central Pacific. *Mar. Pollut. Bull.* 115(1-2)**,** 225-232. doi: 10.1016/j.marpolbul.2016.11.065.

Dixon, T.J., and Dixon, T.R. (1983). Marine litter distribution and composition in the North Sea. *Mar. Pollut. Bull.* 14(4)**,** 145-148. doi: 10.1016/0025-326x(83)90068-1.

[Dataset] EEA (2015). *Europe coastline shapefile.* Available: https://www.eea.europa.eu/data-and-maps/data/eea-coastline-for-analysis-1/gis-data/europe-coastline-shapefile.

Eriksen, M., Lebreton, L.C., Carson, H.S., Thiel, M., Moore, C.J., Borerro, J.C., et al. (2014). Plastic Pollution in the World's Oceans: More than 5 Trillion Plastic Pieces Weighing over 250,000 Tons Afloat at Sea. *PLoS One* 9(12)**,** e111913. doi: 10.1371/journal.pone.0111913.

Ershova, A., Makeeva, I., Malgina, E., Sobolev, N., and Smolokurov, A. (2021). Combining citizen and conventional science for microplastics monitoring in the White Sea basin

(Russian Arctic). *Mar. Pollut. Bull.* 173(Pt A)**,** 112955. doi: 10.1016/j.marpolbul.2021.112955.

Everaert, G., De Rijcke, M., Lonneville, B., Janssen, C.R., Backhaus, T., Mees, J., et al. (2020). Risks of floating microplastic in the global ocean. *Environ. Pollut.* 267**,** 115499. doi: 10.1016/j.envpol.2020.115499.

Falk-Andersson, J., Berkhout, B.W., and Abate, T.G. (2019). Citizen science for better management: Lessons learned from three Norwegian beach litter data sets. *Mar. Pollut. Bull.* 138**,** 364-375. doi: 10.1016/j.marpolbul.2018.11.021.

Fazey, F.M., and Ryan, P.G. (2016). Biofouling on buoyant marine plastics: An experimental study into the effect of size on surface longevity. *Environ. Pollut.* 210**,** 354-360. doi: 10.1016/j.envpol.2016.01.026.

Furevik, T., Bentsen, M., Drange, H., Johannessen, J.A., and Korablev, A. (2002). Temporal and spatial variability of the sea surface salinity in the Nordic Seas. *J. Geophys. Res. Oceans* 107(C12)**,** SRF 10-11-SRF 10-16. doi: 10.1029/2001jc001118.

Gacutan, J., Johnston, E.L., Tait, H., Smith, W., and Clark, G.F. (2022). Continental patterns in marine debris revealed by a decade of citizen science. *Sci. Total. Environ.* 807(Pt 2)**,** 150742. doi: 10.1016/j.scitotenv.2021.150742.

Goldstein, M.C., Titmus, A.J., and Ford, M. (2013). Scales of spatial heterogeneity of plastic marine debris in the northeast pacific ocean. *PLoS One* 8(11)**,** e80020. doi: 10.1371/journal.pone.0080020.

Grøsvik, B.E., Prokhorova, T., Eriksen, E., Krivosheya, P., Horneland, P.A., and Prozorkevich, D. (2018). Assessment of Marine Litter in the Barents Sea, a Part of the Joint Norwegian–Russian Ecosystem Survey. *Front. Mar. Sci.* 5. doi: 10.3389/fmars.2018.00072.

Gutow, L., Ricker, M., Holstein, J.M., Dannheim, J., Stanev, E.V., and Wolff, J.O. (2018). Distribution and trajectories of floating and benthic marine macrolitter in the south-eastern North Sea. *Mar. Pollut. Bull.* 131(Pt A)**,** 763-772. doi: 10.1016/j.marpolbul.2018.05.003.

Haarr, M.L., Pantalos, M., Hartviksen, M.K., and Gressetvold, M. (2020). Citizen science data indicate a reduction in beach litter in the Lofoten archipelago in the Norwegian Sea. *Mar. Pollut. Bull.* 153**,** 111000. doi: 10.1016/j.marpolbul.2020.111000.

Hidalgo-Ruz, V., Thiel, M. (2015). The Contribution of Citizen Scientists to the Monitoring of Marine Litter. In: Bergmann, M., Gutow, L., Klages, M. (eds) *Marine Anthropogenic Litter*. Springer, Cham. https://doi.org/10.1007/978-3-319-16510-3_16

Hinojosa, I.A., Rivadeneira, M.M., and Thiel, M. (2011). Temporal and spatial distribution of floating objects in coastal waters of central–southern Chile and Patagonian fjords. *Cont. Shelf Res.* 31(3-4)**,** 172-186. doi: 10.1016/j.csr.2010.04.013.

Hoffmann, L., Eggers, S.L., Allhusen, E., Katlein, C., and Peeken, I. (2020). Interactions between the ice algae *Fragillariopsis cylindrus* and microplastics in sea ice. *Environ. Int.* 139**,** 105697.

Holst, J.C., and McDonald, A. (2000). FISH-LIFT: a device for sampling live fish with trawls. *Fish. Res.* 48(1)**,** 87-91.

Koelmans, A.A., Redondo-Hasselerharm, P.E., Nor, N.H.M., de Ruijter, V.N., Mintenig, S.M., and Kooi, M. (2022). Risk assessment of microplastic particles. *Nat. Rev. Mater.* 7(2)**,** 138-152. doi: 10.1038/s41578-021-00411-y.

Kühn, S., and van Franeker, J.A. (2020). Quantitative overview of marine debris ingested by marine megafauna. *Mar. Pollut. Bull.* 151**,** 110858. doi: 10.1016/j.marpolbul.2019.110858.

Kukulka, T., Proskurowski, G., Morét-Ferguson, S., Meyer, D.W., and Law, K.L. (2012). The effect of wind mixing on the vertical distribution of buoyant plastic debris. *Geophys. Res. Lett.* 39(7)**,** doi: 10.1029/2012gl051116.

Law, K.L., Moret-Ferguson, S.E., Goodwin, D.S., Zettler, E.R., Deforce, E., Kukulka, T., et al. (2014). Distribution of surface plastic debris in the eastern Pacific Ocean from an 11-year data set. *Environ. Sci. Technol.* 48(9)**,** 4732-4738. doi: 10.1021/es4053076.

Lebreton, L., Slat, B., Ferrari, F., Sainte-Rose, B., Aitken, J., Marthouse, R., et al. (2018). Evidence that the Great Pacific Garbage Patch is rapidly accumulating plastic. *Sci. Rep.* 8(1)**,** 4666.

Li, D., Liu, K., Li, C., Peng, G., Andrady, A.L., Wu, T., et al. (2020). Profiling the Vertical Transport of Microplastics in the West Pacific Ocean and the East Indian Ocean with a Novel in Situ Filtration Technique. *Environ. Sci. Technol.* 54(20)**,** 12979-12988. doi: 10.1021/acs.est.0c02374.

MacLeod, M., Arp, H.P.H., Tekman, M.B., and Jahnke, A. (2021). The global threat from plastic pollution. *Science* 373(6550)**,** 61-65. doi: 10.1126/science.abg5433.

Mallory, M.L., Baak, J., Gjerdrum, C., Mallory, O.E., Manley, B., Swan, C., et al. (2021). Anthropogenic litter in marine waters and coastlines of Arctic Canada and West Greenland. *Sci. Total Environ.* 783**,** 146971. doi: 10.1016/j.scitotenv.2021.146971.

Mark, F. C. (2015): Cruise Report RV Heincke HE451.1 [Miscellaneous] doi: 10.1594/PANGAEA.855528

Marti, E., Martin, C., Galli, M., Echevarria, F., Duarte, C.M., and Cózar, A. (2020). The Colors of the Ocean Plastics. *Environ. Sci. Technol.* 54(11)**,** 6594-6601. doi: 10.1021/acs.est.9b06400.

Meyer, A. N. (2022). Deep Dives into Arctic Beach Debris. Analysing its Composition and Origin. Bachelor's thesis. Kiel: Christian-Albrechts-Universität zu Kiel

Murphy, E., Nistor, I., Cornett, A., Wilson, J., and Pilechi, A. (2021). Fate and transport of coastal driftwood: A critical review. *Mar. Pollut. Bull.* 170**,** 112649. doi: 10.1016/j.marpolbul.2021.112649.

[Dataset] NE (2019). *World Marine Regions.* Available: https://www.naturalearthdata.com/downloads/10m-physical-vectors/10m-physical-labels/.

Nelms, S.E., Coombes, C., Foster, L.C., Galloway, T.S., Godley, B.J., Lindeque, P.K., et al. (2017). *Marine anthropogenic litter* on British beaches: A 10-year nationwide assessment using citizen science data. *Sci. Total. Environ.* 579**,** 1399-1409.

Olivelli, A., Hardesty, B.D., and Wilcox, C. (2020). Coastal margins and backshores represent a major sink for marine debris: insights from a continental-scale analysis. *Environ. Res. Lett.* 15(7)**,** 074037. doi: 10.1088/1748-9326/ab7836

Ory, N.C., Sobral, P., Ferreira, J.L., and Thiel, M. (2017). Amberstripe scad Decapterus muroadsi (Carangidae) fish ingest blue microplastics resembling their copepod prey along the coast of Rapa Nui (Easter Island) in the South Pacific subtropical gyre. *Sci. Total Environ.* 586**,** 430-437. doi: 10.1016/j.scitotenv.2017.01.175.

[Dataset] OSPAR (2016). *OSPAR Maritime Area and its Regions.* Available: https://odims.ospar.org/en/maps/map-maritime-area-and-its-regions/.

Palatinus, A., Kovac Virsek, M., Robic, U., Grego, M., Bajt, O., Siljic, J., et al. (2019). Marine litter in the Croatian part of the middle Adriatic Sea: Simultaneous assessment of floating and seabed macro and micro litter abundance and composition. *Mar. Pollut. Bull.* 139**,** 427-439. doi: 10.1016/j.marpolbul.2018.12.038.

Parga Martínez, K.B., Tekman, M.B., and Bergmann, M. (2020). Temporal trends in marine litter at three stations of the HAUSGARTEN observatory in the Arctic deep sea. *Front. Mar. Sci.* 7**,** 321. 10.3389/fmars.2020.00321

Peeken, I., Primpke, S., Beyer, B., Gütermann, J., Katlein, C., Krumpen, T., et al. (2018). Arctic sea ice is an important temporal sink and means of transport for microplastic. *Nat. Commun.* 9(1)**,** 1-12.

Persson, L., Carney Almroth, B.M., Collins, C.D., Cornell, S., de Wit, C.A., Diamond, M.L., et al. (2022). Outside the Safe Operating Space of the Planetary Boundary for Novel Entities. *Environ. Sci. Technol.* 56(3)**,** 1510-1521. doi: 10.1021/acs.est.1c04158.

Pham, C.K., Ramirez-Llodra, E., Alt, C.H., Amaro, T., Bergmann, M., Canals, M., et al. (2014). Marine litter distribution and density in European seas, from the shelves to deep basins. *PLoS One* 9(4)**,** e95839. doi: 10.1371/journal.pone.0095839.

Pichel, W.G., Churnside, J.H., Veenstra, T.S., Foley, D.G., Friedman, K.S., Brainard, R.E., et al. (2007). Marine debris collects within the North Pacific Subtropical Convergence Zone. *Mar. Pollut. Bull.* 54(8)**,** 1207-1211. doi: 10.1016/j.marpolbul.2007.04.010.

Pogojeva, M., Zhdanov, I., Berezina, A., Lapenkov, A., Kosmach, D., Osadchiev, A., et al. (2021). Distribution of floating marine macro-litter in relation to oceanographic characteristics in the Russian Arctic Seas. *Mar. Pollut. Bull.* 166**,** 112201. doi: 10.1016/j.marpolbul.2021.112201.

Reisser, J., Shaw, J., Wilcox, C., Hardesty, B.D., Proietti, M., Thums, M., et al. (2013). Marine plastic pollution in waters around Australia: characteristics, concentrations, and pathways. *PLoS One* 8(11)**,** e80466. doi: 10.1371/journal.pone.0080466.

Rothäusler, E., Jormalainen, V., Gutow, L., and Thiel, M. (2019). Low abundance of floating marine debris in the northern Baltic Sea. *Mar. Pollut. Bull.* 149**,** 110522. doi: 10.1016/j.marpolbul.2019.110522.

Ryan, P.G. (2013). A simple technique for counting marine debris at sea reveals steep litter gradients between the Straits of Malacca and the Bay of Bengal. *Mar. Pollut. Bull.* 69(1-2)**,** 128-136. doi: 10.1016/j.marpolbul.2013.01.016.

Ryan, P.G. (2014). Litter survey detects the South Atlantic 'garbage patch'. *Mar. Pollut. Bull.* 79(1-2)**,** 220-224. doi: 10.1016/j.marpolbul.2013.12.010.

Ryan, P.G. (2015). Does size and buoyancy affect the long-distance transport of floating debris? *Environ. Res. Lett.* 10(8)**,** 084019. doi: 10.1088/1748-9326/10/8/084019.

Ryan, P.G., Dilley, B.J., Ronconi, R.A., and Connan, M. (2019). Rapid increase in Asian bottles in the South Atlantic Ocean indicates major debris inputs from ships. *Proc. Natl. Acad. Sci. U.S.A.* 116(42)**,** 20892-20897. doi: 10.1073/pnas.1909816116

Ryan, P.G., Musker, S., and Rink, A. (2014). Low densities of drifting litter in the African sector of the Southern Ocean. *Mar. Pollut. Bull.* 89(1-2)**,** 16-19. doi: 10.1016/j.marpolbul.2014.10.043.

Ryan, P.G., Pichegru, L., Perold, V., and Moloney, C.L. (2020). Monitoring marine plastics - will we know if we are making a difference? *S. Afr. J. Sci.* 116**,** 1-9. doi: 10.17159/sajs.2020/7678

Sa, S., Bastos-Santos, J., Araujo, H., Ferreira, M., Duro, V., Alves, F., et al. (2016). Spatial distribution of floating marine debris in offshore continental Portuguese waters. *Mar. Pollut. Bull.* 104(1-2)**,** 269-278. doi: 10.1016/j.marpolbul.2016.01.011.

Stocker, A.N., Renner, A.H.H., and Knol-Kauffman, M. (2020). Sea ice variability and maritime activity around Svalbard in the period 2012-2019. *Sci. Rep.* 10(1)**,** 17043. doi: 10.1038/s41598-020-74064-2.

Strand, K.O., Huserbråten, M., Dagestad, K.F., Mauritzen, C., Grøsvik, B.E., Nogueira, L.A., et al. (2021). Potential sources of marine plastic from survey beaches in the Arctic and Northeast Atlantic. *Sci. Total Environ.* 790**,** 148009. doi: 10.1016/j.scitotenv.2021.148009.

Suaria, G., and Aliani, S. (2014). Floating debris in the Mediterranean Sea. *Mar. Pollut. Bull.* 86(1-2)**,** 494-504. doi: 10.1016/j.marpolbul.2014.06.025.

Suaria, G., Avio, C.G., Mineo, A., Lattin, G.L., Magaldi, M.G., Belmonte, G., et al. (2016). The Mediterranean Plastic Soup: synthetic polymers in Mediterranean surface waters. *Sci. Rep.* 6**,** 37551. doi: 10.1038/srep37551.

Suaria, G., Melinte-Dobrinescu, M.C., Ion, G., and Aliani, S. (2015). First observations on the abundance and composition of floating debris in the North-western Black Sea. *Mar. Environ. Res.* 107**,** 45-49. doi: 10.1016/j.marenvres.2015.03.011.

Suaria, G., Perold, V., Lee, J.R., Lebouard, F., Aliani, S., and Ryan, P.G. (2020). Floating macro- and microplastics around the Southern Ocean: Results from the Antarctic Circumnavigation Expedition. *Environ. Int.* 136**,** 105494. doi: 10.1016/j.envint.2020.105494.

Tekman, M.B., Krumpen, T., and Bergmann, M. (2017). Marine litter on deep Arctic seafloor continues to increase and spreads to the North at the HAUSGARTEN observatory. *Deep-Sea Res. I: Oceanogr. Res. Pap.* 120**,** 88-99.

Tekman, M.B., Walther, B.A., Peter, C., Gutow, L., and Bergmann, M. (2022). "Impacts of plastic pollution in the oceans on marine species, biodiversity and ecosystems". , 1–221, WWF Germany, Berlin. doi: 10.5281/zenodo.5898684

Tekman, M.B., Wekerle, C., Lorenz, C., Primpke, S., Hasemann, C., Gerdts, G., et al. (2020). Tying up loose ends of microplastic pollution in the Arctic: Distribution from the sea surface through the water column to deep-sea sediments at the HAUSGARTEN observatory. *Environ. Sci. Technol.* 54(7)**,** 4079-4090. doi: 10.1021/acs.est.9b06981

Thiel, M., Hinojosa, I.A., Joschko, T., and Gutow, L. (2011). Spatio-temporal distribution of floating objects in the German Bight (North Sea). *J. Sea Res.* 65(3)**,** 368-379. doi: 10.1016/j.seares.2011.03.002.

Thomas, D.N., Arevalo-Martinez, D.L., Crocket, K.C., Grosse, F., Grosse, J., Schulz, K., et al. (2022). A changing Arctic Ocean. *Ambio* 51(2)**,** 293-297. doi: 10.1007/s13280-021-01677-w.

Thompson, R.C., Olsen, Y., Mitchell, R.P., Davis, A., Rowland, S.J., John, A.W.G., et al. (2004). Lost at sea: Where is all the plastic? *Science* 304**,** 838.

UNEP (2005). "Marine litter: an analytical overview". (Nairobi, Kenya: United Nations Environment Programme).

Unger, B., Herr, H., Viquerat, S., Gilles, A., Burkhardt-Holm, P., and Siebert, U. (2021). Opportunistically collected data from aerial surveys reveal spatio-temporal distribution patterns of marine debris in German waters. *Environ. Sci. Pollut. Res.* 28(3)**,** 2893-2903. doi: 10.1007/s11356-020-10610-9.

van Sebille, E., Aliani, S., Law, K.L., Maximenko, N., Alsina, J.M., Bagaev, A., et al. (2020). The physical oceanography of the transport of floating marine debris. *Environ. Res. Lett.* 15(2)**,** 32. doi: 10.1088/1748-9326/ab6d7d.

van Sebille, E., England, M.H., and Froyland, G. (2012). Origin, dynamics and evolution of ocean garbage patches from observed surface drifters. *Environ. Res. Lett.* 7**,** 044040. doi: 10.1088/1748-9326/7/4/044040

van Sebille, E., Wilcox, C., Lebreton, L., Maximenko, N., Hardesty, B.D., van Franeker, J.A., et al. (2015). A global inventory of small floating plastic debris. *Environ. Res. Lett.* 10(2)**,** 124006. 10.1088/1748-9326/10/12/124006

Vesman, A., Moulin, E., Egorova, A., and Zaikov, K. (2020). Marine litter pollution on the Northern Island of the Novaya Zemlya archipelago. *Mar. Pollut. Bull.* 150**,** 110671. doi: 10.1016/j.marpolbul.2019.110671.

Węsławski, J., and Kotwicki, L. (2018). Macro-plastic litter, a new vector for boreal species dispersal on Svalbard. *Pol. Polar Res.* 39**,** 165-174. doi: 10.24425/118743.

Wilson, C., Aksenov, Y., Rynders, S., Kelly, S.J., Krumpen, T., and Coward, A.C. (2021). Significant variability of structure and predictability of Arctic Ocean surface pathways

affects basin-wide connectivity. *Commun. Earth Environ.* 2(1)**,** 164. doi: 10.1038/s43247-021-00237-0.

Zeri, C., Adamopoulou, A., Bojanic Varezic, D., Fortibuoni, T., Kovac Virsek, M., Krzan, A., et al. (2018). Floating plastics in Adriatic waters (Mediterranean Sea): From the macro- to the micro-scale. *Mar. Pollut. Bull.* 136**,** 341-350. doi: 10.1016/j.marpolbul.2018.09.016.

2.2 Marine litter on deep Arctic seafloor continues to increase and spreads to the North at *the* HAUSGARTEN observatory

Mine B. Tekman[a], Thomas Krumpen[b], Melanie Bergmann[a]

[a] Alfred-Wegener-Institut, Helmholtz-Zentrum für Polar- und Meeresforschung, Am Handelshafen 12, 27570 Bremerhaven, Germany

[b]Alfred Wegener Institut, Helmholtz-Zentrum für Polar- und Meeresforschung, Bussestraße 24, D-27570 Bremerhaven

Deep Sea Research Part I: Oceanographic Research Papers, January 2017, doi: 10.1016/j.dsr.2016.12.011

Abstract

The increased global production of plastics has been mirrored by greater accumulations of plastic litter in marine environments worldwide. Global plastic litter estimates based on field observations account only for 1% of the total volumes of plastic assumed to enter the marine ecosystem from land, raising again the question 'Where is all the plastic?'. Scant information exists on temporal trends on litter transport and litter accumulation on the deep seafloor. Here, we present the results of photographic time-series surveys indicating a strong increase in marine litter over the period of 2002-2014 at two stations of the HAUSGARTEN observatory in the Arctic (2500 m depth).

Plastic accounted for the highest proportion (47%) of litter recorded at HAUSGARTEN for the whole study period. When the most southern station was considered separately, the proportion of plastic items was even higher (65%). Increasing quantities of small plastics raise concerns about fragmentation and future microplastic contamination. Analysis of litter types and sizes indicate temporal and spatial differences in the transport pathways to the deep sea for different categories of litter. Litter densities were positively correlated with the counts of ship entering harbour at Longyearbyen, the number of active fishing vessels and extent of summer sea ice. Sea ice may act as a transport vehicle for entrained litter, being released during periods of melting. The receding sea ice coverage associated with global change has opened hitherto largely inaccessible environments to humans and the impacts of tourism, industrial activities including shipping and fisheries, all of which are potential sources of marine litter.

2.2.1 Introduction

Accumulations of marine litter on beaches or coastal areas as well as deleterious effects on marine mammals, turtles, birds and, to some extent, also on fish have attracted wide public attention as they can be directly observed by stakeholders. Marine litter has been recorded from everywhere on Earth including Antarctica and the Arctic (Galgani et al., 2015), proving that even the Polar Regions, some of the remotest areas of our planet, are not immune to litter pollution. During the last decade, the number of marine litter studies has increased drastically (Ryan, 2015), in part due to the discovery of the six so called 'garbage patches' and increasing quantities of microplastics (Thompson et al., 2004). Marine litter is defined as 'any persistent, manufactured or processed solid material discarded, disposed of or abandoned in the marine and coastal environment' (UNEP, 2009), with plastic being the most common material observed due to its durability, wide usage and high disposal rates (Andrady, 2015). The spatial variability of marine litter is high, depending on population levels, coastal usage, hydrodynamics, riverine drainage and shipping traffic (Galgani et al., 2015). Latest figures indicate that the global plastic production has increased to 322 million t a^{-1} in 2015 (PlasticsEurope, 2015). The large discrepancy between global estimates of plastic litter inputs from land (Jambeck et al., 2015) and global plastic litter figures derived from field studies (Cózar et al., 2014; Eriksen et al., 2014; van Sebille et al., 2015) suggests the presence of hidden sinks of plastic in the oceans. Fragmentation into microplastics of larger fragments could be one explanation for 'missing' marine litter (van Sebille et al., 2015). Still, recent research suggests that litter is widely spread in the deep sea (Pham et al., 2014). As with microplastics, the deep-sea realm is difficult to observe, which may render this remote ecosystem another potential sink for the 'missing' amounts of litter.

More than 60% of the Earth's surface is covered with oceans deeper than 2000 m (Smith et al., 2009). Technical issues caused by extreme hydrostatic pressure as well as the causticity of the oceans (Smith et al., 2009) prevented direct observations of the deep seafloor until the late 1970s, prior to which the deep seafloor was often portrayed as a huge near lifeless desert, making it appear as a suitable place onto which to dump waste (Ramirez-Llodra et al., 2011). Even though large-scale waste disposal at sea was banned in 1972 (London Convention), the problem persists. The deep seafloor has not only already accumulated litter from the period preceding this ban but has also continued to receive waste from illegal dumping, coastal waste, riverine discharge, loss of fishing gear and maritime accidents (Ramirez-Llodra et al., 2011). The deep sea has therefore likely become one of the largest regions of marine litter

accumulation (Pham et al., 2014). Even though technological progress has eased access to the deep ocean floor and there is a growing attention paid to the ecosystem as a result of rekindled mineral exploration interests, it remains the least explored ecosystem on Earth. A number of recent studies have reported considerable amounts of litter from the deep seafloor (Bergmann and Klages, 2012; Mordecai et al., 2011; Pham et al., 2014; Ramirez-Llodra et al., 2013; Schlining et al., 2013; Tubau et al., 2015). Litter densities on the deep seafloor vary greatly depending on topography (Pham et al., 2014) and hydrodynamic conditions (Tubau et al., 2015), nearby coastal usage related with population densities (Mordecai et al., 2011), changing environmental conditions or catastrophic events (Goto and Shibata, 2015) and riverine inputs (Rech et al., 2014).

Despite the current lack of standardisation of quantification methods, it is essential to increase our knowledge base on the distribution of litter on the deep seafloor in order to be able to identify any hidden sinks and to quantify the true extent of litter in our oceans. Unfortunately, most studies report litter densities from a particular point in time, or over a rather limited time-period, which precludes the observation of any long-term trends, which are needed to assess the compliance and efficiency of regulations. Sinking rates of buoyant litter items are largely unknown, so there is potential for a delay in the arrival of such material to the seafloor. Systematic long-term observations of litter over time, analysed in the context of anthropogenic activities, the efficiency of legislation and environmental changes, will enable us to identify more accurately the possible sources, transport pathways and transport mechanisms of marine litter.

One of the few longer-term studies available (Bergmann and Klages, 2012) showed that marine litter densities had increased between 2002 and 2011 at one station of the LTER observatory HAUSGARTEN (Arctic). Here, we extend the study to include new data from a station even further to the north and from HAUSGARTEN central station after 2011 to gauge if litter densities continued to increase. This enabled us to quantify temporal and spatial variability between two stations from the latitudinal HAUSGARTEN gradient. Analysis of seafloor photographs taken between 2002 and 2014 produced data on counts, types and sizes of marine litter. In addition, we assess encounters between megafauna and litter to evaluate ecological impacts on benthic biota to fill another important knowledge gap on how such waste products may be interacted with by the marine benthic communities.

2.2.2 Material and Methods

Study site

In 1999, the Alfred Wegener Institute established the LTER (long-term ecological research) observatory HAUSGARTEN (Soltwedel et al., 2016). It is located in the eastern Fram Strait and comprises currently 21 stations along a bathymetric gradient and a latitudinal gradient. These stations are sampled annually to assess temporal variability in faunal, bacterial, biogeochemical and geological properties as well as on hydrography and sedimentation patterns that may be affected by global change. Here, we focus on two stations of the latitudinal gradient at ca. 2500 m depth: the central station HG4 and N3, located 60 km to the north (Fig. 2.2.1).

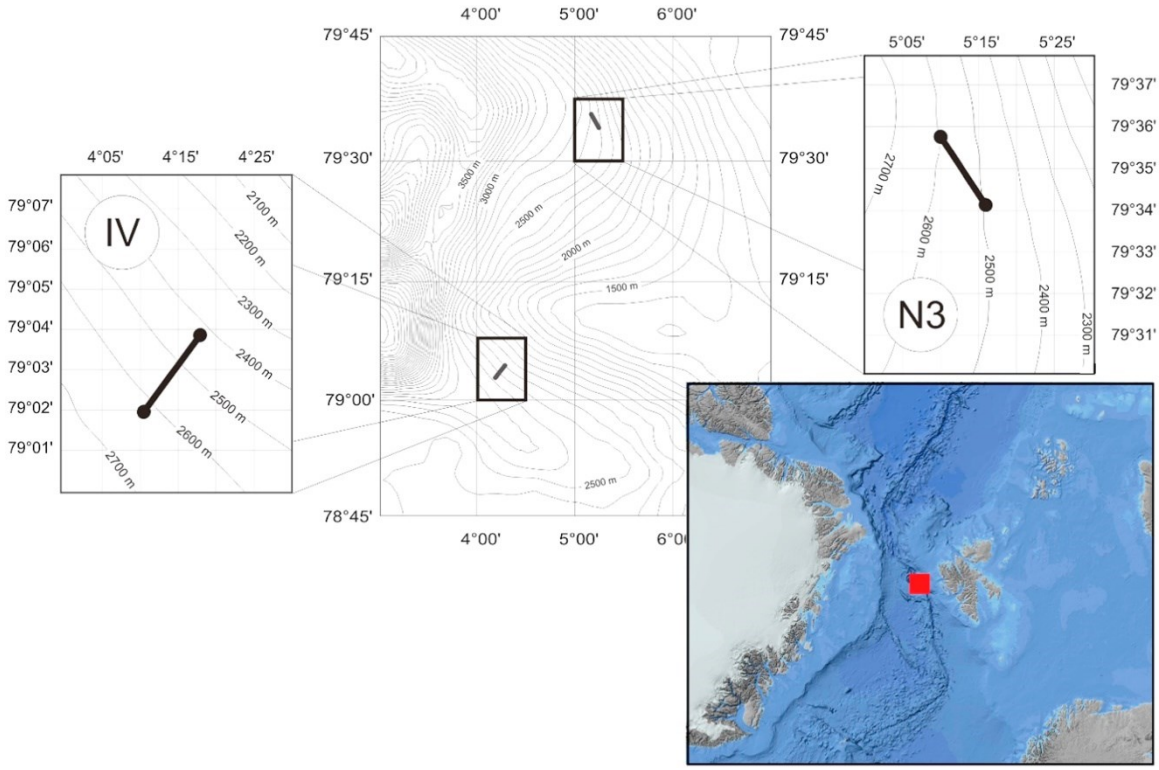

Figure 2.2.1 Positions of Ocean Floor Observation System transects at the LTER observatory HAUSGARTEN (red point indicates HAUSGARTEN observatory) (map courtesy of T. Soltwedel, AWI, produced in CorelDraw version 16, PanMAP version 0.9.6, ArcMap 10.3.1).

Photographic surveys

Photographic surveys were undertaken by a towed camera system (Ocean Floor Observation System, OFOS)(Bergmann and Klages, 2012) during expeditions in 2002 (ARK XVIII/1), 2004 (ARK XX/1), 2007 (ARK XXII/1), 2011 (ARK-XXVI/2), 2012 (ARK-XXVII/2), 2014 (ARK-XXVIII/2) of the German research ice-breaker RV *Polarstern* and RV *MS Merian* expedition in 2013 (MSM29) to the HAUSGARTEN observatory. Images were

taken along the same track at HG4 in 2012 and 2014 and at N3 in 2004, 2007, 2011, 2012, 2013 and 2014 and analysed for litter. Published data (Bergmann and Klages, 2012) from earlier HG4 transects (2002, 2004, 2007, 2011) were included in our data analysis.

Information regarding research cruises and OFOS, camera and lighting configurations for each sampling were detailed in (Bergmann and Klages, 2012; Bergmann *et al.*, 2011; Meyer *et al.*, 2013) for 2002 - 2012. The camera setup of the OFOS changed in 2014 to Canon EOS 5D Mark III (modified for underwater applications by Isitec, Germany). The OFOS lighting set-up in 2013 and 2014 comprised two Sea&Sea YS-250PRO strobes (modified by Isitec for underwater applications) and four Multi-Sealite LED Lights. Three stable laser pointers (Oktopus, Germany) produced three laser points at 50 cm distance to each other and were used as reference points for area calculations. To allow for the strobe illumination to recharge and to avoid overlap between successive images, a timer was used to take a photograph every 30 s'. Additionally, manually triggered images were taken if an object of particular interest occurred in the field of view. The OFOS was controlled by the winch operator and towed for ~4 h at ~0.5 - 0.7 knots and a target distance to the seafloor of 1,5 m although there was variation due to swell and variability in bottom topography.

Image analysis and litter identification

Images were analysed for litter using BIIGLE (Bio-Image Indexing and Graphical Labelling Environment) (Ontrup *et al.*, 2009). In total, 5,018 images were analysed for litter, 3,635 of which were taken at N3 (2004, 2007, 2011, 2012, 2013, 2014) and 1,383 images at HG4 (2012, 2014). All analyses were done in a shaded room, with the same 20'' computer monitor connected to a PC to avoid variation resulting from the resolution or brightness characteristics of differing monitors. A zoom of 120% was used and images were labeled temporarily by five parallel lines during analysis to ensure not to miss any part of the images. Firstly, all images were analysed and items which could easily be identified as litter were labeled. Moreover, any object or shape in the image which could not with certainty be evaluated as biological or environmental was labeled as possible litter item. After completing the first assessment of all images, these images with possible litter items were evaluated several times by the authors until the final decision was reached if the object should or should not be identified as litter. In cases of final uncertainty, the item was not considered as litter.

The three laser points present in each image were detected by a computer algorithm (Schoening *et al.*, 2015) and used to calculate the area covered by the image. As the distance

to the seafloor of the camera varied with bottom topography and sea swell, the area of each image varied from between 0.63 and 14.70 m^2. Images of poor quality were excluded from the analysis, as were those overlapping the previous imaged area. The longest dimension of each item was measured using the BIIGLE measurement tool and grouped into small (<10 cm), medium (10–50 cm) and large (>50 cm) size categories (Bergmann and Klages, 2012). The material comprising each item was categorised as plastic (including Polystyrene and rubber), glass, rope, timber, paper/cardboard, fabric, metal or pottery. Rope, being most likely of ship origin, was set aside as a separate category and was not categorized according to its material because even though synthetic materials are nowadays primarily being used, lost ropes may also be made from natural fibres, a distinction which could not be deduced from the images alone. Encounters with epi-benthic megafauna were noted. Fragments of the hexactinelid sponge *Caulophacus*, which were covered with sediments and were probably dead remains, were termed *Caulophacus* debris. Fauna-litter interactions were categorised as contact (i.e. entangled/entrapped/coverage/touching), colonisation and other (i.e. shrimp on litter item).

Litter density data analysis

The data from Bergmann and Klages (2012) were included in our analysis (2,134 images, 8,570 m^2) to compare spatial and temporal changes of litter at N3 and HG4 between 2002 and 2014 as a whole. However, the results from 2008 at HG4 were excluded since the laser points did not work in 2008, preventing area calculations. Data were grouped into transects/years to assess differences in mean litter densities between N3 and HG4 transects for every sampling year and between sampling years at HAUSGARTEN (N3 and HG4 combined). Each image was treated as a sample for statistical analysis. The areas of the images varied, litter count of each image was converted to litter density in items x km^{-2} by the formula $n_i \times A_i^{-1}$, where n_i is the litter count per image and A_i is the area of the image in km^2. The same dataset obtained after this conversion was used in mean, standard error calculations and statistical tests. Mean annual litter density (ALD) was calculated as ($\sum$ litter density) / N, where ($\sum$ litter density) is the sum of litter densities and N is the total number of the images per transect/year, depending on the analysis in question. Standard errors were obtained based on litter density of each image using standard routines. Similarly, litter types/sizes grouped into categories, litter densities of the images within a category were summed up and divided by total number of the images per transect/year (N) to calculate ALD of each category. Litter count per km^2 was computed by dividing the total count of litter items by the total area in km^2 of the transect/year to allow a comparison with published data relying on this method. Megafaunal interactions were used as

the number of interactions without any transformation as the data were considered as an indication of the interaction, not the species itself, and species density data were not available for all transects for such a calculation. Spatial differences in megafauna interactions were analysed by calculating percentages of the distribution.

All outputs were computed using R Studio (version 0.99.480) and R (version 3.0.3) based on ALD of every station and HAUSGARTEN. ALD of litter type and size categories per transect/year were plotted to illustrate trends in litter density. In addition, ALD of plastic litter items per transect/year were plotted according to size category to illustrate spatial and temporal changes in plastic litter item size.

The dataset was characterised by a high number of zero values as only 82 out of 7,058 images showed litter. Non-parametric tests were initially applied as the data were not normally distributed (Kolmogorov-Smirnov test, $p < 0.05$). PRIMER 6.1.16 and PERMANOVA 1.0.6 using Bray Curtis similarity of litter density with 4^{th}-root transformation was used for the analysis since PERMANOVA does not require a normal distribution in data and is insensitive to high zero counts (Anderson and Walsh, 2013). A one-way PERMANOVA was conducted to compare litter densities, size and type categories between and within stations for all transects. When a significant difference was found between transects, a pair-wise PERMANOVA was applied to compare transects.

Maritime information, sea ice extent and drift trajectories

Data for ship calls, provided by the Harbour Master of Longyearbyen (Svalbard) were analysed for temporal trends and correlations with litter density at N3, HG4 and HAUSGARTEN total. Ship calls included tourism (cruise vessels, day-tour boats, private yachts), cargo, research, fishing, navy / coastguard and Governors vessel categories between 2002 – 2014 and were plotted. The fishing category was removed from the data to eliminate overlap with the fisheries data obtained from the Norwegian Directorate of Fisheries from coastguard patrols. Fishing vessel inspection data from west Svalbard were plotted by country of origin. Since litter density data are not normally distributed, Spearman's rank correlation was used to test for a correlation with ship calls at Longyearbyen and fishing vessel sightings made during coast guard patrols.

Sea-ice extent data was provided by the Centre for Satellite Exploitation and Research (CERSAT) at the Institut Français de Recherche pour l'Exploitation de la Mer (IFREMER), France (Ezraty *et al.*, 2007). Ice extent was calculated based on the ARTIST Sea Ice (ASI)

algorithm developed at the University of Bremen, Germany (Spreen *et al.*, 2008). Sea-ice extent data from HAUSGARTEN (78.3N – 80.3N, 1.7E – 7.7E) was extracted. Mean values for summer months (May – September) between the study period 2002 – 2014 were used for Spearman's rank correlation analysis with ALD's at N3, HG4 and HAUSGARTEN total. All analyses and figures were done using R Studio (version 0.99.480) and R (version 3.0.3).

An approximation for potential source areas of sea ice passing over the HAUSGARTEN site can be obtained by tracking sea ice backward in time using a combination of low-resolution ice drift information and concentration obtained from the National Snow and Ice Data Center (NSIDC) and CERSAT (Krumpen *et al.*, 2015). Here, the tracking of ice parcels was limited to the summer months (May – September, between 2002 and 2014), when ice coverage was high enough and information on ice drift was available. Sea-ice drift trajectories and corresponding plots were produced by IDL 8.4.1 from Exelis Visual Information Solutions.

2.2.3 Result

Spatial and temporal changes in litter density.

A total area of 28,161 m^2 showed 89 litter items in 82 of 7,058 images from HAUSGARTEN total (central HG4 and northern N3 stations combined) taken between 2002 and 2014 (Table 2.2.1).

Table 2.2.1. Summary of area covered, image count, litter count, litter count per km^2, mean and standard error of litter densities at HG4, N3 and HAUSGARTEN Total (TOTAL) between 2002 and 2014.

Year	Station	Area Photographed (m^2)	Image Count	Litter Count (items)	Total Litter Items (items x km^{-2})	Mean Litter Density ± Standard error (items x km^{-2})
2002	HG4	1,926	648	7	3,635	3,523 ± 1,354
2004	N3	2,561	749	1	390	346
	HG4	2,471	658	3	1,214	1,018 ± 603
	TOTAL	5,032	1,407	4	795	660 ± 337
2007	N3	3,570	750	4	1,121	1,049 ± 546
	HG4	2,747	449	2	728	577 ± 419
	TOTAL	6,316	1,199	6	950	873 ± 376
2011	N3	1,195	302	2	1,674	1,642 ± 1,168
	HG4	1,427	379	11	7,710	7,785 ± 3,710
	TOTAL	2,622	681	13	4,959	5,061 ± 2,130
2012	N3	3,637	759	10	2,750	4,284 ± 1,739
	HG4	2,661	812	14	5,260	5,459 ± 1,495
	TOTAL	6,298	1,571	24	3,811	4,891 ± 1,141
2013	N3	2,020	536	10	4,950	4,731 ± 1,642
2014	N3	1,819	452	14	7,699	8,082 ± 2,372
	HG4	2,129	564	11	5,166	5,351 ± 1,716
	TOTAL	3,948	1,016	25	6,333	6,566 ± 1,422
2002 - 2014	N3	14,801	3,548	41	2,770	3,096 ± 567
	HG4	13,361	3,510	48	3,593	3,878 ± 660
	TOTAL	28,161	7,058	89	3,160	3,485 ± 435

Varying distances of OFOS to the seafloor during surveys resulted in image areas with a mean value of 3.99 m^2 (0.63 - 14.70 m^2). Litter items were ubiquitously distributed along the transects. Mean annual litter density (ALD) ranged between 660 (± 337 SEM) and 6,566 (± 1,422 SEM) items km^{-2}, but the two stations did not show significant spatial differences in ALD (PERMANOVA: Pseudo-F = 0.67, p = 0.4). However, there were significant temporal differences at HAUSGARTEN, the northern station N3 and the central station HG4 (PERMANOVA: Pseudo-F = 4.66, p = 0.002; Pseudo-F = 4.39, p = 0.002 and Pseudo-F = 2.19, p = 0.049, respectively), indicating an increase in litter over time (Fig. 2.2.2). At N3, ALD increased 23-fold within the timeframe of a decade (2004 – 2014), with a particularly strong

increase in 2012 (Fig. 2.2.2b). Even though significant difference was found at HG4 between years, it did not show a clearly increasing trend in observed densities (Fig. 2.2.2c).

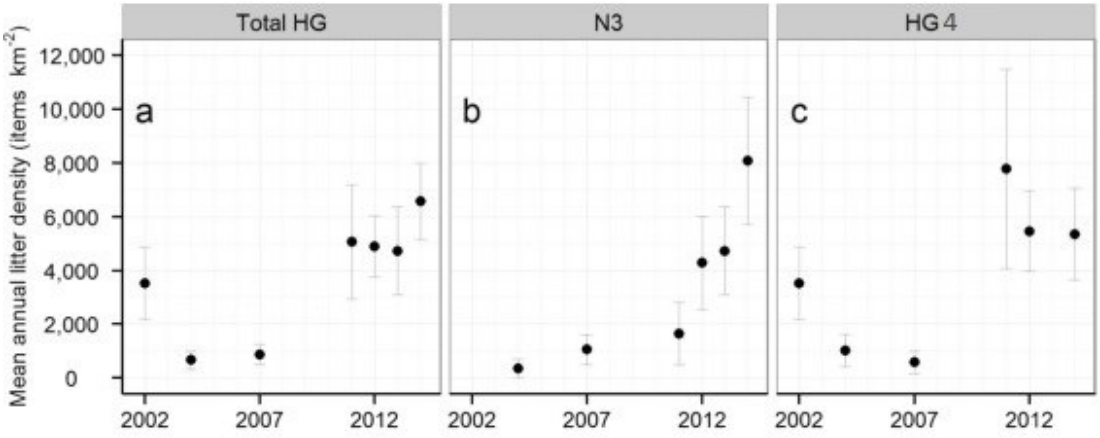

Figure 2.2.2 Mean annual litter densities (items km-2) grouped by station. Total HG represents mean annual litter densities for the two HAUSGARTEN stations combined. Error bars represent standard error of the mean.

Litter size and type

Small litter items constituted 57 % of the litter at HAUSGARTEN total, followed by medium-sized (40%) and large items (4%). Eighty percent of the litter at N3 was small-sized with a strong temporal increase from zero to 100% between 2004 and 2014 (Supporting Information (SI) Table 5.2.1). Conversely, medium-sized litter was the most abundant category at HG4 (57%). PERMANOVA indicated significant differences in the size of plastic litter items between years at N3 (Pseudo-F = 4.69, p = 0.001) but not at HG4 (Pseudo-F = 1.88, p = 0.055). If the data of the two stations were pooled, a comparison of ALD of size groups at HAUSGARTEN total indicated significant difference between years (PERMANOVA: Pseudo-F = 4.26, p = 0.002), but not between stations (PERMANOVA: Pseudo-F = 2.54, p = 0.071).

Plastic was the dominant litter type accounting for 47 % at HAUSGARTEN total, followed by glass (26%), rope (11%), metal (7%), fabric (6%), paper/cardboard, pottery and timber (4%) (Fig. 2.2.3). Annual plastic counts ranged between two and 15 items (SI, Table 5.2.2), reaching a maximum ALD of 4,060 items km^{-2} in 2014 (Fig. 2.2.3).

The comparison of ALD for the different litter types showed significant differences between stations and years at HAUSGARTEN total (PERMANOVA: Pseudo-F = 3.43, p = 0.035 and Pseudo-F = 3.70, p = 0.001, respectively). Glass items, which dominated at N3 (56%), started to appear in 2012 and increased thereafter (Fig. 2.2.3e). By contrast, a higher

proportion of plastic characterised images from HG4 (60 %), followed by rope (16%) and fabric (7 %). The contribution of litter types of N3 and HG4 to the overall HAUSGARTEN were different, 31 of the 42 plastic litter items at HAUSGARTEN were observed at HG4 (SI, Table 5.2.2).

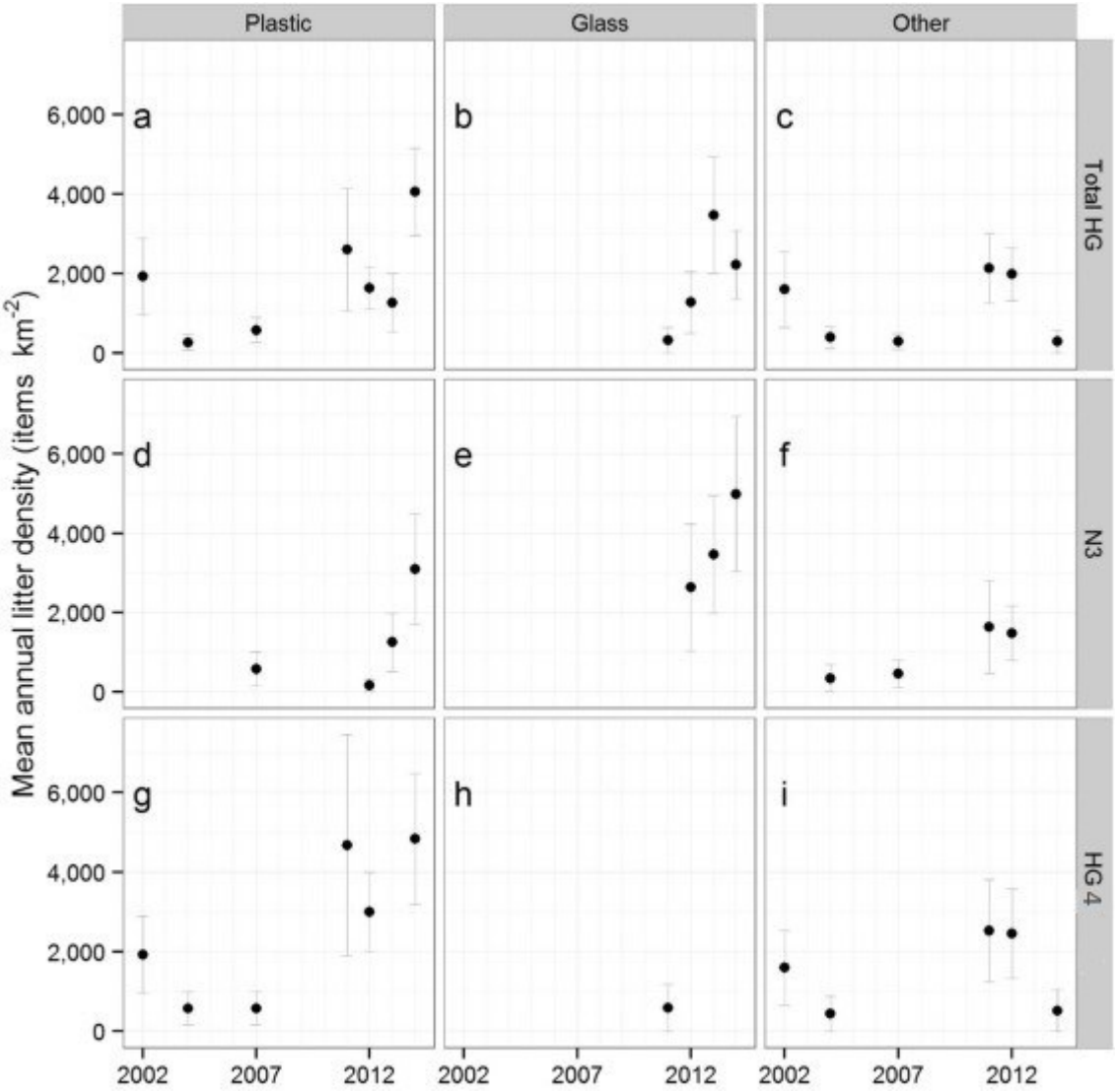

Figure 2.2.3 Mean annual litter densities (items km^{-2}) grouped by station and litter type. Total HG represents mean annual litter densities of the two HAUSGARTEN stations combined. 'Other' comprises fabric, metal, paper, pottery, rope, timber. Error bars represent standard error of the mean.

Plastic litter items were grouped separately according to their size, as this is important in the context of fragmentation into microplastics (Fig. 2.2.4). The majority of plastic items at N3 were small (Fig. 2.2.4d), whereas medium-sized plastic items dominated at HG4 (Fig. 2.2.4h).

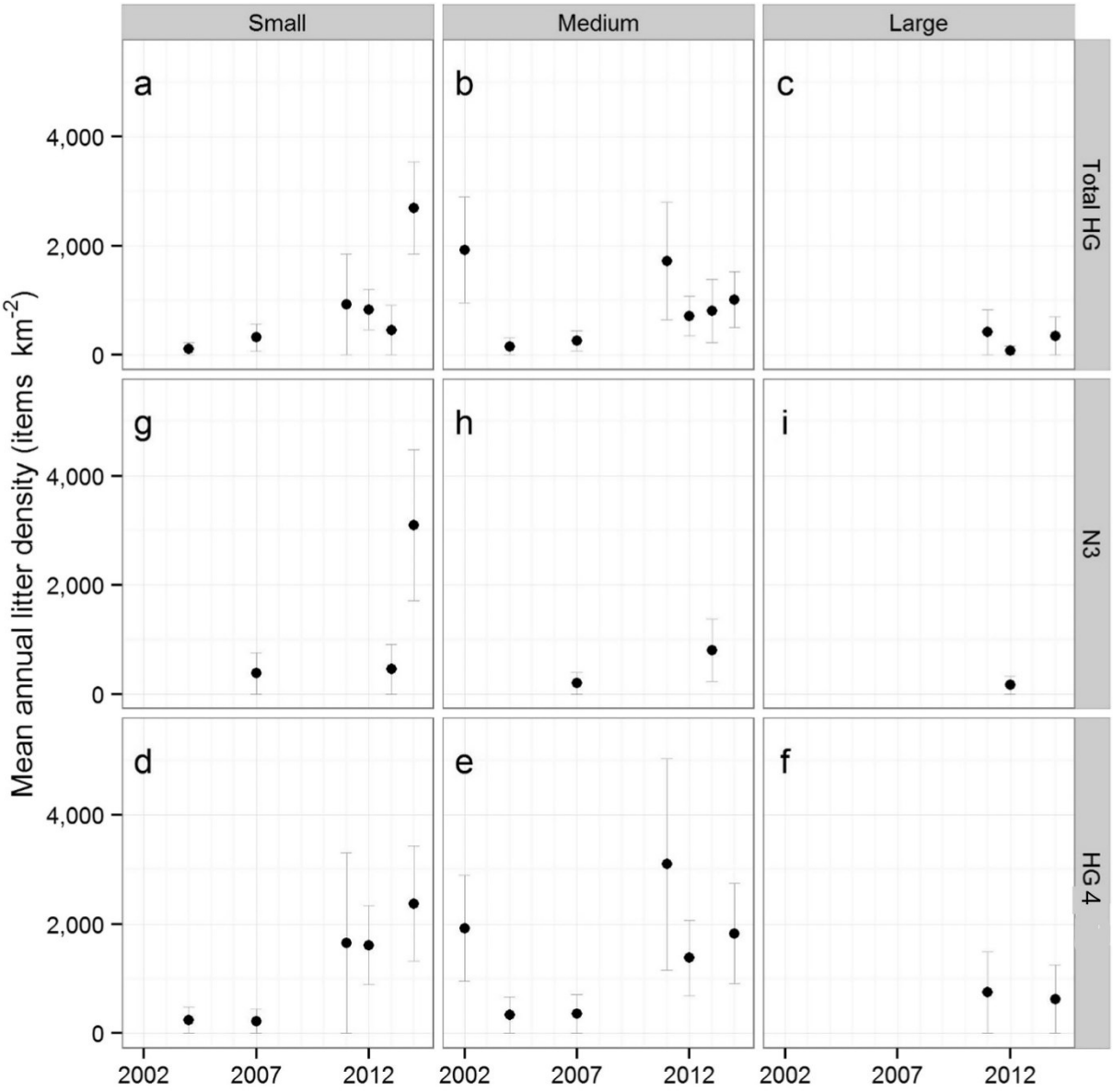

Figure 2.2.4. Mean annual litter densities (items km^{-2}) for plastic, grouped by station and item size. Total HG represents mean annual litter densities of the two HAUSGARTEN stations combined. Error bars represent standard error of the mean.

Encounters of megafauna with anthropogenic litter

Fifty of the 89 litter items observed were in some way interacting with megafauna (biota > 1.5 cm) including hydrozoans, the sponges *Cladorhiza gelida,* cf. Pachastrellidae, *Caulophacus arcticus* and *Caulophacus* debris, the stalked sea lily *Bathycrinus carpenterii*, the sea anemone cf. *Bathyphellia margaritacea* and Hormathiidae as well as shrimps (*Bythocaris* spp.) (Fig. 2.2.5 and 2.2.6). A total of 60 encounters of fauna with marine litter were observed (SI, Table 5.2.3). In some images, multiple encounters with different organisms were observed. Eighty percent of all interactions were identified as "contact" (see methods section), of which 63 % where with suspension feeders (*C. gelida, C. arcticus, B. carpenterii*). Forty-one of the 60 encounters were with plastic litter. There was a clear distinction between the two stations with regard to megafaunal encounters. The number of litter items 'associated' with megafauna was higher at HG4 compared with N3 (35 and 15, respectively), as well as the number of all types of interactions (45 and 15, respectively).

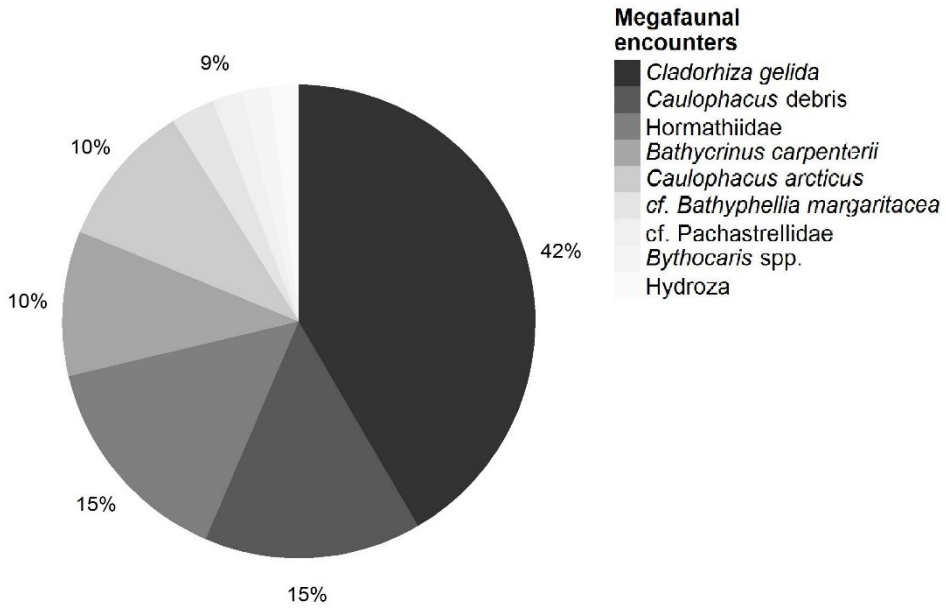

Figure 2.2.5. Proportions of epibenthic megafaunal encounters with litter items.

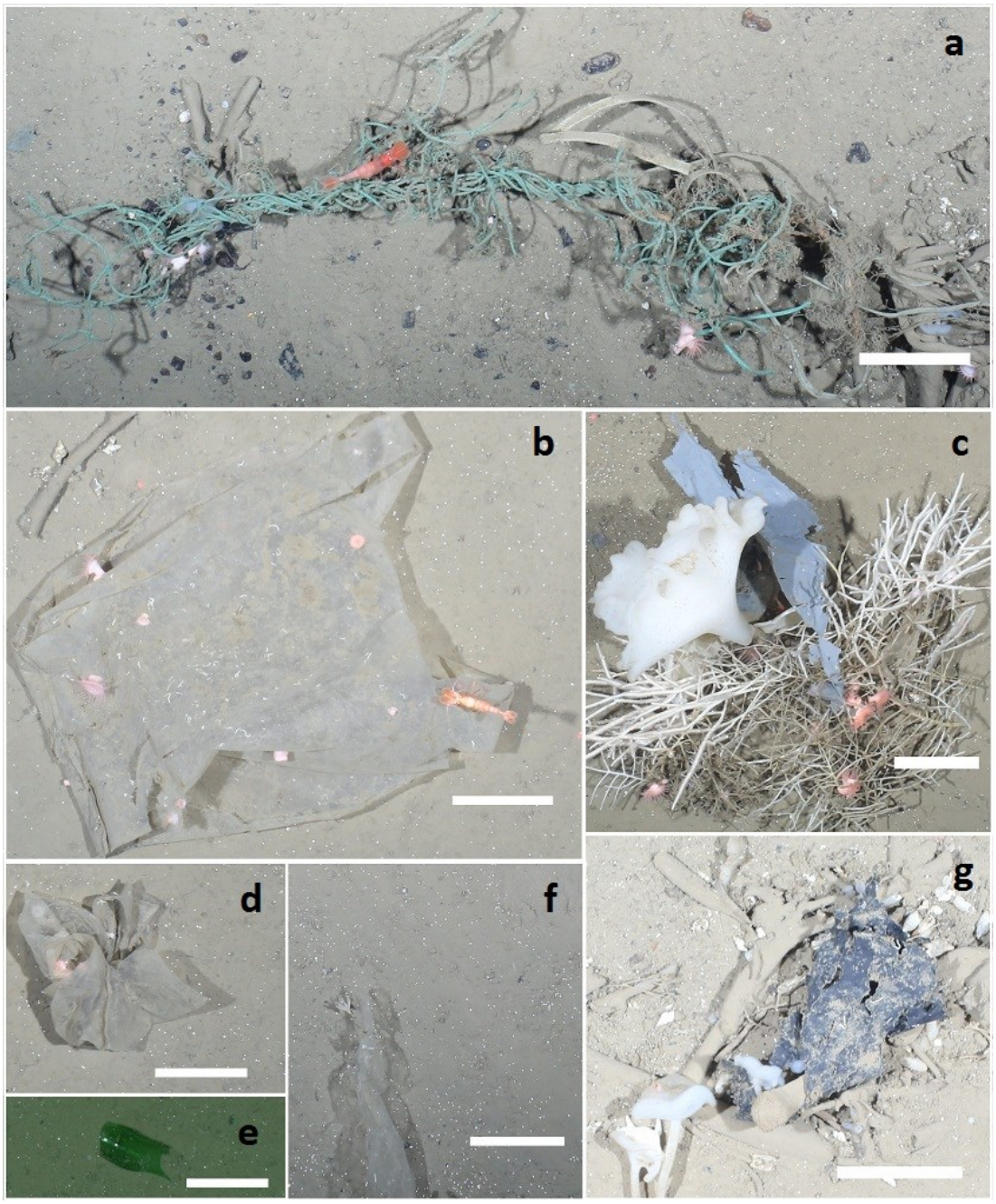

Figure 2.2.6. Sample of images with litter from HAUSGARTEN. (a) Fishing gear and plastic strips entangled with *Caulophacus* debris, colonised by *Amphianthus* sp. and held on to by *Bythocaris* sp., (b) plastic bag colonised by *Amphianthus* sp. and held on to by *Bythocaris* sp., (c) plastic fragments entangled with *C. arcticus* and *C. gelida*, (d) plastic bag/fragment buried partly into sediment and colonised by *Amphianthus* sp., (e) piece of glass bottle, (f) plastic fragment entangled with *B. carpenterii*, (g) piece of fabric entangled with *Caulophacus* debris. Scale bars represent 10 cm.

Maritime traffic, summer sea-ice extent and trajectories

Analysis of annual maritime data and mean litter density indicate significant positive correlations between litter densities at N3 and total ship counts (harbour ship calls and fishing vessel sighting counts combined: $\rho = 0.94$, p = 0.017), total harbour ship calls ($\rho = 0.94$, p = 0.017) and tourism vessel harbour calls ($\rho = 1$, p = 0.003). Litter densities at HAUSGARTEN total were also positively correlated with total ship counts ($\rho = 0.89$, p = 0.012), total harbour ship calls ($\rho = 0.79$, p = 0.048), other-category ship harbour calls ($\rho = 0.89$, p = 0.012), and the number of docking days of tourism vessels ($\rho = 0.86$, p = 0.023). While our figures imply a general increase in maritime traffic in the area over time, the increase in tourism and fishing vessels sightings west off Svalbard showed the strongest increase among maritime traffic information (Fig. 2.2.7).

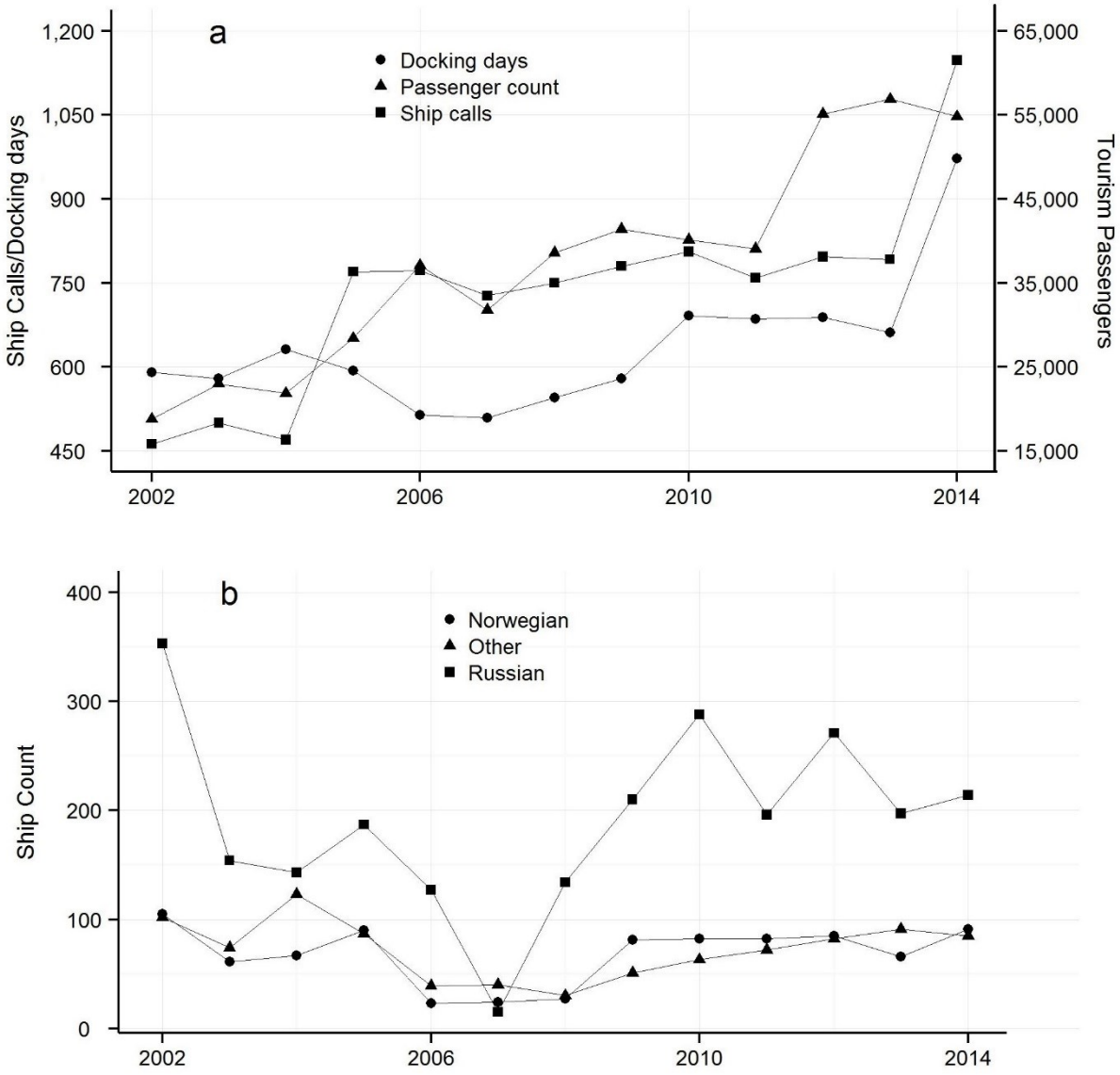

Figure 2.2.7. Temporal trends in tourism and shipping between 2002 and 2014 around the LTER observatory HAUSGARTEN. (a) Annual ship arrivals (tourism, cargo, research, navy / coastguard, governor vessel), docking days and tourism passenger counts at the harbour of Longyearbyen (Svalbard) between 2002 and 2014 (source: Harbourmaster of Longyearbyen). (b) Annual counts of fishing vessel sightings west of Svalbard recorded during patrols by Svalbard's coastguard (source: Norwegian Directorate of Fisheries).

The mean summer sea-ice extent between 2002 – 2014 was also positively correlated with litter densities at N3 (ρ = 0.83, p = 0.042). Drift trajectories indicated that the sea ice above HAUSGARTEN had its origin in the Laptev and Kara Seas (Fig. 2.2.8).

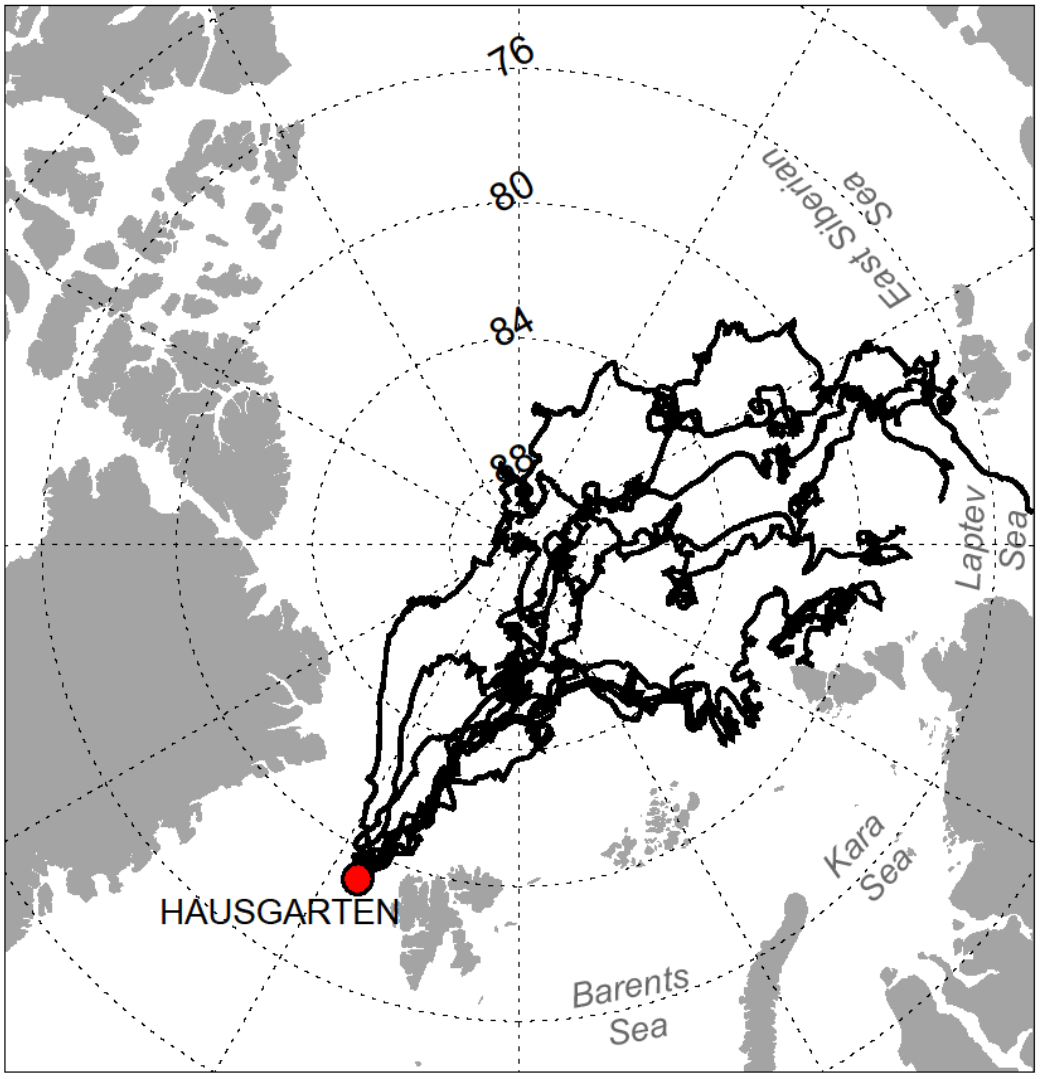

Figure 2.2.8. Drift trajectories and source areas of sea ice tracked backward in time starting from the HAUSGARTEN observatory (red dot).

2.2.4 Discussion

Our data show that litter densities at HAUSGARTEN have continued to increase after 2011 (Bergmann and Klages, 2012). The fact that a similar trend was observed at another station further north indicates that the earlier results were not an outlier but that the region is facing a pollution problem and that there is reason for real concern: in 2014, the mean litter density at HAUSGARTEN reached 6,566 items km^{-2}, similar to litter densities reported from the Lisbon Canyon (6,620 items km^{-2}) (Mordecai *et al.*, 2011), which is in close vicinity to the densely populated capital Lisbon. From the Atlantic and Indian Ocean seafloor, 480 and 550 items km^{-2} were reported during ROV dives in 2011 and 2013 (Woodall *et al.*, 2015), whereas our figures from 2011 and 2013 indicate 4,600 items km^{-2}. Considering the remote location of the stations at HAUSGARTEN, the high density of litter found at HAUSGARTEN is surprising.

Quantification of litter is often not the main target of field work, but is carried out as an additional task to complement another focus of research (Ramirez-Llodra *et al.*, 2011; Spengler and Costa, 2008). Although type and size of each litter item, litter count and density in items per area have been indicated as basic requirements of standards for marine litter studies (Spengler and Costa, 2008), sampling and analysis methods still lack standardisation, even in this primary area. Imaging surveys yield indirect samples as images or video footages introducing the challenge of quantification and qualification. Litter items buried in the sediment could easily be missed in imaging surveys, as can small and ambiguous items. Technological advances have led to an increasing number of imaging survey studies on litter on the deep seafloor. However, financial, logistical and technical limitations still restrict the area surveyed in deep-sea research. While calculating litter densities per km^2 in trawl, sea surface or beach sampling studies does not necessarily imply extrapolations due to large survey areas, the same method would lead to bias in deep-sea debris studies. Therefore, it should be noted that litter densities given in this study should not be considered as extrapolations or actual amounts, instead, they are transformations of litter counts into area (Spengler and Costa, 2008). For the reasons outlined above, when calculated litter densities are taken into account directly as actual litter densities, it may lead under- or overestimation of marine litter at HAUSGARTEN.

Until the 1990s, there was an ongoing increase in the quantities of plastic litter entering into the open ocean, with this flux stabilising in the 1990s, though increasing coastal litter quantities continued to be recorded (Barnes *et al.*, 2009). Either litter has been washed up to the coastal areas, or it sank to the deep seafloor unnoticed. In addition, plastic litter may

fragment into smaller pieces (microplastic), which cannot be observed directly. With a growing focus on microplastic research, more studies have emerged describing the potential fragmentation mechanisms, pathways and sinks and evidence suggest an increase in microplastics (Thompson *et al.*, 2004). Contrary to the common notion that most plastic litter floats at the sea surface, 50 % of plastic from municipal waste sources has a higher density than seawater and can thus sink directly to the seafloor (Engler, 2012). Solar radiation and heat cause fragmentation of plastic into smaller pieces aided by wind and wave actions. Biofilm formation on the plastic surface can slow down degradation processes (O'Brine and Thompson, 2010). Regardless of density, plastic fragments can still be transported by currents (Engler, 2012). Additionally, hydrographic processes such as vertical mixing (Kukulka *et al.*, 2012) and deep-water cascading events (Tubau *et al.*, 2015) may play a significant role in the distribution of plastic and may have aided transport of plastic litter to the deep Arctic seafloor. Indeed, a cascading event was reported in 2002 (Wobus *et al.*, 2013) which may explain the relatively high quantities of litter at the central HAUSGARTEN station in 2002 at the beginning of our time series. On the deep seafloor, low temperatures and the absence of solar radiation and strong wave action may cause plastic to be even more persistent than in shallower areas (Andrady, 2015), which can lead to relatively higher densities of plastic litter on the deep Arctic seafloor compared with other locations.

Previous studies have shown that the highest densities of litter on the seafloor are found in submarine canyons, driven by their associated hydrodynamic regime (Mordecai *et al.*, 2011; Ramirez-Llodra *et al.*, 2013; Tubau *et al.*, 2015), followed by seamounts, banks, mounds, continental slopes and ocean ridges (Galgani *et al.*, 2015; Pham *et al.*, 2014). Although the two HAUSGARTEN stations only represent open-slope environments, the litter densities in 2011 at HG4 and in 2014 at N3 were close to 8,000 items km^{-2}. This is a figure similar to one of the highest litter densities ever reported from the deep seafloor, in La Fonera and Cap de Creus canyons (NW Mediterranean), with litter densities of ~15,000 and ~8,000 items km^{-2}, respectively (Tubau *et al.*, 2015). There is a general consensus that land-based inputs are the prime sources of marine litter (Barnes and Milner, 2005; Galgani *et al.*, 2000; Mordecai *et al.*, 2011; Pham *et al.*, 2014). However, it was concluded that the strong increase in litter densities at HAUSGARTEN after 2008 were unlikely to be caused by direct terrestrial inputs from Svalbard, whose population decreased during that time (Bergmann and Klages, 2012). If the litter from HAUSGARTEN is of terrestrial origin, it probably entered into the Atlantic or North Sea and was transported by currents over long distances to the North (Bergmann and Klages,

2012) as supported by recent evidence from model projections (van Sebille *et al.*, 2016). Marine litter is known to travel long distances; bivalves from SE USA or the Caribbean have been found on plastic jars on British and Irish coasts, proving their long trans-Atlantic journey (Holmes *et al.*, 2015). Most of the litter observed at HAUSGARTEN could not be clearly allocated to any particular industrial sector, looking more like general household litter, which matches findings from the Atlantic (Woodall *et al.*, 2015).

Surface currents converge in specific locations because of wind and geostrophic forces. To date, five such convergence zones have been identified as accumulation areas of marine litter, so-called 'garbage patches', which match subtropical convergence zones and harbour very high litter quantities (Maximenko *et al.*, 2012). In the context of our results, the projection of a sixth garbage patch in the Barents Sea, fed by litter from the North Atlantic (van Sebille *et al.*, 2012), is particularly striking as it could explain increasing litter densities further north in the HAUSGARTEN area. Indeed, microplastic concentrations from the nearby Barents Sea surface resembled quantities reported from the North Pacific (Lusher *et al.*, 2015) and corroborate this projection. Floating litter was also recently reported in the Fram Strait and Barents Sea (Bergmann *et al.*, 2015). Although strictly speaking the data are not comparable because of important differences in the methodology adopted, the density of floating litter was 1-2 orders of magnitude lower compared with litter on the seafloor in the same area, indicating that the seafloor may act as a sink for litter.

There are only very few long-term studies for inter-annual variation of litter from deep-sea regions. Most of these are based on specific sampling times. However, a study from the Pacific coast off northern Japan (Goto and Shibata, 2015) showed a two- to six-fold increase in litter densities from 54 – 94 items km^{-2} in the 2003/2004 period to 233 – 332 items km^{-2} in 2011 after the Tohoku earthquake and tsunami. Intriguingly, our results indicate a much higher increase in mean litter densities at HAUSGARTEN for the same years, without any known catastrophic event. On the contrary, recent time-series studies of litter from other marine ecosystems do not indicate any clear temporal trends. Figures for litter from the open NW Atlantic (Moret-Ferguson *et al.*, 2010) did not show any temporal increase in litter counts, nor did those from SE North Sea coasts and beaches (Schulz *et al.*, 2015a; Schulz *et al.*, 2015b). Still, litter density at the central HAUSGARTEN station almost doubled in 2011 compared to 2002, and there is a clear peak in 2014 at the northern station. So, what factors could have driven this strong increase in litter?

Maritime activities including fisheries have been indicated as one of the main sources of anthropogenic litter in various studies (Pham *et al.*, 2014; Ramirez-Llodra *et al.*, 2013; Vieira *et al.*, 2015). Data for ship calls at Longyearbyen can be considered as an indicator of maritime traffic west of Svalbard, although these ships may not necessarily have passed HAUSGARTEN, or there may be ships operating in the area that have not called at Longyearbyen. Interestingly, even though N3 is located in the marginal ice zone, the strong correlation between tourism ship counts and litter densities at N3 may imply tourism activities around Svalbard as a possible source of anthropogenic litter. Touristic areas generate up to 40 % more marine litter on beaches during summer. (Galgani *et al.*, 2015). It should be noted, however, that a strong correlation between tourism ship counts and litter densities indicating a similar increase over time, does not necessarily mean increasing litter discharges from ships. On the other hand, one cruise ship of 2500 passengers and 800 crew can generate 1 ton of solid waste in a day (National Research Council, 1995) and even though most of the vessels probably strictly abide with regulations, accidental loss of solid waste from such a quantity of garbage may be inevitable. Unfortunately, it is difficult to obtain precise information for fishing activities in the area, as there is no obligation for vessels to report their activity outside the 12-nm limit and Automatic Identification System (AIS) data from the Norwegian satellite AISSAT-1 only commenced in 2011. However, counts of sightings during coastguard patrols indicate a strong increase in fishing activities west of Svalbard from 47 sightings in 2002 to 102 in 2014. Additionally, evidence from the programme 'Clean Up Svalbard' suggests that a great proportion of washed-up litter originates from fisheries (Governor of Svalbard, unpubl. data). The positive correlation between litter densities and total ship counts indicates that the increased presence of ships west of Svalbard has contributed to the increased litter densities observed at HAUSGARTEN.

Between 2000 and 2013, mean sea-ice thickness has decreased by 0.58 m (Lindsay and Schweiger, 2015) and sea-ice extent measured in the month of September has decreased by 24 % decade^{-1} (Meier *et al.*, 2014) in the Arctic. These changes may affect the temporal and spatial variability of litter at HAUSGARTEN. The Fram Strait is the only place for intermediate and deep-water mass exchange between the North Atlantic and the Arctic Ocean (Fahrbach *et al.*, 2001; Rudels *et al.*, 2000). The inflow of warm Atlantic water from Nordic Seas into the central Arctic Ocean characterises the water masses. The eastern and western currents meet at the East Greenland Polar Front (Soltwedel *et al.*, 2016). These dynamic currents also affect the sea-ice cover: while the western areas are covered with ice year-round, the south-eastern areas are ice-

free and changing ice cover is observed in the central and NE Fram Strait depending on the season. The northern station in our HAUSGARTEN study, which is located within the marginal ice zone, saw an extensive increase in litter density, especially in the amount of small-sized plastic and glass litter, between 2004 and 2014. The decreased ice cover could have allowed more maritime activities in the area, which may have played an indirect role in the increase of litter. This explanation is supported by the correlation found between shipping and litter density. Since glass can be assumed to sink quickly to the seafloor close to its entry point, the high density of glass at the northern station in recent years proves increasing ship traffic in the marginal ice zone and indicates ships as sources. Glass items were seen at the northern HAUSGARTEN in the last three years of the study only. It should be noted that the disposal of glass in this area was only prohibited by MARPOL in 2013.

Recent research suggests that sea ice is an important sink of microplastic (Obbard *et al.*, 2014). Drift ice in the Arctic Ocean is known to contain ice-rafted debris, driftwood and biota (Johansen and Hytteborn, 2001). Indeed, debris and driftwood were analysed to assess their origin and transportation pathways in several studies. It was shown that driftwood came from Siberian rivers pouring their waters into the Kara Sea, where they were entrained in drift ice (Johansen, 1999). Most debris on the Arctic seafloor originates from shelf areas (Nurnberg *et al.*, 1994), river discharges and from terrestrial sources transported by winds. Even though ice-rafted debris mostly comprises fine-grained small-sized particulate matter, up to 8 mm carbonate minerals in many shapes were observed in the samples from particle traps in the eastern Fram Strait, whose source was rafting ice (Sanchez-Vidal *et al.*, 2015). Unlike driftwood or particle trap samples, image surveys do not generate physical samples, which prevented the assessment of source and transportation pathways. However, our results indicated positive correlation between litter and summer sea ice extent and the drift trajectories concur with an earlier study based on driftwood specimen analysis (Johansen, 1999). Along with the finding of sea ice trapping microplastic, it can be suggested that the presence of sea ice probably facilitates the release of plastic litter entrained in drifting sea ice upon melting, which may partly explain the observed increase in smaller plastic items at the northern station.

Impacts of marine litter, plastics in particular, on ‘charismatic megafauna’ such as turtles, marine birds, mammals or fishes have been relatively well documented compared to on other biota (Kühn *et al.*, 2015) . Deep-sea ecosystems are still poorly known, thus, it is not surprising that studies about the impacts of marine litter on deep-sea fauna are scarce (but see (Bergmann and Klages, 2012; Fabri *et al.*, 2014; Mordecai *et al.*, 2011; Taylor *et al.*, 2014)).

One of the reasons for the scarcity of these studies may be that only camera-based methods show litter *in situ* with species. Our study showed a high proportion of megafaunal encounters with litter, particularly with suspension feeders. Surprisingly, the encounter rate was higher at the central station compared with the northern one, despite the fact that the northern station harbours a significantly higher megafaunal stock, including the sponges *C. gelida* and *C. arcticus* (Taylor *et al.*, 2016), in which most litter items were entangled. On the contrary, a long-term litter study in Monterey Canyon (California) showed that litter was used primarily as shelter or hard substratum for settlement by hydroids, anemones, asteroids, serpulid worms, crinoids, holothurians and rockfish (Schlining *et al.*, 2013). Most interaction with megafauna was reported as 'simple' entanglement in other deep-sea studies (Pham *et al.*, 2013; Woodall *et al.*, 2015). Entanglement can cause abrasion and necrosis of tissue increasing the risk of predation or infection (Chiappone *et al.*, 2005). Although several studies showed toxic leaching of additives to marine animals in laboratory studies (Browne *et al.*, 2013; Lithner *et al.*, 2011), in situ concentrations in marine environments, pathways into the marine food web and consequences to human health is not yet clear. Plastic was more often colonised by actinians at HAUSGARTEN than other litter items, which may be due to the material's long persistence. Marine litter provides hard substratum for sessile organisms to settle on, which could be considered a positive effect on muddy or sandy ecosystems with few hard substrata available. However, a study of litter that was experimentally deployed on the Greek seafloor showed that it altered both species abundance and community structure (Katsanevakis *et al.*, 2007). Increasing litter quantities thus raise questions about effects on biodiversity. During our study, some plastic items were also observed covering sediments. A study in intertidal sediments has shown that plastic covering sediments caused anoxic conditions in the sediment underneath, reduced primary production, organic matter and the number of infaunal invertebrates (Green *et al.*, 2015). Such changes in ecosystem composition and function may occur in deep-sea communities, too.

2.2.5 Conclusions

Our findings indicate that the Arctic faces a pollution problem and that it is spreading to the north. Litter densities at HAUSGARTEN were substantially higher compared with other locations, despite its remote location. Small-sized plastics increased in observed abundance between 2002 and 2014, which indicates fragmentation of plastic litter and raises concerns about contamination by microplastics. Increasing quantities of litter from northern Europe may drift to the North and the receding sea ice has opened hitherto largely inaccessible

environments to human activities, including shipping, fisheries and tourism. Considering the variety of matter transported by drift ice, increasing amount of plastic items at HAUSGARTEN in recent years raises the question if sea ice is a transport vehicle also for plastic. Whatever the causes, the present study highlights once more that our current waste management frameworks are inadequate to tackle the problem of marine litter pollution and that we have to re-think our usage of plastic materials. Considering the importance of the Arctic region for global climate and ecosystem health, identifying the changes in anthropogenic stress and its direct or indirect sources provide information for future projections to regulate human activities.

2.2.6 Acknowledgements

The authors thank the crew of RVs Polarstern and MS Merian, B. Sablotny, T. Soltwedel, I. Schewe, J. Taylor, E. Bauerfeind, R. Degen, and the HGF-MPG Group for Deep-Sea Ecology and Technology of AWI in general for gathering the data and support needed for the analysis of the data during this study. C. Hasemann gave valuable advice on statistical data analysis. T. Soltwedel kindly provided a map of the study area (Fig. 2.2.1). The authors thank the Harbour Master of Longyearbyen, K. Bråten, for sharing information about ship calls, P. Finne from FMC Norway Directorate of Fisheries for providing VMS and inspection data of fishing vessels and D. Langenkämper for BIIGLE user support.

MB was funded by the Helmholtz Alliance ROBEX (Robotic Exploration of Extreme Environments), and this study contributes to the Pollution Observatory of the Helmholtz-funded programme FRAM (Frontiers in Arctic Marine Research). This publication is Eprint ID 31691 of the Alfred-Wegener-Institut, Helmholtz-Zentrum für Polar- und Meeresforschung.

2.2.7 References

"Clean Up Svalbard" Oceanwide Expeditions [Online]. Available: https://oceanwide-expeditions.com/partner/sval [Accessed August 08, 2022].

Anderson, M.J., and Walsh, D.C.I. (2013). PERMANOVA, ANOSIM, and the Mantel test in the face of heterogeneous dispersions: What null hypothesis are you testing? *Ecol. Monogr.* 83(4), 557-574. doi: 10.1890/12-2010.1.

Andrady, A.L. (2015). "Persistence of Plastic Litter in the Oceans," in *Marine Anthropogenic Litter*, eds. M. Bergmann, L. Gutow & M. Klages. (Berlin: Springer), 57-72.

Barnes, D.K., Galgani, F., Thompson, R.C., and Barlaz, M. (2009). Accumulation and fragmentation of plastic debris in global environments. *Philos. Trans. R. Soc. Lond.*, B, Biol. Sci. 364(1526), 1985-1998. doi: 10.1098/rstb.2008.0205.

Barnes, D.K.A., and Milner, P. (2005). Drifting plastic and its consequences for sessile organism dispersal in the Atlantic Ocean. *Mar. Biol.* 146(4), 815-825. doi: 10.1007/s00227-004-1474-8.

Bergmann, M., and Klages, M. (2012). Increase of litter at the Arctic deep-sea observatory HAUSGARTEN. *Mar. Pollut. Bull.* 64(12), 2734-2741. doi: 10.1016/j.marpolbul.2012.09.018.

Bergmann, M., Sandhop, N., Schewe, I., and D'Hert, D. (2015). Observations of floating anthropogenic litter in the Barents Sea and Fram Strait, Arctic. *Polar Biol.* 39(3), 553-560. doi: 10.1007/s00300-015-1795-8.

Bergmann, M., Soltwedel, T., and Klages, M. (2011). The interannual variability of megafaunal assemblages in the Arctic deep sea: Preliminary results from the HAUSGARTEN observatory (79 degrees N). *Deep Sea Res. Part I Oceanogr. Res. Pap.* 58(6), 711-722. doi: 10.1016/j.dsr.2011.03.007.

Browne, M.A., Niven, S.J., Galloway, T.S., Rowland, S.J., and Thompson, R.C. (2013). Microplastic moves pollutants and additives to worms, reducing functions linked to health and biodiversity. *Curr. Biol.* 23(23), 2388-2392. doi: 10.1016/j.cub.2013.10.012.

Chiappone, M., Dienes, H., Swanson, D.W., and Miller, S.L. (2005). Impacts of lost fishing gear on coral reef sessile invertebrates in the Florida Keys National Marine Sanctuary. *Biol. Conserv.* 121(2), 221-230. doi: 10.1016/j.biocon.2004.04.023.

Cózar, A., Echevarria, F., Gonzalez-Gordillo, J.I., Irigoien, X., Ubeda, B., Hernandez-Leon, S., et al. (2014). Plastic debris in the open ocean. *Proc. Natl. Acad. Sci. U.S.A.* 111(28), 10239-10244. doi: 10.1073/pnas.1314705111.

Engler, R.E. (2012). The complex interaction between marine debris and toxic chemicals in the ocean. *Environ. Sci. Technol.* 46(22), 12302-12315. doi: 10.1021/es3027105.

Eriksen, M., Lebreton, L.C., Carson, H.S., Thiel, M., Moore, C.J., Borerro, J.C., et al. (2014). Plastic Pollution in the World's Oceans: More than 5 Trillion Plastic Pieces Weighing over 250,000 Tons Afloat at Sea. *PLoS One* 9(12), e111913. doi: 10.1371/journal.pone.0111913.

Ezraty, R., Girard-Ardhuin, F., Pioll, J.F., Kaleschke, L., and Heygster, G. (2007). "Arctic and Antarctic sea ice concentration and Arctic sea ice drift estimated from Special Sensor Microwave Imager data. User's manual, Version 2.1".).

Fabri, M.C., Pedel, L., Beuck, L., Galgani, F., Hebbeln, D., and Freiwald, A. (2014). Megafauna of vulnerable marine ecosystems in French mediterranean submarine canyons: Spatial distribution and anthropogenic impacts. *Deep Sea Res. Part II Top. Stud. Oceanogr.* 104(0), 184-207. doi: 10.1016/j.dsr2.2013.06.016.

Fahrbach, E., Meincke, J., Osterhus, S., Rohardt, G., Schauer, U., Tverberg, V., et al. (2001). Direct measurements of volume transports through Fram Strait. *Polar Res.* 20(2), 217-224. doi: DOI 10.1111/j.1751-8369.2001.tb00059.x.

Galgani, F., Hanke, G., and Maes, T. (2015). "Global distribution, composition and abundance of marine litter," in *Marine Anthropogenic Litter*, eds. M. Bergmann, L. Gutow & M. Klages. (Berlin: Springer), 29-56.

Galgani, F., Leaute, J.P., Moguedet, P., Souplet, A., Verin, Y., Carpentier, A., et al. (2000). Litter on the sea floor along European coasts. *Mar. Pollut. Bull.* 40(6), 516-527. doi: Doi 10.1016/S0025-326x(99)00234-9.

Goto, T., and Shibata, H. (2015). Changes in abundance and composition of anthropogenic marine debris on the continental slope off the Pacific coast of northern Japan, after the March 2011 Tohoku earthquake. *Mar. Pollut. Bull.* 95(1), 234-241. doi: 10.1016/j.marpolbul.2015.04.011.

Green, D.S., Boots, B., Blockley, D.J., Rocha, C., and Thompson, R. (2015). Impacts of discarded plastic bags on marine assemblages and ecosystem functioning. *Environ. Sci. Technol.* 49(9), 5380-5389. doi: 10.1021/acs.est.5b00277.

Holmes, A.M., Oliver, P.G., Trewhella, S., Hill, R., and Quigley, D.T.G. (2015). Trans-Atlantic Rafting of Inshore Mollusca on Macro-Litter: American Molluscs on British and Irish Shores, New Records. *J. Conchol.* 42(1), 41-49.

Jambeck, J.R., Geyer, R., Wilcox, C., Siegler, T.R., Perryman, M., Andrady, A., et al. (2015). Marine pollution. Plastic waste inputs from land into the ocean. *Science* 347(6223), 768-771. doi: 10.1126/science.1260352.

Johansen, S. (1999). Origin of driftwood in north Norway and its relevance for transport routes of drift ice and pollution to the Barents Sea. *Sci. Total Environ.* 231(2-3), 201-225. doi: 10.1016/s0048-9697(99)00101-1.

Johansen, S., and Hytteborn, H. (2001). A contribution to the discussion of biota dispersal with drift ice and driftwood in the North Atlantic. *J. Biogeogr.* 28(1), 105-115. doi: DOI 10.1046/j.1365-2699.2001.00532.x.

Katsanevakis, S., Verriopoulos, G., Nicolaidou, A., and Thessalou-Legaki, M. (2007). Effect of marine litter on the benthic megafauna of coastal soft bottoms: a manipulative field experiment. *Mar. Pollut. Bull.* 54(6), 771-778. doi: 10.1016/j.marpolbul.2006.12.016.

Krumpen, T., Gerdes, R., Haas, C., Hendricks, S., Herber, A., Selyuzhenok, V., et al. (2015). Recent summer sea ice thickness surveys in the Fram Strait and associated volume fluxes. *The Cryosphere Discuss.* 9(5), 5171-5202. doi: 10.5194/tcd-9-5171-2015.

Kühn, S., Bravo Rebolledo, E.L., and van Franeker, J.A. (2015). "Deleterious effects of litter on marine life," in *Marine Anthropogenic Litter*, eds. M. Bergmann, L. Gutow & M. Klages. (Berlin: Springer), 75-116.

Kukulka, T., Proskurowski, G., Morét-Ferguson, S., Meyer, D.W., and Law, K.L. (2012). The effect of wind mixing on the vertical distribution of buoyant plastic debris. *Geophys. Res. Lett.* 39(7), n/a-n/a. doi: 10.1029/2012gl051116.

Lindsay, R., and Schweiger, A. (2015). Arctic sea ice thickness loss determined using subsurface, aircraft, and satellite observations. *Cryosphere* 9(1), 269-283. doi: 10.5194/tc-9-269-2015.

Lithner, D., Larsson, A., and Dave, G. (2011). Environmental and health hazard ranking and assessment of plastic polymers based on chemical composition. *Sci. Total Environ.* 409(18), 3309-3324. doi: 10.1016/j.scitotenv.2011.04.038.

Lusher, A.L., Tirelli, V., O'Connor, I., and Officer, R. (2015). Microplastics in Arctic polar waters: the first reported values of particles in surface and sub-surface samples. *Sci. Rep.* 5, 14947. doi: 10.1038/srep14947.

Maximenko, N., Hafner, J., and Niiler, P. (2012). Pathways of marine debris derived from trajectories of Lagrangian drifters. *Mar. Pollut. Bull.* 65(1-3), 51-62. doi: 10.1016/j.marpolbul.2011.04.016.

Meier, W.N., Hovelsrud, G.K., van Oort, B.E.H., Key, J.R., Kovacs, K.M., Michel, C., et al. (2014). Arctic sea ice in transformation: A review of recent observed changes and impacts on biology and human activity. *Rev. Geophys.* 52(3), 185-217. doi: 10.1002/2013RG000431.

Meyer, K.S., Bergmann, M., and Soltwedel, T. (2013). Interannual variation in the epibenthic megafauna at the shallowest station of the HAUSGARTEN observatory (79 degrees N, 6 degrees E). *Biogeosciences* 10(6), 3479-3492. doi: 10.5194/bg-10-3479-2013.

Mordecai, G., Tyler, P.A., Masson, D.G., and Huvenne, V.A.I. (2011). Litter in submarine canyons off the west coast of Portugal. *Deep Sea Res. Part II Top. Stud. Oceanogr.* 58(23-24), 2489-2496. doi: 10.1016/j.dsr2.2011.08.009.

Moret-Ferguson, S., Law, K.L., Proskurowski, G., Murphy, E.K., Peacock, E.E., and Reddy, C.M. (2010). The size, mass, and composition of plastic debris in the western North Atlantic Ocean. *Mar. Pollut. Bull.* 60(10), 1873-1878. doi: 10.1016/j.marpolbul.2010.07.020.

National Research Council (1995). "Clean Ships, Clean Ports, Clean Oceans: Controlling Garbage and Plastic Wastes at Sea", in: *National Academy Press*: Washington, DC.).

Nurnberg, D., Wollenburg, I., Dethleff, D., Eicken, H., Kassens, H., Letzig, T., et al. (1994). Sediments in Arctic Sea-Ice - Implications for Entrainment, Transport and Release. *Mar. Geol.* 119(3-4), 185-214. doi: Doi 10.1016/0025-3227(94)90181-3.

O'Brine, T., and Thompson, R.C. (2010). Degradation of plastic carrier bags in the marine environment. *Mar. Pollut. Bull.* 60(12), 2279-2283. doi: 10.1016/j.marpolbul.2010.08.005.

Obbard, R.W., Sadri, S., Wong, Y.Q., Khitun, A.A., Baker, I., and Thompson, R.C. (2014). Global warming releases microplastic legacy frozen in Arctic Sea ice. *Earths Future* 2(6), 315-320. doi: 10.1002/2014EF000240.

Ontrup, J., Ehnert, N., Bergmann, M., & Nattkemper, T. W. (2009, May). BIIGLE-Web 2.0 enabled labelling and exploring of images from the Arctic deep-sea observatory HAUSGARTEN. In OCEANS 2009-EUROPE (pp. 1-7). IEEE.

Pham, C.K., Gomes-Pereira, J.N., Isidro, E.J., Santos, R.S., and Morato, T. (2013). Abundance of litter on Condor seamount (Azores, Portugal, Northeast Atlantic). *Deep Sea Res. Part II Top. Stud. Oceanogr.* 98(0), 204-208. doi: 10.1016/j.dsr2.2013.01.011.

Pham, C.K., Ramirez-Llodra, E., Alt, C.H., Amaro, T., Bergmann, M., Canals, M., et al. (2014). Marine litter distribution and density in European seas, from the shelves to deep basins. *PLoS One* 9(4), e95839. doi: 10.1371/journal.pone.0095839.

PlasticsEurope (2015). "Plastics-The Facts 2015: An analysis of European latest plastics production, demand and waste data", in: PlasticsEurope.).

Ramirez-Llodra, E., De Mol, B., Company, J.B., Con, M., and Sarda, F. (2013). Effects of natural and anthropogenic processes in the distribution of marine litter in the deep Mediterranean Sea. *Prog. Oceanogr.* 118(0), 273-287. doi: 10.1016/j.pocean.2013.07.027.

Ramirez-Llodra, E., Tyler, P.A., Baker, M.C., Bergstad, O.A., Clark, M.R., Escobar, E., et al. (2011). Man and the last great wilderness: human impact on the deep sea. *PLoS One* 6(8), e22588. doi: 10.1371/journal.pone.0022588.

Rech, S., Macaya-Caquilpan, V., Pantoja, J.F., Rivadeneira, M.M., Jofre Madariaga, D., and Thiel, M. (2014). Rivers as a source of marine litter--a study from the SE Pacific. *Mar. Pollut. Bull.* 82(1-2), 66-75. doi: 10.1016/j.marpolbul.2014.03.019.

Rudels, B., Meyer, R., Fahrbach, E., Ivanov, V.V., Osterhus, S., Quadfasel, D., et al. (2000). Water mass distribution in Fram Strait and over the Yermak Plateau in summer 1997. *Ann. Geophys.* 18(6), 687-705. doi: DOI 10.1007/s00585-000-0687-5.

Ryan, P.G. (2015). A Brief History of Marine Litter Research. In: Bergmann, M., Gutow, L., Klages, M. (Eds.), *Marine Anthropogenic Litter*. Springer, Berlin, 1-25. doi: 10.1007/978-3-319-16510-3_1.

Sanchez-Vidal, A., Veres, O., Langone, L., Ferre, B., Calafat, A., Canals, M., et al. (2015). Particle sources and downward fluxes in the eastern Fram strait under the influence of the west Spitsbergen current. *Deep Sea Res. Part I Oceanogr. Res. Pap.* 103(0), 49-63. doi: 10.1016/j.dsr.2015.06.002.

Schlining, K., von Thun, S., Kuhnz, L., Schlining, B., Lundsten, L., Stout, N.J., et al. (2013). Debris in the deep: Using a 22-year video annotation database to survey marine litter in Monterey Canyon, central California, USA. *Deep Sea Res. Part I Oceanogr. Res. Pap.* 79(0), 96-105. doi: 10.1016/j.dsr.2013.05.006.

Schoening, T., Kuhn, T., Bergmann, M., and Nattkemper, T.W. (2015). DELPHI - fast and adaptive computational laser point detection and visual footprint quantification for arbitrary underwater image collections. *Front. Mar. Sci.* 2. doi: 10.3389/fmars.2015.00020.

Schulz, M., Clemens, T., Forster, H., Harder, T., Fleet, D., Gaus, S., et al. (2015a). Statistical analyses of the results of 25 years of beach litter surveys on the south-eastern North Sea coast. *Mar. Environ. Res.* 109, 21-27. doi: 10.1016/j.marenvres.2015.04.007.

Schulz, M., Krone, R., Dederer, G., Watjen, K., and Matthies, M. (2015b). Comparative analysis of time series of marine litter surveyed on beaches and the seafloor in the southeastern North Sea. *Mar. Environ. Res.* 106(0), 61-67. doi: 10.1016/j.marenvres.2015.03.005.

Smith, K.L., Jr., Ruhl, H.A., Bett, B.J., Billett, D.S., Lampitt, R.S., and Kaufmann, R.S. (2009). Climate, carbon cycling, and deep-ocean ecosystems. *Proc. Natl. Acad. Sci. U.S.A.* 106(46), 19211-19218. doi: 10.1073/pnas.0908322106.

Soltwedel, T., Bauerfeind, E., Bergmann, M., Bracher, A., Budaeva, N., Busch, K., et al. (2016). Natural variability or anthropogenically-induced variation? Insights from 15 years of multidisciplinary observations at the arctic marine LTER site HAUSGARTEN. *Ecol. Indic.* 65, 89-102. doi: 10.1016/j.ecolind.2015.10.001.

Spengler, A., and Costa, M.F. (2008). Methods applied in studies of benthic marine debris. *Mar. Pollut. Bull.* 56(2), 226-230. doi: 10.1016/j.marpolbul.2007.09.040.

Spreen, G., Kaleschke, L., and Heygster, G. (2008). Sea ice remote sensing using AMSR-E 89-GHz channels. J. Geophys. Res. Oceans 113(C2). doi: Artn C02s03
10.1029/2005jc003384.

Taylor, J., Krumpen, T., Soltwedel, T., Gutt, J., and Bergmann, M. (2016). Regional- and local-scale variations in benthic megafaunal composition at the Arctic deep-sea observatory HAUSGARTEN. Deep Sea Res. Part I Oceanogr. Res. Pap. 108, 58-72. doi: 10.1016/j.dsr.2015.12.009.

Taylor, J.R., DeVogelaere, A.P., Burton, E.J., Frey, O., Lundsten, L., Kuhnz, L.A., et al. (2014). Deep-sea faunal communities associated with a lost intermodal shipping container in the Monterey Bay National Marine Sanctuary, CA. *Mar. Pollut. Bull.* 83(1), 92-106. doi: 10.1016/j.marpolbul.2014.04.014.

Thompson, R.C., Olsen, Y., Mitchell, R.P., Davis, A., Rowland, S.J., John, A.W., et al. (2004). Lost at sea: where is all the plastic? *Science* 304(5672), 838. doi: 10.1126/science.1094559.

Tubau, X., Canals, M., Lastras, G., Rayo, X., Rivera, J., and Amblas, D. (2015). Marine litter on the floor of deep submarine canyons of the Northwestern Mediterranean Sea: The role of hydrodynamic processes. *Prog. Oceanogr.* 134(0), 379-403. doi: 10.1016/j.pocean.2015.03.013.

UNEP (2009). Marine Litter: A Global Challenge. Nairobi.

van Sebille, E., England, M.H., and Froyland, G. (2012). Origin, dynamics and evolution of ocean garbage patches from observed surface drifters. *Environ. Res. Lett.* 7(4), 044040. doi: 10.1088/1748-9326/7/4/044040.

van Sebille, E., Spathi, C., and Gilbert, A. (2016). "The ocean plastic pollution challenge: towards solutions in the UK". Grantham Institute, Imperial College London).

van Sebille, E., Wilcox, C., Lebreton, L., Maximenko, N., Hardesty, B.D., van Franeker, J.A., et al. (2015). A global inventory of small floating plastic debris. *Environ. Res. Lett.* 10(12). doi: Artn 124006
10.1088/1748-9326/10/12/124006.

Vieira, R.P., Raposo, I.P., Sobral, P., Goncalves, J.M.S., Bell, K.L.C., and Cunha, M.R. (2015). Lost fishing gear and litter at Gorringe Bank (NE Atlantic). *Journal of Sea Research* 100, 91-98. doi: 10.1016/j.seares.2014.10.005.

Wobus, F., Shapiro, G.I., Huthnance, J.M., and Maqueda, M.A.M. (2013). The piercing of the Atlantic Layer by an Arctic shelf water cascade in an idealised study inspired by the

Storfjorden overflow in Svalbard. *Ocean Model.* 71(0), 54-65. doi: 10.1016/j.ocemod.2013.03.003.

Woodall, L.C., Robinson, L.F., Rogers, A.D., Narayanaswamy, B.E., and Paterson, G.L.J. (2015). Deep-sea litter: a comparison of seamounts, banks and a ridge in the Atlantic and Indian Oceans reveals both environmental and anthropogenic factors impact accumulation and composition. *Front. Mar. Sci.* 2. doi: 10.3389/fmars.2015.00003.

3 Tying up Loose Ends of Microplastic Pollution in the Arctic: Distribution from the Sea Surface through the Water Column to Deep-Sea Sediments at the HAUSGARTEN Observatory

Mine B. Tekman [a], Claudia Wekerle [b], Claudia Lorenz [c], Sebastian Primpke [c], Christiane Hasemann [a], Gunnar Gerdts [c], Melanie Bergmann [a]

[a] Alfred-Wegener-Institut, Helmholtz-Zentrum für Polar- und Meeresforschung, Am Handelshafen 12, 27570 Bremerhaven, Germany

[b] Alfred-Wegener-Institut, Helmholtz-Zentrum für Polar- und Meeresforschung, Klußmannstr. 3d, 27570 Bremerhaven, Germany

[c] Alfred-Wegener-Institut, Helmholtz-Zentrum für Polar- und Meeresforschung, Kurpromenade, 27498 Helgoland, 27570 Bremerhaven, Germany

Environmental Science & Technology, March 2020, doi: 10.1021/acs.est.9b06981

Abstract

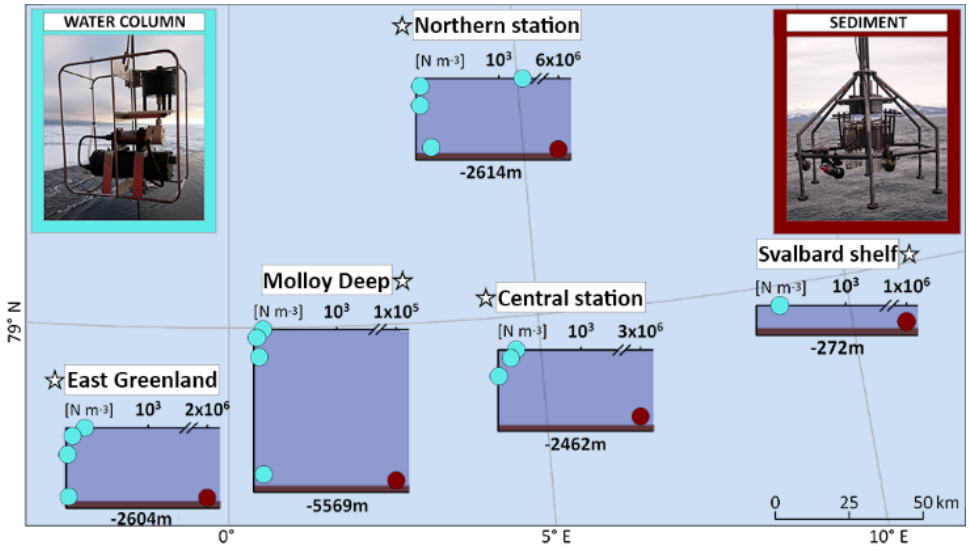

Recent studies have shown that despite its remoteness, the Arctic region harbors some of the highest microplastic (MP) concentrations worldwide. Here, we present the results of a sampling campaign to assess the vertical distribution of MP particles (>11 µm) at five stations of the HAUSGARTEN observatory. Water column samples were taken with large volume pumps by filtering 218 – 561 liters of seawater at two to four depth strata (near-surface, ~300 m, ~1000 m and above seafloor) and sediment samples with a multiple corer. MP concentrations in the water column ranged between 0 – 1,287 N m^{-3} and in the sediment from 239 – 13,331 N kg^{-1}. Fourier transform infrared spectroscopy (FTIR) imaging with automated data analysis showed that polyamide (39%) and ethylene-propylene-diene rubber (23%) were the most abundant polymers within the water samples and polyethylene-chlorinated (31%) in

sediments. MPs ≤25 µm accounted for more than half of the synthetic particles in every sample. The largest MP particle recorded was in the 200 µm size class. The concentrations of fibers were not reported, as fiber detection by FTIR imaging was not available at the time of analyses. Two- and three-dimensional simulations of particle transport trajectories suggest different pathways for certain polymer types. A positive correlation between MP size composition and particulate organic carbon indicates interactions with biological processes in the water column.

3.1 Introduction

Over the last decade, the pollution of our oceans with plastic has aroused great attention in both environmental research and public discourse (Borrelle et al., 2017). The more research has been conducted, the more the extent of the problem has been unveiled (Bergmann et al., 2017a). Microplastic (MP) particles further complicate our comprehension of the problem, as these small particles (<5 mm) have been observed throughout the world oceans (Law et al., 2014) including in sea ice (Obbard et al., 2014; Peeken et al., 2018b), on the deep seafloor (Bergmann et al., 2017b) and within biota (Kühn et al., 2018). Additionally, MP particles have not been found exclusively in marine compartments of the global ecosystem, but also within the atmosphere (Allen et al., 2019; Bergmann et al., 2019), freshwater (Schmidt et al., 2017) and terrestrial (Qi et al., 2020) environments. There is still uncertainty as to the scope and severity of any detrimental effects MP may have on organisms (Wright et al., 2013), though some health implications have been identified (Kim et al., 2012; Jin et al., 2018; Lu et al., 2018).

Rapid changes in the world's climate has drawn particular attention to the Arctic regions, where plastic pollution has, alongside environmental change, been recognized as a growing problem (Bergmann and Klages, 2012; Tekman et al., 2017). As a result of the recent research activities, our knowledge on plastic and MP pollution in the Arctic is improving (Peeken et al., 2018a). However, within Arctic waters (and the world oceans in general) MP concentrations and transport pathways within the water column remains understudied. Concentrations reported from a limited number of water column studies have shown great variation in measured quantities (Courtene-Jones et al., 2017; Kanhai et al., 2018; Peng et al., 2018; Choy et al., 2019), though indicating a ubiquitous presence in the water column globally. Moreover, MP has been suggested to incorporate into marine particles (Long et al., 2015; Cole et al., 2016; Long et al., 2017; Zhao et al., 2017; Mao et al., 2018; Möhlenkamp et al., 2018; Porter et al., 2018; Zhao et al., 2018; Wieczorek et al., 2019) and alter sinking velocities (Cole et al., 2016; Möhlenkamp et al., 2018; Wieczorek et al., 2019). These findings are important in the context

of the biological pump. The biological pump is the process by which photosynthetically-produced organic matter is exported to the deep ocean via sinking particles, which are subjected during settling to advection, vertical mixing and potential removal from the water column to organisms via consumption (Turner, 2015). Given that this pump drives the food supply to the deep ocean (Iversen and Ploug, 2010), it is crucial to understand how the presence of MP may affect the sinking behavior and the efficiency of organic matter export pathways from the surface waters to the deep seafloor.

Aside from settling behavior and abundance, another important MP parameter is the size of the particles. MP particles of 10 µm may be transferred to upper trophic levels within the planktonic food web (Setälä et al., 2014). The majority of studies identifying and quantifying MP conducted to date via visual selection and subsequent verification by Fourier transform infrared spectroscopy (FTIR), allows the detection of particles >100 µm. FTIR imaging with a lower detection limit of 11µm (Bergmann et al., 2017b) has shown that particles ≤25 µm represent the highest proportion of MP particles in environmental samples, suggesting that there is no lower limit on MP size following fragmentation (Bergmann et al., 2017b; Bergmann et al., 2019; Haave et al., 2019; Lorenz et al., 2019). Therefore, it is plausible to assume that many hitherto reported environmental MP concentrations have underestimated abundances and potentially, size-related interactions of small MP particles (<100 µm) with organisms have been unnoticed.

The Fram Strait is the deep-water connection between the Arctic Ocean and the North Atlantic, characterized by contrasting water masses (Wekerle et al., 2018). Warm Atlantic water entering the Fram Strait as West Spitzbergen Current (WSC) facilitates melting of sea ice and subsequent release of particles and organisms from within this melted ice, contributing to the downward flux of particles (Wekerle et al., 2018). A fraction of the WSC recirculates at ~79°N and subducts underneath cold polar waters that exit the Arctic Ocean. The East Greenland Current (EGC) carries both these water masses southward. This complex structure of currents from different origins affects the particle distribution locally within the water column (Wekerle et al., 2018).

Here, we analyzed samples taken from near-surface waters, the deep water column and deep-sea sediments for MP (excluding fibers) at five stations of the HAUSGARTEN observatory. The distribution of MP particles was studied in the context of simulated particle trajectories and environmental parameters to investigate possible sources, transportation pathways and accumulation mechanisms of MP in the Fram Strait. To this end, we assessed:

(i) the spatial distribution of MP particles among stations and depths; (ii) differences between the water column and sediments; (iii) possible interactions with the biological pump; (iv) effect of sea ice on the MP distribution; (v) potential source areas of MP particles.

3.2 Material and Methods

Sampling procedure

Water and sediment sampling were conducted in the summer of 2016 during the *RV Polarstern* expedition PS99.2 from the HAUSGARTEN observatory. In 1999, the Alfred Wegener Institute Helmholtz Centre for Polar and Marine Research (AWI) initiated the long-term ecological research (LTER) observatory HAUSGARTEN in the Fram Strait (Soltwedel et al., 2016). Twenty-one stations along a bathymetric and latitudinal gradient have been sampled annually, to assess the effects of climate change on faunal, bacterial, biogeochemical, geological, hydrographic and sedimentation processes. Four deep and one shallow station from the HAUSGARTEN observatory stations were selected for the current study, covering the full range of oceanographic regimes found within the Fram Strait. These stations were 1) EGIV, located in the East Greenland Current (2604 m depth); 2) N5, the closest station to the marginal ice zone (2614 m depth); 3) The Molloy Deep (HG9), the deepest depression within Fram Strait (5569 m depth); 4) HG4, located at the center of the strait (2462 m depth); 5) SVI, the station on the Svalbard shelf (272 m depth). Four McLane Large Volume Water Transfer Systems (WTS-LVs) were attached to a standard CTD wire to sample MP from within the near-surface (1 – 3 m), ~300 m (250 – 308 m), ~1000 m (974 – 1022 m) and above seafloor (2449 – 5350 m) depth layers during CTD rosette casts (*Table 3.1*). After 1 h of filtering (218 – 561 liters) through a stainless steel filter of 32 µm mesh size and 142 mm diameter (MP filter, Supporting Information (SI), Fig. 5.3.1a) at the target depth layer, WTS-LVs were retrieved and MP filters stored in glass jars at -20 °C. A total of 18 MP filters were obtained. Samples for particulate organic carbon (POC), particulate organic nitrogen (PON) and total particulate matter (TPM) were taken by a rosette sampler equipped with SEA-BIRD CTD system and 24 Niskin bottles (12 L), with subsamples processed onboard (see Engel et al. (2019) (Engel et al., 2019) for the details). A video-guided multiple corer (MUC; Oktopus GmbH) holding eight cores of 100 mm diameter was used to sample sediments and environmental parameters according to Bergmann et al. (2017) (Bergmann et al., 2017b) at the same stations as the water samples were taken. The top 5 cm of three sediment cores taken at each station were sliced off with a metal spatula, wrapped into tin foil and stored at -20 °C.

Sample purification and microplastic identification

MP filters were thawed, removed from the glass jars and placed into MP reactors. A MP reactor is a semi-enclosed unit, which contains stainless steel metal filters of 20 µm mesh size at both ends. This unit allows the addition and removal of solutions by vacuum and pressure filtration without sample transfer (SI Fig. 5.3.1b, see Lorenz et al. (2019) (Lorenz et al., 2019) for the details of MP reactors). Glass jars were thoroughly rinsed with Milli-Q water and subsequently with 35% pre-filtered ethanol into the reactors to wash off particles adhering to the inner surfaces of the jars. The samples were purified in the reactors by an enzymatic-oxidative treatment with sodium dodecyl sulfate (SDS), protease, cellulase and hydrogen peroxide as described in Löder et al. (2017) (Löder et al., 2017). Visual inspection returned no particles >500 µm size on MP filters. After purification, the MP filters were taken out of the MP reactors and rinsed with Milli-Q water into the reactors (SI, Fig. 5.3.1c). Each MP filter was then inspected by stereomicroscope (Olympus SZX16) to ensure that no particles remained. Purified water samples were obtained by removing the filters from the bottom ends of the MP reactors and rinsing these into 100 mL glass bottles (Lorenz et al., 2019).

Separation and size fractionation of the sediments were carried out as described in Bergmann et al. (2017) (Bergmann et al., 2017b). Size fractionation resulted in particles of >500 µm size, which were manually sorted, inspected under a stereo microscope (Olympus SZX16, Olympus) at a 100 – 320x magnification and putative MPs identified using an attenuated total reflection (ATR, SI, Paragraph 5.3.2) FTIR unit (Bruker Optik GmbH) (Bergmann et al., 2017b). Before the purification of <500 µm size fraction, a comparison of enzymatic-oxidative (as used for water samples) and Fenton's reagent purification (as used in a previous study on Arctic sediments (Bergmann et al., 2017b) was performed on another set of Arctic sediments (SI, Paragraph 5.3.3). The aim of this analysis was to assess if FTIR analyses of identical sediments, which have been purified with each of these two methods, result in different particle type and size measurements. Since this analysis did not reveal significant differences between methodologies, Fenton's reagent was selected to comply with the purification method of the earlier study of HAUSGARTEN sediments (Bergmann et al., 2017b).

Focal Plane Array (FPA) based FTIR imaging analysis was applied to measure the small size fraction (11 - 500 µm) of the water and sediment samples (Löder et al., 2015; Bergmann et al., 2017b; Lorenz et al., 2019). The mesh size of the MP filters (32 µm) and eventually also the filters of the MP reactors (20 µm) mark the lower size limit of the collected particles.

However, MP incorporated aggregates within samples (Zhao et al., 2018) and a decrease over time in fluid permeability during the filtering processes (Redner and Datta, 2000) may have led to a capture of yet smaller particles. Therefore, our measured concentrations of particles in 11 µm, 25 µm (>11≤25µm) and partly in 50 µm (>25≤50µm) size classes are semi-quantitative. An appropriate quantity of water and sediment subsamples was assessed by FlowCam (Fluid Imaging Technologies, Scarborough, USA) (Bergmann et al., 2017b) to prevent filter overload (Lorenz et al., 2019). Subsamples (*Table 3.1*) were concentrated on aluminum oxide filters (Ø = 25 mm; pore size, 0.2 µm; Anodisc, Whatman, Germany) (SI, Fig. 5.3.1d). These Anodisc filters (filter area: 184 mm^2, 77 × 77 FPA fields) were subsequently dried at 30 °C for two days and measured via FTIR imaging (SI, Paragraph 5.3.4). Fiber detection (Primpke et al., 2019) was not available at the time of analyses, therefore fibers were excluded from the results as they were in comparable previous studies (Bergmann et al., 2017b; Peeken et al., 2018b; Haave et al., 2019; Lorenz et al., 2019; Mani et al., 2019).

Automated Analysis of FTIR data. The measured FTIR data were analyzed via the automated analysis pipeline (Bergmann et al., 2017b) excluding human bias. Within this process the spectrum was compared twice against the reference database (Primpke et al., 2018) using spectra correlation of the raw and the first derivative data. A spectrum is identified if both methods yield the same polymer type and the result is transferred into an image. Particle numbers, polymer size classes and types were obtained via image analysis using Python 3.4 scripts and Simple ITK functions (see Primpke et al (2017) (Bergmann et al., 2017b) for details).

Contamination prevention

Water and sediment sampling equipment (tweezers, glass jars, spatula, ruler) were rinsed thoroughly with Milli-Q (0.22 µm filtered water, Millipore) before every deployment. MP filters were placed and retrieved with metal tweezers. Contamination prevention in the laboratory and creation of procedural blanks of sediment samples were conducted according to Lorenz et al. (2019) (Lorenz et al., 2019). Glass or metal equipment were used throughout, with the exceptions of tubing and seals (silicone), $ZnCl_2$ filters (polypropylene; pleated cartridge 37 filters) and squeeze bottles (polytetrafluorethylene). All chemicals were filtered before usage through 0.2 µm (GTTP, polycarbonate), enzymes and sodium dodecyl sulfate (SDS) over 0.45 µm (cellulose nitrate) or 1.2 µm (GF/F 40 glass fiber) filters to remove particles from the solutions. Dustboxes (DB1000, G4 prefiltration, HEPA-H14 final filtration, Q = 950 m^3/h, Möcklinghoff Lufttechnik) were placed at the sediment separation, purification

and FTIR imaging laboratories to prevent contamination of the samples by airborne particles. The purification with the MP reactors and filtration of the samples were processed in a laminar flow cabinet (ScanLaf 43 Fortuna 1800, LaboGene, Lillerød, Denmark). A blank sample was taken on-board to assess the contamination during the deployments of WTS-LVs. A total of 100 L of pre-filtered freshwater was pumped with a WTS-LV. Pre-filtration was done by attaching a water filter with metal cartridges of 2 – 3 µm mesh to a freshwater source. The MP filter of the blank sample was purified and analyzed together with the water samples. MP amounts in the water samples were blank-corrected for contamination based on the result of the blank sample analysis and in the sediment samples based on the result of the procedural blank as described in Bergmann et al. (2017) (Bergmann et al., 2017b). The contamination, which was caused by certain polymers during the sampling and analysis processes of water the samples were eliminated from the results (SI, Paragraph 5.3.5).

Particle tracking

The origin of MP particles measured in the analyzed water samples was estimated with a Lagrangian particle-tracking algorithm, following the approach of Wekerle et al. (2018) (Wekerle et al., 2018) for 2016. Backward three-dimensional (3D) trajectories of MP particles in the deep water column (300 m, 1000 m, above seafloor) were computed for four stations in the Fram Strait (EGIV, HG4, HG9, N5) with three different settling velocities. Particles were released into a model run once per day during 2016 at corresponding sampling station x depths and tracked backward in time until they reached the sea surface, where they may have commenced sinking (surface origin). Therefore, a reversed flow field was used, as if the particles were rising from the sampling depth to their surface origins via lateral displacement with a negative sinking and reversed horizontal velocity (vertical ocean velocities were neglected). Daily averaged horizontal velocity fields were taken from the Finite-Element Sea-ice Ocean Model (FESOM, version 1.4). The model configuration used in this study was optimized for the Fram Strait region, applying a mesh resolution of 1 km in this area. It covers the time period 2010 – 2016, is forced with atmospheric re-analysis data from Era-interim and is initialized with model fields from the simulation described in Wekerle et al. (2017) (Wekerle et al., 2017). A time step of one hour was used for the trajectory calculations, yielding hourly positions and corresponding values of temperature and salinity. The sampling depths for HG4 above seafloor and SVI 300 m depth layers were not included in the computation since the analyses did not reveal MP particles in these water samples. Previous studies have shown that the settling velocities of marine particles are altered by a factor of -2.87 to 1.64 when MP is

incorporated into them, suggesting a decrease in the settling velocity for most of the cases (between -2.87 and -1.35) (Long et al., 2015; Cole et al., 2016; Wieczorek et al., 2019). To account for this variability, a representative factor of -2.25 was selected from Cole et al. (2016) (Cole et al., 2016) and settling velocities used in Wekerle et al. (2018) (Wekerle et al., 2018) (20 m , 60 m d^{-1}, 120 m d^{-1}) were modified accordingly (9 m, 27 m d^{-1}, 53 m d^{-1}). These settling velocities match with the results of an earlier experimental study (Kaiser et al., 2019).

In addition to the 3D particle trajectories described above, two-dimensional (2D) trajectories were computed for the MP particles in the near-surface water samples by using only the surface velocity field of the ocean model. This was done for all five stations (EGIV, HG4, HG9, N5, SVI). As in the case of the 3D trajectories, particles were released once per day throughout 2016 and tracked backward in time for 365 days. The computation was stopped earlier if the particle reached the coast. Probability maps of the particle distributions were generated by counting the visit of a particle as it crossed a bin and normalizing by the total number of particles (365).

Environmental parameters

Temperature, salinity and dissolved oxygen (O_2) data were obtained from synchronous CTD measurements (Tippenhauer et al., 2017). Where no data were available for the same depth as at which the water column was sampled for MP, measurements from the nearest depths were included in the datasets (SI, Table 5.3.6). Sea ice conditions at the surface were determined from daily concentrations of sea ice retrieved from Centre d'Exploitation et de Recherche SATellitaire (CERSAT; http://cersat.ifremer.fr/) (Krumpen, 2017). Ice coverages were calculated as the percentage of the days (for the near-surface depths and seafloor) and surface origins (for the deep water column) when sea ice concentration was >15% during the corresponding time period (2016 for the water column and 2000 – 2016 for the seafloor, see SI, Paragraph 5.3.6 for the details). POC and PON were analyzed as described in Engel et al. (2019) (Engel et al., 2019) by filtering aliquots of 1 to 6 L of seawater onto combusted GF/F filters and TPM as in Bodungen et al. (2013) (Bodungen et al., 2013). Values for environmental parameters in sediments (porosity, chlorophyll *a*, chloroplastic pigment equivalent, particulate organic carbon, and phospholipids) were obtained as outlined in Bergmann et al. (2017) (Bergmann et al., 2017b) by subsampling additional cores with cutoff syringes of 2 cm diameter, which were analyzed at 1 cm intervals down to 5 cm sediment depth.

Design of permutational multivariate analysis of variance for the analysis of polymer compositions

Multivariate analyses of polymer type and size class composition as concentrations (hereafter polymer composition, unless only type or size class composition is referred) were performed using PRIMER-e version 6.1.16 with PERMANOVA 1.0.6 (Anderson and Walsh, 2013). A permutational multivariate analysis of variance (PERMANOVA) routine with 9999 permutations was carried out to assess differences between a priori groups of stations (EGIV, HG4, HG9, N5, SVI), depth layers (near-surface, 300 m, 1000 m, above seafloor, sediment), water masses (polar, Atlantic, deep waters), surface locations (N5 and EGIV: ice edge, HG4 and HG9: center, SVI: shelf) and realms (water column and sediment). CTD profiles showed waters below 0°C (polar waters) at the near-surface depth layers of the deep stations. Warm waters of Atlantic origin (> 2°C) prevailed at 300 m depth layers at all stations and at SVI. For data analyses, 1000 m and above seafloor layers were categorized as deep waters. Data treatment prior to PERMANOVAs was done based on the sampling realms (i.e. water column only or through the water column and sediment, see subsequent sections). Two-way PERMANOVAs were performed using station x depth layer (without interaction), station x water mass and station x marine realm as fixed factors. Surface locations were compared one-way to evaluate the influence of ice coverage on MPs distribution. Furthermore, a canonical analysis of principal coordinates (CAP) was applied to analyze and visualize significant differences between the a priori defined groups. Temporal changes in MP concentrations and polymer type compositions of the sediments were investigated on the dataset by including in the analysis results from a previous HAUSGARTEN study (Bergmann et al., 2017b) in 2015, by running PERMANOVA on Bray Curtis similarity matrix of square-root transformed dataset of polymer type compositions. MP concentrations from two years were compared with one-way analysis of variance (ANOVA).

Analysis of the microplastic distribution in the water column

Univariate statistical analyses were performed with Sigmaplot 14.0 on water column MP concentrations. A Kolmogorov-Smirnov normality test failed for MP concentrations (K-S Dist. = 0.387, P = 0.037) because of the high MP abundance in the N5 near-surface sample. Therefore, this station was excluded from univariate analyses to achieve normality (K-S Dist. = 0.168, $P > 0.2$) and mean MP concentrations were then calculated by excluding this sample. Stations, depth layers, water masses and surface locations were compared with ANOVA followed by a Holm-Sidak test to assess differences between different groups. A Spearman

rank order correlation was used to assess the relationships between MP concentrations and environmental parameters (sampling depth, temperature, salinity, O_2, ice coverage, POC, PON, TPM). A PERMANOVA routine was executed on Bray Curtis similarity matrix of square-root transformed datasets of polymer compositions. Polymer compositions of different stations, depths, water masses and surface locations were compared. The similarity percentage (SIMPER) routine of PRIMER-e was performed to assess within group (stations, depth layers, water masses, surface locations) similarities and between group dissimilarities. The distance-based linear model (DistLM) routine of PRIMER-e was applied to investigate multivariate multiple regressions between polymer compositions and environmental parameters. Ice coverage, POC, PON and TPM values were not obtained for all of the depth layers of HG4, HG9 and SVI. Therefore, three sample groups (1 – 3) of polymer compositions (SI, Table 5.3.7a, see SI, Paragraph 5.3.7 for the details) were created for DistLM analyses based on the availability of these values. Marginal tests of the DistLM routine were run with 9999 permutations to assess the correlations between polymer composition and individual environmental parameter. The "Best" selection procedure with the "Akaike information criterion (AIC)" was used to find the regression models. Following the selection of the fitting model (SI, Paragraph 5.3.7), the relations were visualized with distance-based redundancy analysis (dbRDA).

Analysis of the microplastic distribution through the water column and sediment

The Hellinger dissimilarity measure is not sensitive to magnitude differences in abundances, and therefore it was applied to square-root transformed standardized datasets of polymer compositions of water column and sediment in combination (Lorenz et al., 2019). A PERMANOVA was applied to assess the differences in polymer compositions between stations, depths, marine realms and station x marine realm interactions. Total polymer types (S) and Pielou's evenness (J') of polymer compositions were calculated to assess the diversity of polymer compositions since these two diversity measures are not based on abundances. PERMANOVA was run for stations, depth layers and realms on Euclidean distances of log(x+1) transformed diversity dataset.

3.3 Results

Between 218 and 561 liters of water were filtered with large volume pumps. Depending on the particle load of each sample, 5 – 100% of the purified sampled volume were measured by FTIR imaging (*Table 3.1*). MPs were found in 16 out of 18 samples ranging from 9 – 1,287

N m^{-3} (Fig. 3.1a) with a mean concentration of 95 ± 85 N m^{-3} (±SD; 161 ± 293 N m^{-3} if N5 near-surface included). A total of 15 types of synthetic polymers in a size range of 11 – 150 µm were identified (Fig. 3.1b). The highest mean MP concentration through the entire water column was detected at the coastal SVI (131 ± 185 N m^{-3}) and the lowest mean at the deep HG9 (84 ± 39 N m^{-3}). The highest mean concentration through the water column of the deep stations was found at N5 (98 ± 77 N m^{-3}, excluding near-surface). ANOVA indicated no significant difference between stations ($P > 0.050$). Comparison of depth layers revealed a significant difference (ANOVA: F = 5.97, df = 3, $P = 0.009$) caused by the disparity of samples taken near-surface and at 300 m (Holm-Sidak: t = 3.41, $P = 0.023$) and between near-surface and 1000 m depth layers (Holm-Sidak: t = 3.89, $P = 0.011$). No significant difference was found between water masses and different surface locations ($P > 0.050$).

The highest MP concentration within sediments was detected at N5 (13,331 N kg^{-1}) and the lowest at HG9 (239 N kg^{-1}) (*Table 3.1*). Four to 52% of each purified sediment sample volume was measured by FTIR imaging, giving a mean concentration of 4,730 ± 5,107 N kg^{-1} (Fig 3.1a). A total of 12 polymer types in a size range of 11 – 200 µm were identified (Fig 3.1 b – d). ANOVA showed no significant difference between 2015 and 2016 ($P > 0.050$).

Table 3.1 Microplastic concentrations in Arctic sediment and water samples taken at different depths.

Station	**Realm**	**Sampling depth (m)**	**Sample volume (L) and dry weight (g) [a]**	**Subsample volume for FTIR (%)**	**MP (N m^{-3}) [b]**	**MP (N kg^{-1})**
EGIV (78.8°N, 2.8°E)	water column	-1	218 L	100%	227	
		-303	490 L	55%	78	
		-993	556 L	77%	16	
		-2,574	541 L	64%	29	
	sediment	-2,604	823 g	12%	1.9×10^6	2,437
		-3	223 L	5%	1.287	

N5 (79.9°N, 3.1°W)	water column	-289	499 L	41%	54	
		-999	554 L	48%	53	
		-2,549	546 L	27%	186	
	sediment	-2,614	513 g	4%	6.3×10^6	13,331
HG4 (79.1°N, 4.2°W)	water column	-1	223 L	49%	218	
		-302	501 L	90%	152	
		-974	559 L	80%	9	
		-2,449	546 L	26%	0	
	sediment	-2,462	582 g	5%	3.2×10^6	5,099
HG9 (79.1°N, 2.8°W)	water column	-2	228 L	35%	113	
		-308	496 L	6%	38	
		-1,022	561 L	17%	65	
		-5,350	542 L	11%	119	
	sediment	-5,569	509 g	52%	0.1×10^6	239
SVI (79.0°N, 11.1°W)	water column	-1	424 L	100%	262	
		-250	544 L	64%	0	
	sediment	-272	630 g	11%	1.3×10^6	2,542

[a] Sample volume (L) and dry weight (g) column represents total in-situ filtered volume of the water samples and total weight of the sediment samples.

[b] Sediment microplastic concentrations in N m^{-3} were calculated by multiplying the concentrations in N kg^{-1} with (dry) sediment density. The dry weight (wet weight × porosity) was divided by the volume of the subsample to obtain the sediment density (kg m^{-3}) at each station. Weight, volume and porosity values were measured from additional sediment cores taken to analyze environmental parameters.

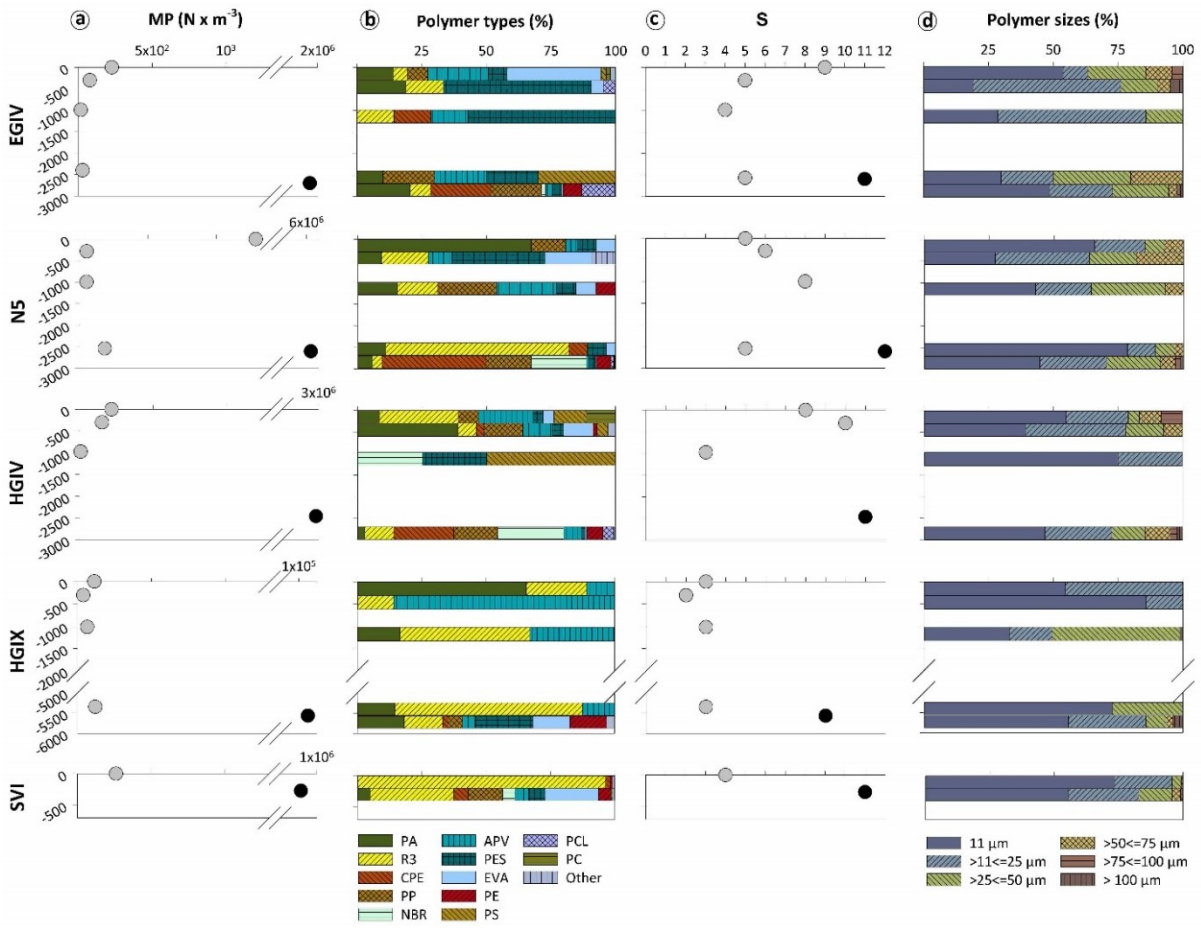

Figure 3.1 Microplastic concentrations, percentages of polymer types, total polymer counts and percentages of polymer size classes of each sample. For visual purpose, the sampling depths of the above seafloor and sediment layers were adjusted to prevent the bars from overlapping. **a.** MP concentrations. Gray dots represent MP concentrations in the water samples and black dots in the sediments; **b.** Percentages of polymer types (PA: polyamide, R3: ethylene-propylene-diene rubber, CPE: polyethylene-chlorinated, PP: polypropylene, NBR: nitrile rubber, APV: acrylates/polyurethanes/varnish/lacquer, PES: polyester, EVA: ethylene-vinyl-acetate, PE: polyethylene, PS: polystyrene, PCL: polycaprolactone, PC: polycarbonate, other: polyvinylchloride, rubber type 1, polysulfone, cellulose acetate) (Primpke et al., 2018); **c.** Total polymer type counts (S) in the water and sediment samples.Gray dots represent S in the water samples and black dots in the sediments; **d.** Percentages of polymer size classes.

Polymer types. Six polymer types accounted for 96% of all synthetic particles found in water samples (Polyamide [PA]: 39%, ethylene-propylene-diene rubber [R3]: 23%, acrylates/polyurethanes/varnish/lacquer [APV]: 10%, polypropylene [PP]: 8%, polyester [PES]: 8%, ethylene-vinyl-acetate [EVA]: 8%) (Fig. 3.1b, SI, Table 5.3.4a). PERMANOVA

of polymer types for station x depth groups revealed significant differences between stations (Pseudo-F = 2.02, *P (perm)* = 0.017) but not between depth layers. The polymer composition at HG9 was significantly different from N5 (t = 2.31, *P (perm)* = 0.036) and the CAP routine revealed a similar result (SI, Fig. 5.3.8a). Analysis of station x water mass groups did not show any difference (*P (perm)* > 0.050). HG9 harbored only PA, APV and R3 at all depth layers with a 66% within group similarity whereas the within group similarity of the other stations ranged between 16% – 39%. The lowest dissimilarity between stations was observed between EGIV and N5 (57%) and the highest between EGIV and SVI (94%). Surface locations showed significant differences (Pseudo-F = 1.83, *P (perm)* = 0.049), which was also confirmed by the CAP routine (SI, Fig. 5.3.8b). Polyethylene-chlorinated (CPE: 31%), nitrile rubber (NRB: 18%) and PP (17%) comprised the highest proportions in sediments whereas other polymer types contributed 1% – 9%. There was no significant difference in polymer type compositions of sediments sampled in 2015 (Bergmann et al., 2017b) and 2016 (Pseudo-F = 1.55, *P (perm)* = 0.140)

Data analyses on MP concentrations through the water column and sediment at stations and realms revealed significant differences between stations (for station x depth layer: Pseudo-F = 1.73, *P (perm)* = 0.020) (SI, Fig. 5.3.8c) and realms (for station x realm: Pseudo-F = 3.37, *P (perm)* = 0.003) (SI, Fig. 5.3.8e). Polymer type compositions at HG9 were significantly different from N5 (Pseudo-F = 1.94, *P (perm)* = 0.039). Polymer diversity was higher in sediment samples compared to water samples (Fig. 3.1c). PERMANOVA results of diversity indices (S and J') for station x depth layer showed significant differences between depth layers (Pseudo-F = 3.12, *P (perm)* = 0.011) due to the differences between sediment and 1000 m (Pseudo-F = 4.79, *P (perm)* = 0.014) and sediment and above seafloor layers (Pseudo-F = 3.49, *P (perm)* = 0.038). Water column and sediment diversity indices (S and J') between stations and realms were significantly different (station: Pseudo-F = 2.31, *P (perm)* = 0.0002; realm: Pseudo-F = 13.93, *P (perm)* = 0.039, respectively).

Polymer size classes. There were no significant differences in the polymer size composition between stations, realms, depth layers, water masses, station x water mass interactions and surface locations but diversity indices between realms were significantly different for station x realm groups (Pseudo-F = 11.12, *P (perm)* = 0.0013). The largest MP particle found within the water column was in the 150 µm size class (>125≤150µm, SI, Table 5.3.4b). Twenty-three putative MP particles >500 µm including 14 fibers (SI, Table 5.3.2, Fig. 5.3.2a, e) were detected in the sediment samples. The measurements by ATR-FTIR did not

reach hit quality above 700 in repeated measurements (SI, Table 5.3.2). Therefore, they were not included in the data analyses. The largest MP particle detected by FTIR imaging was in the 200 µm size class (>175≤200µm, SI, Table 5.3.4b). MP of 11 – 25 µm size classes accounted for 82% of the synthetic particles (Fig. 3.1d, SI, Table 5.3.4b) in the water column and 72% in the sediment. Only 0.15% of the particles exceeded 100 µm in the water column and 1% in the sediment.

Environmental parameters. MP concentrations in the water column were positively correlated with POC (Spearman: $\rho = 0.66$, $P = 0.01$), PON ($\rho = 0.60$, $P = 0.022$), TPM ($\rho = 0.61$, $P = 0.025$), sampling depth ($\rho = 0.48$, $P = 0.045$), O_2 ($\rho = 0.53$, $P = 0.025$). Marginal tests of polymer size compositions showed statistically significant values for sampling depth, O_2 (for sample groups 1 – 3), POC (for sample groups 2, 3), PON (for sample group 2) and TPM (for sample group 3) (SI, Table 5.3.7b). The multi-collinearity among sampling depth, O_2, POC, PON and TPM (SI, Table 5.3.7c) was taken into account during the selection of multivariate multiple regression model selection (SI, Paragraph 5.3.7). Marginal tests of polymer types showed significant values for sampling depth, O_2 and TPM only for sample group 3 (SI, Table 5.3.7b). Considering the multi-collinearity among O_2, POC, PON, TPM, as well as the significant correlation between polymer compositions and these parameters, any of them (or in combination) would explain the modelled variation among the samples. For the polymer size compositions, the multivariate regression models of O_2 and, salinity were selected as the distance-based linear models for the sample groups 1 and 2 (SI, Fig. 5.3.7a, $R^2 = 0.30$, $AIC = 110$ and SI, Fig. 5.3.7b, $R^2 = 0.41$, $AIC = 88$, respectively). If environmental parameters including TPM were examined (sample group 3), the models of sampling depth and TPM were selected for polymer size and type compositions (SI, Fig. 5.3.7c, $R^2 = 0.27$, $AIC = 92$ and SI, Fig. 5.3.7d, $R^2 = 0.47$, $AIC = 81$, respectively). MP concentrations in sediments were not correlated with environmental parameters.

Particle Tracking. 2D trajectories showed distinct patterns of source areas of the MP particles in the near-surface samples (Fig. 3.2). An area to the south of Svalbard was exclusively projected as the source area of particles arriving at SVI, which were carried by the Svalbard Coastal Current. At EGIV, the trajectories suggested a pathway from the North to the sampling station. Particles at HG4 were estimated to originate from an area to the south of the Fram Strait driven by WSC. By contrast, particles arriving at N5 and HG9 were projected to be carried from north of Svalbard.

A total of eleven groups of 3D trajectories were obtained for the MP particles in the deep water column samples (300 m, 1000 m, above seafloor) (SI, Fig. 5.3.9). A total of 12,045 surface origin points were computed and a summary dataset was created (SI, Table 5.3.9). 3D trajectories revealed the WSC and EGC as the prime vector for particle transport to HG4, N5 and HG9, yet with different intensities. The slower the settling velocity the larger were the catchment areas. Most of the particles detected at EGIV originated from the sea-ice covered areas (66%) and thus from polar waters and at HG4 from Atlantic waters (73%). Particles at HG9 originated from both water masses; 52% from polar waters and 48% from Atlantic waters. For all stations, 3D trajectories revealed mostly south of the Fram Strait as the source area of the particles settling with a velocity of 9 m d^{-1}.

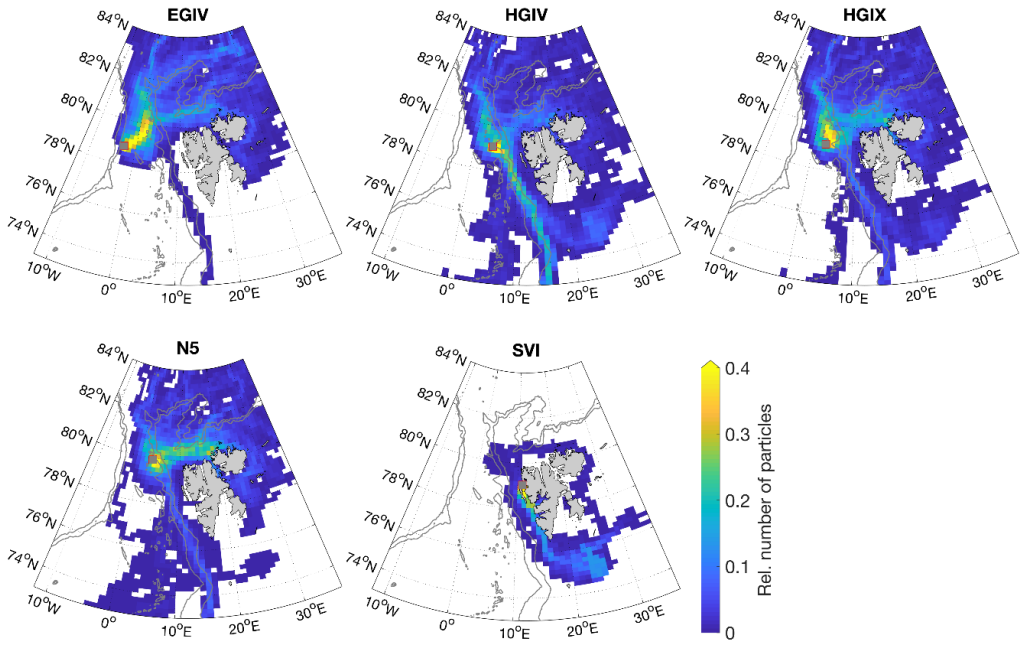

Figure 3.2 Source areas of MP particles detected at the near-surface depth layers at five stations (gray dots) of the HAUSGARTEN LTER Observatory as computed by 2D backward trajectories, using only the surface velocity field of the ocean model. The color scale shows the relative number of particles that crossed a grid box. The grey lines represent the topography at 1000 m and 2000 m depths.

3.4 Discussion

Our results show that MP particles are present throughout the Arctic water column (9 - 1,287 N m^{-3}). Even though MP concentrations in water samples were not as high as in

sediments (present study: 239 – 13,331 N kg^{-1}, earlier study (Bergmann et al., 2017b): 42 – 6,595 N kg^{-1}) and in sea ice (1,100 – 12,000 N L^{-1}) (Peeken et al., 2018b), it should be noted that water samples represent a snapshot in time, whereas sediment and sea ice samples reflect MP accumulation over longer time scales. The mesh size of the sampling and processing filters most likely resulted in the loss of smaller particles (<32 µm and <20 µm, respectively). Therefore, MP concentrations of the 11 µm, 25 µm and partly 50 µm size classes have to be considered as semi-quantitative, indicating that a more abundant number of particles in the small size range of MP may be present as pollution in the Arctic. The fact that sediments harbored 16 × 10^3 times higher quantities than were observed in the water column further proves that the Arctic seafloor constitutes a long-term sink for MP (Woodall et al., 2014; Bergmann et al., 2017b). This was corroborated by a higher polymer diversity being found in the sediments than the water column, which indicates the accumulation of a higher variety of polymers over long time scales. There is currently no standard operational procedure with respect to sampling, analysis and reporting of MP concentrations, but the number of MP per unit volume is the most common unit used for water samples (Bergmann et al., 2017b; Tekman et al., 2018). A conversion of quantities to m^3 may result in extrapolation of MP counts, yet such a conversion is necessary to allow comparisons between studies. The large-volume pumps used in the current study filtered between 218 and 561 liters of seawater per sample, resulting in a similar or lesser magnitude of extrapolation when compared to the earlier deep water column studies (Courtene-Jones et al., 2017; Kanhai et al., 2018; Peng et al., 2018) (except Choy et al. (2019) (Choy et al., 2019)). For some samples, particle concentrations within the purified volume were high, and care had to be taken to ensure that Anodisc filters were not overloaded. Thus, for example, only 5% of the near-surface sample of the northern station could be analyzed, which showed the highest MP concentration of all water samples (1,287 N m^{-3}). While this value was treated as an outlier in univariate analyses, the high abundance did not come as a surprise as this station is located closest to the marginal ice zone. Indeed, globally, some of the highest MP concentrations have been found in Arctic sea ice (Obbard et al., 2014; Peeken et al., 2018b). Furthermore, the highest MP concentration among above seafloor samples and in HAUSGARTEN sediments (from surveys in 2015 (Bergmann et al., 2017b) and 2016) was found at the northern station.

Combining results from sediments with those from water samples provided more insight into accumulation mechanisms of MP particles. However, different sampling realms, methods and large discrepancies in concentrations constrain the assessment of MP distribution

throughout these ecosystem compartments. As samples from Arctic waters have not been analyzed with our methods before, the concentrations in the water column were completely unknown and the samples were purified following enzymatic-oxidative treatment, the efficiency of which was proven for several environmental matrices (Lorenz et al., 2019). On the other hand, our sediment samples were a part of a time-series of the HAUSGARTEN observatory, with samples purified with Fenton's reagent. Therefore, Fenton's reagent was used for the purification of the sediment samples to maintain the consistency of the time series since the comparison of the two treatments did not show any difference in polymer compositions. Most previous studies on MP in Arctic sediments (Mu et al., 2019; Kanhai et al., 2019) have relied on visual selection of putative particles, which were verified by FTIR (except earlier study of HAUSGARTEN (Bergmann et al., 2017b)). Indeed, HAUSGARTEN sediments seem to harbor many more MP particles (239 – 13,331 N kg^{-1}) compared to other Arctic locations (5 – 69 N kg^{-1}) (Mu et al., 2019), but if we limit the comparison to the >100 µm size range, MP concentrations at HAUSGARTEN are in a similar magnitude (8 – 142 N kg^{-1}). However, if fibers were excluded, which account for 64% of the MP particles at other Arctic locations (Mu et al., 2019), HAUSGARTEN sediments show substantially higher MP concentrations.

MP from near-surface layers has been reported from Antarctica (Cincinelli et al., 2017) (0.17 N m^{-3}), NE Pacific (Desforges et al., 2014) (8 – 9,180 N m^{-3}), Monterey Bay (Choy et al., 2019) (2,900 N m^{-3}), European coasts (Enders et al., 2015) (~300 N m^{-3}) and North Atlantic Subtropical Gyre (Enders et al., 2015) (~100 N m^{-3}). The latter two are pertinent to compare with the HAUSGARTEN observatory results directly as Enders et al. (2015) (Enders et al., 2015) identified MPs down to 7 µm. Near-surface concentrations at HAUSGARTEN appear higher (113 –1,287 N m^{-3}) than measured in the North Atlantic Subtropical Gyre (Enders et al., 2015). Levels of 0 to 31 N m^{-3} with fibers (except Morgana et al. (2018) (Morgana et al., 2018)) accounting for 91% – 96% were reported from the near-surface layers of the Arctic Ocean (Lusher et al., 2015; Barrows et al., 2018; Kanhai et al., 2018; Morgana et al., 2018). Only one of the near-surface samples contained MP particles >100 µm at HAUSGARTEN. Overall, 99.9% of MPs in the water column were between 10 and 100 µm, highlighting once more (Bergmann et al., 2017b; Peeken et al., 2018b; Bergmann et al., 2019; Haave et al., 2019; Lorenz et al., 2019) how crucial it is to detect small MP particles (<100 µm) to quantify the true extent of MP pollution in the environment. There may well be high abundances of smaller MP particles below our current detection limit (11 µm). Such information affects the outcome

of risk assessments (Everaert et al., 2018). A higher contribution of particles >100 µm in the sediment compared to the water column indicates a lower residence time of small MP in surface waters, which contradicts earlier studies (Enders et al., 2015; Fazey and Ryan, 2016). Whether this inconsistency is due to hitherto unnoticed amounts of small MP or due to possible interactions with water column processes is an important research question.

The highest MP concentrations were found in the near-surface samples from all stations, except for the Molloy Deep. While increasing concentrations with depth were reported from the Mariana Trench (2,060 – 13,510 N m $^{-3}$) (Peng et al., 2018), no clear pattern was found at the Arctic Central Basin (0 – 375 N m^{-3}) (Kanhai et al., 2018) and highest concentrations were observed between 200 and 600 m at Monterey Bay (15,000 N m^{-3}) (Choy et al., 2019). In the present study, the mean MP concentration decreased six-fold towards the 1000 m depth layer resulting in profiles similar to those of POC (Engel et al., 2019), with concentrations doubling above the seafloor. Interestingly, the vertical distribution of particles at the Molloy Deep indicated a different mechanism in the MP flux, which implies the importance of the local ocean circulation for the distribution of MP. A similar polymer type composition was found at all depth layers of the Molloy Deep, whereas at the other stations polymer diversity varied between depth layers. Additionally, the Molloy Deep is the only station where no positively buoyant polymers were found and where the highest MP concentration among different sampling depths occurred at the closest sampling location to the seafloor. The Molloy Deep is the deepest known depression in the Arctic Ocean, which acts as a trap for organic matter due to its depth, topography and hydrography (Cathalot et al., 2015). Model studies indicated that one of the two main recirculation branches of the WSC cyclonically encircles the Molloy Deep (Hattermann et al., 2016; Wekerle et al., 2017). As in the case of eddies, the cyclonic loop leads to upwelling at its center and divergence of particles at the surface (Bakun, 2017). The higher concentration above the sea floor, in contrast, might be related to the steep slopes around the Molloy Deep, which may facilitate accumulation of particles towards nepheloid layer. Even though the full depth of this station is twice the depth of most of the other HAUSGARTEN stations, 3D trajectories showed a catchment area identical to other stations.

The positive correlation between MP concentrations and O_2, POC, PON, TPM in the HAUSGARTEN water column is remarkable. Correlations alone may not be sufficient to draw firm conclusions, but earlier studies have already shown that MP particles incorporate into marine snow (Zhao et al., 2017; Porter et al., 2018), fecal pellets (Cole et al., 2016; Wieczorek et al., 2019) and phytoplankton hetero-aggregates (Long et al., 2015; Long et al., 2017; Mao et

al., 2018; Möhlenkamp et al., 2018) indicating biological pathways in the downward flux of MP particles. Zhao et al. (2018) (Zhao et al., 2018) identified MP in 73% of the marine aggregates collected during field surveys and proposed that they act as a transport medium for MP in the water column. Despite the 32 µm mesh size of the sampling filters used, the detection of particles <32 µm in the HAUSGARTEN water column corroborates these findings. The occurrence of MP particles in phytoplankton hetero-aggregates is interesting in the context of the Arctic Ocean since the POC concentration in the upper water column of the Fram Strait is strongly related to phytoplankton growth (Engel et al., 2019). Processes related to sea ice are driving factors for the biological pump in the Arctic Ocean (Codispoti et al., 1991). Sea-ice derived cryogenic gypsum enhanced carbon export during under-ice blooms of the haptophyte *Phaeocystis* (Wollenburg et al., 2018). Such ballasting effects may also enhance the flux of MP to the deep ocean. Inter-annual variability affects MP amounts in aquatic environments (Cheang et al., 2018). The sampling at the HAUSGARTEN observatory was carried out in June – July, during a period of phytoplankton blooms, which may have led to the correlation of MP with POC.

Earlier studies used MP fragments and beads in a range of 2 – 500 µm (Cole et al., 2013; Long et al., 2015; Porter et al., 2018; Wieczorek et al., 2019) to experimentally investigate whether they incorporate into marine particles or not. However, there are currently no data available as to how the size of MP affects the rate of this incorporation since experimental studies have investigated specific concentrations, polymer types or sizes (Cole et al., 2013; Long et al., 2015; Porter et al., 2018; Wieczorek et al., 2019). The distribution of MP size classes at HAUSGARTEN did not show any difference throughout the water column, which concurs with the particle and plankton size distribution from the upper water column in the Fram Strait (Trudnowska et al., 2018). Multivariate correlation between MP size classes and POC indicates size-related interactions of MP particles with biological processes. MP particles have been detected in larvaceans from 200 – 400 m depth (Katija et al., 2017; Choy et al., 2019) and in zooplankton (Cole et al., 2013; Wieczorek et al., 2019). Another Arctic-specific example is the ingestion of MP by polar cod (*Boreogadus saida*) (Kühn et al., 2018; Morgana et al., 2018), which is considered a keystone species and whose juveniles are particularly dependent on sea ice. Thus, another understudied mechanism of downward flux of MP particles may be the transportation by pelagic organisms through the water column. Small MP particles have been shown to decrease the survival and reproduction of the rotifer *Brachionus plicatilis* (Sun et al., 2019). Along with the finding of almost all MP particles in the water column being <100

µm, these other observations also validate the concerns as to how much MP enters into the food chain and what effects this may have on the well-being of organisms, including humans.

Considering the complex hydrographic structure of the Fram Strait, it is crucial to adopt a holistic approach in the efforts of identifying sources, pathways and sinks of MP. A validated model simulation (Wekerle et al., 2018) was used in the present study to track MP particles in the water column back to their potential source areas at the ocean surface. 3D particle trajectories emphasized the importance of lateral advection and variable particle settling velocities in the vertical distribution of MP particles. The vertical ocean velocities were neglected and a constant sinking speed was used in the model, which may be a particularly important parameter at frontal regions, and thus needs to be investigated in future simulation efforts. It was estimated that MP particles detected above the seafloor traveled distances between 604 and 654 km. Therefore, when considering the sinking of MP particles, the focus should be rather on downward flux mechanisms than direct vertical transport. With the slowest settling velocity of 9 m d^{-1}, particles are exposed to the currents to a greater extent, and thus the influence of the WSC and of its recirculating branch, present at the surface and at intermediate depths of all deep stations, is much higher. Correspondingly, 3D trajectories suggested that most of these particles were carried to the Fram Strait from the south, which may be a pathway for positively buoyant polymers.

2D particle trajectories validated distinct spatial patterns in the transport of certain polymers. Ethylene-propylene-diene rubber was abundant in almost all water column samples and made up 96% of all the MPs detected at the surface layer of the Svalbard shelf station. 2D trajectories revealed south of Svalbard and the Barents Sea as the only source of these particles, suggesting North Atlantic and European origins. Ethylene-propylene-diene rubber is widely used in roofs, the automotive industry (as sealing material) and for artificial turf filling (Kim et al., 2012). The latter is notable since it is widely used and poses a risk for human health (Kim et al., 2012). Another distinct pattern was noticed in the near-surface samples of the station located in the East Greenland Current region. This layer contained the highest proportion of ethylene vinyl acetate (36%) among all samples and the modelled trajectories indicated polar waters as the only likely origin. This material is widely used in products such as paints, coatings, safety glass, packaging, adhesives and textiles (ACC, 2018). This polymer accounted for up to 10% of the MP particles identified in an ice core from East Greenland (Peeken et al., 2018b) corroborating a sea ice origin. 3D trajectories also suggested a sea ice origin for the majority of the particles found in the deep waters of East Greenland. Polyamide dominated all

water column samples and has been observed in Arctic sediments (Bergmann et al., 2017b), ice cores (Obbard et al., 2014; Peeken et al., 2018b) and snow (Bergmann et al., 2019) albeit in lower proportions. It is widely used in synthetic fabrics, carpets, sails and fishing nets and is one of the dominant polymers used in European fisheries (Oxvig, 2007). Because of its widespread usage, it is impossible to draw firm conclusions as to exact origins and transportation pathways of the polyamide particles observed in the current study. It may be speculated that increased fishery activity, an indirect consequence of the declining sea ice, may be a source for polyamide in Fram Strait waters. Acrylates/polyurethanes/varnish/lacquer, one of the most abundant polymers in the water column, is widely used as coating material in architectural, automotive, shipping and wind turbine applications to protect or decorate surfaces (ACC, 2018). It has also been a dominant polymer found in snow and ice cores (Peeken et al., 2018b; Bergmann et al., 2019). Sea ice trajectories revealed the Laptev Sea as the potential origin of such material in one of the ice cores with a high abundance (Peeken et al., 2018b).

Our data indicate a widespread MP pollution of the Arctic Ocean and support the hypotheses that the Arctic is an accumulation area for MP particles transported (i) from the North Atlantic via the thermohaline circulation (Cózar et al., 2017), (ii) from the north of the Fram Strait entrained in sea ice and released during melting (Peeken et al., 2018b), (iii) from the Barents Sea (van Sebille et al., 2012) (iv) via local emissions from increasing shipping activities (Tekman et al., 2017), (v) from different directions through the atmosphere and precipitation[6] and (vi) from the discharge of rivers (Schmidt et al., 2017). The findings from the Molloy Deep highlight the importance of local circulation features for the distribution of MP particles. Size-dependent relations between MP and biogenic particles suggest that biotic processes throughout the water column affect MP distribution. The POC flux to the Arctic seafloor is low (Cai et al., 2010), however sea ice decline in the Arctic and longer summer periods stimulate primary production (Arrigo and van Dijken, 2015; Wassmann et al., 2015). It is unclear how incorporation of MP into marine aggregates affects the efficiency of the biological pump and consequently deep-sea ecosystem functions in the Arctic. Nevertheless, increasing plastic leakage into our oceans (Brandon et al., 2019), especially into an ecosystem which has already been stressed by climate change as the Arctic Ocean, may well have unknown ecological repercussions.

3.5 Acknowledgements

We thank the officers and crew of *RV Polarstern* and chief scientist of expedition PS99.2, T. Soltwedel. I. Schewe operated the multiple corer. S. Tippenhauer and S. Torres-Valdes operated the CTD. We thank G. Wegener, MPI and MARUM for lending the pumps and S. Becker and J. Rapp for assistance with pump operations. N. Knüppel sampled and analyzed POC, POC and TPM, E-M. Nöthig provided the dataset and gave advice on water column processes along with M. Iversen. A. Purser gave advice on the language and graphical abstract. C. Peter helped with the assessment of the data in LITTERBASE. This work contributes to the Pollution Observatory of the Helmholtz-funded infrastructure program FRAM (Frontiers in Arctic Marine Research), which funded MBT, CW. German Federal Ministry of Education and Research (Project BASEMAN - Defining the baselines and standards for microplastics analyses in European waters; BMBF grant 03F0734A) funded GG, SP. CL was funded by a Ph.D. scholarship of the Deutsche Bundesstiftung Umwelt (DBU) and MB, CH were funded by the Helmholtz-Gemeinschaft Deutscher Forschungszentren. This publication is Eprint ID #### of the Alfred-Wegener-Institut Helmholtz-Zentrum für Polar- und Meeresforschung.

Supporting Information Available

Processing of the water column samples. Identification of particles >500 µm by attenuated total reflection (ATR) FTIR unit. Comparison of the purification methods. FTIR measurements. Contamination elimination. Environmental parameters in the water column and sediments. Relationships between polymer compositions and environmental parameters in the water column. CAP of polymer type compositions. Simulation of the 3D backward particle trajectories. This information is available free of charge via the Internet at http://pubs.acs.org.

3.6 References

ACC (2018). *Elements of the Business of Chemistry.* The American Chemistry Council.

Allen, S., Allen, D., Phoenix, V.R., Le Roux, G., Durántez Jiménez, P., Simonneau, A., et al. (2019). Atmospheric transport and deposition of microplastics in a remote mountain catchment. *Nature Geoscience* 12(5)**,** 339-344. doi: 10.1038/s41561-019-0335-5.

Anderson, M.J., and Walsh, D.C.I. (2013). PERMANOVA, ANOSIM, and the Mantel test in the face of heterogeneous dispersions: What null hypothesis are you testing? *Ecol. Monogr.*83(4)**,** 557-574. doi: 10.1890/12-2010.1.

Arrigo, K.R., and van Dijken, G.L. (2015). Continued increases in Arctic Ocean primary production. *Prog. Oceanogr.* 136**,** 60-70. doi: 10.1016/j.pocean.2015.05.002.

Bakun, A. (2017). Climate change and ocean deoxygenation within intensified surface-driven upwelling circulations. *Philos. Trans. Royal Soc. A* 375(2102)**,** 20160327. doi: 10.1098/rsta.2016.0327.

Barrows, A.P.W., Cathey, S.E., and Petersen, C.W. (2018). Marine environment microfiber contamination: Global patterns and the diversity of microparticle origins. *Environ. Pollut.* 237**,** 275-284. doi: 10.1016/j.envpol.2018.02.062.

Bergmann, M., and Klages, M. (2012). Increase of litter at the Arctic deep-sea observatory HAUSGARTEN. *Mar. Pollut. Bull.* 64(12)**,** 2734-2741. doi: 10.1016/j.marpolbul.2012.09.018.

Bergmann, M., Mutzel, S., Primpke, S., Tekman, M.B., Trachsel, J., and Gerdts, G. (2019). White and wonderful? Microplastics prevail in snow from the Alps to the Arctic. *Sci. Adv.* 5(8)**,** eaax1157. doi: 10.1126/sciadv.aax1157.

Bergmann, M., Tekman, M.B., and Gutow, L. (2017a). Marine litter: Sea change for plastic pollution. *Nature* 544(7650)**,** 297. doi: 10.1038/544297a.

Bergmann, M., Wirzberger, V., Krumpen, T., Lorenz, C., Primpke, S., Tekman, M.B., et al. (2017b). High Quantities of Microplastic in Arctic Deep-Sea Sediments from the HAUSGARTEN Observatory. *Environ. Sci. Technol.* 51(19)**,** 11000-11010. doi: 10.1021/acs.est.7b03331.

Bodungen, B.V., Wunsch, M., and Fürderer, H. (2013). "Sampling and Analysis of Suspended and Sinking Particles in the Northern North Atlantic," in *Marine Particles: Analysis and Characterization*.), 47-56.

Borrelle, S.B., Rochman, C.M., Liboiron, M., Bond, A.L., Lusher, A., Bradshaw, H., et al. (2017). Opinion: Why we need an international agreement on marine plastic pollution. *Proc. Natl. Acad. Sci. U.S.A.*114(38)**,** 9994-9997. doi: 10.1073/pnas.1714450114.

Brandon, J.A., Jones, W., and Ohman, M.D. (2019). Multidecadal increase in plastic particles in coastal ocean sediments. *Sci. Adv.* 5(9)**,** eaax0587. doi: 10.1126/sciadv.aax0587.

Cai, P., Rutgers van der Loeff, M., Stimac, I., Nöthig, E.M., Lepore, K., and Moran, S.B. (2010). Low export flux of particulate organic carbon in the central Arctic Ocean as revealed by 234 Th: 238 U disequilibrium *J. Geophys. Res. Oceans* 115(C10). doi: 10.1029/2009jc005595.

Cathalot, C., Rabouille, C., Sauter, E., Schewe, I., and Soltwedel, T. (2015). Benthic Oxygen Uptake in the Arctic Ocean Margins - A Case Study at the Deep-Sea Observatory HAUSGARTEN (Fram Strait). *PLoS One* 10(10)**,** e0138339. doi: 10.1371/journal.pone.0138339.

Cheang, C.C., Ma, Y., and Fok, L. (2018). Occurrence and Composition of Microplastics in the Seabed Sediments of the Coral Communities in Proximity of a Metropolitan Area. *Int. J. Environ. Res. Public Health* 15(10)**,** 12. doi: 10.3390/ijerph15102270.

Choy, C.A., Robison, B.H., Gagne, T.O., Erwin, B., Firl, E., Halden, R.U., et al. (2019). The vertical distribution and biological transport of marine microplastics across the epipelagic and mesopelagic water column. *Sci. Rep.* 9(1)**,** 7843. doi: 10.1038/s41598-019-44117-2.

Cincinelli, A., Scopetani, C., Chelazzi, D., Lombardini, E., Martellini, T., Katsoyiannis, A., et al. (2017). Microplastic in the surface waters of the Ross Sea (Antarctica): Occurrence, distribution and characterization by FTIR. *Chemosphere* 175**,** 391-400. doi: 10.1016/j.chemosphere.2017.02.024.

Codispoti, L.A., Friederich, G.E., Sakamoto, C.M., and Gordon, L.I. (1991). Nutrient cycling and primary production in the marine systems of the Arctic and Antarctic. *J. Mar. Syst.* 2(3-4)**,** 359-384. doi: 10.1016/0924-7963(91)90042-s.

Cole, M., Lindeque, P., Fileman, E., Halsband, C., Goodhead, R., Moger, J., et al. (2013). Microplastic ingestion by zooplankton. *Environ. Sci. Technol.* 47(12)**,** 6646-6655. doi: 10.1021/es400663f.

Cole, M., Lindeque, P.K., Fileman, E., Clark, J., Lewis, C., Halsband, C., et al. (2016). Microplastics Alter the Properties and Sinking Rates of Zooplankton Faecal Pellets. *Environ. Sci. Technol.* 50(6)**,** 3239-3246. doi: 10.1021/acs.est.5b05905.

Courtene-Jones, W., Quinn, B., Gary, S.F., Mogg, A.O.M., and Narayanaswamy, B.E. (2017). Microplastic pollution identified in deep-sea water and ingested by benthic invertebrates in the Rockall Trough, North Atlantic Ocean. *Environ. Pollut.* 231(Pt 1)**,** 271-280. doi: 10.1016/j.envpol.2017.08.026.

Cózar, A., Marti, E., Duarte, C.M., Garcia-de-Lomas, J., van Sebille, E., Ballatore, T.J., et al. (2017). The Arctic Ocean as a dead end for floating plastics in the North Atlantic branch of the Thermohaline Circulation. *Sci. Adv.* 3(4)**,** e1600582. doi: 10.1126/sciadv.1600582.

Desforges, J.P., Galbraith, M., Dangerfield, N., and Ross, P.S. (2014). Widespread distribution of microplastics in subsurface seawater in the NE Pacific Ocean. *Mar. Pollut. Bull.* 79(1-2)**,** 94-99. doi: 10.1016/j.marpolbul.2013.12.035.

Enders, K., Lenz, R., Stedmon, C.A., and Nielsen, T.G. (2015). Abundance, size and polymer composition of marine microplastics >/=10mum in the Atlantic Ocean and their modelled vertical distribution. *Mar. Pollut. Bull.* 100(1)**,** 70-81. doi: 10.1016/j.marpolbul.2015.09.027.

Engel, A., Bracher, A., Dinter, T., Endres, S., Grosse, J., Metfies, K., et al. (2019). Inter-Annual Variability of Organic Carbon Concentration in the Eastern Fram Strait During Summer (2009–2017). *Front. Mar. Sci.* 6**,** 187. doi: 10.3389/fmars.2019.00187.

Everaert, G., Van Cauwenberghe, L., De Rijcke, M., Koelmans, A.A., Mees, J., Vandegehuchte, M., et al. (2018). Risk assessment of microplastics in the ocean: Modelling approach and first conclusions. *Environ. Pollut.* 242(Pt B)**,** 1930-1938. doi: 10.1016/j.envpol.2018.07.069.

Fazey, F.M., and Ryan, P.G. (2016). Biofouling on buoyant marine plastics: An experimental study into the effect of size on surface longevity. *Environ. Pollut.* 210**,** 354-360. doi: 10.1016/j.envpol.2016.01.026.

Haave, M., Lorenz, C., Primpke, S., and Gerdts, G. (2019). Different stories told by small and large microplastics in sediment - first report of microplastic concentrations in an urban recipient in Norway. *Mar. Pollut. Bull.* 141**,** 501-513. doi: 10.1016/j.marpolbul.2019.02.015.

Hattermann, T., Isachsen, P.E., Appen, W.J., Albretsen, J., and Sundfjord, A. (2016). Eddy-driven recirculation of Atlantic Water in Fram Strait. *Geophys. Res. Lett.* 43(7)**,** 3406-3414. doi: 10.1002/2016gl068323.

Iversen, M.H., and Ploug, H. (2010). Ballast minerals and the sinking carbon flux in the ocean: carbon-specific respiration rates and sinking velocity of marine snow aggregates. *Biogeosciences* 7(9)**,** 2613-2624. doi: 10.5194/bg-7-2613-2010.

Jin, Y., Xia, J., Pan, Z., Yang, J., Wang, W., and Fu, Z. (2018). Polystyrene microplastics induce microbiota dysbiosis and inflammation in the gut of adult zebrafish. *Environ. Pollut.* 235**,** 322-329. doi: 10.1016/j.envpol.2017.12.088.

Kaiser, D., Estelmann, A., Kowalski, N., Glockzin, M., and Waniek, J.J. (2019). Sinking velocity of sub-millimeter microplastic. *Mar. Pollut. Bull.* 139**,** 214-220. doi: 10.1016/j.marpolbul.2018.12.035.

Kanhai, D.K., Gardfeldt, K., Lyashevska, O., Hassellov, M., Thompson, R.C., and O'Connor, I. (2018). Microplastics in sub-surface waters of the Arctic Central Basin. *Mar. Pollut. Bull.* 130**,** 8-18. doi: 10.1016/j.marpolbul.2018.03.011.

Kanhai, L.D.K., Johansson, C., Frias, J.P.G.L., Gardfeldt, K., Thompson, R.C., and O'Connor, I. (2019). Deep sea sediments of the Arctic Central Basin: A potential sink for microplastics. *Deep Sea Res. Part I Oceanogr. Res. Pap.* 145**,** 137-142. doi: 10.1016/j.dsr.2019.03.003.

Katija, K., Choy, C.A., Sherlock, R.E., Sherman, A.D., and Robison, B.H. (2017). From the surface to the seafloor: How giant larvaceans transport microplastics into the deep sea. *Sci. Adv.* 3(8)**,** e1700715. doi: 10.1126/sciadv.1700715.

Kim, S., Yang, J.Y., Kim, H.H., Yeo, I.Y., Shin, D.C., and Lim, Y.W. (2012). Health risk assessment of lead ingestion exposure by particle sizes in crumb rubber on artificial turf considering bioavailability. *Environ. Health. Toxicol.* 27**,** e2012005. doi: 10.5620/eht.2012.27.e2012005.

[Dataset] Krumpen, T. (2017). *Sea Ice and Amtospheric Conditions at HAUSGARTEN between 2000 - 2016 (daily resolution), link to model results.* PANGAEA. doi: 10.1594/PANGAEA.878244. Available: https://doi.org/10.1594/PANGAEA.878244.

Kühn, S., Schaafsma, F.L., van Werven, B., Flores, H., Bergmann, M., Egelkraut-Holtus, M., et al. (2018). Plastic ingestion by juvenile polar cod (*Boreogadus saida*) in the Arctic Ocean. *Polar Biol.* 41(6)**,** 1269-1278. doi: 10.1007/s00300-018-2283-8.

Law, K.L., Moret-Ferguson, S.E., Goodwin, D.S., Zettler, E.R., Deforce, E., Kukulka, T., et al. (2014). Distribution of surface plastic debris in the eastern Pacific Ocean from an 11-year data set. *Environ. Sci. Technol.* 48(9)**,** 4732-4738. doi: 10.1021/es4053076.

Löder, M.G.J., Imhof, H.K., Ladehoff, M., Loschel, L.A., Lorenz, C., Mintenig, S., et al. (2017). Enzymatic Purification of Microplastics in Environmental Samples. *Environ. Sci. Technol.* 51(24)**,** 14283-14292. doi: 10.1021/acs.est.7b03055.

Löder, M.G.J., Kuczera, M., Mintenig, S., Lorenz, C., and Gerdts, G. (2015). Focal plane array detector-based micro-Fourier-transform infrared imaging for the analysis of microplastics in environmental samples. *Environmental Chemistry* 12(5)**,** 563-581. doi: 10.1071/en14205.

Long, M., Moriceau, B., Gallinari, M., Lambert, C., Huvet, A., Raffray, J., et al. (2015). Interactions between microplastics and phytoplankton aggregates: Impact on their respective fates. *Mar. Chem.* 175**,** 39-46. doi: 10.1016/j.marchem.2015.04.003.

Long, M., Paul-Pont, I., Hegaret, H., Moriceau, B., Lambert, C., Huvet, A., et al. (2017). Interactions between polystyrene microplastics and marine phytoplankton lead to species-specific hetero-aggregation. *Environ. Pollut.* 228**,** 454-463. doi: 10.1016/j.envpol.2017.05.047.

Lorenz, C., Roscher, L., Meyer, M.S., Hildebrandt, L., Prume, J., Löder, M.G.J., et al. (2019). Spatial distribution of microplastics in sediments and surface waters of the southern North Sea. *Environ. Pollut.* 252(Pt B)**,** 1719-1729. doi: 10.1016/j.envpol.2019.06.093.

Lu, L., Wan, Z., Luo, T., Fu, Z., and Jin, Y. (2018). Polystyrene microplastics induce gut microbiota dysbiosis and hepatic lipid metabolism disorder in mice. *Sci Total Environ* 631-632**,** 449-458. doi: 10.1016/j.scitotenv.2018.03.051.

Lusher, A., Tirelli, V., O'Connor, I., and Officer, R. (2015). Microplastics in Arctic polar waters: the first reported values of particles in surface and sub-surface samples. *Sci. Rep.* 5, 14947 (2015). doi: 10.1038/srep14947.

Mani, T., Primpke, S., Lorenz, C., Gerdts, G., and Burkhardt-Holm, P. (2019). Microplastic Pollution in Benthic Midstream Sediments of the Rhine River. *Environ. Sci. Technol.* 53(10)**,** 6053-6062. doi: 10.1021/acs.est.9b01363.

Mao, Y., Ai, H., Chen, Y., Zhang, Z., Zeng, P., Kang, L., et al. (2018). Phytoplankton response to polystyrene microplastics: Perspective from an entire growth period. *Chemosphere* 208**,** 59-68. doi: 10.1016/j.chemosphere.2018.05.170.

Möhlenkamp, P., Purser, A., Thomsen, L., Deming, J.W., and Barkay, T. (2018). Plastic microbeads from cosmetic products: an experimental study of their hydrodynamic behaviour, vertical transport and resuspension in phytoplankton and sediment aggregates. *Elementa: Science of the Anthropocene* 6(1)**,** 61. doi: 10.1525/elementa.317.

Morgana, S., Ghigliotti, L., Estevez-Calvar, N., Stifanese, R., Wieckzorek, A., Doyle, T., et al. (2018). Microplastics in the Arctic: A case study with sub-surface water and fish samples off Northeast Greenland. *Environ. Pollut.* 242(Pt B)**,** 1078-1086. doi: 10.1016/j.envpol.2018.08.001.

Mu, J.L., Qu, L., Jin, F., Zhang, S., Fang, C., Ma, X., et al. (2019). Abundance and distribution of microplastics in the surface sediments from the northern Bering and Chukchi Seas. *Environ. Pollut.* 245, 122-130. doi: 10.1016/j.envpol.2018.10.097

Obbard, R.W., Sadri, S., Wong, Y.Q., Khitun, A.A., Baker, I., and Thompson, R.C. (2014). Global warming releases microplastic legacy frozen in Arctic Sea ice. *Earth's Future* 2(6)**,** 315-320. doi: 10.1002/2014ef000240.

Oxvig, U.H., Ulrik Jes (2007). *Fishing gears.* Fiskericirklen.

Peeken, I., Bergmann, M., Gerdts, G., Katlein, C., Krumpen, T., Primpke, S., et al. (2018a). "Microplastics in the Marine Realms of the Arctic with Special Emphasis on Sea Ice [in Arctic Report Card 2018]".).

Peeken, I., Primpke, S., Beyer, B., Gutermann, J., Katlein, C., Krumpen, T., et al. (2018b). Arctic sea ice is an important temporal sink and means of transport for microplastic. *Nat. Commun.* 9(1)**,** 1505. doi: 10.1038/s41467-018-03825-5.

Peng, X., Chen, M., Chen, S., Dasgupta, S., Xu, H., Ta, K., et al. (2018). Microplastics contaminate the deepest part of the world's ocean. *Geochem. Perspect. Lett.* 9**,** 1-5. doi: 10.7185/geochemlet.1829.

Porter, A., Lyons, B.P., Galloway, T.S., and Lewis, C. (2018). Role of Marine Snows in Microplastic Fate and Bioavailability. *Environ. Sci. Technol.* 52(12)**,** 7111-7119. doi: 10.1021/acs.est.8b01000.

Primpke, S., A. Dias, P., and Gerdts, G. (2019). Automated identification and quantification of microfibres and microplastics. *Analytical Methods* 11(16)**,** 2138-2147. doi: 10.1039/c9ay00126c.

Primpke, S., Wirth, M., Lorenz, C., and Gerdts, G. (2018). Reference database design for the automated analysis of microplastic samples based on Fourier transform infrared (FTIR) spectroscopy. *Anal. Bioanal. Chem.* 410(21)**,** 5131-5141. doi: 10.1007/s00216-018-1156-x.

Qi, R., Jones, D.L., Li, Z., Liu, Q., and Yan, C. (2020). Behavior of microplastics and plastic film residues in the soil environment: A critical review. *Sci Total Environ* 703**,** 134722. doi: 10.1016/j.scitotenv.2019.134722.

Redner, S., and Datta, S. (2000). Clogging time of a filter. *Phys. Rev. Lett.* 84(26 Pt 1)**,** 6018-6021. doi: 10.1103/PhysRevLett.84.6018.

Schmidt, C., Krauth, T., and Wagner, S. (2017). Export of Plastic Debris by Rivers into the Sea. *Environ. Sci. Technol.* 51(21)**,** 12246-12253. doi: 10.1021/acs.est.7b02368.

Setälä, O., Fleming-Lehtinen, V., and Lehtiniemi, M. (2014). Ingestion and transfer of microplastics in the planktonic food web. *Environ. Pollut.* 185**,** 77-83. doi: 10.1016/j.envpol.2013.10.013.

Soltwedel, T., Bauerfeind, E., Bergmann, M., Bracher, A., Budaeva, N., Busch, K., et al. (2016). Natural variability or anthropogenically-induced variation? Insights from 15 years of multidisciplinary observations at the arctic marine LTER site HAUSGARTEN. *Ecol. Indic.* 65**,** 89-102. doi: 10.1016/j.ecolind.2015.10.001.

Sun, Y., Xu, W., Gu, Q., Chen, Y., Zhou, Q., Zhang, L., et al. (2019). Small-sized microplastics negatively affect rotifers: Changes in the key life-history traits and Rotifer–*Phaeocystis* population dynamics. *Environ. Sci. Technol.* 53(15)**,** 9241-9251. doi: 10.1021/acs.est.9b02893.

Tekman, M.B., Bergmann, M., and Gutow, L. (2018). *LITTERBASE* [Online]. Available: litterbase.org [Accessed].

Tekman, M.B., Krumpen, T., and Bergmann, M. (2017). Marine litter on deep Arctic seafloor continues to increase and spreads to the North at the HAUSGARTEN observatory. *Deep Sea Res. Part I Oceanogr. Res. Pap.* 120**,** 88-99.

[Dataset] Tippenhauer, S., Torres-Valdés, S., Fong, A.A., Krauß, F., Huchler, M., and Wisotzki, A. (2017). *Physical oceanography during POLARSTERN cruise PS99.2 (ARK-XXX/1.2).* PANGAEA. doi: 10.1594/PANGAEA.871949. Available: https://doi.org/10.1594/PANGAEA.871949.

Trudnowska, E., Sagan, S., and Błachowiak-Samołyk, K. (2018). Spatial variability and size structure of particles and plankton in the Fram Strait. *Prog. Oceanogr.* 168**,** 1-12. doi: https://doi.org/10.1016/j.pocean.2018.09.005.

Turner, J.T. (2015). Zooplankton fecal pellets, marine snow, phytodetritus and the ocean's biological pump. *Prog. Oceanogr.* 130**,** 205-248. doi: https://doi.org/10.1016/j.pocean.2014.08.005.

van Sebille, E., England, M.H., and Froyland, G. (2012). Origin, dynamics and evolution of ocean garbage patches from observed surface drifters. *Environ. Res. Lett.* 7**,** 044040.

Wassmann, P., Kosobokova, K.N., Slagstad, D., Drinkwater, K.F., Hopcroft, R.R., Moore, S.E., et al. (2015). The contiguous domains of Arctic Ocean advection: Trails of life

and death. *Prog. Oceanogr.* 139**,** 42-65. doi: https://doi.org/10.1016/j.pocean.2015.06.011.

Wekerle, C., Krumpen, T., Dinter, T., von Appen, W.J., Iversen, M.H., and Salter, I. (2018). Properties of Sediment Trap Catchment Areas in Fram Strait: Results From Lagrangian Modeling and Remote Sensing. *Front. Mar. Sci.*5**,** 407. doi: 10.3389/fmars.2018.00407.

Wekerle, C., Wang, Q., von Appen, W.-J., Danilov, S., Schourup-Kristensen, V., and Jung, T. (2017). Eddy-Resolving Simulation of the Atlantic Water Circulation in the Fram Strait With Focus on the Seasonal Cycle. *J. Geophys. Res. Oceans* 122(11)**,** 8385-8405. doi: 10.1002/2017jc012974.

Wieczorek, A.M., Croot, P.L., Lombard, F., Sheahan, J.N., and Doyle, T.K. (2019). Microplastic ingestion by gelatinous zooplankton may lower efficiency of the biological pump. *Environ. Sci. Technol.* 53(9)**,** 5387-5395. doi: 10.1021/acs.est.8b07174.

Wollenburg, J.E., Katlein, C., Nehrke, G., Nöthig, E.M., Matthiessen, J., Wolf- Gladrow, D.A., et al. (2018). Ballasting by cryogenic gypsum enhances carbon export in a *Phaeocystis* under-ice bloom. *Sci. Rep.* 8(1)**,** 7703. doi: 10.1038/s41598-018-26016-0.

Woodall, L.C., Sanchez-Vidal, A., Canals, M., Paterson, G.L.J., Coppock, R., Sleight, V., et al. (2014). The deep sea is a major sink for microplastic debris. *Roy. Soc. open sci.* 1(4)**,** 140317. doi: 10.1098/rsos.140317.

Wright, S.L., Thompson, R.C., and Galloway, T.S. (2013). The physical impacts of microplastics on marine organisms: A review. *Environ. Pollut.* 178**,** 483-492. doi: 10.1016/j.envpol.2013.02.031.

Zhao, S., Danley, M., Ward, J.E., Li, D., and Mincer, T.J. (2017). An approach for extraction, characterization and quantitation of microplastic in natural marine snow using Raman microscopy. *Analytical Methods* 9(9)**,** 1470-1478. doi: 10.1039/C6AY02302A.

Zhao, S., Ward, J.E., Danley, M., and Mincer, T.J. (2018). Field-Based Evidence for Microplastic in Marine Aggregates and Mussels: Implications for Trophic Transfer. *Environ. Sci. Technol.* 52(19)**,** 11038-11048. doi: 10.1021/acs.est.8b03467.

4 General Discussion

4.1 Overview

This dissertation investigated macro-debris and microplastic distribution in open Arctic waters. However, the temporal and spatial distribution of floating marine debris in Arctic waters presented in Chapter 2.1 covered not only Arctic waters but also the temperate North Atlantic, enabling a comparison of concentrations between these two oceanic regions. The concentrations of floating macro-debris ranged from zero to 356 items km^{-2} with no statistically significant differences in concentrations or compositions between the studied regions. A median concentration of 11 items km^{-2} was measured in both Arctic and temperate North Atlantic waters. Although Chapter 2.1 is on marine debris, given that plastics including ropes and nets accounted for 91% of all debris items, the chapter is mainly on plastic pollution in surface waters. The pollution levels in Arctic waters were similar to those in the North Atlantic (Thiel et al., 2011; Gutow et al., 2018), higher than in the Southern Ocean (Ryan et al., 2014; Suaria et al., 2020) but lower than in hotspot areas, such as in the Mediterranean Sea (Zeri et al., 2018; Palatinus et al., 2019) or North Pacific subtropical region (Goldstein et al., 2013). The most frequently observed plastic items were fragments, films (including foils, sheets and bags), ropes and nets, packaging materials, expanded polystyrene pieces and straps. These types of plastic debris constituted 50% of 1,149 floating items observed in total. Medium-sized items accounted for 46%, followed by small (36%) and large (5%) items. White and transparent items dominated the observations with 55% of the total debris count. Debris concentrations measured in summer were significantly higher than those detected in spring and autumn, suggesting an indirect effect of sea ice decline, which has led to an increase in maritime activities in the Arctic Ocean. The analysis of environmental parameters suggested a weak but significant relation to debris concentrations, yet it only explained a small portion of the variability. This indicates how complex it is to cover all influential factors when distribution of floating debris was explored.

Chapter 2.2 focused on the spatial and temporal variability of marine debris on the deep seafloor of the Fram Strait by reporting the results of the analyses of images taken between 2002 and 2014 at the central and northern stations of the HAUSGARTEN Observatory. Photographic surveys were undertaken by a camera system towed by the research vessel along the same transects in every sampling year. Chapter 2.2 is a part of the time series, which included the debris concentrations observed between 2002 and 2012 at the central HAUSGARTEN station (Bergmann and Klages, 2012). Despite the remoteness of the Fram

Strait, the mean debris concentration measured (3,485 items km^{-2}) was in a similar range as those recorded in more populated areas(Mordecai et al., 2011). In contrast to size distribution of floating debris (Chapter 2.1), the majority of the items on the seafloor was small-sized (57%), followed by medium-sized items (40%). Plastic accounted for the majority of the items, yet with a lower proportion (47%) than in surface waters (91%). Glass (26%), rope (11%), metal (7%), fabric (6%), paper/cardboard, pottery and timber (4%) were other types of debris. An increase in debris concentrations from 2002 to 2014 was observed, which was attributed to the increase in maritime operations in the Arctic including touristic cruises. In case of sea ice being a transportation medium for debris, drift trajectories indicated Kara and Laptev Seas as the source areas. Marine debris concentration on the deep seafloor of the Fram Strait was 500 times higher than that observed floating in the Greenland Sea (9 items km^{-2}), indicating that the deep Arctic seafloor constitutes a sink for continuous debris accumulation. Interactions of marine debris with hydrozoans, sponges, sea lilies and anemones and shrimps were observed for 56% of the debris items.

Chapter 3 dealt with microplastic pollution throughout the water column and in sediments of the Fram Strait. Water samples were taken with large volume in-situ filtration devices deployed at four different depth levels and sediment samples with a video guided multi-corer. The water column samples were taken from 1 – 3 m below the surface (near-surface), 300 m, 1000 m and above the seafloor. Microplastics were found in all samples with a range from nine to 1,287 items m^{-3}, except for the samples taken above the seafloor of the central HAUSGARTEN and of the station close to the Svalbard coast. A significant difference in microplastic concentrations between the sampling stations were found. However, it should be noted that all sampling stations were at the HAUSGARTEN Observatory, thus, the spatial variability of microplastics evaluated in Chapter 3 was at a smaller scale than surface observations (Chapter 2.1). Significant differences in microplastic concentrations and compositions among stations indicated a specific vertical distribution pattern at the Molloy Deep, which differed from all other stations and pointed to the importance of local conditions in particle distribution. Microplastic concentrations were correlated with organic matter concentrations, suggesting an interaction between marine aggregates and anthropogenic particles. Microplastic concentrations in sediments at the Fram Strait were very high, ranging from 239 to 13,331 items m^{-3}.

The three main studies of this dissertation deal only with a part of the findings of the FRAM Pollution Observatory. In addition to them, macro-debris concentrations at Svalbard

beaches (Bergmann et al., 2017a; Meyer, 2022) and microplastic particles in deep-sea sediments (Bergmann et al., 2017b), in snow (Bergmann et al., 2019), in sea ice (Peeken et al., 2018) and ingested by zooplankton (Botterell et al., 2022) and polar cod (Kühn et al., 2018) were investigated in other studies of the FRAM Pollution Observatory. Moreover, a later study extended Chapter 2.2 by evaluating the seafloor images taken from the southernmost station of the HAUSGARTEN observatory between 2002 and 2017 and new images taken between 2015 and 2017 from the central and northern stations (Parga Martínez et al., 2020). Such an extensive assessment of marine debris and microplastic pollution from a region is extremely rare and deserves special attention. Therefore, in the remaining part of this chapter, I will synthesise all studies of the FRAM Pollution Observatory in order to provide the best picture of anthropogenic pollution in the European Arctic. Therefore, even though this dissertation is mainly divided into two parts based on the size classification of marine debris, in the following sections, I will focus on ecosystem compartments and summarise the findings obtained from studies other than those in the main chapters.

As a short synthesis, the following results have been reported by all studies of the FRAM Pollution Observatory. The deep seafloor images taken between 2002 and 2017 showed a mean marine debris concentration of 4,571 ± 1,628 items km^{-2} [Chapter 2.2 and (Bergmann and Klages, 2012; Parga Martínez et al., 2020)], with plastic bags, packaging material and fishing gear accounting for 41% of all observed items. A mass beach debris concentration ranging from 0 to 524 g m^{-2} reported by two studies (Bergmann et al., 2017a; Meyer, 2022), which analysed the samples collected from 20 beaches on Svalbard by citizen scientists between 2016 and 2021. Fisheries debris accounted for 44–100% of the total debris mass at Svalbard beaches. Surveys of nine beaches yielded a mean concentration of 0.37 items m^{-2} by count, which was by far the highest macro-debris concentration compared to those reported from any other ecosystem compartment. This value corresponds to a concentration of 370,000 items km^{-2}, which is two orders of magnitude higher than that reported from the seafloor and four orders of magnitude higher than that reported from the sea surface. Microplastic particles from the sea surface, the water column, sediment, sea ice and snow were analysed by combining the latest sampling technology with state-of–the-art harmonised µFT-IR analyses [Chapter 3 and (Bergmann et al., 2017b; Peeken et al., 2018; Bergmann et al., 2019)]. The highest microplastic concentration throughout the water column was at the near-surface layer, ranging from 113 to 1,287 items m^{-3}. But microplastic particles were also found in all water column samples of the remaining depth layers with concentrations ranging between 9 to 186 items m^{-3} except for

samples taken above the seafloor at the central HAUSGARTEN and Svalbard stations (Chapter 3). The analyses of sediment cores showed microplastic concentrations of 42 to 13,331 N kg^{-1} [Chapter 3 and (Bergmann et al., 2017b)]. Polymer diversity in sediments was higher compared to the diversity in the water column samples, probably because the seafloor is a long-term sink for microplastic and has thus accumulated more and more different particles over longer time scales. The highest microplastic concentrations in water and sediments were measured at the northernmost station in the marginal ice zone and polymer compositions resembled those of sea ice indicating this as a possible source. In the sea ice, the highest microplastic concentration (1.2 ± 1.4) $\times 10^7$ items m^{-3}) was detected in an ice core taken in the pack ice of Fram Strait (Peeken et al., 2018). A median concentration of 224 items per litre melted snow was measured in the samples taken from Svalbard and ice floes in the Fram Strait, which is an indicator of atmospheric deposition of microplastic particles (Bergmann et al., 2019). In addition, 64 plastic fragments were detected in 1,417 individuals of zooplankton from Fram Strait. All these numerical results were summarised in Fig. 4.1.

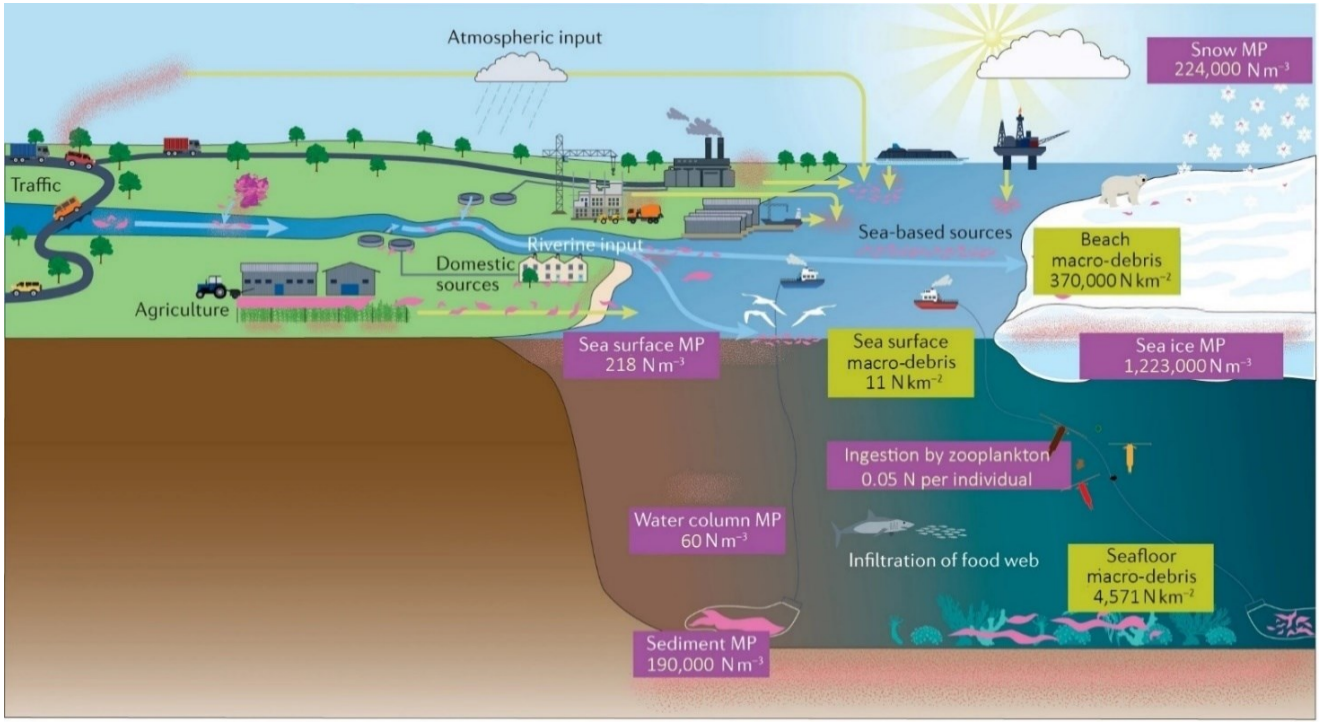

Figure 4.1 Microplastic levels were presented as median concentrations. To enable a comparison, they were converted to N (items) m^{-3}. For macro-debris, the mean concentrations reported in the studies were used and beach debris concentration was converted to N (items) km^{-2} to enable a comparison with those from the seafloor and sea surface. Adapted from Fig.1 in "Plastic pollution in the Arctic" by M. Bergmann, F. Collard, J. Fabres, G. W. Gabrielsen,

A comparison of debris concentrations between different marine ecosystem compartments is very challenging. For example, in Chapter 2.1, macro-debris concentrations at the sea surface were compared to those measured on the seafloor. Although both compartments were assessed by visual methods, the results obtained by different sampling methods are not strictly comparable. For example, the observation altitude was greater for sea surface than seafloor observations. Sea surface observations had to be categorised instantly whereas seafloor photographs could be scrutinized repeatedly by several experts and physical samples from beaches could even be examined by citizen scientists. Multivariate analyses of size and material compositions were conducted for all studies in this dissertation, in order to obtain additional information on composition patterns so that marine debris in different ecosystem compartments can be compared qualitatively. Although the microplastic samples of FRAM Pollution Observatory were obtained from different marine compartments, they all were purified with similar filters, inspected with Fourier transform infrared spectroscopy imaging (µ-FTIR) and spectral data was evaluated with automated data analysis (Primpke et al., 2017). Unlike the macro-debris studies, the use of the same analytical approach in all samples enables quantitative and qualitative comparisons of microplastic. However, for example, sediment microplastic concentrations in Chapter 3 were estimated in items per m^3 dry sediment in order to provide a comparison with the water column, yet the quantities per volume water is not strictly comparable to quantities per volume sediment. In this dissertation, particle size detection limits of studies are always considered in comparisons of concentrations. Despite these drawbacks, globally, our knowledge on the spatial distribution, transportation pathways and accumulation mechanisms of marine debris pollution is limited and if possible, comparisons of debris concentrations in different marine compartments are essential to identify the sources and sinks of marine debris pollution. Therefore, globally, the FRAM Pollution Observatory provides one of the few case-studies to assess regional marine debris and microplastic pollution obtained from different ecosystem compartments in a holistic approach. Huntington et al. (2020) conducted a regional assessment of microplastic pollution, but not of macro-debris in different ecosystem compartments of Canadian Arctic waters and Miller et al. (2021) and Zhu et al. (2021) of San Francisco Bay.

The debris observations and analyses at the FRAM Pollution Observatory have not allowed me to draw firm conclusions as to the sources, pathways and sinks of plastic pollution. However, this is not specific to the studies of the FRAM Pollution Observatory. Even when physical samples are collected, this is challenging. For example, I contacted the producer of the floating bucket retrieved from the Fram Strait bearing the writing "Glidden" (Chapter 2.1) to find out if I can obtain any more information about its history and received the following reply:

"Unfortunately, our products are sold to commercial, residential and light industrial contractors as well as consumers throughout the US and Canada. In addition, our customers frequently continue to use empty paint buckets on the job and/or in their homes long after the paint is used up. With that in mind it would be impossible to tell where the container was used and when or where it entered the water. I can tell you that I agree with your assertion that the container has been around for a very long time. Based on the picture you provided it would appear that the paint pail you found is not currently in use in our distribution. In fact, I checked with several of our associates who were with Glidden prior to PPG's acquisition of that brand several years ago. Some of these associates have more than 20 years of experience with that brand. I was not able to find anyone who recalls Glidden stencilling their name on pails as it is observed on the specimen you found. Also, the apparent erosion of the plastic in many areas of your picture points to severe abrasion incurred over time."

In the best case, we can only obtain information about the production date and place of the debris, as was done for the beach debris from Svalbard (Meyer, 2022). Therefore, the studies of the FRAM Pollution Observatory have investigated all possible aspects including the properties of individual pieces and the distribution and composition patterns. Moreover, the drift trajectories of floating and sinking particles and sea ice were simulated in order to investigate the possible pathways of plastic pollution in the Arctic. In the following section, I will summarise the findings obtained from each ecosystem compartment in order to elucidate the distribution, sources, transportation pathways and sinks of plastic pollution in the Arctic. By doing so, I will also summarise the results generated by studies other than those included in the main body of this dissertation. Moreover, I will provide a first comparison of microplastic compositions obtained from the water column, sediment and snow.

4.2 Sea Surface, Sea Ice and Snow

In addition to the concentrations of marine debris and microplastic floating at the sea surface of the Fram Strait investigated in Chapter 2.1 and Chapter 3, Botterell et al. (2022) measured microplastic concentrations in the Fram Strait in order to explore how spatial differences in concentrations affect the ingestion rates of microplastic by zooplankton. The water samples were taken at 6.5 m water depth of six stations with plastic bottles from the underway system. Spectral imaging (µFTIR) in combination with the SIMPLE automated polymer identification software (Primpke et al., 2020) was used for the quantification and qualification, allowing the detection of particles down to 6.25 µm in size. Fig. 4.2 shows the distribution of microplastic in the near-surface waters of the Fram Strait based on the data from Chapter 3 and Botterell et al. (2022).

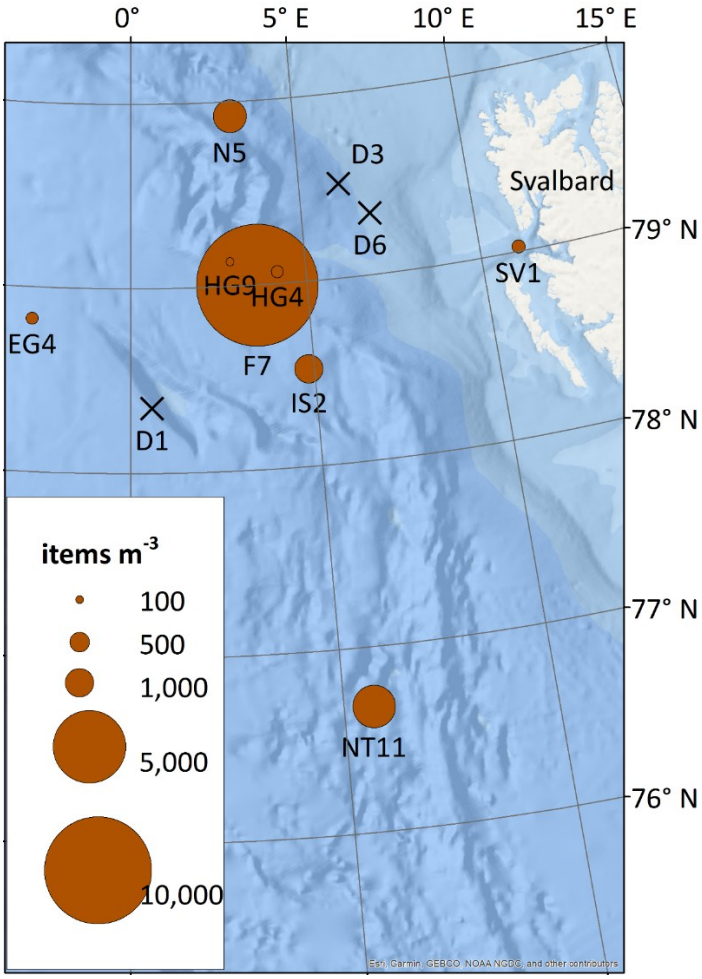

Figure 4.2. Near-surface distribution of microplastic particles reported in Chapter 3 (based on the samples taken from stations EG4, N5, HG4, HG9 and SV1) and by Botterell et al. (2022) (based on the samples taken from stations D1, D3, D6, F7, IS2, N11). The sizes of the points are proportional and represent microplastic concentrations in items m^{-3}. Crosses denote the absence of microplastic particles.

The average microplastic concentration of 7,000 items m^{-3} reported in (Botterell et al., 2022) is 32 times higher than the median microplastic concentration in near-surface samples reported in Chapter 3. Such a difference could have arisen because of two reasons: (i) (Botterell et al., 2022) include both fragments and fibres, whereas fibre detection was not yet available when the analyses for Chapter 3 were conducted. Future studies of the FRAM Pollution Observatory should also focus on the distribution of anthropogenic fibres because a model based on water masses, current velocity and winds concluded that globally microfibre concentrations are highest in the Arctic Ocean (Lima et al., 2021). Indeed, snow samples taken from ice floes in the Fram Strait and Svalbard showed a microfibre concentration ranging from 0.043×10^3 to 10.2×10^3 items L^{-1}, with the highest value observed in the sample taken from an ice floe in the Fram Strait, indicating considerable atmospheric deposition in the Arctic (Bergmann et al., 2019). (ii) Only two litres of sea water were sampled by (Botterell et al., 2022), which may be not as representative as samples taken during the study in Chapter 3 (Li et al., 2020; Yakushev et al., 2021).

As for other Arctic regions, microplastic analyses for particles > 10 µm in surface waters in the fjord Nuup Kangerlua close to Nuuk revealed a concentration of 142 items m^{-3} (Rist et al., 2020), which is similar to those obtained from the near-surface waters of the Fram Strait (Chapter 3). For microplastic particles > 7 µm, a concentration of ~100 items m^{-3} was detected in the North Atlantic Subtropical Gyre (Enders et al., 2015). The surface concentrations of microplastic particles > 11 µm ranged from 0.1 to 245 in the southern North Sea (Lorenz et al., 2019). As with the floating debris observations, Arctic waters appear to be as polluted with microplastics as waters from lower latitudes of the North Atlantic, which are closer to urban centres.

A high contribution of miscellaneous plastic fragments reported in Chapter 2.1 concurs with results from the North Pacific subtropical gyre (Lebreton et al., 2018) and indicates a long residence time in the ocean. Indeed, drift trajectories in other studies (Cózar et al., 2017; Strand et al., 2021), as well as those presented in Chapter 3 suggest that much of the floating debris originates from the Atlantic Ocean. Cózar et al. (2017) estimated that in one to three years, floating plastics can reach the northernmost parts of the Greenland and Barents Sea where deep-water formation occurs. While waters sink to deeper layers, buoyant plastics remain afloat leading to an accumulation. Therefore, the study concluded that the Arctic Ocean, especially the deep seafloor, is the ultimate dead end for floating plastic. In Chapter 3, 2-D simulations of particle drift trajectories for 365 days revealed similar trajectories to Cózar et al. (2017).

Indeed, a significant positive correlation with salinity presented in Chapter 2.1 indicates a relation to water masses and thus suggests that the temperate regions are a source area of debris floating in Arctic waters. Strand et al. (2021) simulated trajectories of marine debris and microplastic found on seven Arctic beaches back to their origins. In their model, it took six months to one year for marine debris from adjacent seas to strand on the beaches. The residence time of macro plastic in surface waters was longer than that of microplastic, possibly due to windage. Indeed, as shown in Chapter 2.1 and in earlier studies (Kukulka et al., 2012; Suaria et al., 2016), wind has a significant effect on plastic distribution: a higher wind speed leads to lower debris concentrations. Therefore, it was advised to apply a correction coefficient for submerged microplastics (Kukulka et al., 2012; Suaria et al., 2016), which should be taken into consideration for future studies of the FRAM Pollution Observatory. Therefore, it is likely that due to the wind-induced vertical mixing, some debris items were pushed to subsurface waters, thus the reported concentrations in Chapter 2.1 should be considered as the minimum values. One valuable addition to Chapter 2.1 would be the simulation of drift trajectories of floating items, tracking them back to their source areas. The 2D model presented for microplastic in Chapter 3 can be customized for macro plastics by applying a coefficient to simulate the effect of wind drag. Earlier models of floating debris have used multiple coefficients of wind drag because of the various shapes and sizes of debris. For example, Gutow et al. (2018) used 0.0%, 0.5% and 1.0% of the current speed to determine the particle velocities in the North Sea. Cardoso and Caldeira (2021) applied random windage coefficients ranging from 0 to 1%, 1 to 2%, 2 to 3%, 3 to 4%, and 4 to 5% of the wind to the virtual particles released at the Macaronesia Islands in the NE Atlantic.

The Transpolar Drift is known to carry particles along with shelf water from Eurasian basin and sea ice from Siberian Seas to the Central Arctic and the Fram Strait (Charette et al., 2020). Overall, the results from this dissertation suggest that the North Atlantic Current carries more marine debris and microplastic into the Fram Strait than the Transpolar Drift. Similarly, Jiang et al. (2020) identified microplastic particles in the East Greenland current, albeit with lower concentrations than in the Greenland Sea Gyre, which is formed by a branch of the Norwegian Atlantic Current. It is still not exactly known how sea ice distribution affects macro-debris concentrations. Anthropogenic items were not seen trapped in ice floes (Chapter 2.1). Moreover, no floating debris was recorded during transects with extensive sea ice. Therefore, the presence of extensive sea ice can actually be a limitation of visual surveys in the Arctic Ocean, until the fate of floating macro-debris during ice formation or when encountering ice

floes is resolved. In theory, debris items could become submerged, pushed aside or entrained in sea ice. For example, wood is carried over long distances in the Arctic Ocean in sea ice (Murphy et al., 2021). Accordingly, if macro plastic is entrained in sea ice, the sea ice drift trajectories presented in Chapter 2.2 could also be pathways of once floating plastics. These drift trajectories identified the Kara and Laptev Seas as the source area of floating sea ice in the Fram Strait. Therefore, plastic pollution levels and the oceanographic processes in Siberian Seas merit special attention.

Recently, a few studies have investigated the plastic pollution in the Siberian Seas. Surface waters of the Kara, Laptev and East Siberian Seas were free of floating macro-debris in the ice-free season (Pogojeva et al., 2021), which was attributed to the seasonality as the sampling was conducted during autumn, when river discharge is low. Unlike macro-debris, microplastic is present in surface waters of the Siberian Seas, albeit at 140 to 1,600 times lower microplastic concentrations than those measured in the Fram Strait. For microplastic particles larger than 100 µm, a concentration of 0.71 items m^{-3} was reported from the subsurface waters at the east of 65°E (Pakhomova et al., 2022). These waters were identified as the second most polluted region after the Barents Sea compared to the North Atlantic, Central Atlantic and Antarctica (Pakhomova et al., 2022). Another study on surface particles larger than 200 µm and subsurface particles larger than 100 µm measured microplastic concentrations of 0.01 and 0.8 items m^{-3}, respectively (Yakushev et al., 2021). It identified Siberian river discharge as a source of microplastics, which can then stay in shelf areas for several years, as has been simulated for tracers (Golubeva et al., 2019). Pakhomova et al. (2022) suggested that neutrally buoyant microplastics get trapped by turbulent mixing within the near-surface layers and are transported over long distances by Stokes drift associated with surface waves. The sampling for microplastics in Chapter 3 was conducted between one to three meters depth due to the operational requirements of the gear. Accordingly, microplastic concentrations at the sea surface of the Fram Strait can in fact be different to those measured in these near-surface waters. The positively buoyant particles in the surface layer, on the other hand, are mainly affected by wind and waves and thus can be subjected to a random horizontal distribution as suggested in Strand et al. (2021) and supported by the patchiness of the macro-debris observations in Chapter 2.1.

Mountford and Morales Maqueda (2021) investigated the accumulation and transport of microplastics by sea ice by describing three processes for the capture and release of microplastics in sea ice: (i) Microplastic particles get trapped in sea ice via basal accretion. (ii)

A thick snow cover can force the sea ice to sink. Subsequently, particles in the surface layer permeate the submerged part of the snow-ice matrix, assuming that snow is free of microplastics. (iii) Microplastics are released from the sea ice by basal melting and surface-melt (Fig. 4.3). Their model suggests that positively buoyant microplastics dominate in Arctic sea ice, which concurs with Peeken et al. (2018).

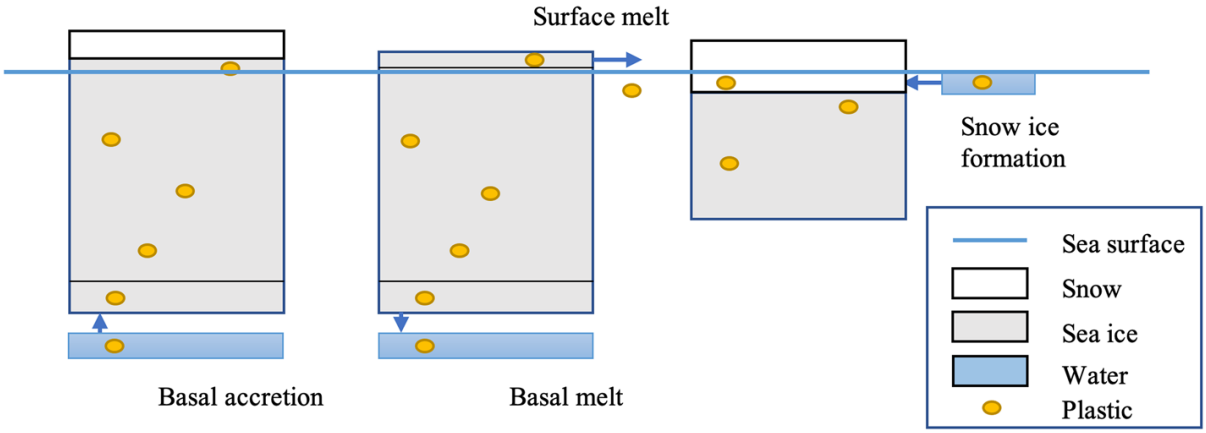

Figure 4.3. Capture and release processes of microplastics in sea ice. Reprinted from Fig. 2 in "Modelling the Accumulation and Transport of Microplastics by Sea Ice" by A. S. Mountford and M. A. Morales Maqueda, 2021, J. Geophys. Res. Oceans, 126 (2), e2020JC016826 with permission from A. S. Mountford.

The first study on microplastic particles in Arctic sea ice reported a concentration of 38 to 234 particles per litre sea ice by analysing cores taken from four locations in the Arctic (Obbard et al., 2014). Peeken et al. (2018) analysed another five ice cores and found microplastic concentrations ranging between 1,100 and 12,000 particles per litre. The highest concentration was found in the pack ice of Fram Strait that originated from the Makarov Basin. Such high concentrations may impact sea ice albedo (Geilfus et al., 2019). The presence of darker microplastics could accelerate the sea ice melt and affect the light penetration depth, having an effect on photochemical and photo-biological processes in sea ice accelerating melt rates (Bergmann et al., 2022).

Kanhai et al. (2020) detected 2 – 17 items L^{-1} in 25 ice cores taken from the Central Arctic Basin. However, their minimum particle detection limit was 100 µm, whereas, particles of size down to 11 µm were identified in Peeken et al. (2018). The majority of the particles were smaller than 100 µm with 67% being in the smallest size category of 11 µm. Therefore, the concentrations in Kanhai et al. (2020) are most likely a great underestimate of actual pollution levels although they included fibres, whose identification was not available at the

time of analyses of Peeken et al. (2018). As for other regions of the world, 8 to 41 particles larger than 63 µm were detected in per litre sea ice of the Baltic Sea (Geilfus et al., 2019), and an average of 12 particles larger than 20 µm per litre melted sea ice was measured in one core sampled from coastal land-fast sea ice in East Antarctica (Kelly et al., 2020), which are considerably lower than those reported by Peeken et al. (2018) for Arctic ice cores.

Measurements in Chapter 3 and by Kanhai et al. (2020) and Kim et al. (2021) support the hypothesis of sea ice being a temporary and intermediate sink of microplastics. Microplastic concentrations in land-fast ice (Peeken et al., 2018) were 19,000 times higher than those reported from near-surface waters of Fram Strait (Chapter 3) and three orders of magnitude higher than those reported from below the sea ice (Kanhai et al., 2020). Moreover, the highest near-surface microplastic concentration of the Fram Strait was found in the sample from the northernmost station at the marginal ice zone, suggesting the release of particles during melting. In fact, the microplastic concentration in that sample was up to one order of magnitude higher than those in the remaining samples, thus, in Chapter 3, this sample was even treated as an outlier and excluded in univariate analyses. Similarly, von Friesen et al. (2020) measured 158 anthropogenic particles larger than 50 µm per litre of floating sea ice around Svalbard, a concentration up to two orders of magnitude higher than the concentrations they detected in seawater. As in Chapter 3, von Friesen et al. (2020) also found the highest subsurface microplastic concentrations at the marginal ice zone.

The salinity and temperature profiles of the near-surface layer in Chapter 3 showed a special pattern. Rudels et al. (1991) identified the polar mixed layer in the Fram Strait as "freezing temperature and salinity of about 32.7 psu". The area of the Fram Strait, where the near-surface samples of central station and Molloy Deep were obtained, fits to this profile with salinity values of 32.9 and 32.4 psu and with temperature values of -0.3 and -0.5 °C, respectively. On the other hand, cooler waters (-0.9 and -1.1) with a higher salinity (33.9 and 33.3) were recorded for the near-surface waters of the northern and East Greenland stations. Based on these profiles and microplastic concentrations, we can speculate that some of the microplastic particles at the near-surface layer of the central station and Molloy Deep were carried along with waters of polar mixed layer, which is also supported by the drift trajectories in Chapter 3. The higher salinity and lower water temperatures measured at the northern and East Greenland stations could indicate that the recirculating Atlantic branch meets with sea ice, causing it to melt and release entrained microplastics.

Snow scavenges airborne particles and pollutants during its passage to Earth's surfaces (Zhao et al., 2015), thus concentrations of anthropogenic particles in snow is a good indicator of atmospheric microplastic pollution. Microplastic occurrence in snow samples taken from Svalbard and ice floes in the Fram Strait was studied by Bergmann et al. (2019). Additional samples were taken from northern Europe (Bremen City, Isle of Heligoland) and the Alps (Davos, Tschuggen, Bavaria) for a comparison with Arctic samples. Microplastic particles and fibres were detected in all samples, with concentrations ranging from 0.02×10^3 to 154×10^3 items L^{-1} and 0.043×10^3 to 10.2×10^3 items L^{-1}, respectively except for one ice floe. The median microplastic concentration in snow samples from Svalbard and the Fram Strait was 224 items L^{-1} with a high-level calculation of snowfall rates of 200 kg m^{-2} on the Fram Strait and 450 kg m^{-2} on Svalbard. This level of microplastic pollution is 1,000 times higher than that in near-surface waters and 4,200 times higher than in the deep-water column. However, compared with concentrations in sea ice and sediments, microplastic concentrations in snow are one to two orders of magnitude lower. Evangeliou et al. (2020) estimated that 140,000 metric tons of microplastics from the wear of car tyres and brakes are carried by winds to the oceans and that these particles can even be transported by atmospheric circulations to the Arctic with hot spots on Greenland. In addition, microfibers from synthetic textiles and fabrics could add 7 – 34 metric tons per year to the ocean (Liu et al., 2020). However, the transport mechanisms and sinks of atmospheric particles are poorly constrained with estimates ranging from 0.013 to 25 million metric tons per year of micro(nano)plastics being transported within the marine atmosphere and deposited in the oceans (Allen et al., 2022). Ferrero et al. (2022) suggested that while particles are carried by wind, a continuous deposition and emission at the sea-air interface occurs, which may be well the case at the sea ice-air interface in the Arctic. Air samples taken from sea-air interface on the French Atlantic showed an average microplastic concentration of 2.9 items m^{-3} during onshore and 9.6 items m^{-3} during offshore winds, yielding estimates of 136,000 metric tons of microplastic blown out to the sea (Allen et al., 2020). Therefore, it is plausible to assume that microplastic particles in Arctic snow become incorporated into the sea ice matrix or blown back to the atmosphere by wind, thus they indirectly or partially contribute to the pollution in Arctic waters.

According to the data in Bergmann et al. (2019), the median microplastic concentration of particles > 11 µm and fibres in Arctic snow (224 and 218 items L^{-1}) was lower than that in the Alps (2,700 and 986 items L^{-1}) and North Europe (11,800 and 1,983 items L^{-1}). Since the sampling method and minimum size detection limit of the particles differ among studies, it is

challenging to compare our concentrations with those of other studies. For example, an aircraft sampling whilst flying up to 3,500 m over Spain reported a microplastic concentration of particles > 9.8 µm ranging from 1.5 items m^{-3} above rural areas to 13.9 items m^{-3} above urban areas (González-Pleiter et al., 2021). Above rural areas, the dominant type of particles were fibres with up to 84%, whereas fragments accounted for up to 67% of the microparticles over urban areas (González-Pleiter et al., 2021). Snow samples from the Mount Everest revealed a concentration of 30 items L^{-1} for microplastic particles > 30 µm, which were mainly polyester fibres, likely released from climber's clothing and equipment (Napper et al., 2020). Microplastic particles > 50 µm had an average concentration of 29 items L^{-1} in Antarctic snow, again, fibres constituting the majority of the microplastics (Aves et al., 2022). Atmospheric microplastic can interact with solar radiation and thus influence the carbon cycle by absorbing and scattering radiation, hence affecting climate processes (Revell et al., 2021). In addition, these particles have been found in human lung tissue (Pauly et al., 1998). Considering that bioaerosols carrying pathogens can adhere to athmospheric microplastics, they have a potential to carry diseases over long distances (VishnuRadhan et al., 2021). Therefore, the high microplastic concentrations in Arctic snow should be considered as an early warning sign of possible repercussions on human health and climate processes.

4.3 Arctic Beaches (Svalbard)

Although the distribution of anthropogenic debris on Arctic beaches was not assessed in the main chapters of this dissertation, it has been an important part of the FRAM Pollution Observatory. A total of 20 Svalbard beaches were surveyed between 2016 and 2021 by citizen scientists. The results obtained during the island visits of tourist cruises in 2016 were reported by Bergmann *et al.* (Bergmann et al., 2017a). A total of 991 kg of litter was collected from an area of 11,732 m^2 on six beaches, corresponding to a debris concentration between 9 and 524 g m^{-2} with a mean (± SEM) mass of 102 ± 84 g m^{-2} (Fig. 4.4). Such a pollution level is higher than those reported from densely populated South China beaches (3 g m^{-2}) (Cheung et al., 2016) or India (<1 and 29 g m^{-2}) (Kaladharan et al., 2012; Jayasiri et al., 2013) but lower than the remote and uninhabited Henderson Island in the South Pacific (40 – 1,250 g m^{-2}) (Lavers and Bond, 2017). The mass of fisheries-related plastic accounted for 44 – 100% of the total debris, followed by other plastic items (0 – 48%), glass (0 – 12%) and clothes (0 – 5%).

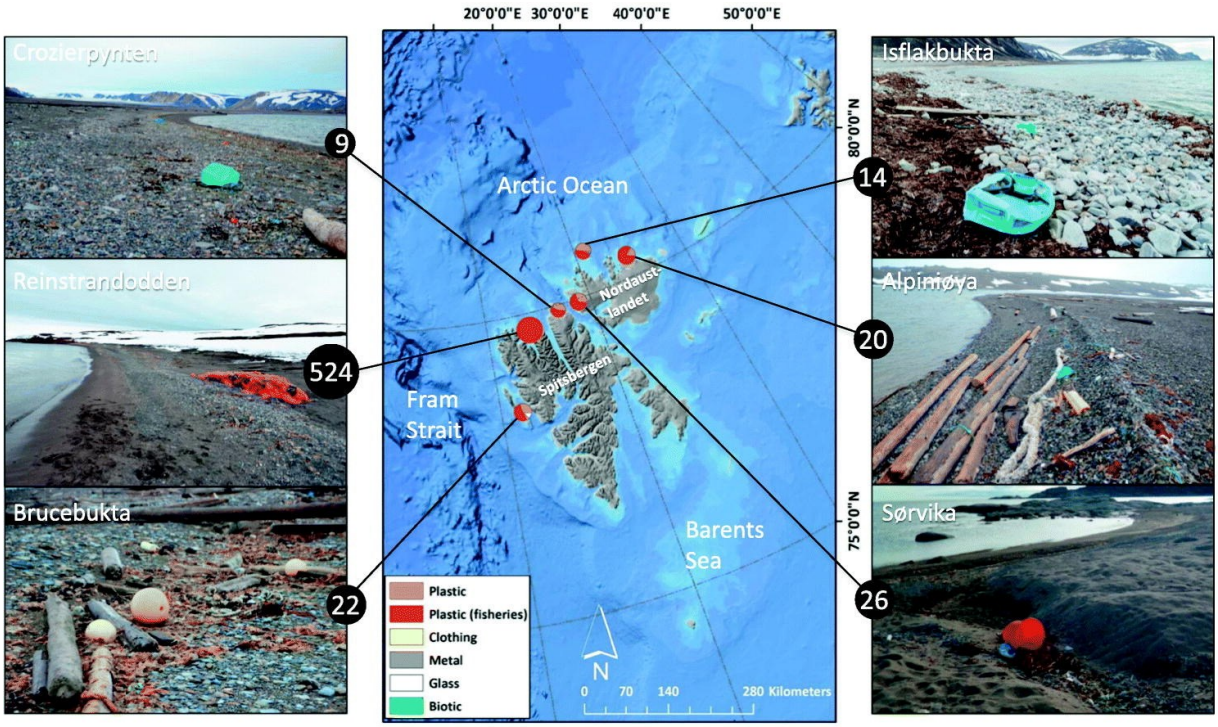

Figure. 4.4 "Location and photos of beach surveys conducted by citizen scientist on the Svalbard Archipelago. Bubble size reflects debris mass (log (g m^{-2})) and composition and numbers refer to total litter mass (g m^{-2}). All images were taken by B. Lutz except for Isflabukta (J. Hager) and Alpiniøya (F. Kruse)." Reprinted from Fig. 1 in "Citizen scientists reveal: Marine litter pollutes Arctic beaches and affects wild life" by M. Bergmann, B. Lutz, M.B. Tekman, L. Gutow., 2017, Marine Pollution Bulletin, 125(1-2), 535-540. Copyright by CC BY-NC-ND 4.0 (https://creativecommons.org/licenses/by-nc-nd/4.0/).

In general, a high mass contribution of fishing nets in the Arctic indicates fishing activities as a substantial source of debris pollution in the region (Bergmann et al., 2017a; Buhl-Mortensen and Buhl-Mortensen, 2017; Vesman et al., 2020; Benzik et al., 2021; Strand et al., 2021). An increase of shipping operations (fishing and tourism) due to sea ice retreat and the related increase in debris concentrations on the seafloor were presented in Chapter 2.2 and in Parga Martinez *et al.* (Parga Martínez et al., 2020). In Arctic surface waters, ropes and nets accounted for only 7% of the observed items by number and unlike in other studies [i.e. (Lebreton et al., 2018)], mega-sized fisheries-related bundles were not present. Indeed, the presence of a single particularly heavy fishing net at Reinstrandodden and in the Hinlopen Strait (Bergmann et al., 2017a; Meyer, 2022) is also in contrast with surface observations. I do not have any explanation for this contradiction except one speculation that debris originating from local fishing operations near the coast washes ashore in a rather short time and thus was not observed afloat. This suggestion is supported by Strand *et al.* (Strand et al., 2021), pointing

out the significant contribution of local fishing activities as a source of debris on Arctic beaches.

It should be noted that in (Bergmann et al., 2017a), no count measures were given. Thus, it is impossible to compare the composition of debris between Arctic surface waters and beaches, a challenge, which was partly overcome by a new study conducted between 2017 and 2021 (Meyer, 2022) (Fig. 4.5). A total debris mass of 1,620 kg was collected from an area of 38,000 m^2, with a mean (±SEM) of 41.83 ± 31.62 g m^{-2} , which was dominated by fisheries-related plastic (80 – 92 % of the total debris mass). A total of 23,000 pieces of debris was collected over an area of 25,500 m^2 on nine beaches. Accordingly, the mean debris concentration (± SEM) was 0.37± 0.17 items m^{-2}. The most frequently observed material was plastic (99.6%), including both general (76.9%) and fisheries/shipping-related plastic (22.7%). This study allowed a comparison with macro-debris concentrations obtained from other ecosystem compartments of the Arctic.

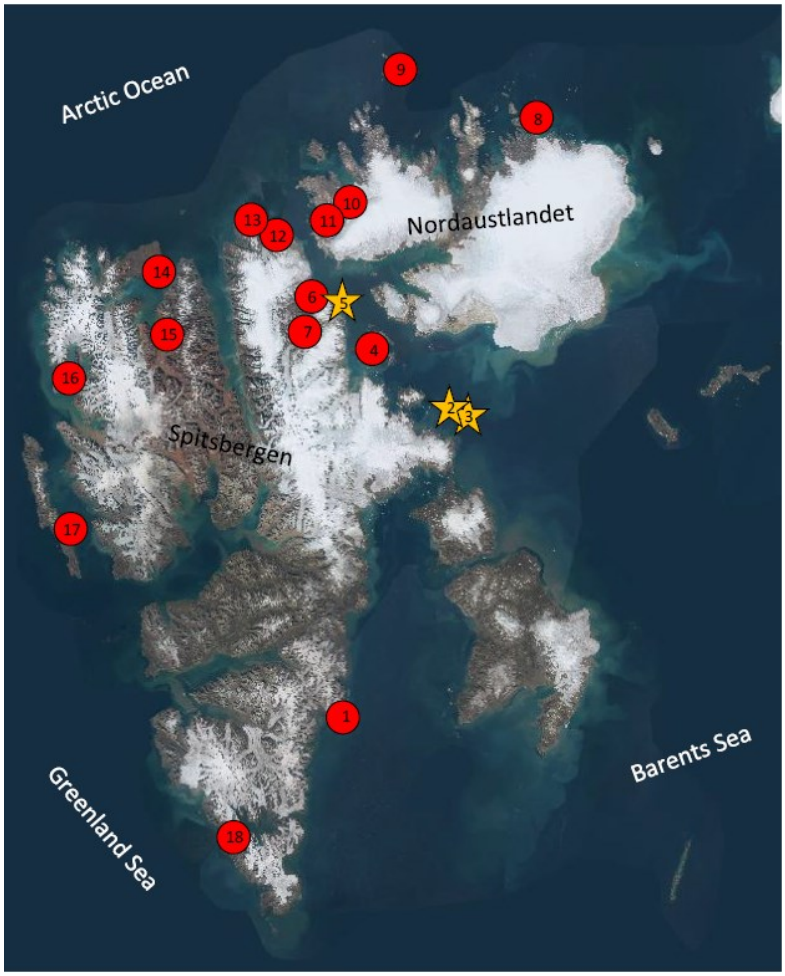

Figure 4.5 "Red dots represent 15 beach locations around Svalbard, that were monitored by citizen scientists, numbered in order of surrounding Svalbard. Stars mark the locations where big packs were collected. (Map © Norwegian Polar Institute)." Reprinted from Fig.1 in "Deep Dives into Arctic Beach Debris. Analysing its Composition and Origin" by A. N. Meyer, 2022, Bachelor's thesis. Kiel: Christian-Albrechts-Universität zu Kiel with permission from A.N. Meyer

Physical samples from Kiepertøya and Tollemen beach were examined in detail in order to identify the origin of debris items (Fig. 4.6). Items originating from Norway, Denmark and Russia accounted for 44% of the 359 pieces. The proportion of the items produced in distant countries such as Canada, USA, Brazil, Argentina, Japan, Korea, China and Philippines was 3.9%, indicating long-distance transport. Items subject to global distribution (i.e. Tetra Pak, Nestlé, Coca Cola) accounted for 18%. Twenty-two percent originated from European states with Germany contributing the highest number (6%). The oldest piece was from the 1960's. Although goods produced in nearby Arctic and European countries and those that are globally distributed constitutes the majority of plastic debris on Svalbard beaches, as with the bucket collected in the Fram Strait (Chapter 2.1), it should be noted that the identification of the county and date of production does not necessarily show how and when an item was disposed. However, by considering additional information, such analyses can in fact provide important information about the origins of a debris item. For example, (Ryan et al., 2019) investigated stranded bottles on an uninhabited island in the Tristan da Cunha archipelago, central South Atlantic Ocean. The study estimated the time taken for a possible drift from India and Southeast Asian countries (3 – 5 years) and concluded that bottles produced within a shorter time period, had likely been dumped by ships. Accordingly, an increase in Asian bottles discarded from ships were reported.

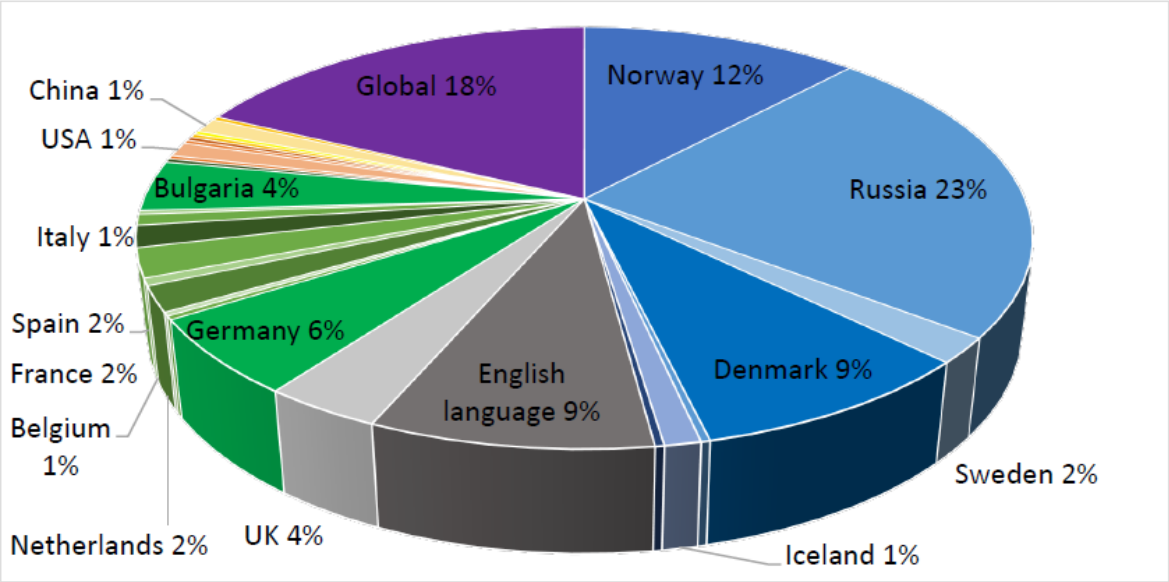

Figure 4.6. "Pie chart showing the proportion of debris items from different countries. Country and percentage are shown for countries with 1% or more. Local provenience is depicted in shades of blue, European provenience in shades of green and grey, Asian provenience in shades of orange, American provenience in shades of yellow and Global in purple." Reprinted from Fig.10 in " Deep Dives into Arctic Beach Debris. Analysing its Composition and Origin" by A. N. Meyer, 2022, Bachelor's thesis. Kiel: Christian-Albrechts-Universität zu Kiel with permission from A.N. Meyer

The debris concentration measured on Svalbard's beaches amounted to 370,000 items km^{-2} (Meyer, 2022). While a large extrapolation should be treated with care, such a conversion is required for high-level comparisons of concentrations among different ecosystem compartments. Accordingly, the highest macro-debris pollution was found on beaches (370,000 items km^{-2}), followed by the seafloor [ranging from 813 ± 525 (SEM) to 6,717 ± 2,044 (SEM) items km^{-2}, (Parga Martínez et al., 2020)] and lowest levels at the sea surface (11 items km^{-2}, Chapter 2.1). In fact, a recent study based on data from 605 peer-reviewed publications suggested that globally, the median marine macro-debris concentration on beaches is highest compared to other marine compartments [Fig. 4.7, (Tekman et al., 2022)]. For example, macro-debris concentrations at beaches are two orders of magnitude higher than those on the seafloor (Tekman et al., 2022), which concurs with the results obtained from the FRAM Pollution Observatory.

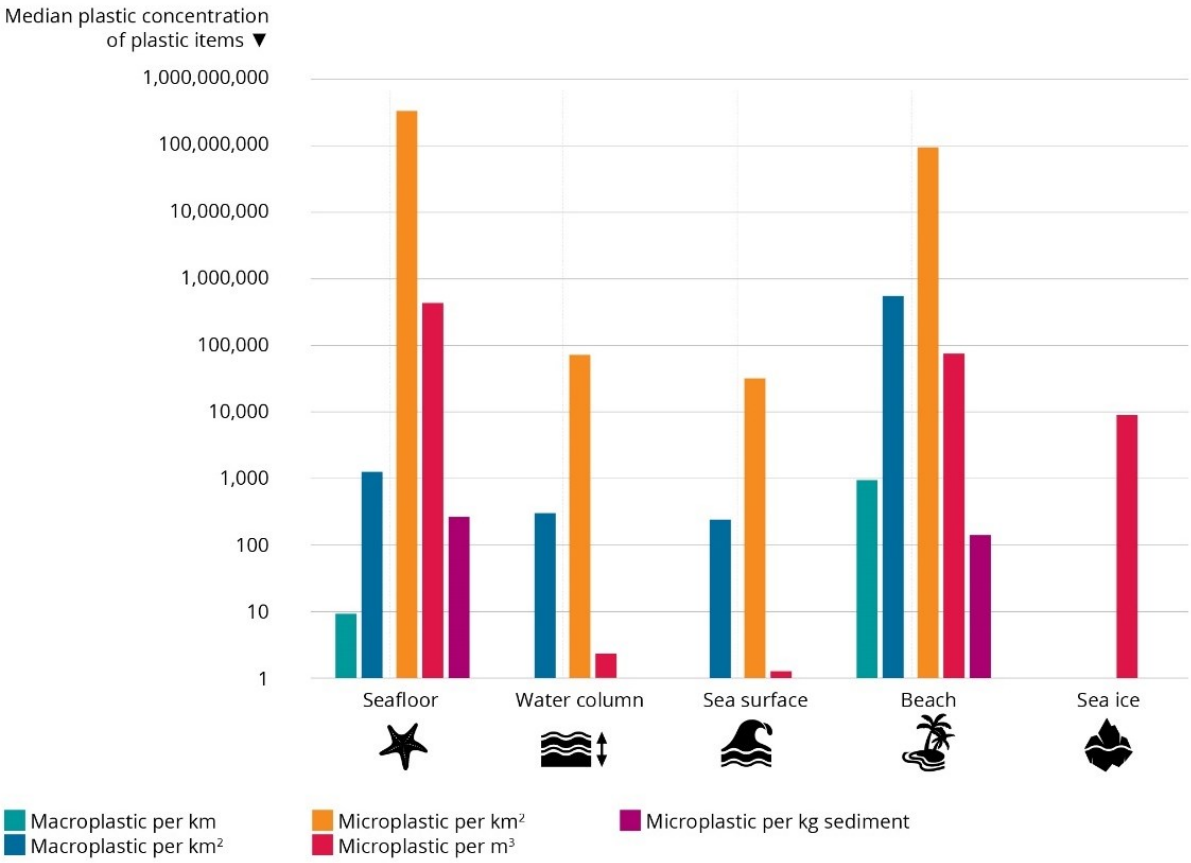

Figure 4.7 "Median plastic debris quantities in different environmental compartments. Since amounts reported in different units are not comparable, a colour code was used to depict quantities per km, km², m³ and kg of sediment. Plastic concentrations are shown on a logarithmic scale. This analysis is based on 605 publications (LITTERBASE)." Reprinted from Fig. 5 in "Impacts of plastic pollution in the oceans on marine species, biodiversity and ecosystems" by M.B. Tekman, B.A. Walther, C. Peter, L. Gutow, M. Bergmann, 1–221, WWF Germany, Berlin, with permission from Bernhard Bauske from WWF Germany.

The transportation mechanisms of anthropogenic debris towards the seafloor were described in Chapter 3, the accumulation on the seafloor in Chapter 2.2 and both will be discussed later in this chapter. However, by an either lateral or a direct vertical pathway, the accumulation on the deep seafloor is relatively straightforward and more importantly, it can be assumed that once a debris item reaches the deep seafloor, it does not resurface. On the contrary, beaches are more dynamic environments and thus debris accumulation is influenced by several factors, which was described by Ryan et al. (2020) (Fig. 4.8), who suggest that beaches are intermediate sinks of marine debris: (i) floating debris items wash ashore, (ii) visitors leave litter on the beaches, and (iii) debris items are blown to beaches from land by wind. A debris item stays there until it is (i) removed by beach-cleaning activities, (ii) blown

away by wind or carried by tides and waves back to the sea, or (iii) moved along the beach, to the backshore and/or buried into the sediment. Debris items reaching the backshore often get entrapped by vegetation. A fragmentation model suggests that large plastic debris becomes trapped on beaches, fragmented after stranding, and these fragments enter the ocean after a short residence time (Kaandorp et al., 2021). Accordingly, floating fragments, as well as microplastics in surface waters of the Arctic Ocean may have originated from the coasts as fragments of larger pieces on Arctic beaches.

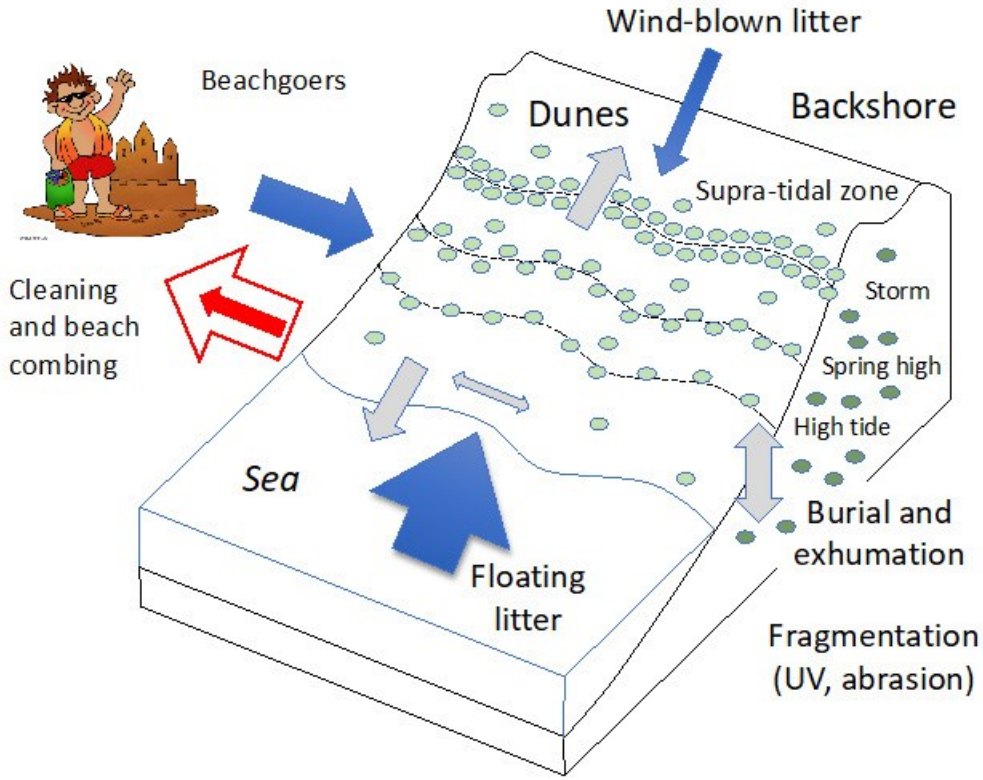

Figure 4.8 "The factors affecting plastic debris standing stocks on sandy beaches. Most debris typically washes ashore, but beach visitors and wind-blown debris from the land also contribute debris inputs (blue arrows). Debris (green circles) tends to accumulate in a series of strand lines linked to wave action, tidal cycles and storm events. Within the beach, debris is moved by the wind, tides and waves (grey arrows), which may carry debris back into the sea, into the backshore where it is often trapped by vegetation, or along the shore, or debris may be buried (darker circles) and can be re-exposed if the beach is cut back by storm seas. Over the long term, items exposed to UV radiation become brittle and break down, aided by mechanical abrasion. Beach cleaning (red arrows), which selectively removes larger debris items from beaches, typically has increased over time" Reprinted from Fig. 2 in "Monitoring marine plastics – will we know if we are making a difference?" by P.G. Ryan, L. Pichegru, V. Perolod,

In the Arctic region, freeze-thaw events could also lead to fragmentation of plastic. Wu et al. (2022) investigated the effect of freeze-thaw alternating from -30 to 20 ℃ on the release of plasticizers and microplastic particles released from plastic mulch films and found a strong correlation between plasticizers and microplastic concentrations and that freeze-thaw events can significantly promote the release of plasticizers. Arctic beaches could thus not only be considered accumulation zones for macroplastic but also a significant source for microplastic, driven by UV light (24 h during summer), wind and wave action as well as repeated freeze-thaw cycles.

Chapter 2.1 and the two studies from Svalbard beaches and snow collections on Svalbard (Bergmann et al. 2019) have proven that citizen science campaigns can significantly feed scientific data collection. In fact, beach clean-ups have become very popular among the tourists in the Arctic region. The Governor of Svalbard and Arctic Expedition Cruise Operators have set up the long-term programme “Clean-up Svalbard” in order to collect marine debris. (Falk-Andersson et al., 2019) Sea ice retreat led to an increase in cruise and fishing activities around Svalbard (Stocker et al., 2020) and accordingly a conceptual framework for citizen science in the Arctic has been proposed, which recognises beach surveys as a tool for debris pollution assessments (Taylor et al., 2020).

4.4 The Water Column

The microplastic pollution at the near-surface layer of the Fram Strait was discussed earlier in the current chapter. Here, I will focus on the deep-water column. By definition, the deep sea is the region below the continental shelf starting from 200 m depth and supports diverse ecosystems (Gage and Tyler, 1991). It has a volume of $1{,}368 \times 10^6$ km^3 (Ramirez-Llodra et al., 2011) and is the least studied marine compartment for microplastic pollution (Tekman et al., 2022). The water column of the Arctic Ocean is not an exception. Prior to the study of Chapter 3, only Kanhai et al. (2018) reported the abundance of particles in the Arctic water column, yet those concentrations only included particles bigger than 250 µm, which precluded a direct comparison. Since 99% of the particles were smaller than 100 µm, it is not surprising that the concentrations reported in Chapter 3 are hundreds of times higher than those reported in Kanhai et al. (2018).

With regard to the deep-water layers, three important findings of Chapter 3 deserve particular attention: (i) Small-scale circulation features are important to consider in microplastic distribution as shown with the specific distribution and composition at the Molloy Deep. (ii) A positive correlation between microplastic and organic matter concentrations suggested incorporation of microplastics into marine aggregates, which can have implications for carbon and nutrient cycles (MacLeod et al., 2021). (iii) Particle trajectories suggested lateral sinking with an estimated total traveling distance of 604 – 654 km of particles detected above the seafloor, indicating that research should not focus exclusively on direct vertical sinking; there are much more complex mechanisms at play in terms of settling of particles.

A higher load of microplastics in the upper Arctic Ocean (218 items m^{-3}) compared to deeper layers (60 items m^{-3}) was discussed at the beginning of this chapter in relation to sea ice melt. For the deeper layers, the origin of water masses and stratification deserve further attention. The 300-m layer of the deep stations (Chapter 3) fits to the temperature and salinity profile of Atlantic waters with salinities around 35 psu and temperatures ranging from 2.9 to 3.8 (Rudels et al., 1991). The temperature and salinity profiles at the 1000-m and above-seafloor layers correspond to Arctic deep waters. Our analyses did not reveal any differences in microplastic concentrations, polymer type and size compositions between these water masses. Similarly, Kanhai et al. (2018) did not find significant differences in microplastic concentrations between the water masses in the Arctic. In the West Pacific, microplastic concentrations between 200 and 4,000 m depth ranged from 0.2 and 1.5 items m^{-3} and in the East Indian Ocean, from 0.2 to 2.3 items m^{-3}, with no significant difference in concentrations between different sampling depths (Li et al., 2020). Even in the stratified Baltic Sea, microplastic concentrations at different depths did not show any significant difference, yet higher concentrations were detected in thin layers of the halocline and thermocline (Uurasjärvi et al., 2021). These findings show that the concentrations of microplastic particles are not related to the water depth. Contrary to these findings increasing concentrations with depth were reported from the Mariana Trench (2,060 – 13,510 N m^{-3}) (Peng et al., 2018) and highest concentrations were observed between 200 and 600 m at Monterey Bay (15,000 N m^{-3}) (Choy et al., 2019). The differences in concentrations in these two studies could be due to special local features as observed in the Molloy Deep (Chapter 3).

Once plastic items reach open waters, their subsequent trajectories depend on several factors. In theory, items with a higher material density than seawater sink, whereas the others float. However, photochemical reactions change the material properties of plastics, leading to

slightly lower densities than the densities of pristine particles (Bond et al., 2022). Therefore, applying the basic rules of physics to plastic trajectories can be misleading. Indeed, Chapter 3 showed that 25 types of plastic material have been found throughout the water column, with no statistically significant difference in polymer composition between the depth layers. Polyethylene particles were also detected in the sediments (Chapter 3), although they have a lower density than seawater. Ye and Andrady (1991) suggested an oscillated movement depending on the latitude and season, at least at the initial phase of sinking, as the algal growth slows down due to down-welling irradiance or organisms feed on the organic material on plastic debris. Clay minerals or quartz grains were also observed to be attached to microplastic particles, which could facilitate ballasting processes (Kowalski et al., 2016) as could cryogenic gypsum as observed for under-ice phytoplankton blooms (Wollenburg et al., 2018).

To my knowledge, except for records from the Barents Sea (Grøsvik et al., 2018) and the one item found in a jelly fish in Svalbard waters (Chapter 2.1), there are no reports on macro-debris in the Arctic water column. Considering that in Chapter 2.1 the water column was not the main focus and marine debris was observed in 301 pelagic trawls from the Barents Sea (Grøsvik et al., 2018), I believe the marine debris pollution in the Arctic water column urgently requires further research.

4.5 The Deep Seafloor

Globally, plastic accounts for 62% of the debris on the seafloor (Canals et al., 2021) and submarine canyons are accumulation hotspots (Pham et al., 2014). The deep seafloor covers an area of 360 million km^2 (Ramirez-Llodra et al., 2011) making it a long-term sink for marine debris pollution. Positively buoyant plastic debris can vertically move in both direction in the upper ocean fouling and de-fouling (Kooi et al., 2017) but within three years they are assumed to be lost to deeper layers (Koelmans et al., 2017), reaching the seafloor unless consumed by pelagic organisms. Flash floods and deep-water cascading events can aid transport of particles to depths (Tubau et al., 2015; Pierdomenico et al., 2019; Canals et al., 2021) and such features have been recorded in the study area (Wobus et al., 2013).

Bergmann and Klages (2012) published the first assessment of macro-debris quantities on the deep Arctic seafloor based on images taken during photographic surveys between 2002 and 2011 at the central station (HG4) of the HAUSGARTEN Observatory. Chapter 2.2 extended this study to the northern station (N3) and images of three additional years. Parga Martínez et al. (2020) added images from the southern station (S3) and extended the time series

to 2017 for all stations. The coverage of these studies is summarised in Table 4.1. In the following section, I focus on Parga Martínez et al. (2020) due to its highest coverage, which includes the data of Chapter 2.2.

Table 4.1 The stations and sampling years of photographic surveys reported by Bergmann and Klages (2012), Chapter 2.2 and Parga Martínez et al. (2020).

	Stations			Total number of images	Total survey area in m^2
	2002 – 2011	2012 – 2014	2015 – 2017		
Bergmann and Klages (2012)	Central			2,882	8,570
Chapter 2.2	Northern and Central	Northern and Central		7,058	28,161
Parga Martínez et al. (2020)	Northern, Central and Southern	Northern, Central and Southern	Northern, Central and Southern	16,157	60,563

The marine debris and plastic concentrations are summarized in Table 4.2 and 4.3, respectively. The concentrations were calculated using the same method as in Chapter 2.2, i.e. the total number of anthropogenic items detected in one transect was divided by the total coverage area of images within the same transect.

Table 4.2. Marine debris concentrations (all types of debris) at three different stations along the latitudinal gradient of HAUSGARTEN Observatory (items km^{-2})

Year	Central	Northern	Southern	HAUSGARTEN
2002	3,635	-	-	3,635
2004	1,214	390	1,089	899
2007	728	1,121	884	932
2011	7,710	1,674	3,603	4,489
2012	5,261	2,750	6,263	4,383
2013	-	4,950	3,613	4,251
2014	5,166	7,699	-	6,333
2015	6,517	7,946	3,103	5,783
2016	3,763	9,930	4,193	5,757
2017	6,838	5,981	3,507	5,614
TOTAL	4,329	4,429	3,144	4,029

Table 4.3 Plastic concentrations at three different stations along the latitudinal gradient of HAUSGARTEN Observatory (items km^{-2})

Year	Central	Northern	Southern	HAUSGARTEN
2002	2,077			2,077
2004	809	0	363	385
2007	728	560	0	466
2011	2,804	0	1,441	1,496
2012	3,382	275	2,088	1,704
2013		1,485	2,709	2,125
2014	4,696	2,750		3,800
2015	3,476	497	887	1,674
2016	3,136	2,069	2,096	2,503
2017	4,179	2,990	1,002	2,875
TOTAL	3,538	1,461	1,863	2,312

Additional univariate statistical analyses were performed on the data in Tables 4.2 and 4.3 including a Shapiro-Wilk test to test if parametric tests can be used. As the evaluation of concentrations at each station and at HAUSGARTEN (all stations combined) showed that the data have a normal distribution ($0.85 < W\text{-Statistic} < 0.97$, $0.06 < P < 0.85$), a two-way analysis of variance (ANOVA) was applied on year × station concentrations of marine debris and plastic items in order to identify spatial and temporal differences at each station and sampling year. Interactions could not be assessed due to the missing sampling campaigns at HG4 in 2013, at N3 in 2002 and at S3 in 2002 and 2014. Moreover, an ANOVA of linear regression was run on the dataset of debris and plastic concentrations measured at each station and at HAUSGARTEN between 2002 and 2017 in order to evaluate the significance of the observed increase. In case of significant differences, pairwise comparisons were assessed with a Holm-Sidak test. The results of two-way ANOVA showed significant differences in plastic concentrations between both stations ($DF = 2$, $F = 12.05$, $P < 0.001$) and years ($DF = 9$, $F = 4.35$, $P = 0.007$) but not in marine debris concentrations. The plastic debris concentrations at HG4 were significantly higher than those at N3 ($t = 4.750$, $P < 0.001$) and S3 ($t = 3.681$, $P = 0.005$). The debris distribution at HG4 is mainly influenced by the North Atlantic Current as shown by drift trajectories in Chapter 3 and thus we can address it as the main transport medium of plastic accumulation at the Fram Strait.

Although several studies investigated the distribution on the deep seafloor using long-term footage (Schlining et al., 2013; Chiba et al., 2018), only a few of them analysed temporal trends (Barnes et al., 2018; Gerigny et al., 2019). The ANOVA of linear regression showed a

significant temporal increase between 2002 and 2017 in concentrations of marine debris and plastics at HAUSGARTEN (Fig. 4.9 and 4.10, respectively). When the stations were evaluated separately, plastic concentrations at HG4 and N3 showed a significant temporal increase but not S3. Regarding all types of debris, only the concentrations at N3 showed a significant temporal increase. Overall, marine debris pollution levels have risen, but plastic accumulation over time is less intense in the south compared to the stations further north.

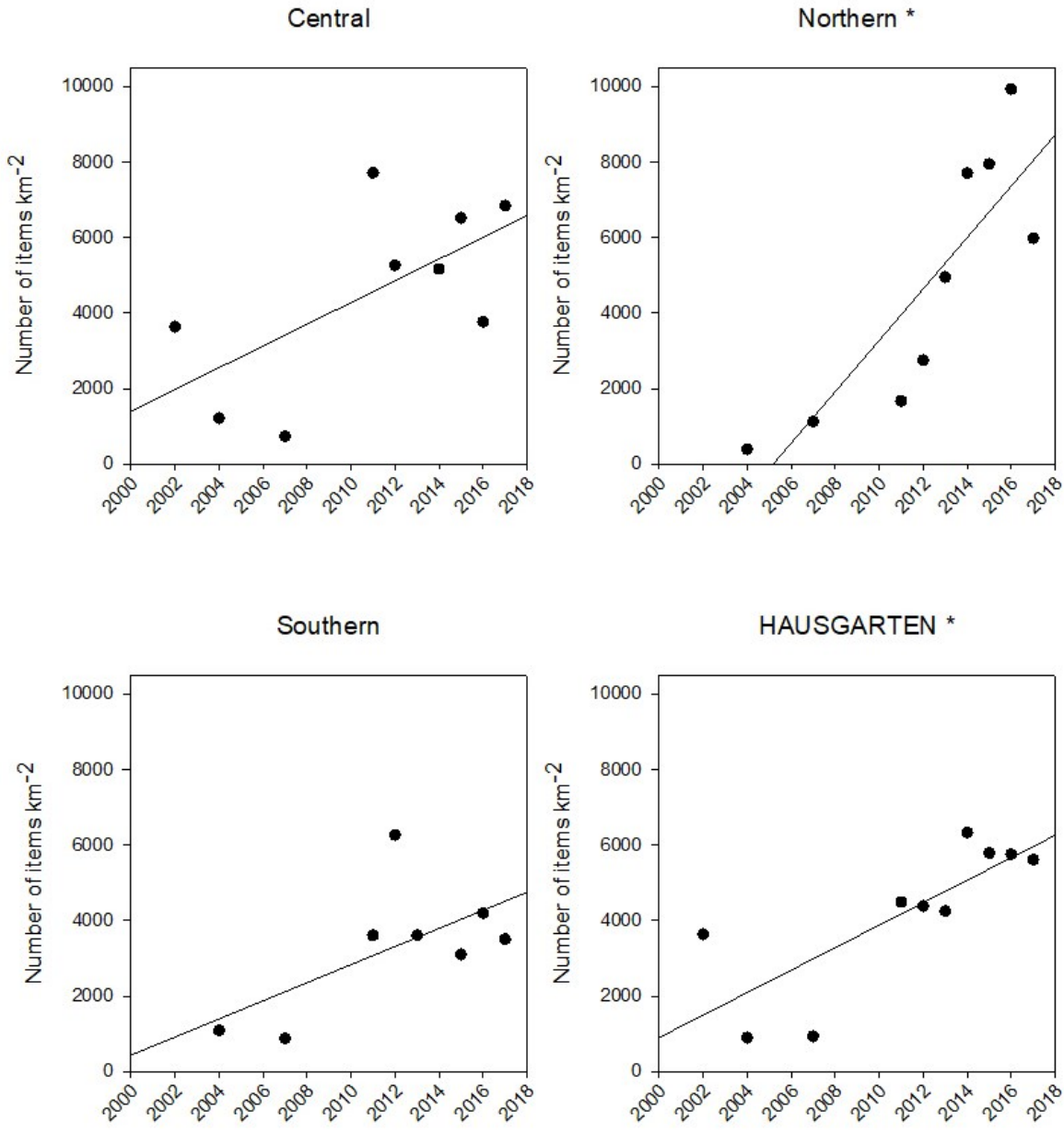

Figure 4.9 Marine debris (all types) concentrations over 15-year period at the central (Linear Regression: N = 9, $r^2 = 0.41$, Analysis of variance of the regression model: F = 4.86, P = 0.06), northern (Linear Regression: N = 9, $r^2 = 0.72$, Analysis of variance of the regression model: F = 18.31, P = 0.004), southern (Linear Regression: N = 8, $r^2 = 0.39$, Analysis of

variance of the regression model: F = 3.90, P = 0.10) stations and at all stations combined of HAUSGARTEN Observatory (Linear Regression: N = 10, r^2 = 0.63, Analysis of variance of the regression model: F = 13.46, P = 0.006). * indicates significant temporal differences.

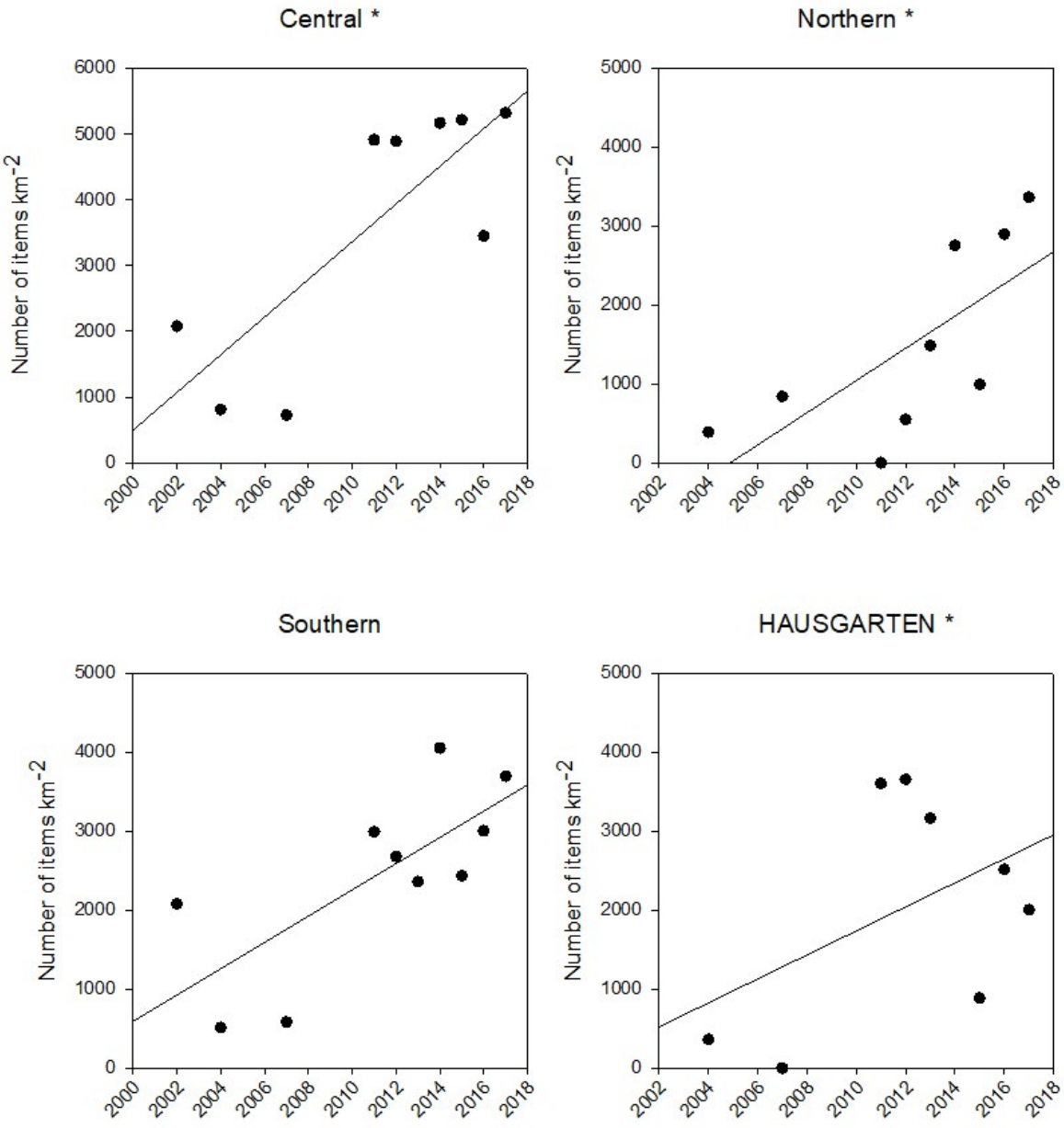

Figure 4.10 Plastic debris concentrations over 15-year period at the central (Linear Regression: N = 9, r^2 = 0.64, Analysis of variance of the regression model: F = 12.61, P = 0.009), northern (Linear Regression: N = 9, r^2 = 0.50, Analysis of variance of the regression model: F = 7.02, P = 0.033), southern (Linear Regression: N = 8, r^2 = 0.22, Analysis of variance of the regression model: F = 1.69, P = 0.24) stations and at the all stations combined of

HAUSGARTEN Observatory (Linear Regression: N = 10, $r^2 = 0.54$, Analysis of variance of the regression model: F = 9.39, P = 0.015). * indicates significant temporal differences.

The 3D particle drift trajectories in Chapter 3 provided information on the catchment areas of particles in the water column. Although the microplastic sampling was not performed at the same stations as the seafloor imaging, the northern station (N5) is in close vicinity to N3. Our 3D simulation showed that 57% of the particles found above the seafloor of N5 originated from polar waters. As the North Atlantic Current is the main source of debris pollution at the central Fram Strait, it is plausible to suggest that the additional source of pollution at the seafloor of N3 seafloor could be the Transpolar Drift or the increasing maritime activities in the area or both. The release of debris from the melting sea ice at the marginal ice zone and the effect of the Transpolar Drift as a conveyer of anthropogenic debris pollution to the Fram Strait were already evaluated earlier in this chapter, thus will not be repeated.

A decreasing sea ice extent (Stocker et al., 2020) including a lengthening ice-free period (Rodrigues, 2009) allow more ships to operate further north as confirmed by. analyses of maritime activities in Chapter 2.2, Parga Martínez et al. (2020) and Stocker et al. (2020) (Fig. 4.11). Indeed, marine debris concentrations at HAUSGARTEN between 2002 and 2017 showed significant positive correlations with fishing activities of Russian vessels and the number of tourist ships calling at Longyearbyen and cruise ship passengers [Fig. 4.11, (Parga Martínez et al., 2020)]. In the Eurasian Arctic, the trawls from the Kara Sea had an average macro-debris weight of 1,320 kg km^{-2}, which was attributed to the fishing operations in the Barents Sea, whereas no debris was found in trawls from the Laptev and East Siberian Seas (Benzik et al., 2021).

(Buhl-Mortensen and Buhl-Mortensen, 2017) assessed the marine debris distribution on the seafloor below 100 m depth in open waters and coastal areas of the Barents and Norwegian Seas and measured debris concentrations of 289 and 171 items km^{-2}, respectively. These concentrations are one order of magnitude lower than those at HAUSGARTEN. However, they found a debris concentration of 2,706 items km^{-2} at depths lower than 100 m off the Norwegian coast, indicating a higher abundance closer to European sources. Footage taken by a Remotely Operated Vehicle (ROV) in the submarine canyons of the northwest Mediterranean (140 to 1,731 m depth) revealed a debris concentration of 15,057 and 8,090 items km^{-2} at the La Fonera and Cap de Creus canyons, respectively (Tubau et al., 2015). These values are two to four times higher than those detected at HAUSGARTEN, which is not surprising considering the high amounts of marine debris in the Mediterranean Sea (Chapter 2.1).

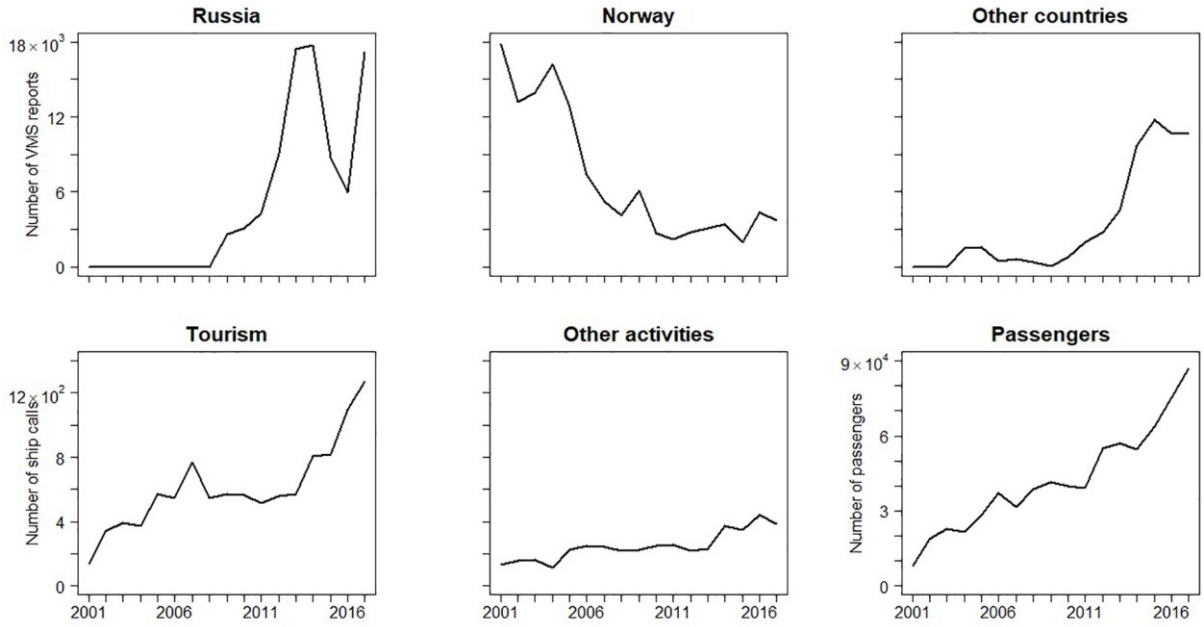

Figure 4.11 "Temporal trend in the number of VMS reports from Russia, Norway, and other countries (upper panel, from left to right, source: Norwegian Directorate of Fisheries). Number of ships calling at the port of Longyearbyen (Svalbard) from tourism, other-type activities, and number of passengers of leisure craft (bottom panel, source: Harbormaster of Longyearbyen)." Reprinted from Fig. 6 in "Temporal trends in marine litter at three stations of the HAUSGARTEN observatory in the Arctic deep sea" by K.B. Parga Martínez, M.B. Tekman, M. Bergmann, 2020, Frontiers in Marine Science, 7, 321. Copyright by CC BY 4.0 (https://creativecommons.org/licenses/by/4.0/).

Although the HAUSGARTEN camera surveys aim to cover the same tracks on the seafloor, it is highly unlikely to succeed at taking images from the exact same locations as the system is towed at a wire of ~2,500 m length. Still, remarkably, the same plastic item entangled in a sponge (*Caulophacus arcticus*) was photographed in 2014 and 2016 (Fig. 4.12). In fact, the fate of macro plastic debris, once it reaches the deep seafloor, is unknown. It can be assumed that the low water temperatures, absence of UV-light and wave action creates relatively stable conditions for debris items (Andrady, 2015), as indicated by 30- year- old plastic recovered from the deep sea of Japan without any signs of deterioration (Kuroda et al., 2020). On the other hand, bottom currents in the Tyrrhenian Sea, reaching up to 20 cm s^{-1} (Kane et al., 2020) or in the NW Mediterranean Sea, reaching up to 30 cm s^{-1} were shown to carry plastics (Dominguez-Carrio et al., 2020), which may be well the case for plastics at the HAUSGARTEN Observatory with an average bottom current speed of 7.8 ± 0.9 cm s^{-1} (Meyer-

Kaiser et al., 2019). The plastic debris in Fig. (4.12) may have not been carried further by bottom currents due to its entanglement with the sponge. In any case, fragmentation into smaller pieces cannot be ruled out, since increasing quantities of small plastic items were observed during the study period (Chapter 2.2).

Figure 4.12 Images taken at the central HAUSGARTEN station in 2014 (upper image) and 2016 (lower image), showing that a piece of plastic sheet is entangled in an aggregation of the two sponges *Cladorhiza gelida* and *Caulophacus arcticus*. Images were taken by Melanie Bergmann (OFOS/AWI).

As with the debris pollution at the sea surface, the findings in this section deal with both macro-debris and microplastic concentrations. The very high quantities of microplastics in sediments of the FRAM Pollution Observatory indicate that the seafloor is a long-term sink not only for macro plastic but also for microplastic [Chapter 3 and (Bergmann et al., 2017b). The µFTIR measurements revealed that up to 13,000 kg^{-1} microplastic particles > 11 µm are present in sediments between 2,500 and 5,500 m depths. The concentration of microplastic particles larger than 100 µm with a concentration of 8 – 142 items kg^{-1} were in the same range as those reported between 855 and 4,353 m depths of the Central Arctic (0 – 200 items kg^{-1}) (Kanhai et al., 2019) and between 148 and 352 m depths of a fjord in Svalbard (430 ± 110 items kg^{-1}) (Collard et al., 2021). Considering that 95 – 99% of the particles in Fram Strait sediments were smaller than 100 µm, the concentrations of this size range deserve particular attention. However, only one other study from the Canadian Arctic investigated this size range in Arctic sediments with a mean concentration of 1,940 ± 4,120 items kg^{-1} for particles exceeding 0.25 µm (Huntington et al., 2020), which is in the same range as concentrations in the Fram Strait (239 - 13,331 items kg^{-1}). Sediment samples from three other regions were also analysed with µFTIR and automated spectra identification including the Kuril Kamchatka Trench at depths from 5,143 to 8,250 m [14 – 209 items kg^{-1}, (Abel et al., 2021)], the southern North Sea [3 – 1,180 items kg^{-1}, (Lorenz et al., 2019)] and deep regions of an urban Norwegian fjord [12,000 – 200,000 particles kg^{-1}, (Haave et al., 2019)]. The microplastic levels in Fram Strait sediments seemed a little higher than those in the North Sea, especially when the northernmost station was considered, which had a magnitude higher concentration.

4.6 Comparison of polymer compositions in snow, water column and sediment

The polymer type and size compositions from snow (Bergmann et al., 2019) and sediments sampled in 2015 (Bergmann et al., 2017b) were combined with the polymer dataset of Chapter 3 in order to investigate the differences between ecosystem compartments by applying the same multivariate statistical approach as in Chapter 3, which was used to compare the composition and diversity of microplastic in the water column and sediment. A PERMANOVA with 999 permutations was applied to assess the differences in polymer type and size compositions obtained from the water column, sediments and snow. Prior to

PERMANOVA, Hellinger dissimilarity measure was applied to square-root transformed standardized datasets of polymer type and size compositions. Total polymer types (S) and Pielou's evenness (J') of polymer compositions were calculated to assess the diversity of polymer compositions. A PERMANOVA with 999 permutations was run on Euclidean distances of log(x+1) transformed diversity dataset. The similarity percentage (SIMPER) routine of PRIMER-e was performed to assess which specimens caused the observed differences in compositions. Moreover, multidimensional scaling (MDS) plots were generated to visualize the compositions (Fig. 4.13, 4.14). Sea ice was not included in these analyses since a change had been applied to the database structure after the assessment of sea ice samples.

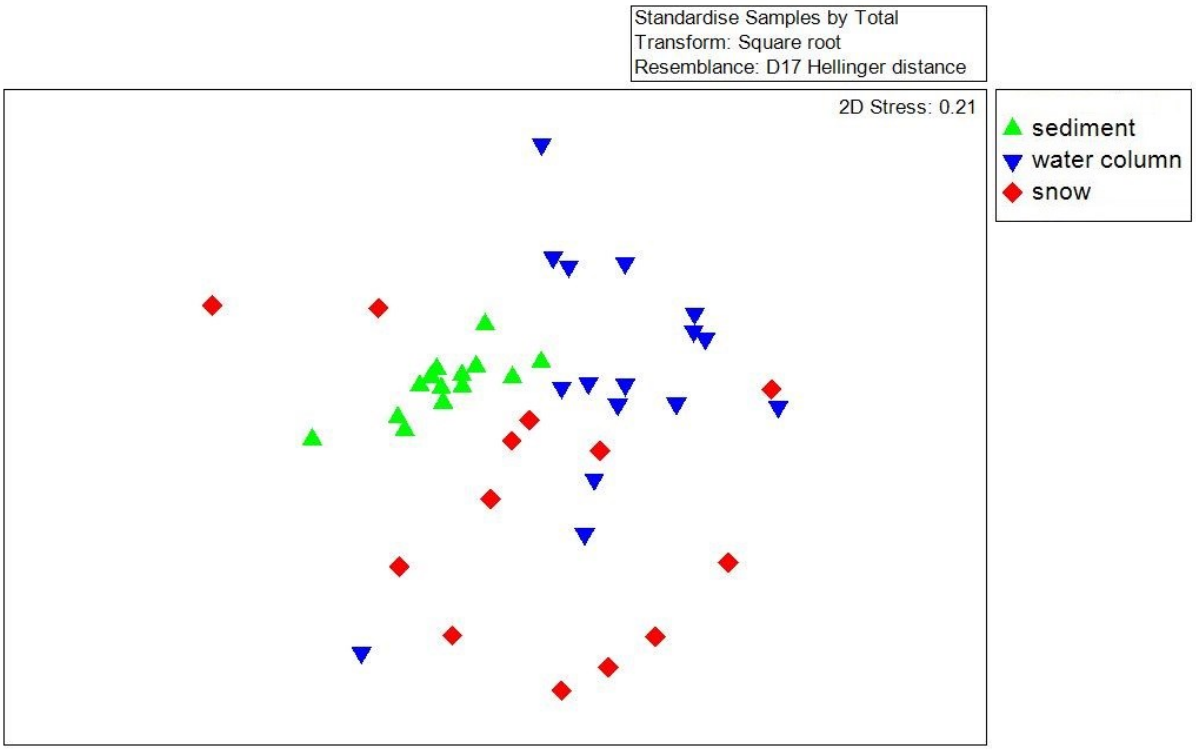

Figure 4.13 Multidimensional scaling plot for polymer type composition in the water column, sediments and snow.

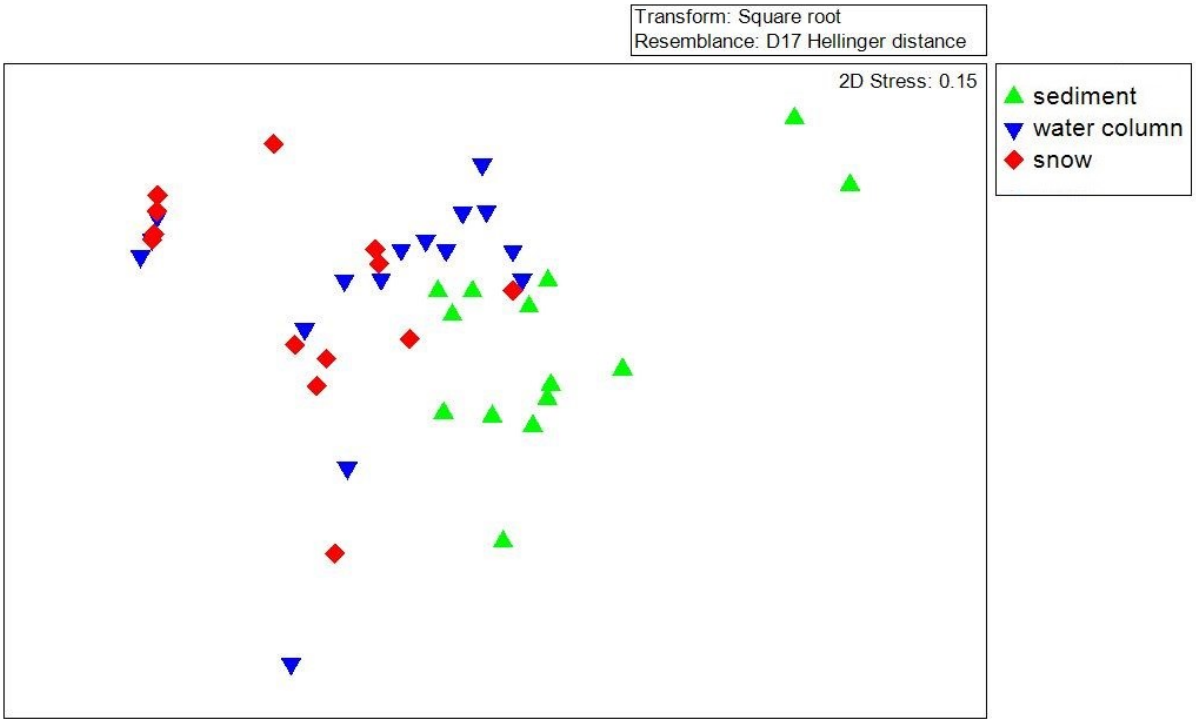

Figure 4.14 Multidimensional scaling plot for microplastic size compositions in the water column, sediments and snow.

PERMANOVA showed a significant difference both in polymer (Pseudo-F = 5.56, P(Perm) = 0.001) and size compositions (Pseudo-F = 5.38, P(Perm) = 0.001). Pairwise tests indicated significant differences in polymer type compositions between all assessed ecosystem compartments (Table 4.4). Polymer size compositions showed a similar result, except for the comparison of the water column and snow samples, which was not statistically significant (Table 4.4). Significant differences were found for both polymer type (Pseudo-F = 12.82, P(Perm) = 0.001) and size class (Pseudo-F = 16.81, P(Perm) = 0.001) diversities. For both size and polymer type diversity compositions, pairwise tests showed that sediment diversities were significantly different compared with the water column and snow samples (Table 4.4). As with the polymer type diversity, the diversity indices of size classes in the water column were not significantly different than those in snow (Table 4.4).

Table 4.4 PERMANOVA Results of polymer composition and diversity. The values represent "t - P(Perm)"

COMPOSITION		
Polymer Type	Sediment	Snow
Snow	2.29 - 0.001	
Water Column	3.06 - 0.001	1.82 - 0.001

DIVERSITY		
Polymer Type	Sediment	Snow
Snow	4.51 - 0.001	
Water Column	5.26 - 0.001	0.33 - 0.818

Polymer Size	Sediment	Snow	**Polymer Size**	Sediment	Snow
Snow	2.92 - 0.001		Snow	4.86 - 0.001	
Water Column	2.44 - 0.001	1.35 - 0.124	Water Column	5.99 - 0.001	0.28 - 0.864

For polymer type composition, a higher abundance of polyethylene-chlorinated (CPE) in the sediments, of nitrile rubber (NRB) in snow and of ethylene-propylene-diene rubber (R3) in the water column accounted for the highest contribution to the obtained differences. For polymer size compositions, the main difference between ecosystem compartments was due to the presence of > 500 µm particles in the sediment, whereas the size classes of polymers in the water column and snow showed similar abundances.

The preliminary multivariate analyses of the pooled dataset of polymer type and size compositions obtained from the water column, snow and sediment samples underlined the findings, which were discussed earlier in this dissertation. Sediment samples contained more types of polymers than the water column with a higher abundance of CPE. As discussed in Chapter 3, a higher polymer diversity supports the assumption that deep-sea sediments are a long-term sink for microplastics. Particles bigger than 500 µm were only present in sediments. The polymer size composition throughout the water column did not show any difference between depths. Therefore, the presence of particles bigger than 500 µm can only be explained by occasional settling of these large particles on the seafloor. Our analyses of polymer compositions of snow and water samples showed no significant differences, indicating a turnover of particles among these two ecosystem compartments at the sea-air interface (Allen et al., 2020; Ferrero et al., 2022), a suggestion, which was discussed earlier in this chapter with regard to the distribution of atmospheric microplastic. Moreover, high concentrations of the two types of rubber (Nitrile and ethylene-propylene-diene) supports the hypothesis of Evangeliou et al. (2020) that suggested microplastic from the wear of car tyres carried by winds are transported by atmospheric circulations to remote locations including the Arctic.

4.7 Impacts on Arctic biota

As it has been shown in this dissertation, the European Arctic is polluted with marine debris including microplastic. Surely, the ecological impacts of plastic pollution have drawn a lot of attention among the scientific community, especially because vulnerable Arctic ecosystems are already under stress from climate induced changes (Thomas et al., 2022). Except for Botterell et al. (2022) and Kühn et al. (2018), studies of FRAM Pollution Observatory have focused on identifying pollution levels in different ecosystem compartments

so far. Still, all observed biota interactions were always recorded and reported (Chapter 2.1, Chapter 2.2, Bergmann and Klages (2012), Bergmann et al. (2017a), Parga Martínez et al. (2020)). Future studies of the FRAM Pollution Observatory should focus on how current and projected levels of plastic pollution could impact the Arctic fauna by computing ecological threshold values (Everaert et al., 2020). In this section, I will summarise the findings of Botterell et al. (2022), Bergmann et al. (2017a), Chapter 2.2 and Parga Martínez et al. (2020) and give examples of reported biota interactions with marine debris in different marine compartments of the Arctic.

Various records of plastic ingestion in Arctic waters exist (Collard and Ask, 2021). Even during the HE451 cruise along the coasts of Svalbard, a jellyfish was caught that had ingested a plastic film (Chapter 2.1) and polar cod with microplastic in its stomach (Kühn et al., 2018). Botterell et al. (2022) analysed zooplankton samples taken using Bongo and MOCNESS nets from 10 stations in the Fram Strait in 2018 and 2019 for microplastic ingestion (Fig.4.15). In addition, water samples were assessed, which were discussed earlier in this chapter in the context of microplastic distribution at the sea surface.

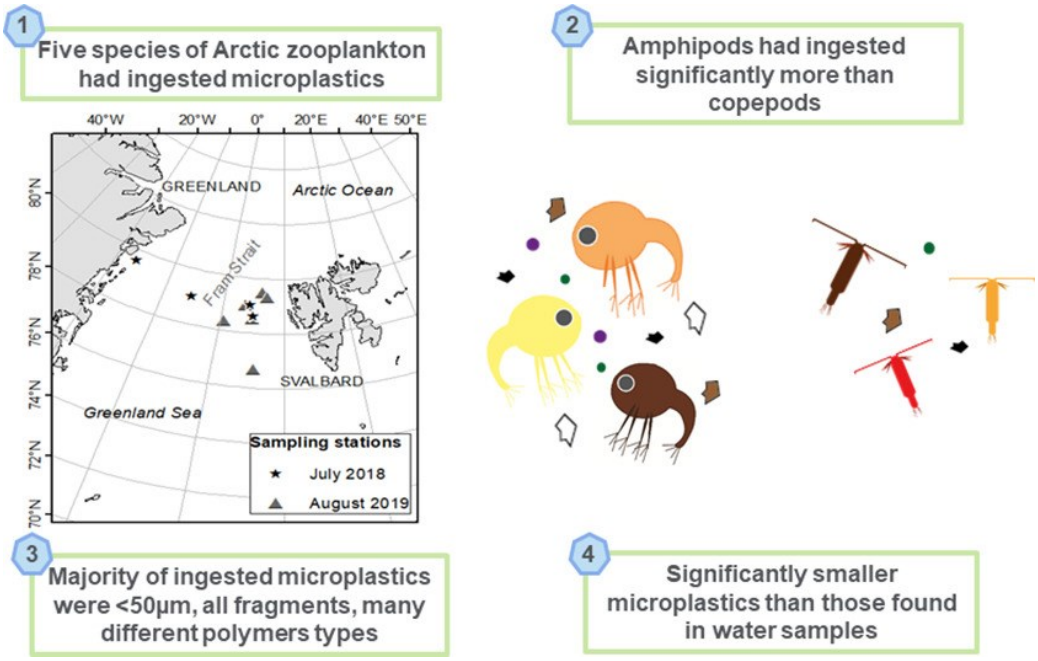

Figure 4.15 Graphical abstract from Botterell et al. (2022). Reprinted from Graphical Abstract in "Microplastic ingestion in zooplankton from the Fram Strait in the Arctic" by Z.L.R. Botterell, M.Bergmann, N. Hildebrand, T. Krumpen, M. Steinke, R.C. Thompson, P.K. Lindeque, 2022, Science of The Total Environment, 831, 154,886. Copyright by CC BY 4.0 (https://creativecommons.org/licenses/by/4.0/).

A total of 64 plastic fragments were detected in 1,417 individuals of the copepods *Calanus hyperboreus* (n = 177) and *Calanus glacialis*/*finmarchicus* (n = 1229), and the amphipods *Themisto libellula* (n = 5), *Themisto abyssorum* (n = 5) and *Apherusa glacialis* (n = 1). The approach of using spectral imaging (µFTIR) in combination with the SIMPLE automated polymer identification software (Primpke et al., 2020), similar to those in (Bergmann et al., 2017b; Peeken et al., 2018; Bergmann et al., 2019) and Chapter 3 allowed to identify particles down to the size of 6.25 µm by avoiding human bias. Overall, on average, 0.045 particles were found to be ingested per individual. An important result was that the amphipods, which are closely associated with surface waters (*Themisto* spp.) or sea ice (*A. glacialis*) ingested more particles (1 – 1.8 particles individual^{-1}) than the copepods (0.01 – 0.21 particles individual^{-1}). The study did not find any relation between microplastic concentrations in water samples and ingested by the animals. However, the microplastic concentrations, including fibres at the sea surface, were so high that they even exceeded the estimated 12,000 microplastic m^{-3} threshold limit of ecological risk (Everaert et al., 2020) at two stations. Such a high level of exposure may have caused the individuals to ingest microplastic particles at the highest amounts possible, especially at times of food paucity, which might be caused by a climate-change induced mismatch between phytoplankton blooms and the hatching time of zooplankton larvae as observed in the area (Leu et al., 2011; Janout et al., 2016). Indeed, exposure to microplastics (200 and 20,000 items L^{-1}) can lead to stress-induced spawning in Arctic copepods, which could cause a mismatch in the timing of larval development and maximum food availability (Rodríguez-Torres et al., 2020). However, this hypothesis should be tested in experiments (Cole et al., 2013) with different concentrations of phytoplankton and microplastics.

The ingested particles were exclusively fragments, of which particles smaller than 50 µm accounted for 75% (Fig. 4.16). A higher ingestion rate of fragments compared to that of fibres by zooplankton was also reported from the coastal ecosystem of the Andaman Islands (Goswami et al., 2020) but in the Canadian Arctic fibres dominated, consisting of 92% of particles (Huntington et al. 2020). A further break down of the distribution within smaller than 50 µm showed that zooplankton ingested a higher number of particles between 11 and 20 µm in size. Indeed, as it was measured in Chapter 3 and Peeken et al. (2018) this size class dominates microplastic particles at the sea surface and in the sea ice. However, the distribution of particles smaller than 50 µm is slightly different in Botterell et al. (2022) than these two studies (Fig. 4.16). Nevertheless, Botterell et al. (2022) is the first study, which assessed microplastic particles down to 6.25 µm in zooplankton specimens and showed that small

microplastic particles pose a greater risk of ingestion. An evaluation of adverse effects of microplastic ingestion by these species is sorely needed in order to complete the picture. To date, studies have suggested that microplastic ingestion can limit natural food uptake, leading to a deficiency in the energy reserves of the zooplankton [i.e. (Cole et al., 2013)]. As with other chemical contaminants, the possibility of biomagnification of microplastic accumulation especially in ice-associated ecosystems might affect ecologically important species such as polar cod (*Boreogadus saida*) and Arctic cod (*Arctogadus glacialis*). Microplastic particles were already identified in polar cod specimens collected during the cruise HE451 around Svalbard (Kühn et al., 2018). Indeed, microplastic analyses in zooplankton, finfish, and shellfish samples from the coastal ecosystem of the Port Blair Bay, Andaman Islands revealed that all species ingested particles (Goswami et al., 2020). The maximum number of fragments was found in the gastrointestinal tract of a planktivorous fish *Alepes djedaba*, indicating bioaccumulation. From a broader perspective, it has been suggested that zooplankton grazing less on primary producers could decrease the oxygen in the water column and accelerate global oxygen inventory loss (Kvale et al., 2021).

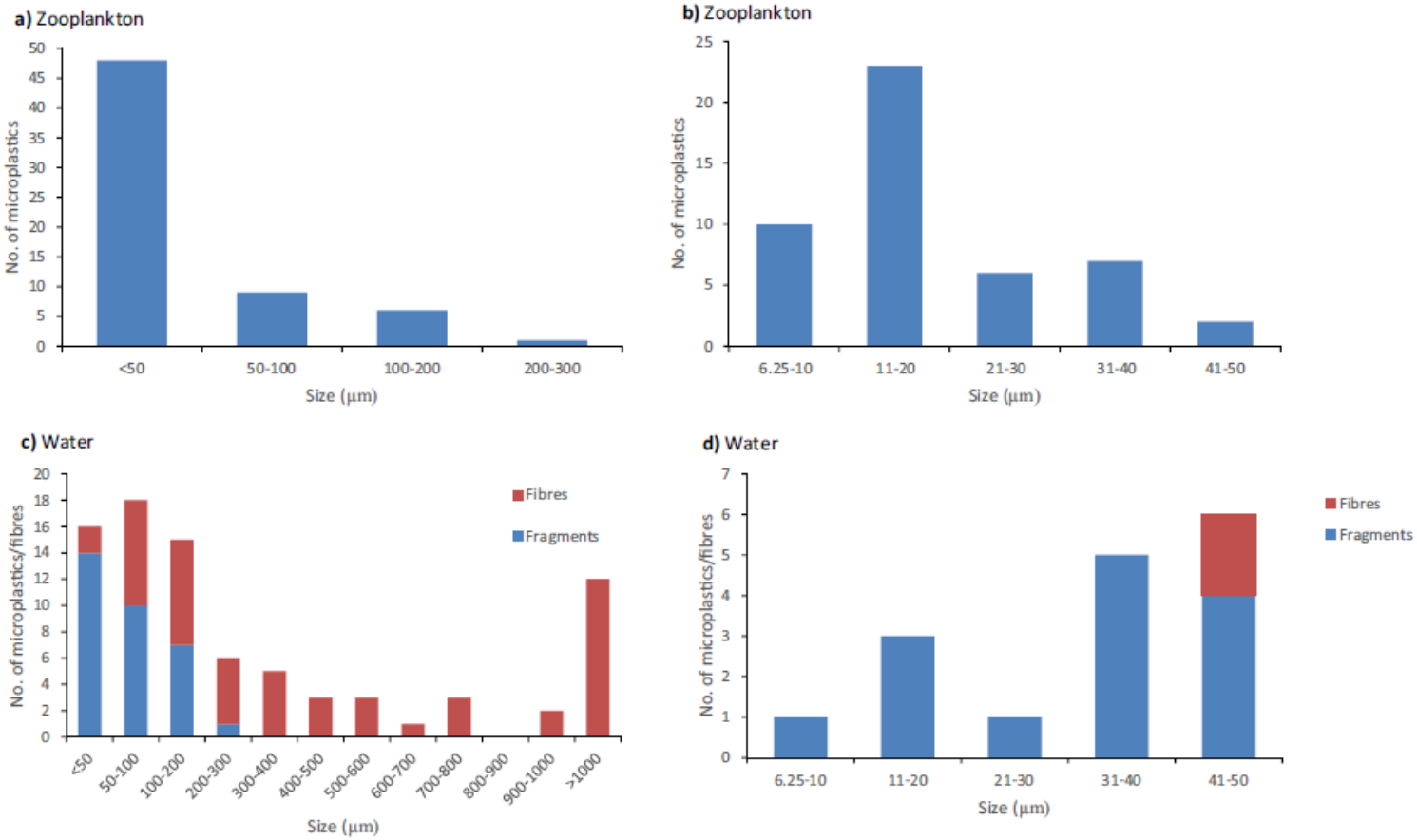

Figure 4.16 "a) Size distribution of microplastic fragments (n = 64) found within the copepod and amphipod samples, b) Size distribution of microplastic fragments smaller than 50

µm (n = 48) in zooplankton, c) Size distribution of the microplastic fragments (n = 32) and fibres (n = 52) found in the water samples, d) Size distribution of fragments (n = 14) and fibres (n = 2) smaller than 50 µm in the water samples." Reprinted from Fig. 2 in "Microplastic ingestion in zooplankton from the Fram Strait in the Arctic" by Z.L.R. Botterell, M.Bergmann, N. Hildebrand, T. Krumpen, M. Steinke, R.C. Thompson, P.K. Lindeque, 2022, Science of The Total Environment, 831, 154886. Copyright by CC BY 4.0 (https://creativecommons.org/licenses/by/4.0/).

One of the most extensive reviews on plastic ingestion in the Arctic was conducted by (Collard and Ask, 2021), which summarised ingestions by invertebrates, fishes and seabirds. The amount of ingested plastic by northern fulmars (*Fulmarus glacialis*) have been used as an indicator in the North Sea for monitoring the ecological quality objective defined by OSPAR for European seas. Northern fulmars prey by surface-seizing with occasional dives up to three metres deep (Garthe and Furness, 2001) and thus plastic ingestion by these species reflects plastic pollution levels in surface waters. A total of 87.5% of the examined individuals of northern fulmars from Svalbard were reported to have ingested plastics, which exceeded the ecological quality objective of OSPAR (Trevail et al., 2015). Among polar cod (*Boreogadus saida*), Atlantic cod (*Gadus morhua*), Greenland cod (*Gadus ogac*), bigeye sculpin (*Triglops nybelini*), Atlantic salmon (*Salmo salar*), Greenland shark (*Somniosus microcephalus*) and capelin (*Mallotus villosus*), up to 34% of the examined animals were found to ingest plastic (Collard and Ask, 2021). Microplastic particles were identified in the stomachs and intestines of all seven examined Beluga whales (*Delphinapterus leucas*) from the Eastern Beaufort Sea (Moore et al., 2020).

Bergmann et al. (2017a) reported sightings of debris encounters of organisms along with the results of beach debris distribution (Fig. 4.17). Severe wounding caused by entanglements in marine debris was observed for a harbour and a bearded seal. A polar bear was seen with a rope around its neck and a plastic sheet in its mouth. Indeed, 13 out of 51 examined polar bears from Alaska ingested plastic, mostly plastic bags [Stimmelmayr et al. (2019) cited by Collard and Ask (2021)]. Microplastic ingestion by walrus (*Odobenus rosmarus*) from west coast of Svalbard was confirmed as well at 34 particles kg^{-1} of faeces (Carlsson et al., 2021).

Figure 4.17 "(A) fishing net bundled up with macroalgae and two entangled antlers and skulls of reindeer (*Rangifer tarandus platyrhynchus*) from Nordaustlandet (credit: J. Hager); (B) harbour seal (*Phoca vitulina*) entangled in rope cutting through the skin, (C) causing severe wounding (credit: F.D. Haug/Governor of Svalbard); (D) bearded seal (*Erignathus barbatus*) with rope tied around its belly in the Hornsund/Bellsund area; (E) polar bear (*Ursus maritimus*) with plastic shred in its mouth on ice floe in Hinlopenstreet (credit: David Shaw Wildlife); (F) dolly rope fibers wrapped around the beak of a perished Arctic tern (*Sterna paradisaea*) (credit: Governor of Svalbard); (G) polar bear with fisheries rope tangled around its neck in the Raudfjord area; (H) Arctic whitlow-grass (*Draba bellii*) in contact with plastic container; (I) polar bear with beached fishing net at Sorgfjorden (credit: T.-A. Hansen/Governor of Svalbard); (J) conglomerate of green algae (cf. Ulva spp.) and dolly rope fibers (credit for D, G, H, J: B. Lutz)." Reprinted from Fig. 2 in "Citizen scientists reveal: Marine litter pollutes Arctic beaches and affects wild life" by M. Bergmann, B. Lutz, M.B. Tekman, L. Gutow., 2017, Marine Pollution Bulletin, 125(1-2), 535-540. Copyright by CC BY-NC-ND 4.0 (https://creativecommons.org/licenses/by-nc-nd/4.0/).

During the visual surveys reported in Chapter 2.1, no organism was observed encountering marine debris in Arctic surface waters. Observations of entanglements in Arctic surface and subsurface waters are scarce as highlighted in an earlier review of ghost gear

entanglements amongst marine mammals, reptiles and elasmobranchs (Stelfox et al., 2016). Sadove and Morreale (1990) identified signs of previous entanglements in five out of 95 examined stranded fin whales in Iceland. A long-term study in the North Atlantic analysed all available photographs of right whales taken between 1980 to 2009 for marks of entanglement with fishing gear and reported that 83% of the animals had been wounded at least once (Knowlton et al., 2012). However, in the context of marine debris, a distinction between discarded and active fishing gear is required, which is impossible in most cases. Nevertheless, our knowledge on entanglements with floating plastic debris of Arctic species is limited.

Chapter 2.2. reported that 50 out of 89 debris items were associated with the deep-sea organisms of *Cladorhiza gelida,* cf. Pachastrellidae, *Caulophacus arcticus* and *Caulophacus* debris, the stalked sea lily *Bathycrinus carpenterii*, the sea anemone cf. *Bathyphellia margaritacea* and Hormathiidae as well as shrimps (*Bythocaris* spp.). The majority of these interactions comprised entanglements of plastic items in *C. gelida*, *C. articus* and *B. carpenterii* or contact between debris and these species.

Up to 31% of the organisms interacted with debris on the deep seafloor of the HAUSGARTEN Observatory (Parga Martínez et al., 2020). The increase in marine debris concentrations was reflected in the number of entanglements within the population of species over the study period. Up to 28% of *C. gelida* at N3 and up to 31% of *C. arcticus* at S3 were observed to suffer entanglements. These figures are concerning because as with corals (Tekman et al., 2022), entanglement with plastic debris can cause injury, disease and death of colonies (Lamb et al., 2018). Only a few studies investigated the impacts of microplastic ingestion by sponges. Mediterranean *Petrosia ficiformis* colonies exposed to microplastic particles showed lower filtration and respiration rates even 72 h after they were transferred to clean water (De Marchi et al., 2022). Species-specific responses and threshold levels of exposure need to be investigated for Arctic species. For example, cold-water coral *Lophelia pertusa* colonies from the northwestern Mediterranean Sea showed reduced growth and capture rates when exposed to microplastic (Mouchi et al., 2019). When covered with macroplastic, the skeletal growth orientation of the colonies changed so as to gain access to water (Mouchi et al., 2019). By contrast, *Madrepora oculata* showed no such response in the same experimental setup (Mouchi et al., 2019).

Anoxic conditions leading to reduced primary production, organic matter and number of infaunal invertebrates were detected in the sediments covered with plastic bags (Green et al., 2015) as in Fig. 2.2.6b. As observed with sea anemones (2.2.6 a – d) macroplastic provides

additional substrate to sessile organisms. In the deep canyons of the Xisha Trough, South China Sea, plastic debris created a biodiversity hotspot by providing an additional habitat for endemic species like soft corals, aplacophoran molluscs, gastropods and even specialized parasitic flatworms, which can induce changes in population dynamics and affect the deep-sea benthic-pelagic coupling processes (Song et al., 2021).

Recently, the ingestion of microplastic particles by benthic amphipod species *Gammarus setosus* collected from Svalbard coasts were reported (Iannilli et al., 2019). Microplastic was identified in the hindguts of over 72% of *Lysianassoidea* amphipod individuals in six deep ocean trenches from around the Pacific Rim (Jamieson et al., 2019). A long-term study showed that two deep-sea benthic invertebrates (*Ophiomusium lymani* and *Hymenaster pellucidus*) from >2000 m deep in the Rockall Trough, North East Atlantic consistently ingested microplastic particles between 1976 and 2015 (Courtene-Jones et al., 2019). Considering the limited food supply to the deep sea and slow growth rate of the organisms, a further increase in debris pollution can lead to population level impacts.

4.8 Outlook

The FRAM Pollution Observatory allowed us to establish a baseline for marine debris and plastic pollution in the Arctic. In contrast to the general perception that the Arctic is a pristine environment, the research showed that this region has also taken its share of anthropogenic debris, especially of plastic pollution. Although these studies established a good understanding of pollution levels in the Arctic, there is still a long way to go to fill the knowledge gaps. In order to fill these knowledge gaps, some issues should be prioritised. Here, I will list the studies in the pipeline along with further suggestions:

- Globally the water column is one of the least studied marine realms for microplastic. Concentrations reported by a limited number of water column studies showed a high disparity in quantities (Courtene-Jones et al., 2017; Kanhai et al., 2018; Peng et al., 2018; Choy et al., 2019), yet proved that microplastic is ubiquitous in this realm. It is essential to understand vertical sinking mechanisms of microplastic particles in the water column, yet these mechanisms have mostly only been studied with model simulations on free-hovering particles. On the other hand, experimental studies have proven that microplastic particles can be incorporated into marine aggregates, alter their buoyancy and settling velocities (Cole et al., 2016; Porter et al., 2018; Wieczorek et al., 2019), which can change the bioavailability of sinking organic matter. As the biological pump facilitates carbon

sequestration and the food supply to the deep ocean, it is a critical research question how the presence of microplastic in surface waters and the deep water column affects its efficiency. In Chapter 3, a significant correlation between microplastic particles and biogenic and lithogenic particles was found. However, these water samples represent a snapshot in time, which does not provide information about microplastic flux and its seasonal variability. The analysis of sediment trap samples for microplastic in relation to organic matter flux could help to understand its role in the biological pump and will be a next step in the Fram Pollution Observatory programme.

- In this dissertation, sea ice and 3D particle drift trajectories were simulated to identify the source areas of marine debris and microplastic pollution. When combined with empirical values, they provided extremely valuable information such as the lateral settling of particles in the Fram Strait with drift trajectories of 604 – 654 km, indicating that there are more complex mechanisms in settling of particles than direct sinking to the seafloor. Future studies of the FRAM Pollution Observatory should focus on numerical models in order to be able to work on future projections and to tackle if current legislations have an impact on mitigating plastic pollution in the Arctic.

- Ecological risk assessments are needed to estimate how current and projected levels of plastic pollution can impact the Arctic fauna. In order to do so, first the identification of ecologically relevant variables and in parallel more studies and a synthesis of ones [i.e. (Kühn et al., 2018; Botterell et al., 2022)] are required in order to elucidate plastic ingestion rates by different ecologically important species. In addition, adverse effects on these species need to be identified in experimental setups. However, this can be extremely challenging for the Arctic, let alone deep-sea biota. The threshold levels of risk can be computed with a similar approach as in (Everaert et al., 2020).

- Neuston samples were collected from the Fram Strait by using a neuston catamaran with a mesh of 330 µm. Even though the results of the analyses of those samples will not be strictly comparable with concentrations reported from the near-surface layer due to different mesh sizes of the sampling gears, the spatial distribution of micro particles would provide valuable information on different sources and could feed numerical models on wind-induced vertical mixing (Kukulka et al., 2012).

- While the macro-debris distribution in surface waters and on the seafloor of the Arctic Ocean was investigated in this dissertation, the transport through the water column has not been studied yet. During the deployments of OFOS, no pelagic debris items were observed and thus this marine compartment was not prioritised to be researched for macro plastic. However, the findings from the Barents Sea showed that marine debris is present in the Arctic water column (Grøsvik et al., 2018). Therefore, it would be beneficial to assess the water column of the Fram Strait with pelagic trawls.

- For all studies of microplastic assessments, a harmonized automated Fourier transform infrared (FTIR) method was used to qualify and quantify microplastic particles in the samples. This method provided a great advantage by not only eliminating human bias, but also enabling identification of particles down to 11 µm. The vast majority of particles in our samples were smaller than 100 µm, highlighting the benefits of this approach, especially considering the bioavailability of this size range. However, the harmonized automated Fourier transform infrared (µFTIR) is still evolving. Even during our FRAM Pollution Observatory studies, improvements have been applied to the pipeline. In fact, the automated analysis was rerun on the dataset of Bergmann et al. (2017b) so that sediment concentrations from 2015 and 2016 could be used together in one dataset. Therefore, it is crucial to keep the analyses updated based on the improvements in the µFTIR pipeline. In fact, the dataset of Peeken et al. (2018) could not be included in the overarching Fram Pollution Observatory analysis of Chapter 4 because a rerun of automated identification is required for that dataset. Therefore, it would be beneficial to have a common repository for the data produced by µFTIR analyses, so that improvements can be easily adjusted in earlier datasets. For example, nowadays fibre detection is possible (Primpke et al., 2019), which was not the case during the time of our studies. As studies from the Arctic have emphasized the high abundances of anthropogenic fibres [i.e. (Ross et al., 2021)], it is crucial to rerun the analyses to identify them in the water column, snow, sea ice and sediment samples.

- Airborne nano- and microplastic can impact ice nucleation efficiency and thus cloud formation, which may exacerbate climate change (Ganguly and Ariya, 2019). As with sea ice (Peeken et al., 2018), anthropogenic particles can penetrate permafrost and be released into the Arctic Ocean with accelerating permafrost thaw driven by climate induced changes (Chen et al., 2021). The distribution of plastic pollution in permafrost, air, snow and sea ice in the Arctic is considerably understudied in the literature (Melvin et al., 2021). Therefore,

future studies of the FRAM Pollution should give a special emphasis on if and how the incorporation of anthropogenic particles into permafrost, air, snow and sea ice may impact the climate processes.

4.9 References

Abel, S.M., Primpke, S., Int-Veen, I., Brandt, A., and Gerdts, G. (2021). Systematic identification of microplastics in abyssal and hadal sediments of the Kuril Kamchatka trench. *Environ. Pollut.* 269**,** 116095. doi: 10.1016/j.envpol.2020.116095.

Allen, D., Allen, S., Abbasi, S., Baker, A., Bergmann, M., Brahney, J., et al. (2022). Microplastics and nanoplastics in the marine-atmosphere environment. *Nature Reviews Earth & Environment* 3(6)**,** 393-405. doi: 10.1038/s43017-022-00292-x.

Allen, S., Allen, D., Moss, K., Le Roux, G., Phoenix, V.R., and Sonke, J.E. (2020). Examination of the ocean as a source for atmospheric microplastics. *PLOS ONE* 15(5)**,** e0232746. doi: 10.1371/journal.pone.0232746.

Andrady, A.L. (2015). "Persistence of Plastic Litter in the Oceans," in *Marine Anthropogenic Litter,* eds. M. Bergmann, L. Gutow & M. Klages. (Berlin: Springer), 57-72.

Aves, A.R., Revell, L.E., Gaw, S., Ruffell, H., Schuddeboom, A., Wotherspoon, N.E., et al. (2022). First evidence of microplastics in Antarctic snow. *The Cryosphere* 16(6)**,** 2127-2145. doi: 10.5194/tc-16-2127-2022.

Barnes, D.K.A., Morley, S.A., Bell, J., Brewin, P., Brigden, K., Collins, M., et al. (2018). Marine plastics threaten giant Atlantic Marine Protected Areas. *Curr. Biol.* 28(19)**,** R1137-R1138. doi: 10.1016/j.cub.2018.08.064.

Benzik, A.N., Orlov, A.M., and Novikov, M.A. (2021). Marine seabed litter in Siberian Arctic: A first attempt to assess. *Mar. Pollut. Bull.* 172**,** 112836. doi: 10.1016/j.marpolbul.2021.112836.

Bergmann, M., Collard, F., Fabres, J., Gabrielsen, G.W., Provencher, J.F., Rochman, C.M., et al. (2022). Plastic pollution in the Arctic. *Nature Reviews Earth & Environment* 3(5)**,** 323-337. doi: 10.1038/s43017-022-00279-8.

Bergmann, M., and Klages, M. (2012). Increase of litter at the Arctic deep-sea observatory HAUSGARTEN. *Mar. Pollut. Bull.* 64(12)**,** 2734-2741. doi: 10.1016/j.marpolbul.2012.09.018.

Bergmann, M., Lutz, B., Tekman, M.B., and Gutow, L. (2017a). Citizen scientists reveal: Marine litter pollutes Arctic beaches and affects wild life. *Mar. Pollut. Bull.* 125(1-2)**,** 535-540. doi: 10.1016/j.marpolbul.2017.09.055.

Bergmann, M., Mutzel, S., Primpke, S., Tekman, M.B., Trachsel, J., and Gerdts, G. (2019). White and wonderful? Microplastics prevail in snow from the Alps to the Arctic. *Sci. Adv.* 5(8)**,** eaax1157. doi: 10.1126/sciadv.aax1157.

Bergmann, M., Wirzberger, V., Krumpen, T., Lorenz, C., Primpke, S., Tekman, M.B., et al. (2017b). High Quantities of Microplastic in Arctic Deep-Sea Sediments from the HAUSGARTEN Observatory. *Environ. Sci. Technol.* 51(19)**,** 11000-11010. doi: 10.1021/acs.est.7b03331.

Bond, T., Morton, J., Al-Rekabi, Z., Cant, D., Davidson, S., and Pei, Y. (2022). Surface properties and rising velocities of pristine and weathered plastic pellets. *Environ. Sci.: Process. Impacts* 24(5)**,** 794-804. doi: 10.1039/D1EM00495F.

Botterell, Z.L.R., Bergmann, M., Hildebrandt, N., Krumpen, T., Steinke, M., Thompson, R.C., et al. (2022). Microplastic ingestion in zooplankton from the Fram Strait in the Arctic. *Sci. Total Environ.* 831**,** 154886. doi: 10.1016/j.scitotenv.2022.154886.

Buhl-Mortensen, L., and Buhl-Mortensen, P. (2017). Marine litter in the Nordic Seas: Distribution composition and abundance. *Mar. Pollut. Bull.* 125(1-2)**,** 260-270. doi: 10.1016/j.marpolbul.2017.08.048.

Canals, M., Pham, C.K., Bergmann, M., Gutow, L., Hanke, G., Van Sebille, E., et al. (2021). The quest for seafloor macrolitter: a critical review of background knowledge, current methods and future prospects. *Environ. Res. Lett.* 16**,** 023001.

Cardoso, C., and Caldeira, R.M.A. (2021). Modeling the Exposure of the Macaronesia Islands (NE Atlantic) to Marine Plastic Pollution. *Front. Mar. Sci.* 8. doi: 10.3389/fmars.2021.653502.

Carlsson, P., Singdahl-Larsen, C., and Lusher, A.L. (2021). Understanding the occurrence and fate of microplastics in coastal Arctic ecosystems: The case of surface waters, sediments and walrus (Odobenus rosmarus). *Sci. Total Environ.* 792**,** 148308. doi: 10.1016/j.scitotenv.2021.148308.

Charette, M.A., Kipp, L.E., Jensen, L.T., Dabrowski, J.S., Whitmore, L.M., Fitzsimmons, J.N., et al. (2020). The Transpolar Drift as a Source of Riverine and Shelf-Derived Trace Elements to the Central Arctic Ocean. *J. Geophys. Res. Oceans* 125(5)**,** e2019JC015920. doi: 10.1029/2019JC015920.

Chen, X., Huang, G., Gao, S., and Wu, Y. (2021). Effects of permafrost degradation on global microplastic cycling under climate change. *J. Environ. Chem. Eng.* 9(5)**,** 106000. doi: 10.1016/j.jece.2021.106000.

Cheung, P.K., Cheung, L.T.O., and Fok, L. (2016). Seasonal variation in the abundance of marine plastic debris in the estuary of a subtropical macro-scale drainage basin in South China. *Sci. Total Environ.* 562**,** 658-665. doi: 10.1016/j.scitotenv.2016.04.048.

Chiba, S., Saito, H., Fletcher, R., Yogi, T., Kayo, M., Miyagi, S., et al. (2018). Human footprint in the abyss: 30 year records of deep-sea plastic debris. *Mar. Policy* 96**,** 204-212. doi: 10.1016/j.marpol.2018.03.022.

Choy, C.A., Robison, B.H., Gagne, T.O., Erwin, B., Firl, E., Halden, R.U., et al. (2019). The vertical distribution and biological transport of marine microplastics across the epipelagic and mesopelagic water column. *Sci. Rep.* 9(1)**,** 7843. doi: 10.1038/s41598-019-44117-2.

Cole, M., Lindeque, P., Fileman, E., Halsband, C., Goodhead, R., Moger, J., et al. (2013). Microplastic ingestion by zooplankton. *Environ. Sci. Technol.* 47(12)**,** 6646-6655. doi: 10.1021/es400663f.

Cole, M., Lindeque, P.K., Fileman, E., Clark, J., Lewis, C., Halsband, C., et al. (2016). Microplastics Alter the Properties and Sinking Rates of Zooplankton Faecal Pellets. *Environ. Sci. Technol.* 50(6)**,** 3239-3246. doi: 10.1021/acs.est.5b05905.

Collard, F., and Ask, A. (2021). Plastic ingestion by Arctic fauna: A review. *Sci. Total Environ.* 786**,** 147462. doi: 10.1016/j.scitotenv.2021.147462.

Collard, F., Husum, K., Eppe, G., Malherbe, C., Hallanger, I.G., Divine, D.V., et al. (2021). Anthropogenic particles in sediment from an Arctic fjord. *Sci. Total Environ.* 772**,** 145575. doi: https://doi.org/10.1016/j.scitotenv.2021.145575.

Courtene-Jones, W., Quinn, B., Ewins, C., Gary, S.F., and Narayanaswamy, B.E. (2019). Consistent microplastic ingestion by deep-sea invertebrates over the last four decades (1976-2015), a study from the North East Atlantic. *Environ. Pollut.* 244**,** 503-512. doi: 10.1016/j.envpol.2018.10.090.

Courtene-Jones, W., Quinn, B., Gary, S.F., Mogg, A.O.M., and Narayanaswamy, B.E. (2017). Microplastic pollution identified in deep-sea water and ingested by benthic invertebrates in the Rockall Trough, North Atlantic Ocean. *Environ. Pollut.* 231(Pt 1)**,** 271-280. doi: 10.1016/j.envpol.2017.08.026.

Cózar, A., Marti, E., Duarte, C.M., Garcia-de-Lomas, J., van Sebille, E., Ballatore, T.J., et al. (2017). The Arctic Ocean as a dead end for floating plastics in the North Atlantic branch of the Thermohaline Circulation. *Sci. Adv.* 3(4)**,** e1600582. doi: 10.1126/sciadv.1600582.

De Marchi, L., Renzi, M., Anselmi, S., Pretti, C., Guazzelli, E., Martinelli, E., et al. (2022). Polyethylene microplastics reduce filtration and respiration rates in the Mediterranean sponge *Petrosia ficiformis*. *Environ. Res.* 211**,** 113094. doi: 10.1016/j.envres.2022.113094.

Dominguez-Carrio, C., Sanchez-Vidal, A., Estournel, C., Corbera, G., Riera, J.L., Orejas, C., et al. (2020). Seafloor litter sorting in different domains of Cap de Creus continental shelf and submarine canyon (NW Mediterranean Sea). *Mar. Pollut. Bull.* 161(Pt B)**,** 111744. doi: 10.1016/j.marpolbul.2020.111744.

Enders, K., Lenz, R., Stedmon, C.A., and Nielsen, T.G. (2015). Abundance, size and polymer composition of marine microplastics ≥ 10 μm in the Atlantic Ocean and their modelled vertical distribution. *Mar. Pollut. Bull.* 100(1)**,** 70-81. doi: 10.1016/j.marpolbul.2015.09.027.

Evangeliou, N., Grythe, H., Klimont, Z., Heyes, C., Eckhardt, S., Lopez-Aparicio, S., et al. (2020). Atmospheric transport is a major pathway of microplastics to remote regions. *Nat. Commun.* 11(1)**,** 3381. doi: 10.1038/s41467-020-17201-9.

Everaert, G., De Rijcke, M., Lonneville, B., Janssen, C.R., Backhaus, T., Mees, J., et al. (2020). Risks of floating microplastic in the global ocean. *Environ. Pollut.* 267**,** 115499. doi: 10.1016/j.envpol.2020.115499.

Falk-Andersson, J., Strietman, W., Larsen, R., Gabrielsen, G., Collard, F., Leemans, E., et al. (2019). "Svalbard Beach Litter Deep Dive".).

Ferrero, L., Scibetta, L., Markuszewski, P., Mazurkiewicz, M., Drozdowska, V., Makuch, P., et al. (2022). Airborne and marine microplastics from an oceanographic survey at the Baltic Sea: An emerging role of air-sea interaction? *Sci. Total Environ.* 824**,** 153709. doi: 10.1016/j.scitotenv.2022.153709.

Ganguly, M., and Ariya, P.A. (2019). Icenucleation of model nanoplastics and microplastics: a novel synthetic protocol and the influence of particle capping at diverse atmospheric environments. *ACS Earth Space Chem.* 3(9)**,** 1729-1739.

Garthe, S., and Furness, R.W. (2001). Frequent Shallow Diving by a Northern Fulmar Feeding at Shetland. *Waterbirds* 24(2)**,** 287-289. doi: 10.2307/1522045.

Geilfus, N.X., Munson, K.M., Sousa, J., Germanov, Y., Bhugaloo, S., Babb, D., et al. (2019). Distribution and impacts of microplastic incorporation within sea ice. *Mar. Pollut. Bull.* 145**,** 463-473. doi: 10.1016/j.marpolbul.2019.06.029.

Gerigny, O., Brun, M., Fabri, M.C., Tomasino, C., Le Moigne, M., Jadaud, A., et al. (2019). Seafloor litter from the continental shelf and canyons in French Mediterranean Water: Distribution, typologies and trends. *Mar. Pollut. Bull.* 146**,** 653-666. doi: 10.1016/j.marpolbul.2019.07.030.

Goldstein, M.C., Titmus, A.J., and Ford, M. (2013). Scales of spatial heterogeneity of plastic marine debris in the northeast pacific ocean. *PLoS One* 8(11)**,** e80020. doi: 10.1371/journal.pone.0080020.

Golubeva, E., Platov, G., Iakshina, D., and Kraineva, M. (2019). A simulated distribution of Siberian river runoff in the Arctic Ocean. *IOP Conf. Ser.: Earth Environ. Sci.* 386(1)**,** 012022. doi: 10.1088/1755-1315/386/1/012022.

González-Pleiter, M., Edo, C., Aguilera, Á., Viúdez-Moreiras, D., Pulido-Reyes, G., González-Toril, E., et al. (2021). Occurrence and transport of microplastics sampled within and above the planetary boundary layer. *Sci. Total Environ.* 761**,** 143213.

Goswami, P., Vinithkumar, N.V., and Dharani, G. (2020). First evidence of microplastics bioaccumulation by marine organisms in the Port Blair Bay, Andaman Islands. *Mar. Pollut. Bullet.* 155**,** 111163. doi: 10.1016/j.marpolbul.2020.111163.

Green, D.S., Boots, B., Blockley, D.J., Rocha, C., and Thompson, R. (2015). Impacts of discarded plastic bags on marine assemblages and ecosystem functioning. *Environ. Sci. Technol.* 49(9)**,** 5380-5389. doi: 10.1021/acs.est.5b00277.

Grøsvik, B.E., Prokhorova, T., Eriksen, E., Krivosheya, P., Horneland, P.A., and Prozorkevich, D. (2018). Assessment of Marine Litter in the Barents Sea, a Part of the Joint Norwegian–Russian Ecosystem Survey. *Front. Mar. Sci.* 5. doi: 10.3389/fmars.2018.00072.

Gutow, L., Ricker, M., Holstein, J.M., Dannheim, J., Stanev, E.V., and Wolff, J.O. (2018). Distribution and trajectories of floating and benthic marine macrolitter in the south-eastern North Sea. *Mar. Pollut. Bull.* 131(Pt A)**,** 763-772. doi: 10.1016/j.marpolbul.2018.05.003.

Haave, M., Lorenz, C., Primpke, S., and Gerdts, G. (2019). Different stories told by small and large microplastics in sediment - first report of microplastic concentrations in an urban recipient in Norway. *Mar. Pollut. Bull.* 141**,** 501-513. doi: 10.1016/j.marpolbul.2019.02.015.

Huntington, A., Corcoran, P.L., Jantunen, L., Thaysen, C., Bernstein, S., Stern, G.A., et al. (2020). A first assessment of microplastics and other anthropogenic particles in Hudson Bay and the surrounding eastern Canadian Arctic waters of Nunavut. *FACETS* 5(1)**,** 432-454. doi: 10.1139/facets-2019-0042.

Iannilli, V., Pasquali, V., Setini, A., and Corami, F. (2019). First evidence of microplastics ingestion in benthic amphipods from Svalbard. *Environ. Res.* 179**,** 108811. doi: 10.1016/j.envres.2019.108811.

Jamieson, A.J., Brooks, L.S.R., Reid, W.D.K., Piertney, S.B., Narayanaswamy, B.E., and Linley, T.D. (2019). Microplastics and synthetic particles ingested by deep-sea amphipods in six of the deepest marine ecosystems on Earth. *R. Soc. Open Sci.* 6(2)**,** 180667. doi: 10.1098/rsos.180667.

Janout, M.A., Hölemann, J., Waite, A.M., Krumpen, T., von Appen, W.-J., and Martynov, F. (2016). Sea-ice retreat controls timing of summer plankton blooms in the Eastern Arctic Ocean. *Geophys. Res. Lett.* 43(24)**,** 12,493-412,501. doi: 10.1002/2016GL071232.

Jayasiri, H.B., Purushothaman, C.S., and Vennila, A. (2013). Quantitative analysis of plastic debris on recreational beaches in Mumbai, India. *Mar. Pollut. Bull.* 77(1-2)**,** 107-112. doi: 10.1016/j.marpolbul.2013.10.024.

Jiang, Y., Yang, F., Zhao, Y., and Wang, J. (2020). Greenland Sea Gyre increases microplastic pollution in the surface waters of the Nordic Seas. *Sci. Total Environ.* 712**,** 136484. doi: 10.1016/j.scitotenv.2019.136484.

Kaandorp, M.L.A., Dijkstra, H.A., and van Sebille, E. (2021). Modelling size distributions of marine plastics under the influence of continuous cascading fragmentation. *Environ. Res. Lett.* 16(5)**,** 054075. doi: 10.1088/1748-9326/abe9ea.

Kaladharan, P., Vijayakumaran, K., Singh, V., Asha, P., Sulochanan, B., Asokan, P., et al. (2012). Assessment of certain Anthropogenic Interventions and their Impacts along the Indian Coastline. *FISHERY TECHNOLOGY* 49**,** 32-37.

Kane, I.A., Clare, M.A., Miramontes, E., Wogelius, R., Rothwell, J.J., Garreau, P., et al. (2020). Seafloor microplastic hotspots controlled by deep-sea circulation. *Science* 368(6495)**,** 1140-1145. doi: 10.1126/science.aba5899.

Kanhai, D.K., Gardfeldt, K., Lyashevska, O., Hassellov, M., Thompson, R.C., and O'Connor, I. (2018). Microplastics in sub-surface waters of the Arctic Central Basin. *Mar. Pollut. Bull.* 130**,** 8-18. doi: 10.1016/j.marpolbul.2018.03.011.

Kanhai, L.D.K., Gardfeldt, K., Krumpen, T., Thompson, R.C., and O'Connor, I. (2020). Microplastics in sea ice and seawater beneath ice floes from the Arctic Ocean. *Sci. Rep.* 10(1)**,** 5004. doi: 10.1038/s41598-020-61948-6.

Kanhai, L.D.K., Johansson, C., Frias, J.P.G.L., Gardfeldt, K., Thompson, R.C., and O'Connor, I. (2019). Deep sea sediments of the Arctic Central Basin: A potential sink for microplastics. *Deep Sea Res. Part I Oceanogr. Res. Pap.* 145**,** 137-142. doi: 10.1016/j.dsr.2019.03.003.

Kelly, A., Lannuzel, D., Rodemann, T., Meiners, K.M., and Auman, H.J. (2020). Microplastic contamination in east Antarctic sea ice. *Mar Pollut Bull* 154**,** 111130. doi: 10.1016/j.marpolbul.2020.111130.

Kim, S.K., Lee, H.J., Kim, J.S., Kang, S.H., Yang, E.J., Cho, K.H., et al. (2021). Importance of seasonal sea ice in the western Arctic ocean to the Arctic and global microplastic budgets. *J. Hazard. Mater.* 418**,** 125971. doi: 10.1016/j.jhazmat.2021.125971.

Knowlton, A.R., Hamilton, P.K., Marx, M.K., Pettis, H.M., and Kraus, S.D. (2012). Monitoring North Atlantic right whale *Eubalaena glacialis* entanglement rates: a 30 yr retrospective. *Mar. Ecol. Prog. Ser.* 466**,** 293-302. doi: 10.3354/meps09923.

Koelmans, A.A., Kooi, M., Law, K.L., and Van Sebille, E. (2017). All is not lost: deriving a top-down mass budget of plastic at sea. *Environ. Res. Lett.* 12(11)**,** 114028. doi: 10.1088/1748-9326/aa9500.

Kooi, M., Nes, E.H.v., Scheffer, M., and Koelmans, A.A. (2017). Ups and Downs in the Ocean: Effects of Biofouling on Vertical Transport of Microplastics. *Environ. Sci. Technol.* 51(14)**,** 7963-7971. doi: 10.1021/acs.est.6b04702.

Kowalski, N., Reichardt, A.M., and Waniek, J.J. (2016). Sinking rates of microplastics and potential implications of their alteration by physical, biological, and chemical factors. *Mar. Pollut. Bull.* 109(1)**,** 310-319. doi: 10.1016/j.marpolbul.2016.05.064.

Kühn, S., Schaafsma, F.L., van Werven, B., Flores, H., Bergmann, M., Egelkraut-Holtus, M., et al. (2018). Plastic ingestion by juvenile polar cod (Boreogadus saida) in the Arctic Ocean. *Polar Biol.* 41(6)**,** 1269-1278. doi: 10.1007/s00300-018-2283-8.

Kukulka, T., Proskurowski, G., Morét-Ferguson, S., Meyer, D.W., and Law, K.L. (2012). The effect of wind mixing on the vertical distribution of buoyant plastic debris. *Geophys. Res. Lett.* 39(7)**,** n/a-n/a. doi: 10.1029/2012gl051116.

Kuroda, M., Uchida, K., Tokai, T., Miyamoto, Y., Mukai, T., Imai, K., et al. (2020). The current state of marine debris on the seafloor in offshore area around Japan. *Mar. Pollut. Bull.* 161(Pt A)**,** 111670. doi: 10.1016/j.marpolbul.2020.111670.

Kvale, K., Prowe, A.E.F., Chien, C.T., Landolfi, A., and Oschlies, A. (2021). Zooplankton grazing of microplastic can accelerate global loss of ocean oxygen. *Nat. Commun.* 12(1)**,** 2358. doi: 10.1038/s41467-021-22554-w.

Lamb, J.B., Willis, B.L., Fiorenza, E.A., Couch, C.S., Howard, R., Rader, D.N., et al. (2018). Plastic waste associated with disease on coral reefs. *Science* 359(6374)**,** 460-462. doi: 10.1126/science.aar3320.

Lavers, J.L., and Bond, A.L. (2017). Exceptional and rapid accumulation of anthropogenic debris on one of the world's most remote and pristine islands. *Proc. Natl. Acad. Sci. U.S.A.* 114(23)**,** 6052-6055. doi: 10.1073/pnas.1619818114.

Lebreton, L., Slat, B., Ferrari, F., Sainte-Rose, B., Aitken, J., Marthouse, R., et al. (2018). Evidence that the Great Pacific Garbage Patch is rapidly accumulating plastic. *Sci. Rep.* 8(1)**,** 4666. doi: 10.1038/s41598-018-22939-w.

Leu, E., Søreide, J.E., Hessen, D.O., Falk-Petersen, S., and Berge, J. (2011). Consequences of changing sea-ice cover for primary and secondary producers in the European Arctic shelf seas: Timing, quantity, and quality. *Prog. Oceanogr.* 90(1)**,** 18-32. doi: 10.1016/j.pocean.2011.02.004.

Li, D., Liu, K., Li, C., Peng, G., Andrady, A.L., Wu, T., et al. (2020). Profiling the Vertical Transport of Microplastics in the West Pacific Ocean and the East Indian Ocean with a Novel in Situ Filtration Technique. *Environ. Sci. Technol.* 54(20)**,** 12979-12988. doi: 10.1021/acs.est.0c02374.

Lima, A.R.A., Ferreira, G.V.B., Barrows, A.P.W., Christiansen, K.S., Treinish, G., and Toshack, M.C. (2021). Global patterns for the spatial distribution of floating microfibers: Arctic Ocean as a potential accumulation zone. *J. Hazard. Mater.* 403**,** 123796. doi: 10.1016/j.jhazmat.2020.123796.

Liu, K., Wang, X., Song, Z., Wei, N., Ye, H., Cong, X., et al. (2020). Global inventory of atmospheric fibrous microplastics input into the ocean: An implication from the indoor origin. *J. Hazard. Mater.* 400**,** 123223. doi: 10.1016/j.jhazmat.2020.123223.

Lorenz, C., Roscher, L., Meyer, M.S., Hildebrandt, L., Prume, J., Löder, M.G.J., et al. (2019). Spatial distribution of microplastics in sediments and surface waters of the southern North Sea. *Environ. Pollut.* 252(Pt B)**,** 1719-1729. doi: 10.1016/j.envpol.2019.06.093.

MacLeod, M., Arp, H.P.H., Tekman, M.B., and Jahnke, A. (2021). The global threat from plastic pollution. *Science* 373(6550)**,** 61-65. doi: 10.1126/science.abg5433.

Melvin, J., Bury, M., Ammendolia, J., Mather, C., and Liboiron, M. (2021). Critical Gaps in Shoreline Plastics Pollution Research. *Front. Mar. Sci.* 8. doi: 10.3389/fmars.2021.689108.

Meyer-Kaiser, K., Bergmann, M., Soltwedel, T., and Klages, M. (2019). Recruitment of Arctic deep-sea invertebrates: Results from a long-term hard-substrate colonization experiment at the Long-Term Ecological Research observatory HAUSGARTEN. *Limnol. Oceanogr.* 64(5)**,** 1924-1938. doi: 10.1002/lno.11160.

Meyer, A.N. (2022). *Deep Dives into Arctic Beach Debris. Analysing its Composition and Origin.* Bachelor, Christian-Albrecht University of Kiel.

Miller, E., Sedlak, M., Lin, D., Box, C., Holleman, C., Rochman, C.M., et al. (2021). Recommended best practices for collecting, analyzing, and reporting microplastics in environmental media: Lessons learned from comprehensive monitoring of San Francisco Bay. *J. Hazard. Mater.* 409**,** 124770. doi: 10.1016/j.jhazmat.2020.124770.

Moore, R.C., Loseto, L., Noel, M., Etemadifar, A., Brewster, J.D., MacPhee, S., et al. (2020). Microplastics in beluga whales (*Delphinapterus leucas*) from the Eastern Beaufort Sea. *Mar. Pollut. Bull.* 150**,** 110723. doi: https://doi.org/10.1016/j.marpolbul.2019.110723.

Mordecai, G., Tyler, P.A., Masson, D.G., and Huvenne, V.A.I. (2011). Litter in submarine canyons off the west coast of Portugal. *Deep Sea Res. Part II Top. Stud. Oceanogr.* 58(23-24)**,** 2489-2496. doi: 10.1016/j.dsr2.2011.08.009.

Mouchi, V., Chapron, L., Peru, E., Pruski, A.M., Meistertzheim, A.L., Vetion, G., et al. (2019). Long-term aquaria study suggests species-specific responses of two cold-water corals to macro-and microplastics exposure. *Environ. Pollut.* 253**,** 322-329. doi: 10.1016/j.envpol.2019.07.024.

Mountford, A.S., and Morales Maqueda, M.A. (2021). Modeling the Accumulation and Transport of Microplastics by Sea Ice. *J. Geophys. Res. Oceans* 126(2). doi: 10.1029/2020JC016826.

Murphy, E., Nistor, I., Cornett, A., Wilson, J., and Pilechi, A. (2021). Fate and transport of coastal driftwood: A critical review. *Mar. Pollut. Bull.* 170**,** 112649. doi: 10.1016/j.marpolbul.2021.112649.

Napper, I.E., Davies, B.F.R., Clifford, H., Elvin, S., Koldewey, H.J., Mayewski, P.A., et al. (2020). Reaching New Heights in Plastic Pollution—Preliminary Findings of Microplastics on Mount Everest. *One Earth* 3(5)**,** 621-630. doi: 10.1016/j.oneear.2020.10.020.

Obbard, R.W., Sadri, S., Wong, Y.Q., Khitun, A.A., Baker, I., and Thompson, R.C. (2014). Global warming releases microplastic legacy frozen in Arctic Sea ice. *Earth's Future* 2(6)**,** 315-320. doi: 10.1002/2014ef000240.

Pakhomova, S., Berezina, A., Lusher, A.L., Zhdanov, I., Silvestrova, K., Zavialov, P., et al. (2022). Microplastic variability in subsurface water from the Arctic to Antarctica. *Environ. Pollut.* 298**,** 118808. doi: https://doi.org/10.1016/j.envpol.2022.118808.

Palatinus, A., Kovac Virsek, M., Robic, U., Grego, M., Bajt, O., Siljic, J., et al. (2019). Marine litter in the Croatian part of the middle Adriatic Sea: Simultaneous assessment of floating and seabed macro and micro litter abundance and composition. *Mar. Pollut. Bull.* 139**,** 427-439. doi: 10.1016/j.marpolbul.2018.12.038.

Parga Martínez, K.B., Tekman, M.B., and Bergmann, M. (2020). Temporal trends in marine litter at three stations of the HAUSGARTEN observatory in the Arctic deep sea. *Front. Mar. Sci.* 7**,** 321. doi: 10.3389/fmars.2020.00321.

Pauly, J.L., Stegmeier, S.J., Allaart, H.A., Cheney, R.T., Zhang, P.J., Mayer, A.G., et al. (1998). Inhaled cellulosic and plastic fibers found in human lung tissue. *Cancer Epidemiol. Biomarkers Prev.* 7(5)**,** 419-428.

Peeken, I., Primpke, S., Beyer, B., Gutermann, J., Katlein, C., Krumpen, T., et al. (2018). Arctic sea ice is an important temporal sink and means of transport for microplastic. *Nat. Commun.* 9(1)**,** 1505. doi: 10.1038/s41467-018-03825-5.

Peng, X., Chen, M., Chen, S., Dasgupta, S., Xu, H., Ta, K., et al. (2018). Microplastics contaminate the deepest part of the world's ocean. *Geochem. Perspect. Lett.* 9**,** 1-5. doi: 10.7185/geochemlet.1829.

Pham, C.K., Ramirez-Llodra, E., Alt, C.H., Amaro, T., Bergmann, M., Canals, M., et al. (2014). Marine litter distribution and density in European seas, from the shelves to deep basins. *PLoS One* 9(4)**,** e95839. doi: 10.1371/journal.pone.0095839.

Pierdomenico, M., Casalbore, D., and Chiocci, F.L. (2019). Massive benthic litter funnelled to deep sea by flash-flood generated hyperpycnal flows. *Sci Rep* 9(1)**,** 5330. doi: 10.1038/s41598-019-41816-8.

Pogojeva, M., Zhdanov, I., Berezina, A., Lapenkov, A., Kosmach, D., Osadchiev, A., et al. (2021). Distribution of floating marine macro-litter in relation to oceanographic characteristics in the Russian Arctic Seas. *Mar. Pollut. Bull.* 166**,** 112201. doi: 10.1016/j.marpolbul.2021.112201.

Porter, A., Lyons, B.P., Galloway, T.S., and Lewis, C. (2018). Role of Marine Snows in Microplastic Fate and Bioavailability. *Environ. Sci. Technol.* 52(12)**,** 7111-7119. doi: 10.1021/acs.est.8b01000.

Primpke, S., A. Dias, P., and Gerdts, G. (2019). Automated identification and quantification of microfibres and microplastics. *Analytical Methods* 11(16)**,** 2138-2147. doi: 10.1039/c9ay00126c.

Primpke, S., Cross, R.K., Mintenig, S.M., Simon, M., Vianello, A., Gerdts, G., et al. (2020). Toward the systematic identification of microplastics in the environment: evaluation of a new independent software tool (siMPle) for spectroscopic analysis. *Appl. Spectrosc.* 74(9)**,** 1127-1138. doi: 10.1177/0003702820917760.

Primpke, S., Lorenz, C., Rascher-Friesenhausen, R., and Gerdts, G. (2017). An automated approach for microplastics analysis using focal plane array (FPA) FTIR microscopy and image analysis. *Analytical Methods* 9(9)**,** 1499-1511. doi: 10.1039/c6ay02476a.

Ramirez-Llodra, E., Tyler, P.A., Baker, M.C., Bergstad, O.A., Clark, M.R., Escobar, E., et al. (2011). Man and the last great wilderness: human impact on the deep sea. *PLoS One* 6(8)**,** e22588. doi: 10.1371/journal.pone.0022588.

Revell, L.E., Kuma, P., Le Ru, E.C., Somerville, W.R.C., and Gaw, S. (2021). Direct radiative effects of airborne microplastics. *Nature* 598(7881)**,** 462-467. doi: 10.1038/s41586-021-03864-x.

Rist, S., Vianello, A., Winding, M.H.S., Nielsen, T.G., Almeda, R., Torres, R.R., et al. (2020). Quantification of plankton-sized microplastics in a productive coastal Arctic marine ecosystem. *Environ. Pollut.* 266**,** 115248. doi: 10.1016/j.envpol.2020.115248.

Rodrigues, J. (2009). The increase in the length of the ice-free season in the Arctic. *Cold Reg. Sci. Technol.* 59(1)**,** 78-101. doi: 10.1016/j.coldregions.2009.05.006.

Rodríguez-Torres, R., Almeda, R., Kristiansen, M., Rist, S., Winding, M.S., and Nielsen, T.G. (2020). Ingestion and impact of microplastics on arctic Calanus copepods. *Aquat. Toxicol.* 228**,** 105631. doi: 10.1016/j.aquatox.2020.105631.

Ross, P.S., Chastain, S., Vassilenko, E., Etemadifar, A., Zimmermann, S., Quesnel, S.-A., et al. (2021). Pervasive distribution of polyester fibres in the Arctic Ocean is driven by Atlantic inputs. *Nat. Commun.* 12(1)**,** 106. doi: 10.1038/s41467-020-20347-1.

Rudels, B., Larsson, A.-M., and Sehlstedt, P.-I. (1991). Stratification and water mass formation in the Arctic Ocean: some implications for the nutrient distribution. *Polar Res.* 10(1)**,** 19-32. doi: 10.3402/polar.v10i1.6724.

Ryan, P.G., Dilley, B.J., Ronconi, R.A., and Connan, M. (2019). Rapid increase in Asian bottles in the South Atlantic Ocean indicates major debris inputs from ships. *Proc. Natl. Acad. Sci. U.S.A.* 116(42)**,** 20892-20897. doi: 10.1073/pnas.1909816116.

Ryan, P.G., Musker, S., and Rink, A. (2014). Low densities of drifting litter in the African sector of the Southern Ocean. *Mar Pollut Bull* 89(1-2)**,** 16-19. doi: 10.1016/j.marpolbul.2014.10.043.

Ryan, P.G., Pichegru, L., Perolod, V., and Moloney, C.L. (2020). Monitoring marine plastics - will we know if we are making a difference? *S. Afr. J. Sci.* 116**,** 1-9. doi: 10.17159/sajs.2020/7678.

Sadove, S.S., and Morreale, S.J. (Year). "Marine mammal and sea turtle encounters with marine debris in the New York Bight and the northeast Atlantic", in: *Proceedings of the Second International Conference on Marine Debris, Honolulu, Hawaii*, eds. R.S. Shomura & M.L. Godfrey: National Oceanic and Atmospheric Administration, U.S. Department of Commerce), 2-7.

Schlining, K., von Thun, S., Kuhnz, L., Schlining, B., Lundsten, L., Jacobsen Stout, N., et al. (2013). Debris in the deep: Using a 22-year video annotation database to survey marine litter in Monterey Canyon, central California, USA. *Deep Sea Res. Part I Oceanogr. Res. Pap.* 79**,** 96-105. doi: 10.1016/j.dsr.2013.05.006.

Song, X.K., Lyu, M.X., Zhang, X.D., Ruthensteiner, B., Ahn, I.Y., Pastorino, G., et al. (2021). Large Plastic Debris Dumps: New Biodiversity Hot Spots Emerging on the Deep-Sea Floor. *Environ. Sci. Tech. Let.* 8(2)**,** 148-154. doi: 10.1021/acs.estlett.0c00967.

Stelfox, M., Hudgins, J., and Sweet, M. (2016). A review of ghost gear entanglement amongst marine mammals, reptiles and elasmobranchs. *Mar. Pollut. Bull.* 111(1-2)**,** 6-17. doi: 10.1016/j.marpolbul.2016.06.034.

Stimmelmayr, R., Adams, B., Kayotuk, C., and M., P. (2019). "Polar Bears, Plastics, and the Pyloric Sphincter: A Volatile Combination", in: *Alaska Marine Science Symposium.*).

Stocker, A.N., Renner, A.H.H., and Knol-Kauffman, M. (2020). Sea ice variability and maritime activity around Svalbard in the period 2012-2019. *Sci. Rep.* 10(1)**,** 17043. doi: 10.1038/s41598-020-74064-2.

Strand, K.O., Huserbraten, M., Dagestad, K.F., Mauritzen, C., Grosvik, B.E., Nogueira, L.A., et al. (2021). Potential sources of marine plastic from survey beaches in the Arctic and Northeast Atlantic. *Sci. Total Environ.* 790**,** 148009. doi: 10.1016/j.scitotenv.2021.148009.

Suaria, G., Avio, C.G., Mineo, A., Lattin, G.L., Magaldi, M.G., Belmonte, G., et al. (2016). The Mediterranean Plastic Soup: synthetic polymers in Mediterranean surface waters. *Sci. Rep.* 6**,** 37551. doi: 10.1038/srep37551.

Suaria, G., Perold, V., Lee, J.R., Lebouard, F., Aliani, S., and Ryan, P.G. (2020). Floating macro- and microplastics around the Southern Ocean: Results from the Antarctic Circumnavigation Expedition. *Environ Int* 136**,** 105494. doi: 10.1016/j.envint.2020.105494.

Taylor, A.R., Barðadóttir, Þ., Auffret, S., Bombosch, A., Cusick, A.L., Falk, E., et al. (2020). Arctic expedition cruise tourism and citizen science: a vision for the future of polar tourism. *J. Tour. Futures* 6(1)**,** 102-111. doi: 10.1108/JTF-06-2019-0051.

Tekman, M. B., Walther, B. A., Peter, C., Gutow, L. and Bergmann, M. (2022): Impacts of plastic pollution in the oceans on marine species, biodiversity and ecosystems, 1–221, WWF Germany, Berlin. Doi: 10.5281/zenodo.5898684

Thiel, M., Hinojosa, I.A., Joschko, T., and Gutow, L. (2011). Spatio-temporal distribution of floating objects in the German Bight (North Sea). *J. Sea Res.* 65(3)**,** 368-379. doi: 10.1016/j.seares.2011.03.002.

Thomas, D.N., Arévalo-Martínez, D.L., Crocket, K.C., Große, F., Grosse, J., Schulz, K., et al. (2022). A changing Arctic Ocean. *Ambio* 51(2)**,** 293-297. doi: 10.1007/s13280-021-01677-w.

Trevail, A.M., Gabrielsen, G.W., Kühn, S., and Van Franeker, J.A. (2015). Elevated levels of ingested plastic in a high Arctic seabird, the northern fulmar (*Fulmarus glacialis*). *Polar Biol.* 38(7)**,** 975-981. doi: 10.1007/s00300-015-1657-4.

Tubau, X., Canals, M., Lastras, G., Rayo, X., Rivera, J., and Amblas, D. (2015). Marine litter on the floor of deep submarine canyons of the Northwestern Mediterranean Sea: The role of hydrodynamic processes. *Prog. Oceanogr.* 134(0)**,** 379-403. doi: 10.1016/j.pocean.2015.03.013.

Uurasjärvi, E., Pääkkönen, M., Setälä, O., Koistinen, A., and Lehtiniemi, M. (2021). Microplastics accumulate to thin layers in the stratified Baltic Sea. *Environ. Pollut.* 268**,** 115700. doi: 10.1016/j.envpol.2020.115700.

Vesman, A., Moulin, E., Egorova, A., and Zaikov, K. (2020). Marine litter pollution on the Northern Island of the Novaya Zemlya archipelago. *Mar. Pollut. Bull.* 150**,** 110671. doi: 10.1016/j.marpolbul.2019.110671.

VishnuRadhan, R., Thresyamma, D.D., Eldho, T.I., and Bhagat, J. (2021). Atmospheric plastics- a potential airborne fomite with an emerging climate signature. *The Journal of Climate Change and Health* 3**,** 100037. doi: 10.1016/j.joclim.2021.100037.

von Friesen, L.W., Granberg, M.E., Pavlova, O., Magnusson, K., Hassellöv, M., and Gabrielsen, G.W. (2020). Summer sea ice melt and wastewater are important local sources of microlitter to Svalbard waters. *Environ. Int.* 139**,** 105511. doi: 10.1016/j.envint.2020.105511.

Wieczorek, A.M., Croot, P.L., Lombard, F., Sheahan, J.N., and Doyle, T.K. (2019). Microplastic ingestion by gelatinous zooplankton may lower efficiency of the biological pump. *Environ. Sci. Technol.* 53(9)**,** 5387-5395. doi: 10.1021/acs.est.8b07174.

Wobus, F., Shapiro, G.I., Huthnance, J.M., and Maqueda, M.A.M. (2013). The piercing of the Atlantic Layer by an Arctic shelf water cascade in an idealised study inspired by the Storfjorden overflow in Svalbard. *Ocean Modelling* 71(0)**,** 54-65. doi: 10.1016/j.ocemod.2013.03.003.

Wollenburg, J.E., Katlein, C., Nehrke, G., Nöthig, E.M., Matthiessen, J., Wolf- Gladrow, D.A., et al. (2018). Ballasting by cryogenic gypsum enhances carbon export in a *Phaeocystis* under-ice bloom. *Scientific Reports* 8(1)**,** 7703. doi: 10.1038/s41598-018-26016-0.

Wu, S., Chen, Z., Zhou, M., Shao, Y., Jin, C., Tang, J., et al. (2022). Freeze-thaw alternations accelerate plasticizers release and pose a risk for exposed organisms. *Ecotoxicol. Environ. Saf.* 241**,** 113742. doi: 10.1016/j.ecoenv.2022.113742.

Yakushev, E., Gebruk, A., Osadchiev, A., Pakhomova, S., Lusher, A., Berezina, A., et al. (2021). Microplastics distribution in the Eurasian Arctic is affected by Atlantic waters and Siberian rivers. *Commun. Earth Environ.* 2(1)**,** 23. doi: 10.1038/s43247-021-00091-0.

Ye, S., and Andrady, A.L. (1991). Fouling of floating plastic debris under Biscayne Bay exposure conditions. *Mar. Pollut. Bull.* 22(12)**,** 608-613. doi: 10.1016/0025-326X(91)90249-R.

Zeri, C., Adamopoulou, A., Bojanić Varezić, D., Fortibuoni, T., Kovač Viršek, M., Kržan, A., et al. (2018). Floating plastics in Adriatic waters (Mediterranean Sea): From the macro- to the micro-scale. *Mar. Pollut. Bull.* 136**,** 341-350. doi: 10.1016/j.marpolbul.2018.09.016.

Zhao, S., Yu, Y., He, J., Yin, D., and Wang, B. (2015). Below-cloud scavenging of aerosol particles by precipitation in a typical valley city, northwestern China. *Atmos. Environ.* 102**,** 70-78. doi: 10.1016/j.atmosenv.2014.11.051.

Zhu, X., Munno, K., Grbic, J., Werbowski, L.M., Bikker, J., Ho, A., et al. (2021). Holistic Assessment of Microplastics and Other Anthropogenic Microdebris in an Urban Bay Sheds Light on Their Sources and Fate. *ACS ES&T Water* 1(6)**,** 1401-1410. doi: 10.1021/acsestwater.0c00292.

5 Supporting Information

5.1 Marine debris floating in Arctic and temperate Northeast Atlantic waters

The protocol form for visual surveys of floating debris

Survey Number			Start time						
Date			Start waypoint no (GPS)						
Survey duration, speed			End time						
Observer			End waypoint no (GPS)						
Animals			Comments						
Waypoint Number	**Material**	**SHAPE/Type/Usage**	**Size (cm)**	**Colour**	**No of items**	**Natural (y/n)**	**Bio-Fouled (y/n)**	**Sub-merged (y/n)**	**Aggre-gated (y/n)**

Table 5.1.1 Numbers of visual ship-based surveys conducted to quantify floating marine debris in different oceans, oceanic regions, and seasons during ten cruises in the NE Atlantic and Arctic Oceans.

	HE451.1	*SV Antigua*	PS99.1	PS99.2	PS101	PS105	PS107	PS108	MSM77	MSM95
Vessel										
RV Polarstern			✓	✓	✓	✓	✓	✓		
RV Maria S. Merian									✓	✓
RV Heincke	✓									
SV Antigua		✓								
Start	11/09/2015	10/05/2016	13/06/2016	23/06/2016	09/09/2016	21/03/2017	23/07/2017	22/08/2017	16/09/2018	09/09/2020
End	29/09/2015	02/07/2016	22/06/2016	16/07/2016	23/10/2016	20/04/2017	19/08/2017	09/09/2017	12/10/2018	07/10/2020
Ocean										
Arctic waters	13	14	24	51	25		49	40	17	14
Temperate NE Atlantic		4	11		8	4				2
Region										
Central Arctic	2	3			5					
Barents Sea	3	1			5					
Greenland Sea	7	6	3	42	1		26	25	13	7
Norwegian Sea	1	5	22	9	15		23	15	4	7
North Sea		3	10		7					2
North Atlantic sector						4				
Season										
Spring		8				4				
Summer		10	35	51			11			
Autumn	13				33		38	40	17	16
Total no. of transects	13	18	35	51	33	4	49	40	17	16

Table 5.1.2 PERMANOVA results of debris concentrations for the material and size groups

		Material		Size	
	Main tests	**Pseudo-F**	**P(perm)**	**Pseudo-F**	**P(perm)**
Region x Year	Region x Year	2.51	0.004	2.42	0.006
Region x Season	Season	4.64	0.003	4.33	0.001
Ocean x Season	Season	8.90	0.001	9.95	0.001
	Ocean x Season	2.58	0.047		
Ship	Ship	1.71	0.087	1.14	0.360
	Pairwise tests	**T**	**P(perm)**	**T**	**P(perm)**
2016	Norwegian Sea, Central Arctic	2.31	0.005	2.35	0.003
	Greenland Sea, Central Arctic	2.24	0.016	2.26	0.011
	Barents Sea, Central Arctic	2.91	0.012	2.76	0.018
2017	Norwegian Sea, Greenland Sea	2.20	0.018	2.88	0.002
Region x Season	Summer, Autumn	2.57	0.002	2.50	0.002
	Summer, Spring	2.10	0.009	2.47	0.002
Ocean x Season	Summer, Autumn	4.01	0.001	4.19	0.001
	Summer, Spring	2.11	0.011	2.59	0.002

Table 5.1.3 Summary of the results of marginal tests of material compositions with environmental parameters.

Variable	SS (trace)	Pseudo-F	P	Proportion
Distance (km)	16,470	17.53	0.001	0.08
Latitude	4,067	4.07	0.019	0.02
Longitude	1,620	1.60	0.204	0.008
Water temperature (°C)	12,550	13.10	0.001	0.06
Salinity (PSU)	16,320	17.34	0.001	0.08
Wind velocity (m s^{-1})	4,565	4.58	0.023	0.02
Chlorophyll a (µg l^{-1})	3,609	3.60	0.033	0.02
Ship speed (kn)	14,565	15.35	0.001	0.07

Table 5.1.4 Summary of the results of marginal tests of size compositions with environmental parameters.

Variable	SS (trace)	Pseudo-F	P	Proportion
Distance (km)	17,470	16.52	0.001	0.07
Latitude	4,796	4.29	0.014	0.02
Longitude	2,116	1.87	0.145	0.009
Water temperature (°C)	15,979	15.01	0.001	0.07
Salinity (PSU)	22,584	21.89	0.001	0.09
Wind velocity (m s^{-1})	6,312	5.68	0.007	0.03
Chlorophyll a (µg l^{-1})	8,546	7.77	0.004	0.04
Ship speed (kn)	21,531	20.74	0.001	0.09

Figure 5.1.1 Photo of fish lift attached to the juvenile fish trawl of RV Heincke (credit: F. Mark/AWI).

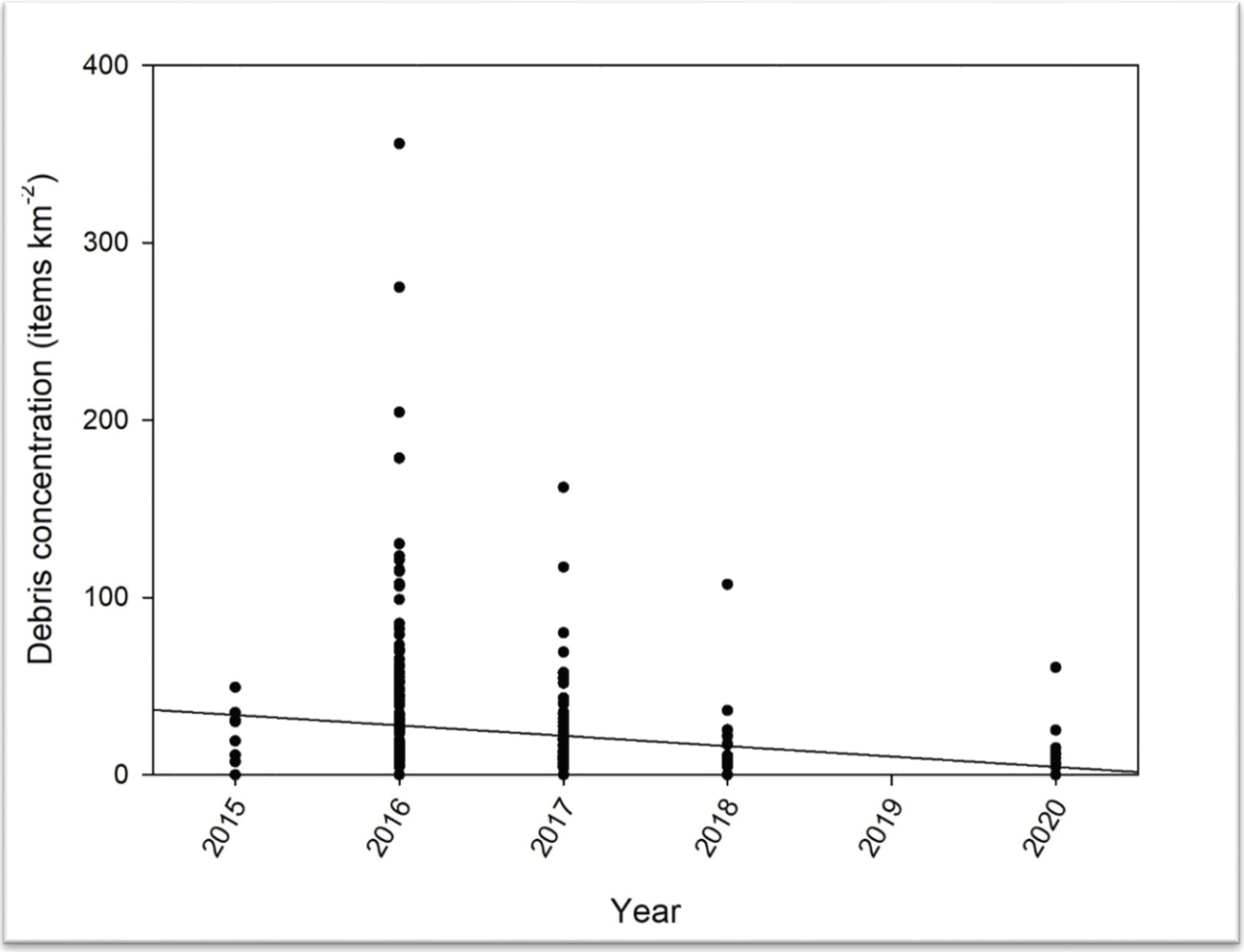

Figure 5.1.2 Debris concentrations over the study period. Linear regression: N = 276, r2 = 0.024. Analysis of variance of the regression model: F = 6.81, P = 0.010.

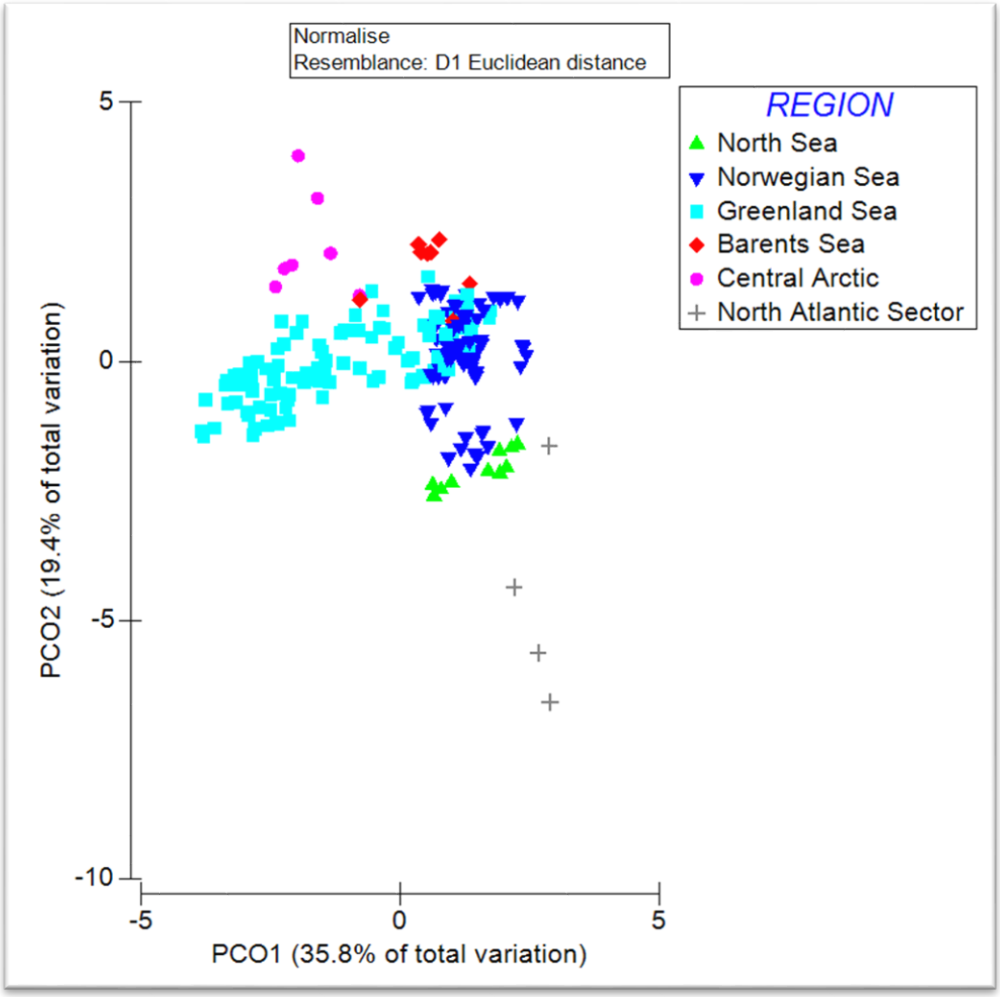

Figure 5.1.3 Principal coordinate analysis of the environmental parameters characterising the marine regions of the NE Atlantic Ocean.

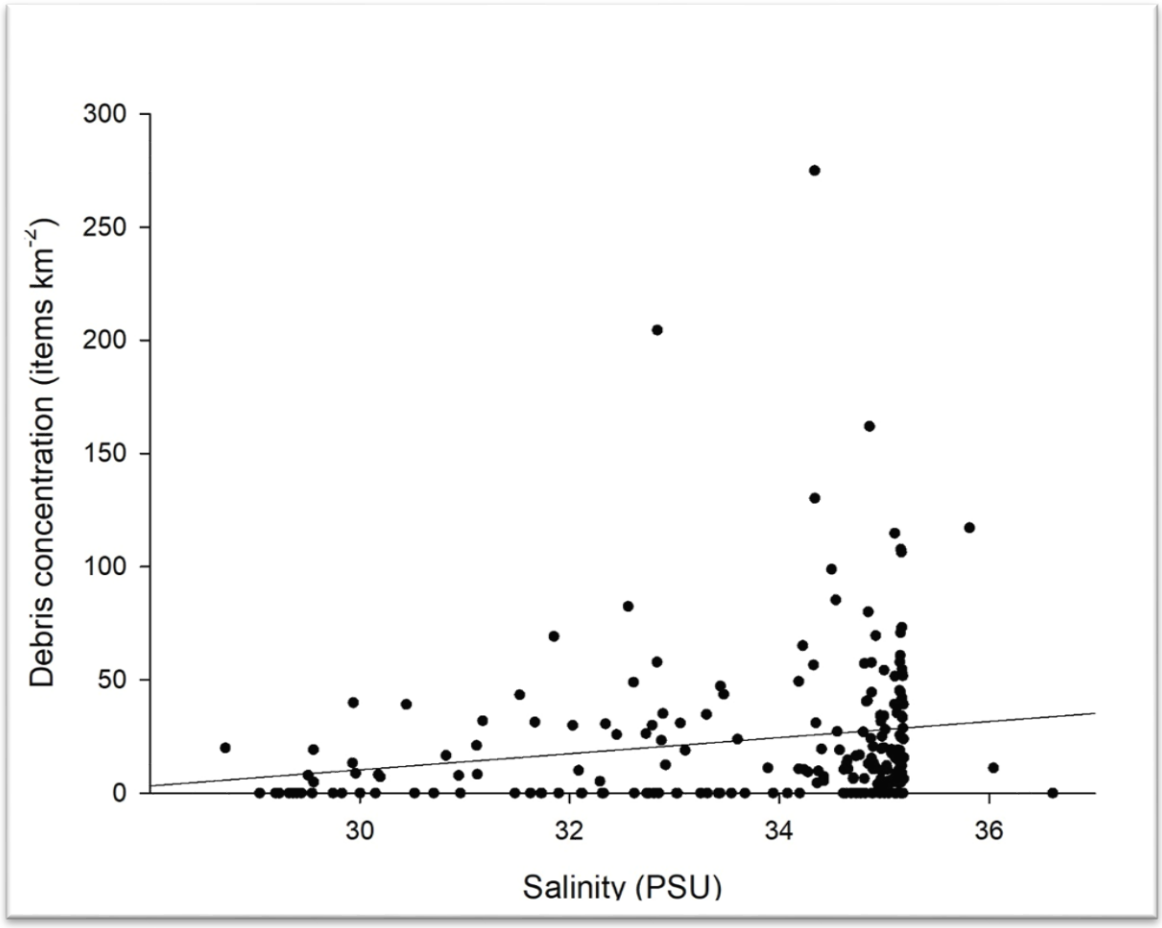

Figure 5.1.4 Scatter plot visualizing the debris concentration in relation to seawater salinity. Spearman's rank test: $\rho = 0.29$, $P < 0.001$. Linear regression: N = 211, r2 = 0.037. Analysis of variance of the regression model: F = 8, P = 0.005.

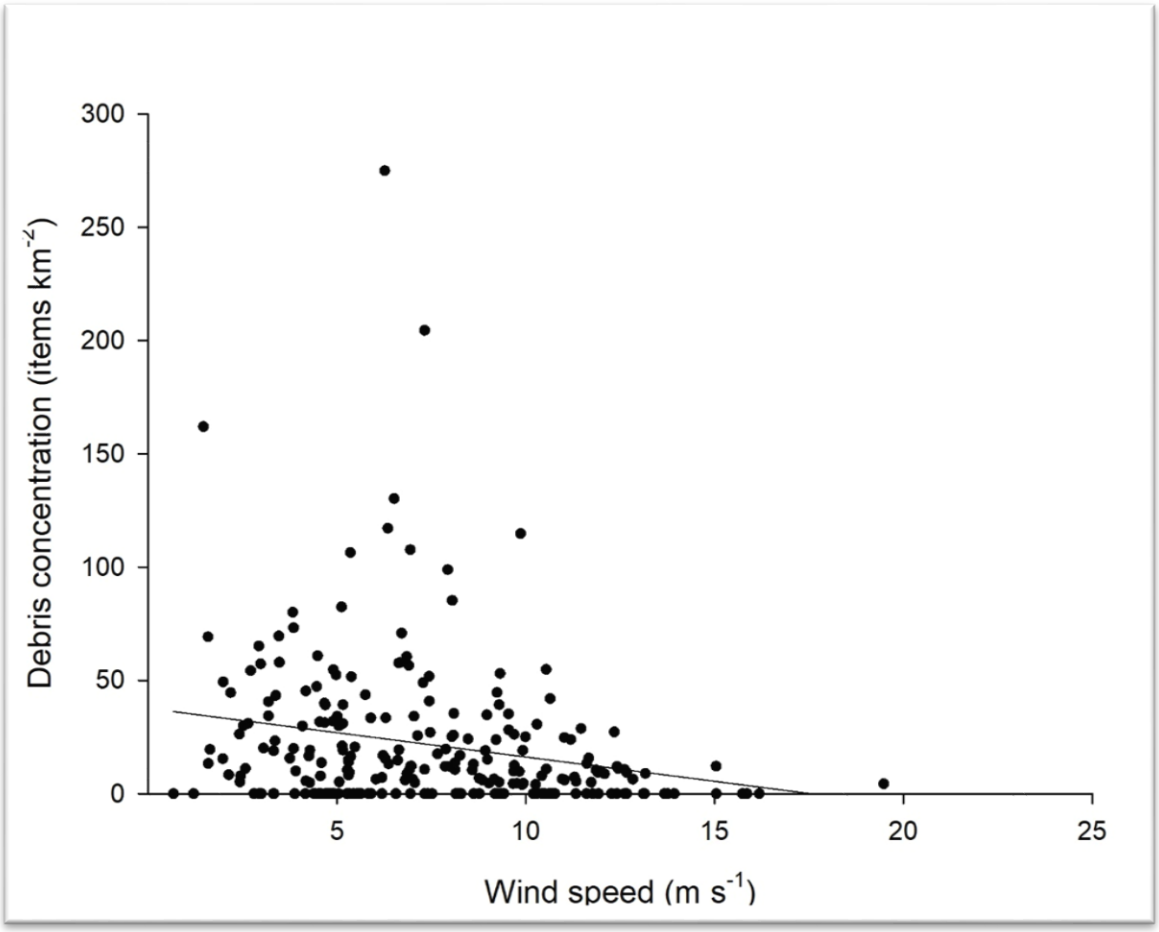

Figure 5.1.5 Scatter plot visualizing the debris concentration in relation to wind speed. Spearman's rank test: $\rho = -0.26$, $P < 0.001$. Linear regression: $N = 241$, $r2 = 0.049$. Analysis of variance of the regression model: $F = 12$, $P < 0.001$.

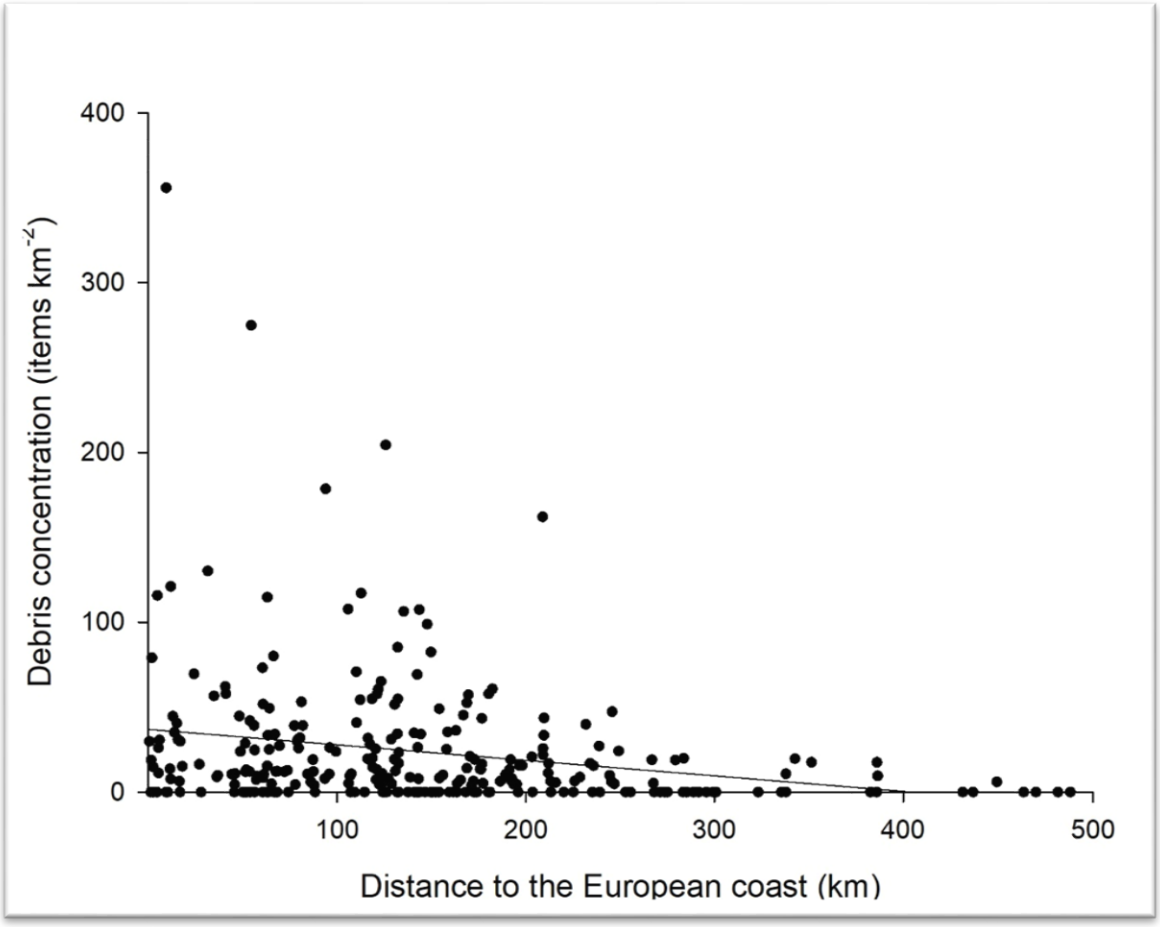

Figure 5.1.6 Scatter plot visualizing the debris concentration in relation to distance to the nearest European coast. Spearman's rank test: $\rho = -0.25$, $P < 0.001$. Linear regression: N = 276, r2 = 0.053. Analysis of variance of the regression model: F = 15, $P < 0.001$.

.

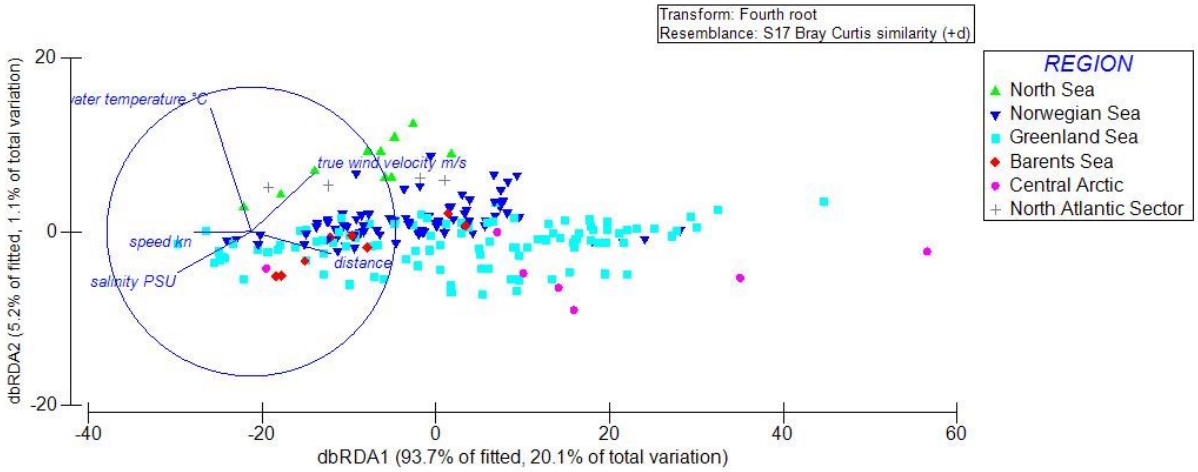

Figure 5.1.7 Plot of the distance-based redundancy analysis to decompose the effects of environmental parameters on the material composition of marine floating debris in the NE Atlantic.

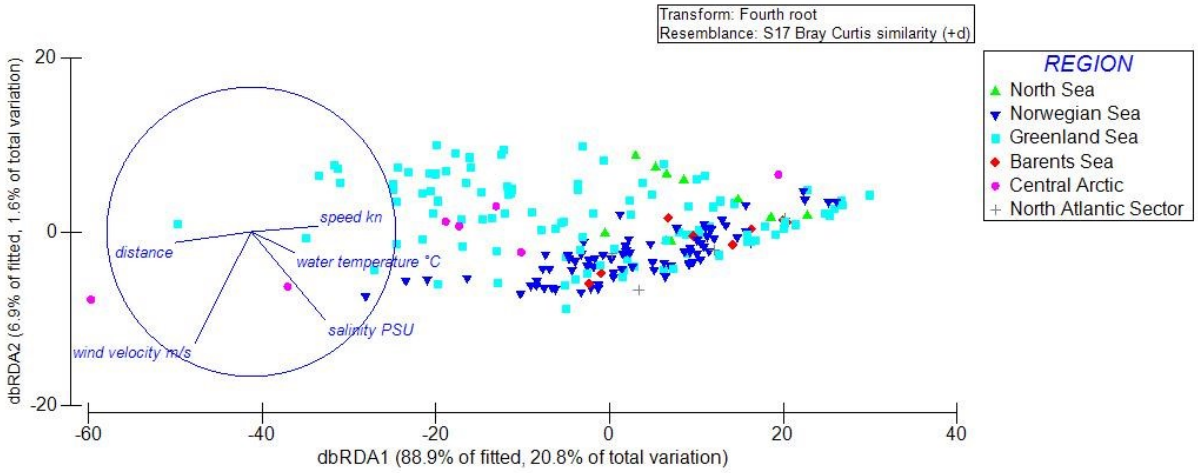

Figure 5.1.8. Plot of the distance-based redundancy analysis to decompose the effects of environmental parameters on the size composition of marine floating debris in the NE Atlantic.

5.2 Marine litter on deep Arctic seafloor continues to increase and spreads to the North at the HAUSGARTEN observatory

Table 5.2.1 Litter items count grouped by litter size.

Year	Station	Small-sized	Medium-sized	Large-sized
2002	HG4	1	6	
2004	N3		1	
	HG4	1	2	
2007	N3	1	2	1
	HG4	1	1	
2011	N3	1	1	
	HG4	3	7	1
2012	N3	7	2	1
	HG4	8	6	
2013	N3	14		
2014	N3	14		
	HG4	5	5	1
	N3	30	9	2
TOTAL	HG4	19	27	2
	HAUSGARTEN	49	36	4

Table 5.2.2 Litter items count grouped by litter type.

Year	Station	Plastic	Glass	Rope	Metal	Fabric	Paper/ Cardboard	Pottery	Timber
2002	HG4	4			1	1	1		
2004	N3			1					
	HG4	2					1		
2007	N3	2		1		1			
	HG4	2							
2011	N3				1	1			
	HG4	6	1	1		2		1	
2012	N3	1	4	1	3				1
	HG4	9		4	1				
2013	N3	3	7						
2014	N3	5	9						
	HG4	10		1					
	N3	11	20	3	4	2			1
TOTAL	HG4	33	1	6	2	3	2	1	
	HAUSGARTEN	44	21	9	6	5	2	1	1

Table 5.2.3 Megafaunal interaction counts grouped by megafaunal species, stations and litter type. Values for HAUSGARTEN represent proportions of epibenthic megafaunal

encounter distributed by species, litter with- and without biota interaction and type of interaction of the two HAUSGARTEN stations combined.

	Station			Litter Type	
	N3	**HG 4**	**HAUSGARTEN**	**Plastic**	**Other**
Cladorhiza gelida	5	20	42%	21	4
Caulophacus debris	6	3	15%	2	7
Hormathiidae	1	8	15%	6	3
Bathycrinus carpenterii		6	10%	3	3
Caulophacus arcticus	2	4	10%	5	1
Bathyphellia margaritacea	1	1	3%	2	
Hydrozoa		1	2%		1
cf. Pachastrellidae		1	2%	1	
Bythocaris spp.		1	2%	1	
Litter with biota interaction	15	35	56%	28	22
Litter with no biota interaction	26	13	44%	14	25
Contact	14	34	54%	35	13
Colonisation	1	10	12%	5	6
Other		1	1%	1	

5.3 Tying up Loose Ends of Microplastic Pollution in the Arctic: Distribution from the Sea Surface through the Water Column to Deep-Sea Sediments at the HAUSGARTEN Observatory

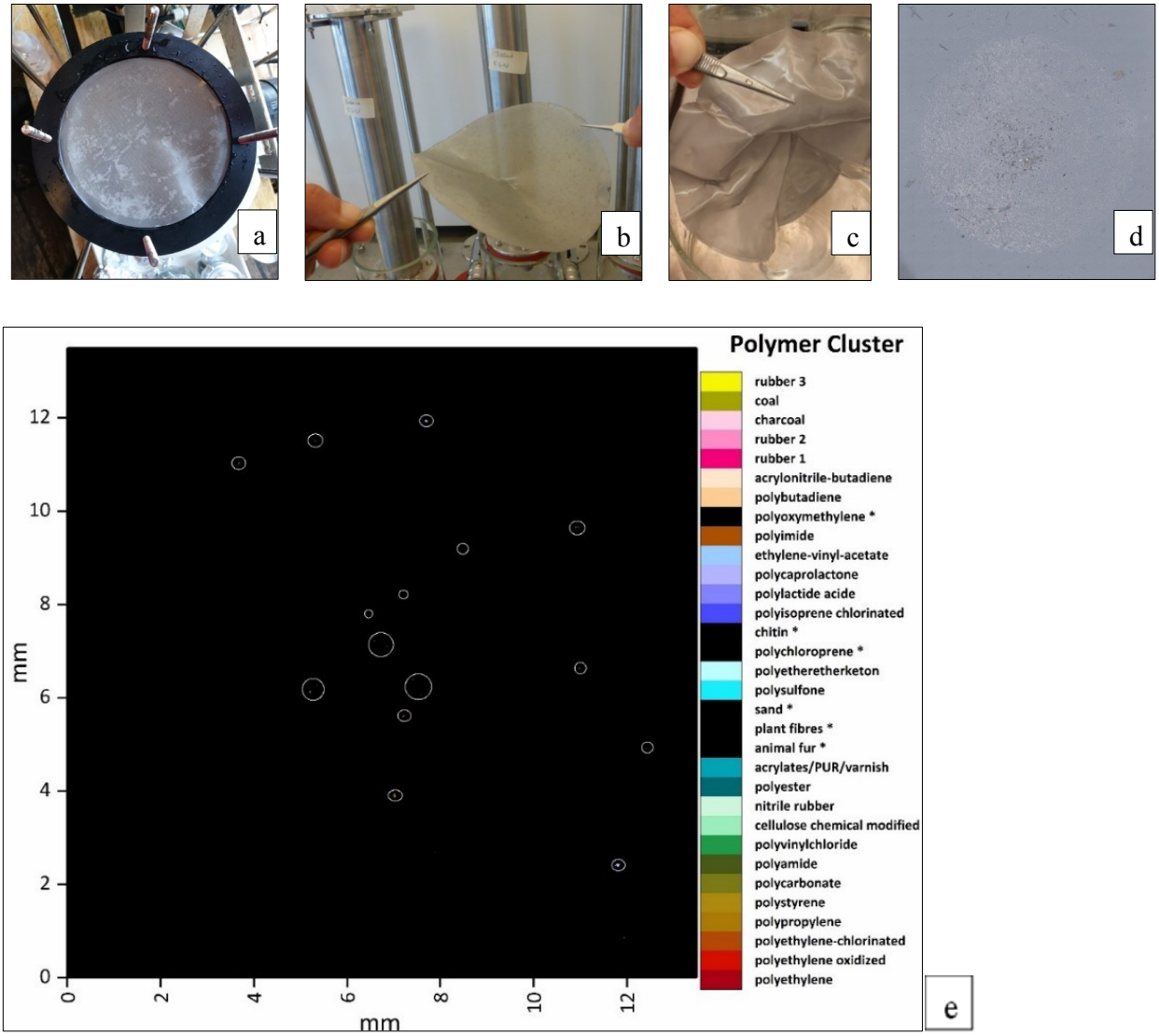

Figure 5.3.1 Processing of the water column samples. **a.** MP filter (stainless steel, 32 µm mesh) after in-situ sampling. **b.** MP filter before the purification with the microplastic reactor [Detailed information about enzymatic-oxidative purification with the microplastic reactor can be found in Lorenz et al. (2019)]. **c.** MP filter after purification. **d.** Anodisc filter with enriched water column sample. **e.** Corresponding polymer-dependent false-color image after FTIR measurement and automated analysis. To improve the visibility of the particles, some of the particles were encircled.

Paragraph 5.3.2 Identification of particles >500 µm by attenuated total reflection (ATR) FTIR unit.

The measurements via attenuated total reflection Fourier Transform Infrared spectroscopy were performed using a Bruker Tensor 27 equipped with a Platinum ATR unit (Bruker Optics GmbH). The spectra were collected using Bruker OPUS 7.5 (Bruker Optics GmbH) in the range of 4000 – 400 cm^{-1} with a resolution of 4 cm^{-1} with 32 co-added scans. Prior to a series of sample measurements, a background spectrum was collected and automatically subtracted from the data by the measurement software. The Fourier transformation was performed with the following parameters: phase Correction: Mertz; apodization function = Blackman-Harris Term 3, Zero filling: 2. The measurement was followed by library search using spectral correlation.

Table 5.3.2 Particles >500 µm in the sediment samples

Station	Particle [a]	Polymer type	Company/ origin of reference	rank /hit [b]	Polymer abbreviation	Colour	Shape	Size [µm]	
								Length	Width
SVI	A1	Could not be measured					fiber		
SVI	A2	Could not be measured					fiber		
SVI	A3	polytetrafluoroethylene	Scientific Polymer Products, Inc.	599 596 615	PTFE	black	film	1,167	813
SVI	A4	Resin dispersion	Hammerite	447 442 432	Resin dispersion	braun	film	1,508	1,332
SVI	A5	Could not be measured					fiber	1,110	-
SVI	A6	Could not be measured					fiber	2,734	-
SVI	A7	cellulose	Scientific Polymer Products, Inc.	461 470	cellulose	transparent	fiber	1,908	-
SVI	A8	algal fucus serratus	-	389	-	-	-	632	275
HG4	A2	Resin dispersion	Hammerite	406	-	red	film	2,253	1,766
		Polyethelene	Uni Bayreuth	497	LDPE	white, transparent			

		Resin dispersion	Hammerite	432	-	red			
		Resin dispersion	Hammerite	432	-	red			
		Polyethelene low density	Schaetti	410	LDPE	transparent			
		Polyethelene	Uni Bayreuth	562	LDPE	white, transparent			
HG4	A2_e	cellulose	Scientific Polymer Products, Inc.	387	-	white	fiber	2,371	-
HG4	A2_e1	fibre_linen2	Faserinstitut Bremen	554	-	braun	fiber	1,354	805
HG4	A3	lost during measurement				transparent	fiber	1,370	464
HG4	A4	lost during measurement				blackish	fiber	1,824	-
HG4	A5	lost during measurement				blackish	fiber	678	-
HG4	A6	lost during measurement					fiber	5,258	1,716
HG4	A7	lost during measurement					fiber		
N5	A1	fibre_linen2	Faserinstitut Bremen	442	-	brown	fiber	10,583	
N5	A2	polytetrafluoroethylene	Scientific Polymer Products, Inc.	559	PTFE	black	film	2,166	839
				603					
				570					

N5	N5_fibers	Aggregation, was not measured, only the picture was taken							
EGIV	A1	fibre_grass	Faserinstitut Bremen	438	-	brown	bead	694 (diameter)	
				441	-				
				433	-				
		ethylene_propylene	Scientific Polymer Products, Inc.	481	ethylene_propylene	light yellow			
		fibre_linen2	Faserinstitut Bremen	436	-	brown			
EGIV	A2	Could not be measured					fiber	10,263	
EGIV	A3	polytetrafluoroethylene	Scientific Polymer Products, Inc.	549	PTFE	black	film	1,487	553
EGIV	A4	polytetrafluoroethylene	Scientific Polymer Products, Inc.	484	PTFE	black	film	1,047	917
				481					
EGIV	A5	polytetrafluoroethylene	Scientific Polymer Products, Inc.	611	PTFE	black	film	1,185	945

[a] Twenty-three putative MP particles, including fibers (14) could be isolated for further ATR analysis. Some fibers from N5 were entangled with each other and it was not possible to separate them without damaging the particles (N5_fibers). These fibers could not be counted and were not analyzed.

[b] The measurements by ATR-FTIR did not reach hit quality above 700 in repeated measurements of the putative particles. Therefore, they were not included as synthetic polymers in the data analysis.

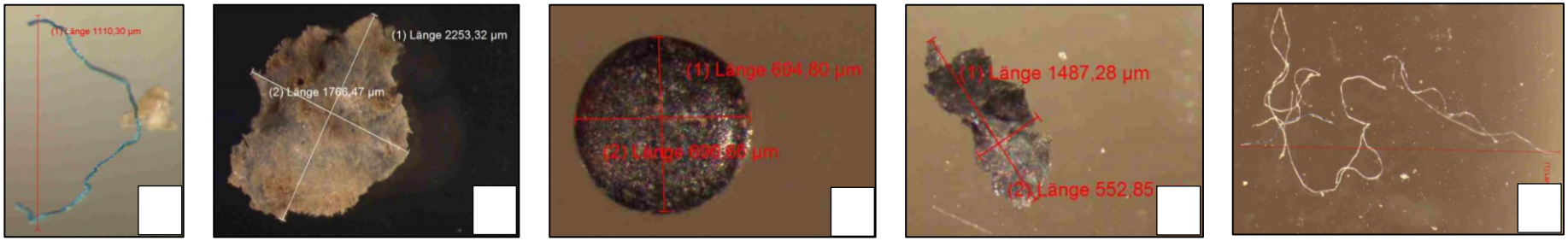

Figure 5.3.2 Examples of particles >500 µm in the sediment samples **a.** Fiber from SVI (particle: A5, measured dimension: 1110 µm) **b.** Particle from HG4 (particle: A2, measured dimensions: 1766 x 2253 µm) **c.** Particle from EGIV (particle: A1, measured diameter: 600 µm) **d.** Particle from EGIV (particle: A3, measured dimensions: 1487 x 553 µm) **e.** Fibers from N5 (particle: N5_fibers, measured dimension: 5368 µm).

Paragraph 5.3.3 Comparison of the purification methods.

Sediment samples which were taken from the HAUSGARTEN observatory during the expeditions ARK 29.2 in the summer of 2015 and PS 99.2 in the summer of 2016 were analyzed prior to the analysis of the actual sediment samples to assess the results of different purification methods (enzymatic-oxidative and Fenton's reagent) on particle identification by FTIR imaging. Four sediment samples were defrosted and pooled into a glass jar. Sediment separation was done as described in Bergmann et al. (2017). After separation, the sample was divided into six subsamples and the contents of these individual subsamples were mixed randomly with each other several times. Six subsamples with the volume of 85 – 109 ml were obtained after mixing process (Fig. 5.3.3-a). Three subsamples were selected randomly for the enzymatic-oxidative treatment and processed with the microplastic reactors as the water samples. Other subsamples were purified using Fenton's reagent according to Bergmann et al. (2017). After purification, an appropriate amount of subsamples was assessed by FlowCam and a consequent FTIR imaging analysis was applied to the subsamples to measure the small size fraction (11 - 500 µm). PERMANOVA was applied to Bray Curtis similarity matrix of square root transformed dataset to compare particle concentrations of the two groups (enzymatic-oxidative and Fenton's reagent purification). Monte Carlo simulation was used for pairwise comparisons if the count of unique permutations was not sufficient enough (< 100) and the significance value of Monte Carlo simulation (P (MC)) was selected. Data analysis did not show any significant difference between Fenton's reagent and enzymatic-oxidative treatment in polymer types (Fig. 5.3.3-b) and polymer size classes (Fig. 5.3.2-c) (Pseudo-F = 1.02, P (MC) = 0.599 and Pseudo-F = 1.13, P (MC) = 0.395, respectively). A similar contribution of polymer types (CPE, NRB, PP, PA, R3, PE, APV) and size classes (25 µm – 100 µm) were observed in both groups. No significant difference was found in particle types (Fig. 5.3.2-d) and size classes (Fig. 5.3.2-e) between treatments (Pseudo-F = 1.17, P (MC) = 0.4 and Pseudo-F = 0.75, P (MC) = 0.608, respectively) when natural particles (plant, animal fur, sand, chitin) were included in the dataset. Cluster analyses showed >70% similarity between treatments in particle types and sizes for every analysis. Therefore, sediment samples were purified with Fenton's reagent to maintain consistency in the purification method of the HAUSGARTEN sediments time series.

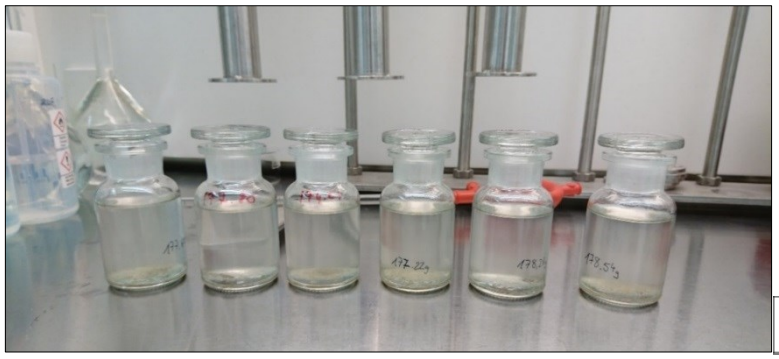

a

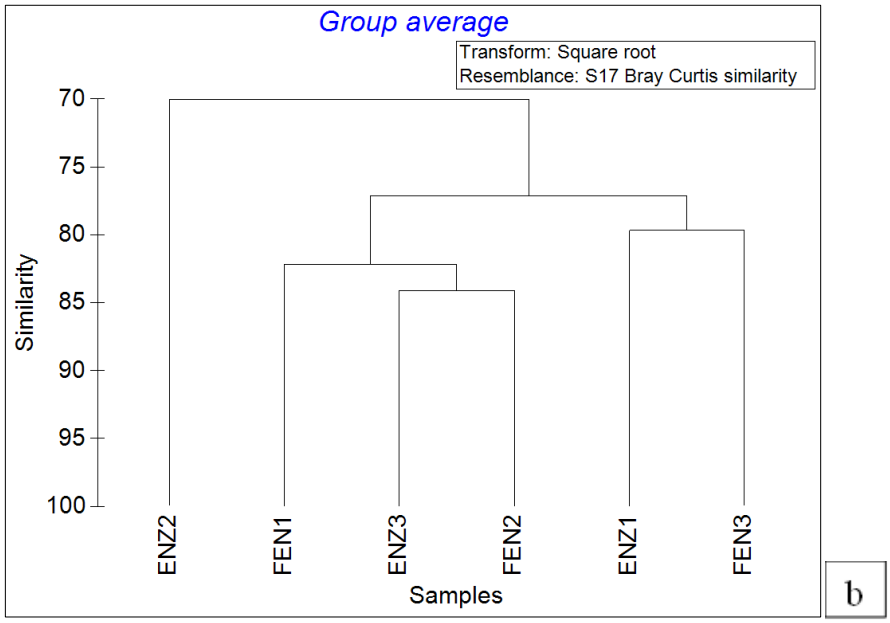

b

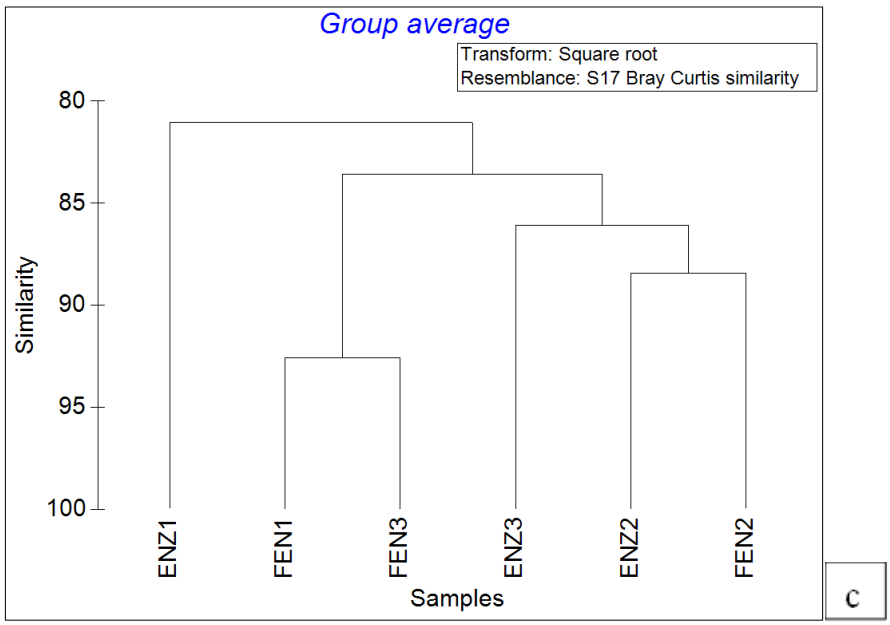

c

Figure 5.3.3 **a.** Samples obtained after sediment separation **b – d:** Cluster analysis of the results obtained by FTIR measurement of the subsamples purified with enzymatic-

oxidative treatment and Fenton's reagent. [**b.** Polymer types **c.** Polymer size classes **d.** Particle (polymer and natural) types. **e.** Particle (polymer and natural) size classes]

Paragraph 5.3.4 Fourier transform infrared spectroscopy (FTIR) measurements.

FTIR imaging was performed using a TENSOR 27 spectrometer (Bruker Optics GmbH) which is connected to a Hyperion 3000 µFTIR microscope equipped with a 4x optical lens and two 15x IR lenses for measurement. The data were collected in the wave number range of 3600−1250 cm^{-1}, with a resolution of 8 cm^{-1} and a binning factor of 4 was applied. The spectra were collected using a FPA detector with 64 × 64 MCT detector elements, yielding a pixel resolution of 11 µm with the applied parameters. The collected data were directly Fourier transformed using the parameters phase correction: Power/No Peak Search; apodization function = Blackman-Harris Term 3, Zero filling: 2).The background was measured on a particle free area of the same Anodisc filter prior to measurement and was automatically subtracted via the measurement software. To monitor spectra performance the polypropylene (PP) support of the Anodisc was used as internal standard and its data removed from the results prior to image analysis.

Table 5.3.4a The concentrations of the polymer types.

Station	Depth layer	Polymer types [a]												
		PA	R3	CPE	PP	NRB	APV	PES	EVA	PE	PS	PCL	PC	Other
N m^{-3}														
EGIV	near-surface	32	12	0	17	0	53	17	82	0	5	0	4	5
	300 m	15	11	0	0	0	0	44	4	0	0	4	0	0
	1000 m	0	2	2	0	0	2	9	0	0	0	0	0	0
	above seafloor	3	0	0	6	0	6	6	0	0	9	0	0	0
N5	near-surface	866	0	0	172	0	56	96	96	0	0	0	0	0
	300 m	5	10	0	0	0	5	20	10	0	0	0	0	5
	1000 m	8	8	0	11	0	11	4	4	4	0	0	0	4
	above seafloor	20	132	13	0	0	0	13	7	0	0	0	0	0
HG4	near-surface	18	67	0	17	0	46	9	9	0	27	0	25	0
	300 m	60	11	4	21	0	18	7	18	2	7	0	0	4
	1000 m	0	0	0	0	2	0	2	0	0	4	0	0	0

	above seafloor	0	0	0	0	0	0	0	0	0	0	0	0	0
HG9	near-surface	74	27	0	0	0	12	0	0	0	0	0	0	0
	300 m	0	5	0	0	0	33	0	0	0	0	0	0	0
	1000 m	11	33	0	0	0	21	0	0	0	0	0	0	0
	above seafloor	17	87	0	0	0	15	0	0	0	0	0	0	0
SVI	near-surface	0	252	5	0	0	0	0	0	2	0	0	0	2
	300 m	0	0	0	0	0	0	0	0	0	0	0	0	0
N kg^{-1}														
EGIV	sediment	498	196	569	475	39	60	92	10	177	-	312	-	8
N5	sediment	757	472	5,399	2,350	2,842	93	379	47	759	-	142	47	44
HG4	sediment	140	566	1,193	869	1,308	351	69	35	319	-	213	-	35
HG9	sediment	44	36	5	13	-	11	55	34	34	-	-	-	7
SVI	sediment	125	828	137	342	121	135	164	526	125	-	-	14	24
N m^{-3} [b]														
EGIV	sediment	382×10^3	151×10^3	437×10^3	365×10^3	30×10^3	46×10^3	71×10^3	8×10^3	136×10^3	-	239×10^3	-	6×10^3
N5	sediment	356×10^3	222×10^3	$2{,}538\times10^3$	$1{,}105\times10^3$	$1{,}336\times10^3$	44×10^3	178×10^3	22×10^3	357×10^3	-	67×10^3	22×10^3	20×10^3
HG4	sediment	88×10^3	357×10^3	753×10^3	549×10^3	826×10^3	222×10^3	44×10^3	22×10^3	201×10^3	-	134×10^3	-	22×10^3

HG9	sediment	19×10^3	15×10^3	2×10^3	6×10^3	-	5×10^3	24×10^3	15×10^3	15×10^3	-	-	-	3×10^3
SVI	sediment	65×10^3	430×10^3	71×10^3	178×10^3	63×10^3	70×10^3	85×10^3	273×10^3	65×10^3	-	-	7×10^3	13×10^3

[a] PA: polyamide, R3: ethylene-propylene-diene rubber, CPE: polyethylene-chlorinated, PP: polypropylene, NBR: nitrile rubber, APV: acrylates/polyurethanes/varnish, PES: polyester, EVA: ethylene-vinyl-acetate, PE: polyethylene, PS: polystyrene, PCL: polycaprolactone, PC: polycarbonate, Other: polyvinylchloride, rubber type 1, polysulfone, cellulose acetate

[b] The values For the sediments, the concentrations in N m^{-3} were calculated by multiplying MP N kg^{-1} with (dry) sediment density. Sediment density (kg m^{-3}) at each station was obtained by dividing the dry weight (wet weight × porosity) by the volume of the subsample. Weight, volume and porosity values were measured from additional sediment cores taken to analyze environmental parameters. All values are blank corrected.

Table 5.3.4b The concentrations of the polymer size classes.

Station	**Depth layer**	**=11µm**	**25 µm size class >11≤25µm**	**50 µm size class >25≤50µm**	**75 µm size class >50≤75µm**	**100 µm size class >75≤100µm**	**125 µm size class >100≤125µm**	**150 µm size class >125≤150µm**	**175 µm size class >150≤175µm**	**200 µm size class >175≤200µm**
N m^{-3}										
EGIV	near-surface	122	22	51	23	9	-	-	-	-
	300 m	15	44	11	4	-	4	-	-	-
	1000 m	5	9	2	-	-	-	-	-	-
	above seafloor	9	6	9	6	-	-	-	-	-
N5	near-surface	846	249	96	96	-	-	-	-	-

	300 m	15	20	10	10	-	-	-	-	-
	1000 m	23	11	15	4	-	-	-	-	-
	above seafloor	145	20	13	7	-	-	-	-	-
HG4	near-surface	120	53	9	18	18	-	-	-	-
	300 m	60	59	22	11	-	-	-	-	-
	1000 m	7	2	-	-	-	-	-	-	-
	above seafloor	-	-	-	-	-	-	-	-	-
HG9	near-surface	62	51	-	-	-	-	-	-	-
	300 m	33	5	-	-	-	-	-	-	-
	1000 m	21	11	32	-	-	-	1	-	-
	above seafloor	87	-	32	-	-	-	-	-	-
SVI	near-surface	204	44	12	2	-	-	-	-	-
	300 m	-	-	-	-	-	-	-	-	-
N kg^{-1}										
EGIV	sediment	1,183	594	529	81	30	-	-	-	21
N5	sediment	5,938	3,435	2,779	755	283	47	-	47	47

HG4	sediment	2,382	1,320	656	493	142	-	35	71	-
HG9	sediment	134	72	19	6	2	8	-	-	-
SVI	sediment	1,409	696	330	81	26	-	-	-	-
N m^{-3} [a]										
EGIV	sediment	908×10^3	456×10^3	406×10^3	62×10^3	23×10^3	-	-	-	16×10^3
N5	sediment	$2{,}792\times10^3$	$1{,}615\times10^3$	$1{,}306\times10^3$	355×10^3	133×10^3	22×10^3	-	22×10^3	22×10^3
HG4	sediment	$1{,}504\times10^3$	833×10^3	414×10^3	311×10^3	90×10^3	-	22×10^3	45×10^3	-
HG9	sediment	58×10^3	31×10^3	8×10^3	2×10^3	1×10^3	3×10^3	-	-	-
SVI	**sediment**	$\mathbf{732\times10^3}$	$\mathbf{361\times10^3}$	$\mathbf{171\times10^3}$	$\mathbf{42\times10^3}$	$\mathbf{14\times10^3}$	**-**	**-**	**-**	**-**

[a] For the sediments, the concentrations in N m^{-3} were calculated by multiplying MP N kg^{-1} with (dry) sediment density. Sediment density (kg m^{-3}) at each station was obtained by dividing the dry weight (wet weight × porosity) by the volume of the subsample. Weight, volume and porosity values were measured from additional sediment cores taken to analyze environmental parameters.

Paragraph 5.3.5 Contamination elimination.

High amounts of polyoxymethylene and polychloroprene particles were present in the water samples. Both polymer types are not common to be found in the Arctic samples (Bergmann et al., 2017; Peeken et al., 2018; Bergmann et al., 2019). Polyoxymethylene particles may have been introduced into the samples from the filter heads of the large volume pumps during in-situ filtering. Investigation about polychloroprene particles showed the humidity in the laboratory as the probable cause of the high amounts. For these reasons, polyoxymethylene and polychloroprene particles were not included in any of the datasets. As for the blank sample, the lid of the filter head had to be left open during sampling due to technical reasons. This may have introduced airborne contamination which is not the case for in-situ filtering. In fact, initially MPs were identified in the samples taken from the above seafloor depth layer of the central HAUSGARTEN (HG4) and 300 m depth layer of the Svalbard shelf (SVI) stations, but they got eliminated from the results after the results were blank-corrected.

Paragraph 5.3.6 Environmental parameters in the water column and sediments.

Table 5.3.6 Environmental parameters in the water column and sediments

WATER COLUMN									
Station	Sampling depth (m)	Ice coverage (%) [a]	CTD sampling depth (m)	Temp (°C)	Salinity	O_2 (µmol L^{-1})	POC (µg L^{-1})	PON (µg L^{-1})	TPM (µg L^{-1})
EGIV	-1	88	-10	-1.1	33.39	451	559	75	-870
	-303	71	-253	3.-	35.03	324	47	4	-13
	-993	63	-1014	-0.2	34.92	322	35	6	-14
	-2,574	65	-2570	-0.8	34.92	304	18	2	-12
N5	-3	41	-15	-0.9	33.95	453	305	48	1430
	-289	49	-254	3.2	35.04	323	12	2	-17
	-999	41	-1017	-0.2	34.92	321	39	6	-25
	-2,549	48	-2468	-0.7	34.93	306	9	1	-15
HG4	-1	1	-10	-0.5	32.95	429	356	48	-85
	-302	13	-253	2.8	35.02	325	41	6	-22
	-974	12	-1013	-0.3	34.91	321	36	5	-12
	-2,449	-	-2438	-0.7	34.92	305	25	3	-71

HG9	-2	28	-10	-0.3	32.41	405	163	32	-50
	-308	36	-101	3.9	35.07	322	-	-	-
	-1,022	36	-1013	-0.2	34.91	312	-	-	-
	-5,350	41	-5632	-0.4	34.93	304	-	-	-
SVI	-1	1	-5	5.1	34.59	366	241	44	-
	-250	-	-263	2.2	34.94	334	-	-	-

SEDIMENT

Station	Sampling depth (m)	Ice coverage (%) [a]	Chlorophyll a ($\mu g\ cm^{-3}$)	Chloroplastic pigment equivalent ($\mu g\ cm^{-3}$)	Phospholipids ($nmol\ ml^{-1}$)	Porosity (%)	POC (%)
EGIV	-2604	89	1.34	7.76	7.95	44.64	0.44
N5	-2614	52	2.28	12.67	19.82	60.80	0.95
HG4	-2462	3	1.67	11.70	22.55	50.94	0.56
HG9	-5569	34	2.47	15.79	17.58	63.26	1.24
SVI	-272	6	20.54	51.93	58.19	57.58	1.86

[a] Ice coverage (%): Sea ice conditions at the surface were determined with daily concentrations of sea ice retrieved from Centre d'Exploitation et de Recherche SATellitaire (CERSAT; http://cersat.ifremer.fr/). For the near-surface depth layers, sea-ice concentrations for 365 days of 2016 were extracted at the coordinates of the sampling stations. For the deep water column this was done at the surface origins of simulated 3D backward particle trajectories (for 2016, 365 trajectories). For the water samples, the number of days whose ice concentrations exceeded 15% at the sampling

coordinates (for the near-surface depth layers) and at their origins at the sea surface (for deep water column layers) were counted and normalized by 365 days to obtain ice coverage. 3D backward particle trajectories were not computed for the particles in the sediments. Therefore, to obtain a representative value of the ice coverage for the sediments, lateral advection was neglected and sea-ice concentrations at the coordinates of the sampling stations were extracted. This was done for the time period of 2000 – 2016 since particles in the sediments accumulate over time. The number of days whose ice concentrations exceeded 15% were counted and normalized by the total number of days between 2000 and 2016.

Paragraph 5.3.7 Relationships between polymer compositions and environmental parameters in the water column.

Three sample groups of polymer compositions were created (Table 5.3.7a) based on the availability of ice coverage, POC, PON and TPM values of the corresponding samples (Table 5.3.6). Bray Curtis similarity matrices were created from square-root transformed datasets of polymer compositions. DistLM routines were performed for each sample group to find the best parameters explaining the variability in polymer composition. Prior to the DistLM analyses, skewness of the data, outliers and multi-collinearity (Table 5.3.7c) were investigated with draftsman plots and log-transformations were applied accordingly. "Best" selection procedure with "Akaike Information Criterion (AIC)" was used to find best fitting model. As O_2, POC, PON, TPM showed multi-collinearity ($|r| > 0.90$) (Table 5.3.7c). "Overall best solutions" suggested by DistLM routine were examined. The solutions containing multi-collinear variables were left out during the selection of the model. Among the remaining models, the ones containing environmental parameters whose marginal tests showed the lowest Pseudo-F and highest p values were eliminated and the solutions with the lowest AIC value explaining the highest percentage of variation were selected as the best fitting model. Distance-based redundancy analysis (dbRDA) plots were done on the environmental parameters of the selected models (Fig. 5.3.7a – d). The analyses reveal similar results for the sample groups 1 and 2. O_2 and salinity were selected as explanatory variables due to a higher variability explained by these parameters than other combinations of environmental parameters.

Table 5.3.7a Sample groups used in DistLM analyses.

Station	**Samples**	**Sample group 1** [x]	**Sample group 2** [y]	**Sample group 3** [z]
EGIV	near-surface	✓	✓	✓
	300 m	✓	✓	✓
	1000 m	✓	✓	✓
	above seafloor	✓	✓	✓
N5	near-surface	✓	✓	✓
	300 m	✓	✓	✓

	1000 m	✓	✓	✓
	above seafloor	✓	✓	✓
HG4	near-surface	✓	✓	✓
	300 m	✓	✓	✓
	1000 m	✓	✓	✓
	above seafloor	×	×	×
HG9	near-surface	✓	✓	✓
	300 m	✓	×	×
	1000 m	✓	×	×
	above seafloor	✓	×	×
SVI	near-surface	✓	✓	×
	300 m	×	×	×

Table 5.3.7b Marginal tests of polymer compositions versus environmental parameters °

	Polymer size classes				**Polymer types**			
	Sample group 1 [x]		Sample group 2 [y]		Sample group 3 [z]		Sample group 3 [z]	
Variable	Pseudo-F	*P*	Pseudo-F	*P*	Pseudo-F	*P*	Pseudo-F	*P*
Log (Depth)	4.16	0.011	5.06	0.007	4.38	0.015	2.10	0.029
Log (Ice (%))	0.70	0.572	0.64	0.600	0.38	0.772	0.55	0.800
Log (Temperature)	0.95	0.431	0.75	0.527	1.18	0.312	0.87	0.540
Log (Salinity)	2.44	0.069	2.42	0.082	2.50	0.070	1.52	0.140
Log (O2)	4.59	0.005	5.09	0.011	4.70	0.010	2.22	0.024
Log (POC)			3.50	0.030	2.95	0.049	1.74	0.090
Log (PON)			3.27	0.035	2.76	0.057	1.68	0.102
Log (TPM)					5.72	0.005	2.61	0.024

Table 5.3.7c Correlations (r) between O2, POC, PON, TPM *

	Log (Depth)	Log (O2)	Log (POC)	Log (PON)
Log (O2)	-0.93 [x], -0.92 [y], -0.97 [z]			
Log (POC)	-0.93	0.92		
Log (PON)	-0.94 [y], -0.95 [z]	0.92	0.99	
Log (TPM)	-0.81	0.91	0.84	0.83

[x] HG4 above seafloor and SVI 300 m depth layers were excluded due to the missing ice coverage values for these samples.

[y] HG4 above seafloor and SVI 300 m, HG9 300 m, HG9 1000 m, HG9 above seafloor depth layers were excluded due to the missing ice coverage, POC and PON values for these samples.

[z] HG4 above seafloor, SVI near-surface, SVI 300 m, HG9 300 m, HG9 1000 m, HG9 above seafloor depth layers were excluded due to the missing ice coverage, POC, PON and TPM values for these samples.

° Marginal tests of polymer types for sample group 1 and sample group 2 versus environmental parameters were not statistically significant ($p > 0.05$), therefore their results were not included in the table.

* If *r* value differed among the analyses of the sample groups, corresponding *r* value was indicated with [x], [y] or [z].

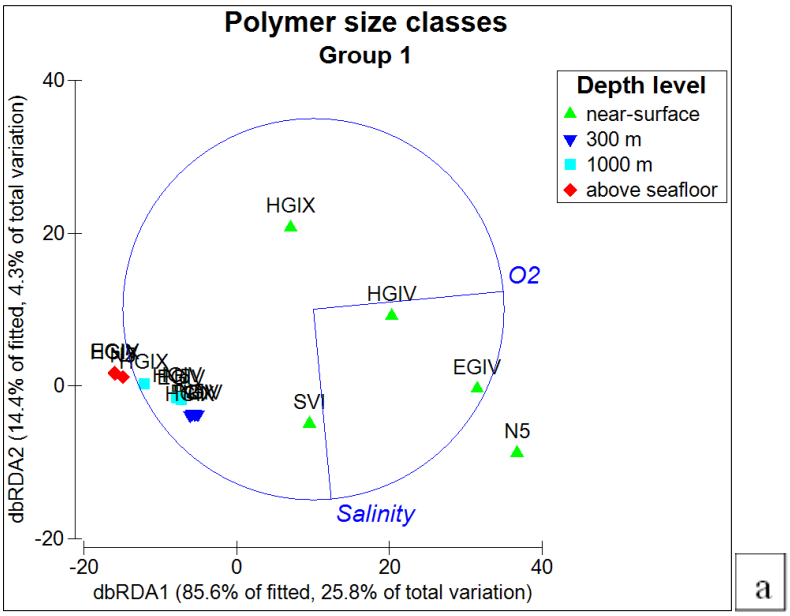

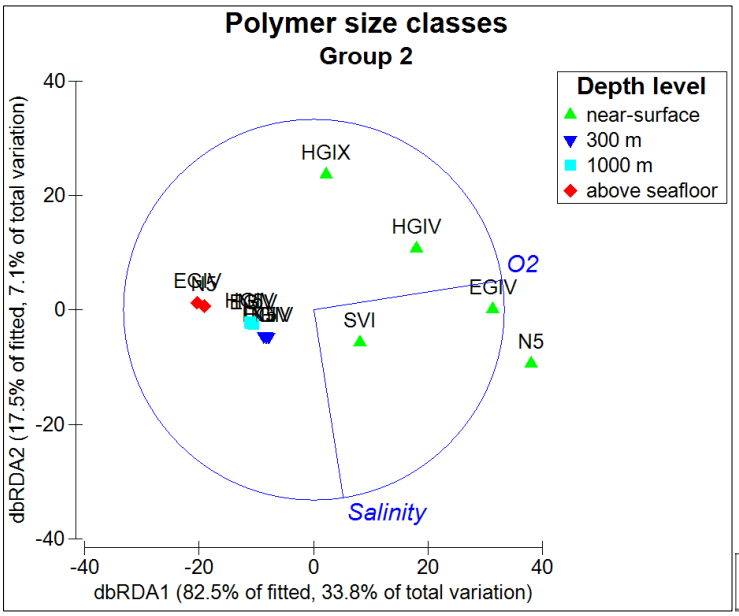
Polymer size classes
Group 2
Depth level
near-surface
300 m
1000 m
above seafloor
HGIX
HGIV
O2
EGIV
SVI
N5
Salinity
dbRDA2 (17.5% of fitted, 7.1% of total variation)
dbRDA1 (82.5% of fitted, 33.8% of total variation)
40
20
0
-20
-40
-40
-20
0
20
40

b

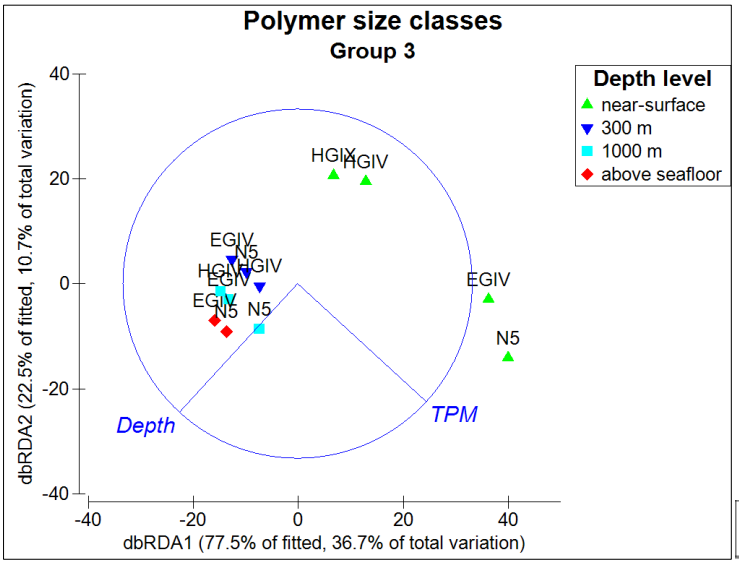
Polymer size classes
Group 3
Depth level
near-surface
300 m
1000 m
above seafloor
HGIX
HGIV
EGIV
N5
Depth
TPM
dbRDA2 (22.5% of fitted, 10.7% of total variation)
dbRDA1 (77.5% of fitted, 36.7% of total variation)
40
20
0
-20
-40
-40
-20
0
20
40

c

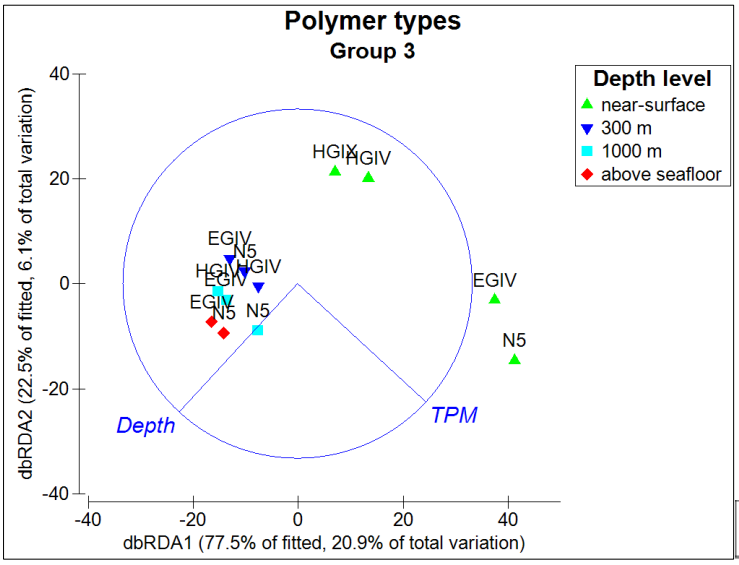
Polymer types
Group 3
Depth level
near-surface
300 m
1000 m
above seafloor
HGIX
HGIV
EGIV
N5
Depth
TPM
dbRDA2 (22.5% of fitted, 6.1% of total variation)
dbRDA1 (77.5% of fitted, 20.9% of total variation)
40
20
0
-20
-40
-40
-20
0
20
40

d

Figure 5.3.7 a – d. Distance-based redundancy analysis (dbRDA) of polymer compositions and best fitting models of environmental parameters in the water column with their vectors (strength and direction of effect of the variable on the ordination plot). Axis legends include the percentage of variation explained by the fitted model and the percentage of total variation explained by the axis. Bray Curtis similarity matrices of square-root transformed datasets of polymer compositions were used for the analyses. dbRDAs were run on log-transformed values of environmental variables.

a. dbRDA of polymer size classes excluding HG4 above seafloor and SVI 300 m depth layers due to the missing ice coverage values for these samples. (R^2 = 0.30, *AIC* = 110) **b.** dbRDA of polymer size classes excluding HG4 above seafloor, SVI 300 m, HG9 300 m, HG9 1000 m, HG9 above seafloor depth layers due to the missing ice coverage, POC or PON values for these samples. (R^2 = 0.41, *AIC* = 88) **c.** dbRDA of polymer size classes excluding HG4 above seafloor, SVI near-surface, SVI 300 m, HG9 300 m, HG9 1000 m, HG9 above seafloor depth layers due to the missing ice coverage, POC, PON or TPM values for these samples. (R^2 = 0.47, *AIC* = 81) **d.** dbRDA of polymer types, excluding HG4 above seafloor, SVI near-surface, SVI 300 m, HG9 300 m, HG9 1000 m, HG9 above seafloor depth layers due to the missing ice coverage, POC, PON or TPM values for these samples (R^2 = 0.27, *AIC* = 92).

Paragraph 5.3.8 Canonical analysis of principal coordinates (CAP) of polymer type compositions.

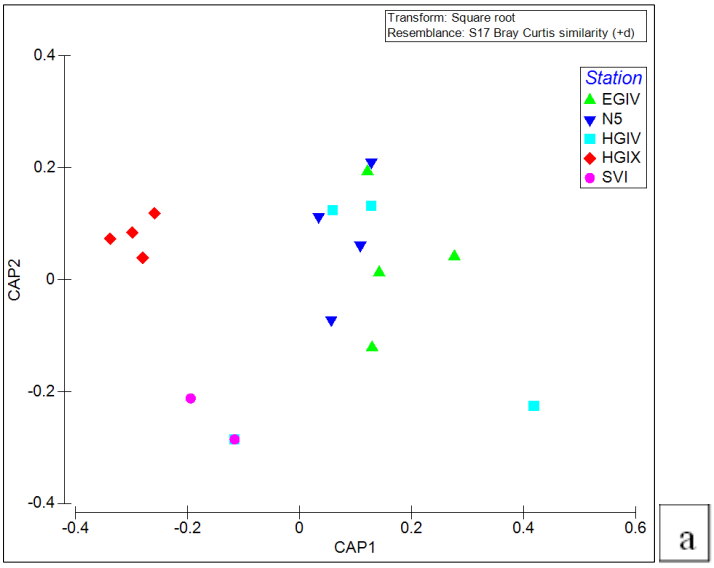

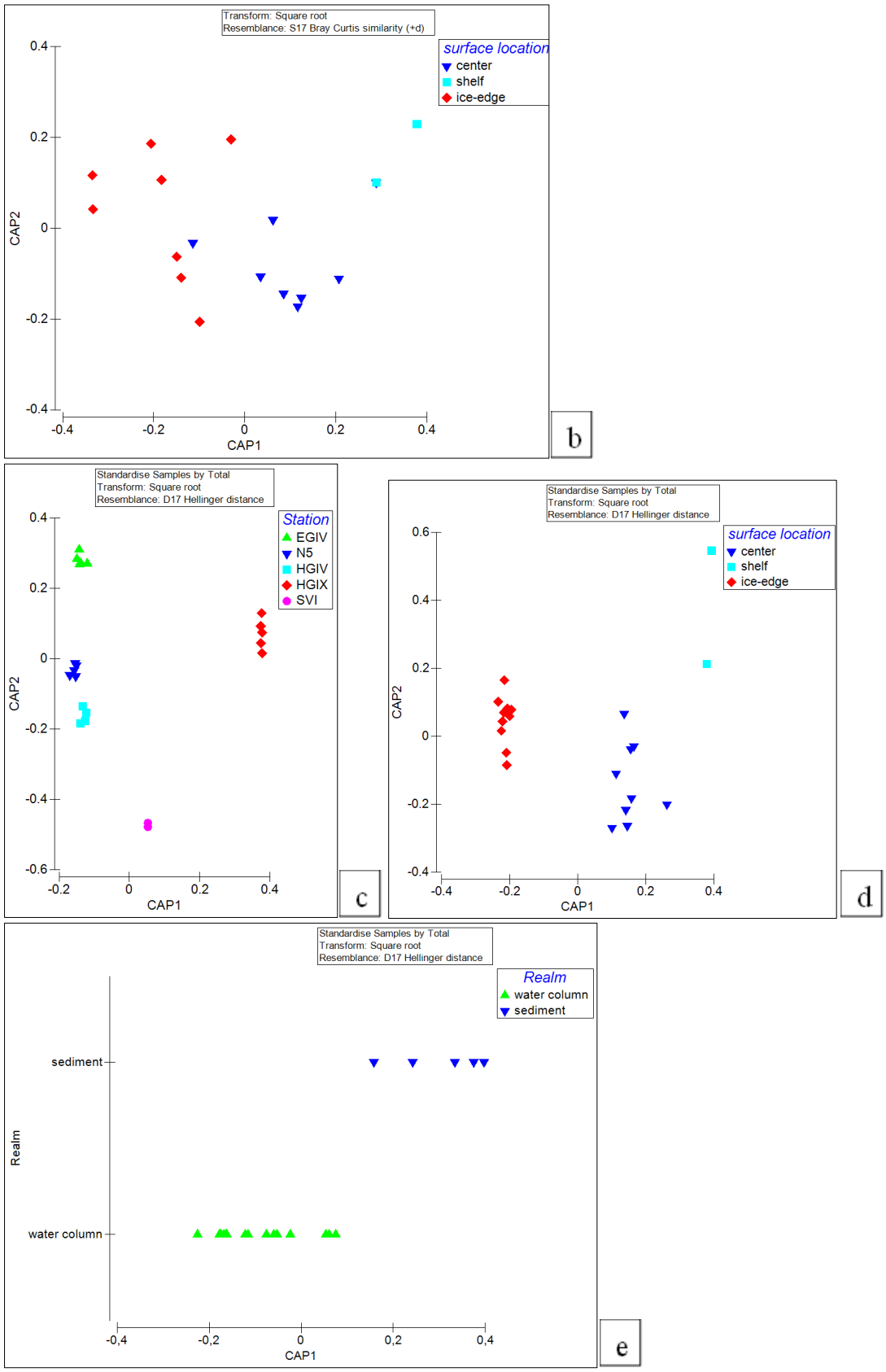

Figure 5.3.8 a – e. CAP of polymer type compositions. Analysis of polymer type compositions of water samples is based on the Bray-Curtis similarity of square-root transformed polymer type compositions (a, b). Analysis of polymer type compositions through

the water column and sediment is based on the Hellinger distance of square-root transformed standardized polymer type compositions (c – e). CAP for the stations was run with a separation of five a priori groups (EGIV, N5, HG4, HG9, SVI) (a, c). CAP for surface locations was run with a separation of three a priori groups (center, shelf and ice-edge) (b, d). CAP for realms was run with a separation of two a priori groups (water column, sediment) (e).

a. CAP of stations in the water column (m=3; δ_1 = 0.87, δ_2 = 0.66, δ_3 = 0.24; mis-classification error = 56%). **b.** CAP of surface locations in the water column (m=6, δ_1 = 0.87, δ_2 = 0.57, mis-classification error = 39%). **c.** CAP of stations through the water column and sediment (m=16; δ_1 = 0.99, δ_2 = 0.99, δ_3 = 0.96, δ_4 = 0.76; mis-classification error = 57%). **d.** CAP of surface locations through the water column and sediment (m=16, δ_1 = 0.99, δ_2 = 0.83, mis-classification error = 43%). **e.** CAP of realms (m=4, δ_1 = 0.87, mis-classification error = 4.8%

Paragraph 5.3.9 Simulation of the three-dimensional (3D) backward particle trajectories.

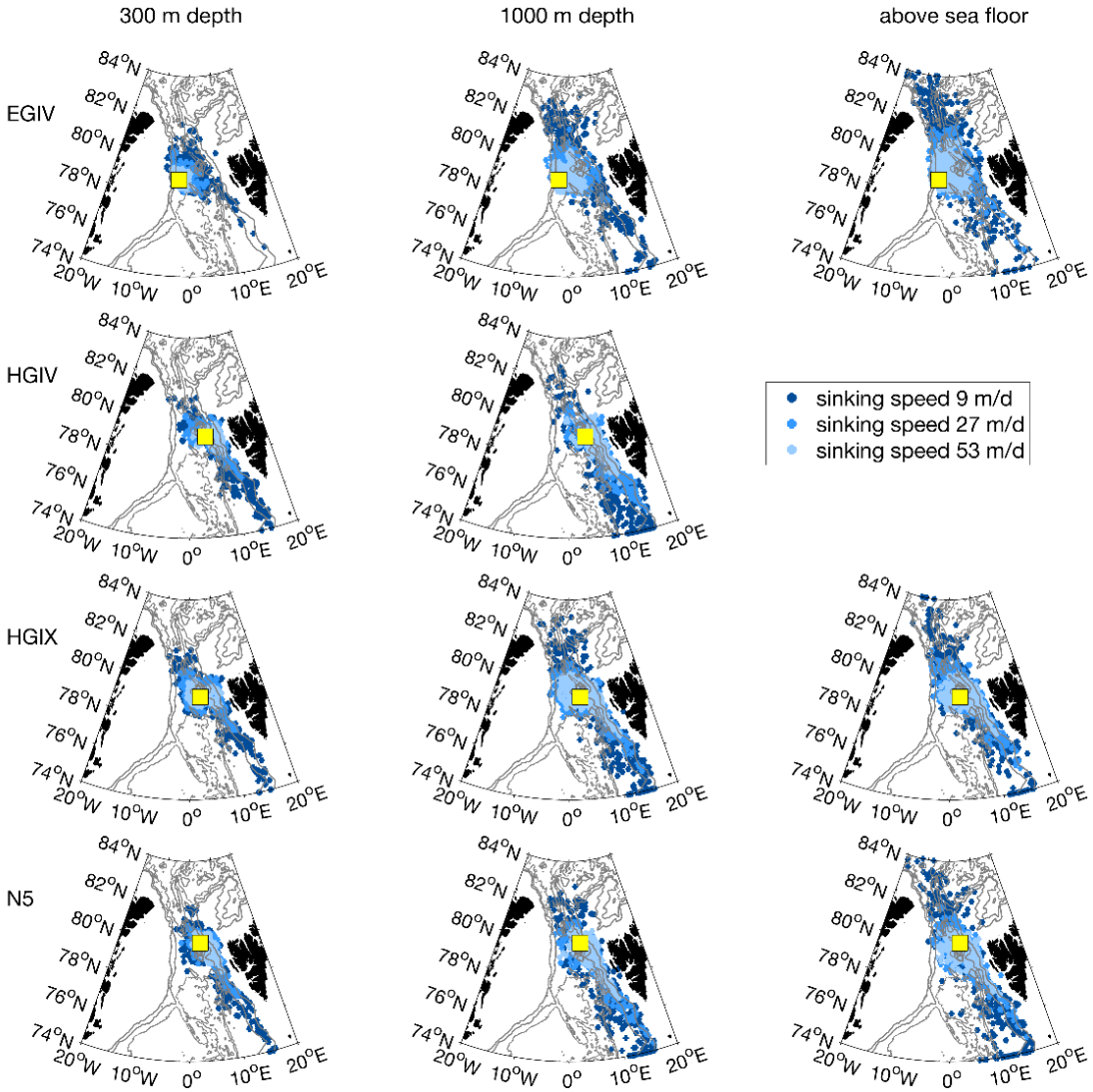

Figure 5.3.9 The simulated origins of the particles detected at the deep water column of the HAUSGARTEN stations.

Table 5.3.9 Summary dataset of the 3D simulation data.

Station x depth layer	Latitude	Longitude	North	West	Ice coverage (ice concentration >15%)	Average distance to sampling point (km)	Average trajectory path length (km)	Average salinity at surface	Polar water	Atlantic water
EGIV 300 m	78.83	-2.77	62%	20%	71%	72.46	144.07	33.04	70%	26%
EGIV 1000 m	78.83	-2.77	65%	16%	63%	140.81	349.50	33.16	63%	30%
EGIV above seafloor	78.83	-2.77	71%	21%	65%	186.89	630.38	33.03	67%	29%
N5 300 m	79.92	3.06	33%	35%	49%	88.46	159.55	33.42	60%	32%
N5 1000 m	79.92	3.06	31%	32%	41%	154.98	372.85	33.68	48%	44%
N5 above seafloor	79.92	3.06	34%	48%	48%	166.26	603.87	33.39	57%	37%
HG4 300 m	79.07	4.18	37%	22%	13%	108.75	185.96	34.37	23%	72%
HG4 1000 m	79.07	4.18	22%	17%	12%	182.43	391.20	34.44	21%	75%
HG9 300 m	79.13	2.85	55%	48%	36%	99.97	204.49	33.58	49%	45%
HG9 1000 m	79.13	2.85	46%	41%	36%	165.65	413.81	33.76	41%	53%
HG9 above seafloor	79.13	2.85	50%	40%	41%	154.15	653.11	33.65	47%	47%
Station										

EGIV	78.83	-2.77	66%	19%	66%	132.95	372.90	33.08	67%	28%
N5	79.92	3.06	33%	38%	46%	136.20	377.69	33.50	55%	38%
HG4	79.07	4.18	30%	19%	12%	144.54	285.64	34.40	22%	73%
HG9	79.13	2.85	51%	43%	38%	139.70	423.24	33.66	46%	48%

The number of the locations at the sea surface (obtained by the simulation of the 3D backward particle tracking) at the north, west of the sampling points; at the ice covered areas (ice concentration > 15%) and at polar, Atlantic waters was normalized by the total number of particles (365, the number of the particles which were released during the simulation period of 2016). Sea ice conditions at the surface were determined from daily concentrations of sea ice retrieved from Centre d'Exploitation et de Recherche SATellitaire (CERSAT; http://cersat.ifremer.fr/).

References

Bergmann, M., Mützel, S., Primpke, S., Tekman, M.B., Trachsel, J., and Gerdts, G. (2019). White and wonderful? Microplastics prevail in snow from the Alps to the Arctic. *Sci. Adv.* 5(8), eaax1157. doi: 10.1126/sciadv.aax1157.

Bergmann, M., Wirzberger, V., Krumpen, T., Lorenz, C., Primpke, S., Tekman, M.B., et al. (2017). High Quantities of Microplastic in Arctic Deep-Sea Sediments from the HAUSGARTEN Observatory. *Environ. Sci. Technol.* 51(19), 11000-11010. doi: 10.1021/acs.est.7b03331.

Peeken, I., Primpke, S., Beyer, B., Gütermann, J., Katlein, C., Krumpen, T., et al. (2018). Arctic sea ice is an important temporal sink and means of transport for microplastic. *Nat. Commun.* 9, 1505. doi: 10.1038/s41467-018-03825-5.

6 Further scientific publications

PEER-REVIEWED JOURNAL ARTICLES

1 Bergmann, M., Collard, F., Fabres, J., Gabrielsen, G.W., Provencher, J.F., Rochman, C.M., van Sebille, E., **Tekman, M.B.** (2022). Plastic pollution in the Arctic. *Nat. Rev. Earth Environ., 3*(5), 323-337. doi:10.1038/s43017-022-00279-8
2 MacLeod, M., Arp, H. P. H., **Tekman, M. B.**, & Jahnke, A. (2021). The global threat from plastic pollution. *Science, 373*(6550), 61-65. doi:10.1126/science.abg5433
3 Parga Martínez, K. B., **Tekman, M. B.**, & Bergmann, M. (2020). Temporal trends in marine litter at three stations of the HAUSGARTEN observatory in the Arctic deep sea. *Front. Mar. Sci., 7*, 321.
4 Hasemann, C., Mokievsky, V., Sablotny, B., **Tekman, M. B.**, & Soltwedel, T. (2020). Effects of sediment disturbance on deep-sea nematode communities: Results from an in-situ experiment at the arctic LTER observatory HAUSGARTEN. *J. Exp. Mar. Biol. Ecol., 533*, 151471. doi: 10.1016/j.jembe.2020.151471
5 Bergmann, M., Mutzel, S., Primpke, S., **Tekman, M. B.**, Trachsel, J., & Gerdts, G. (2019). White and wonderful? Microplastics prevail in snow from the Alps to the Arctic. *Sci. Adv., 5*(8), eaax1157. doi:10.1126/sciadv.aax1157
6 Kühn, S., Schaafsma, F. L., van Werven, B., Flores, H., Bergmann, M., Egelkraut-Holtus, M., **Tekman, M. B.** van Franeker, J. A. (2018). Plastic ingestion by juvenile polar cod (*Boreogadus saida*) in the Arctic Ocean. *Polar Biol., 41*(6), 1269-1278. doi:10.1007/s00300-018-2283-8
7 Bergmann, M., **Tekman, M. B.**, & Gutow, L. (2017). Marine litter: Sea change for plastic pollution. *Nature*, 544(7650), 297. doi:10.1038/544297a
8 Bergmann, M., Lutz, B., **Tekman, M. B.**, & Gutow, L. (2017). Citizen scientists reveal: Marine litter pollutes Arctic beaches and affects wild life. *Mar. Pollut. Bull., 125*(1-2), 535-540. doi:10.1016/j.marpolbul.2017.09.055
9 Bergmann, M., Wirzberger, V., Krumpen, T., Lorenz, C., Primpke, S., **Tekman, M. B.**, & Gerdts, G. (2017). High quantities of microplastic in arctic deep-sea sediments from the HAUSGARTEN observatory. *Environ. Sci. Technol., 51*(19), 11000-11010. doi:10.1021/acs.est.7b03331

IN BOOK

1 Lebreton, L., Kooi, M., Mani, T., Mintenig, S.M., **Tekman, M. B.**, van Emmerik, T. and Wolter, H. (2022). Plastics in Freshwater Bodies. In Plastics and the Ocean, A.L. Andrady (Ed.). https://doi.org/10.1002/9781119768432.ch7
2 Bergmann, M., **Tekman, M. B.**, Walter, A., Gutow, L. (2018). Tackling Marine Litter—LITTERBASE. In: Krause, G. (eds) Building Bridges at the Science-Stakeholder Interface. SpringerBriefs in Earth System Sciences. Springer, Cham. https://doi.org/10.1007/978-3-319-75919-7_13
3 Bergmann, M., **Tekman, M. B.** and Gutow, L. (2017), LITTERBASE: An Online Portal for Marine Litter and Microplastics and Their Implications for Marine Life / Baztan, J., Jorgensen, B., Pahl, S., Thompson, R. and Vanderlinden, J. P. (editors), In: Fate and Impact of Microplastics in Marine Ecosystems, MICRO 2016, Amsterdam, Elsevier, 2 p. doi:10.1016/B978-0-12-812271-6.00104-6, hdl:10013/epic.49729

4 Bergmann, M., Peeken, I., Beyer, B., Krumpen, T., Primpke, S., **Tekman, M. B.** and Gerdts, G. (2017), Vast Quantities of Microplastics in Arctic Sea Ice—A Prime Temporary Sink for Plastic Litter and a Medium of Transport / Baztan, J., Jorgensen, B., Pahl, S., Thompson, R. and Vanderlinden, J. P. (editors), In: Fate and Impact of Microplastics in Marine Ecosystems, MICRO 2016, Amsterdam, Elsevier, 2 p. doi:10.1016/B978-0-12-812271-6.00073-9, hdl:10013/epic.49739

7 Acknowledgements

First of all, I would like to express my extreme gratitude to my supervisor Dr Melanie Bergmann. She gave me a great opportunity to work in a leading marine institute. During these years, she always guided me with great patience, endless support and friendship. Thank you Melanie.

It was a great pleasure to be part of the Deep-sea Ecology and Technology group at the Alfred Wegener Institute. Everyone in the group always helped me whenever I had a question or a need for my work. This PhD work would have not been possible without their continuous support. I also want to thank Annabel for her great kindness.

I want to thank to Pitty, Jenny, Melissa and Claudia W. for their valuable advice both on an academic and personal level. When I felt depressed, they created time for me. I cannot thank them enough for their support.

I also would like to thank to Lars for his continuous mentorship during my PhD and LITTERBASE work.

Claudia L, Gunnar and Sebastian supported my whole life and work on Helgoland. Claudia L. not only accompanied me during the long hours in the laboratory and patiently answered my never-ending questions but also after endless hours of working, we spent great times together. Sidika has become a lifelong friend that I am extremely grateful for.

Even though it was not a part of my PhD, LITTERBASE was one of my works at the AWI. Corina provided endless support for my LITTERBASE work. As we shared the same office, she always motivated me while I was writing my manuscripts.

Without Onur, Ale, Ivo, Mehmet, Özgür and Zeki I do not know how I would have survived in Germany.

Since the first day I met with Annika, she not only has become my scientific soulmate but also an amazing friend. I do not know how I can express my gratitude to her for being my mentor on an academic, professional and personal level. Together with Tilo, they continuously supported my whole life in Germany.

I would also like to thank my mother from the bottom of my heart, whose incredible emotional support made it possible for me to complete this PhD. I thank Zeynep, Ozan, Hilal, Elif, Özlem and their families and children for being my best friends, even when we lived in different countries.

And finally, even though he will never know or be aware, my four-legged flatmate Mahzun kept me sane during the pandemic period of this PhD.